ARMY RESEARCH LABORATORY

A Method of Identifying Supersonic Projectiles Using Acoustic Signatures

Richard B. Loucks
Bradford S. Davis
Linda Moss
Tien Pham
Manfai Fong

ARL-TR-859 September 1995

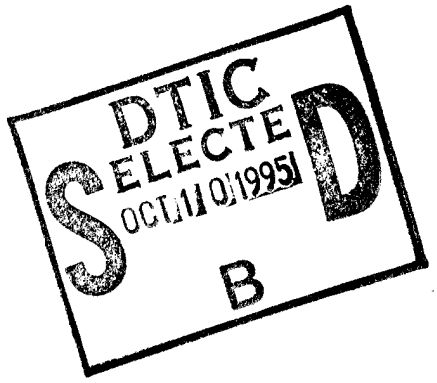

19951005 012

NOTICES

Destroy this report when it is no longer needed. DO NOT return it to the originator.

Additional copies of this report may be obtained from the National Technical Information Service, U.S. Department of Commerce, 5285 Port Royal Road, Springfield, VA 22161.

The findings of this report are not to be construed as an official Department of the Army position, unless so designated by other authorized documents.

The use of trade names or manufacturers' names in this report does not constitute indorsement of any commercial product.

REPORT DOCUMENTATION PAGE

Form Approved
OMB No. 0704-0188

1. AGENCY USE ONLY *(Leave blank)*	2. REPORT DATE	3. REPORT TYPE AND DATES COVERED
	September 1995	April 1992-August 1993

4. TITLE AND SUBTITLE

A Method of Identifying Supersonic Projectiles Using Acoustic Signatures

5. FUNDING NUMBERS

PR: 1L162618AH80

6. AUTHOR(S)

Richard B. Loucks, Bradford S. Davis, Linda Moss, Tien Pham, and Manfai Fong

7. PERFORMING ORGANIZATION NAME(S) AND ADDRESS(ES)

U.S. Army Research Laboratory
ATTN: AMSRL-WT-NC
Aberdeen Proving Ground, MD 21005-5066

8. PERFORMING ORGANIZATION REPORT NUMBER

ARL-TR-859

9. SPONSORING/MONITORING AGENCY NAMES(S) AND ADDRESS(ES)

7th Army Training Center
HQ 7th ATC, Unit 28130
APO, AE 09114

U.S. Army Materiel Command
Field Assistance in Science and Technology Program
Ft. Belvoir, VA 22060-6606

10.SPONSORING/MONITORING AGENCY REPORT NUMBER

11. SUPPLEMENTARY NOTES

12a. DISTRIBUTION/AVAILABILITY STATEMENT

Approved for public release; distribution is unlimited.

12b. DISTRIBUTION CODE

13. ABSTRACT *(Maximum 200 words)*

There was a need to investigate the feasibility of attaching a device to the existing Remote Equipment Target System (RETS) such that RETS would be able to identify the type of projectile that struck the target. A concept was developed to identify projectiles acoustically by measuring some characteristics of N-Wave produced from the projectile's sonic boom. High-fidelity microphones were positioned to provide N-Wave profiles. The distance between the sonic boom's source and the microphone was the most important parameter. An array of six low-fidelity microphones was used to locate the projectile location. By utilizing the sonic boom arrival times and knowledge of the spatial locations of the low-fidelity microphones, the location of the projectile relative to the high-fidelity microphones was determined. The concept development was broken into three phases--feasibility, data collection, and finally validation and verification of the concept's functionality. A prototype unit called a Round Discrimination System (RDS) was fabricated and field tested in the validation/verification phase. The RDS unit was transported to the 7th ATC in Germany for a demonstration. This report provides details of each phase of the development program and the results of the on-site demo in Germany.

14. SUBJECT TERMS

acoustic arrays, acoustic signatures, computer application, decision making, identification, locators, model theory, overpressure, pressure measurements, projectile noise, shock waves, sonic boom, statistical analysis

15. NUMBER OF PAGES

197

16. PRICE CODE

17. SECURITY CLASSIFICATION OF REPORT	18. SECURITY CLASSIFICATION OF THIS PAGE	19. SECURITY CLASSIFICATION OF ABSTRACT	20. LIMITATION OF ABSTRACT
UNCLASSIFIED	UNCLASSIFIED	UNCLASSIFIED	UL

INTENTIONALLY LEFT BLANK.

ACKNOWLEDGMENTS

The authors express their sincere appreciation to the following people for their support during all phases of the FAST Round Discrimination System Project.

We are indebted to Bob Watts and James Lim for their support as advisors during the research-gathering phase, the technical reviews, and the demonstration at 7th ATC. SGT Jackson, Jim Cruthers, and Tim Knowles were also helpful in making those efforts a success. Special thanks go to Lisa Kogel who kept us from self-destructing when we were at 7th ATC.

The authors are also appreciative of Ralph Scutti and Doug Griffen for seeing us through the testing at the U.S. Army Combat Systems Test Activity (CSTA); Don Forsythe for providing excellent technical support at H-Field; the gunners Marvin Baine, Al Atkinson, Dale Simpkins, Glen Griffin, Bill Morgan, Bruce Zeigler, and Bob Newton for safely firing hundreds of rounds under what must have seemed eccentric circumstances; the surveyors Mark Lange, Mike Hitchcock, Vince Costanzi, Charles Moore, and Eric Donald for those precise measurements needed to verify the success of the project; and others such as Ronnie Spangler, John Hoffmann, Curt Janney, Doug Haskins, and Rick Drennan, who provided tireless hours with video scoring and Weibel radar data. These individuals provided us with excellent data at H-Field and High-Velocity Range.

Kit Tram and Jerry Gerber of Sensors, Signatures, and Information (S3I) Processing Directorate are also thanked for their relentless drive to stay up through the night to get the job done. Ron Frankel, David Gonski, Dorthea "Bubbles" Nicali, Mark Probst, L. Scott Miller, Julian "Junior" Knisley, Debra Calomiris, William Hanlon, SFC Percy Johnson, and SFC Keith Francis are also acknowledged for the excellent support in designing, fabricating, and assembling the actual RDS unit.

Thanks also go to Hassan Zadeh of UNISYS for equipment support of the RETS.

Dr. Joel Kalb, Pete Peters, and SGT Johnson, of HRED, contributed to the project by helping with the locating portion of the RDS and supporting pretests of the RDS at M-Range.

William E. Baker and Jerry Thomas provided constructive comments and suggestions that aided the statistical analysis of the data.

The AMC-FAST team of Will Johnson, MAJ Craig Langhauser, SFC Randy Hauser, SFC Jeffrey Witas, SFC John Holmes, and SFC David Morris are acknowledged for their support during weapon maintenance, for answering military questions on training and doctrine, for report documentation support, and for putting up with a couple of young engineers with big ideas and little experience in running shows like this.

The authors thank BG Montgomery Meigs for giving us the idea and letting us run with it, BG Baumann and COL Rowan for strongly supporting us, BG John Michitsch for hearing us out and agreeing to help, and SFC Dean Price, SFC Dennis Woods, and SFC Dennis Buck for spending an entire week showing us the 7th ATC, answering all our questions, and giving us their valuable advice. They all contributed much of their time and reputation to stand behind the authors and trust that they would produce in good Army fashion. Without the support of these people, this project would never have even left the ground.

TABLE OF CONTENTS

INTENTIONALLY LEFT BLANK.

LIST OF FIGURES

INTENTIONALLY LEFT BLANK.

LIST OF TABLES

1. INTRODUCTION

The function of the round discrimination system (RDS) is to improve the scoring accuracy of the remote equipment target system (RETS) currently being used for live-fire training at training centers worldwide. The RDS, which interfaces directly with the RETS, discriminates among different main gun kinetic energy (KE), high-explosive antitank (HEAT), and high-explosive incendiary (HEI) and machine gun (ball and tracer) training practice (TP) ammunition from the following armored vehicles: all M1 Abrams series main battle tanks, the M60A3 main battle tank, and the M2/3 Bradley Fighting Vehicle (BFV). This system can determine whether the incoming projectile could produce a kill during live fire exercises.

The RDS program was conducted in three phases. The first phase was a feasibility test. Acoustic signatures of medium- to large-caliber projectiles from the three types of armored vehicles were collected; these signatures were found to have distinct acoustic features, allowing the program to continue. In the second phase, acoustic signatures of the 35-mm tank precision gunnery in-bore device (TPGID) rounds and small-caliber machine gun rounds were collected so that the database could be completed. An algorithm and a brassboard were developed on the acoustic signature discriminants found. The major discriminants used include the duration of the supersonic shock wave, the location of the round relative to the acoustic sensors, and the terminal velocity of the round. In the third phase, verification/validation, a field test was conducted at Aberdeen Proving Ground (APG), MD. A working brassboard correctly discriminated 90% of the rounds fired. Finally, the RDS brassboard was demonstrated as a proof-of-concept to the sponsor, the Seventh Army Training Command (7th ATC) in Grafenwoehr, Germany.

This report summarizes the background material, the round discrimination algorithm, and the current RDS brassboard design. The test data, software development, and system components are mentioned in the discussion.

2. BACKGROUND

2.1 RDS Program. The RDS program was initiated by the Army Materiel Command Field Assistance in Science and Technology Junior (AMC-FAST Jr.) engineers at the U.S. Army Research Laboratory (ARL), in response to a request by the AMC-FAST Science Advisor at the 7th ATC in 1992. The request from the 7th ATC reads as follows: "The 7th ATC requires a target RDS, which identifies the round

location within an area which extends 1 m beyond the target edge and classifies the round type into four band size categories: <20 mm, 20–30 mm, 30–90 mm, and >90 mm." At the very least, the Commander of the 7th ATC wanted a system able to discriminate between projectiles <30 mm (small caliber and BFV main gun projectiles) and >30 mm (M1A1 main gun projectiles) with a per unit (system) cost of around $5k. Table 1 identifies the projectile's group by band and caliber. Several sensor technologies were explored as potential candidates, including acoustics, infrared, radar, and video. The acoustic approach was chosen for two reasons: cost and the ability to exploit the uniqueness of acoustic signatures of armored vehicle rounds.

Table 1. Projectiles Tested

Projectile Caliber (In-bore) (mm)	Projectile Caliber (In-flight) (mm)	Projectile Nomenclature	Projectile Description	Projectile Group by Band (mm)	Projectile Group by Caliber (mm)
7.62	7.82	M59	Ball	<20	7.62
7.62	7.82	M62	Tracer	<20	7.62
12.7	12.95	M33	Ball	<20	12.7
12.7	12.95	M17	Tracer	<20	12.7
25	16.2	M910	TPDS-T	<20	25 KE
25	25	M793	TP-T	20–30	25 HEI
35	35	XM?	TPL-T	30–90	35 TPGID
35	35	DM18	HEAT-TP-T	30–90	35 TPGID
35	35	DM68	HEAT-TP-T	30–90	35 TPGID
105	63.5	M724	TPDS-T	30–90	105/120 KE
120	38	M865	TPCSDS-T	30–90	105/120 KE
105	105	M490	TP-T	>90	105/120 HE
120	120	M831	HEAT-TP-T	>90	105/120 HE

2.2 RETS. The RETS, as seen in Figure 1, uses vibration sensors (also called hit sensors) that are attached to the target and connect to the RETS electronic control unit (ECU). When the sensors detect a hit, the ECU conveys a hit signal to a range control tower via a hardwired or radio link. This activates an electromechanical mechanism that lowers the plywood tank target, thus indicating a kill. A deficiency of the current system is the absence of a mechanism to discriminate between rounds, locate the rounds, and activate the target only in response to those rounds that can produce a kill. A 12.7-mm (.50 cal.) machine gun round, for example, can currently be credited with killing a T-72 tank target. RETS can be

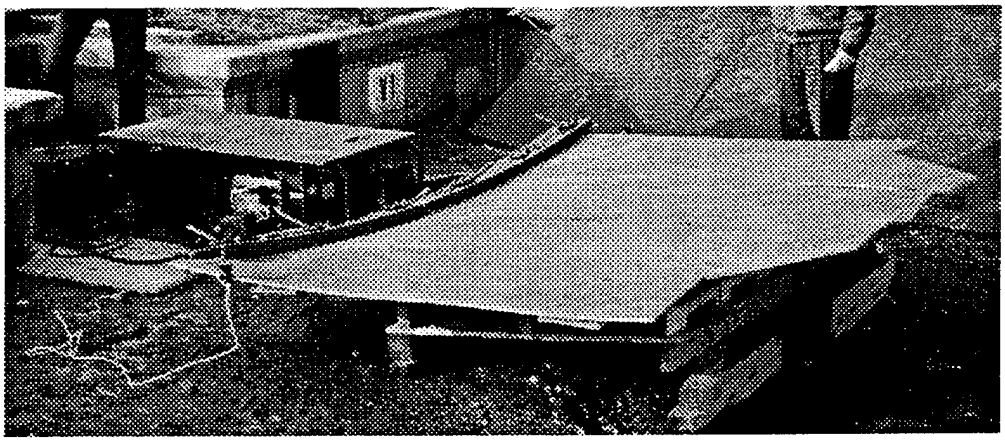

Figure 1. Remote equipment target system.

fooled by debris from ricocheting rounds or by small-caliber machine gun fire onto the target, simulating a main gun round vibration pattern. As a result, armor kills by non-armor-defeating projectiles erroneously inflate the training unit's score. In addition, this deficiency prohibits an accurate after-action evaluation of the trainee's ability to choose the proper ammunition for the mission at hand. The RDS eliminates this deficiency and increases the accuracy of the training process.

3. RDS CONCEPT

An extensive literature search of existing scoring systems and potential signature-producing technologies was undertaken. The techniques investigated included using video cameras, colored tracers, lasers, radar, and acoustics. Many were dismissed due to cost, practicality, or lack of technology. The two most promising concepts recommended by the FAST Jr. team were analysis of acoustical signatures and radar signatures of the passing projectile. Analysis of the radar signature approach was subsequently deemed not feasible due to high cost. It was determined that the simplest and most cost-effective method of discrimination would be an acoustic approach.

In order to explore the feasibility of an acoustic RDS system, a three-test program was proposed that included participants from three ARL directorates—the Weapons Technology Directorate (WTD), the Survivability/Lethality Analysis Directorate (SLAD), and the Sensors, Signatures, Signal and Information (S3I) Processing Directorate. A test matrix was developed to include all possible rounds and engagement distances used on a live-fire gunnery range during a Combined Arms Live-Fire Exercise (CALFEX), as dictated by FM 17-12-1 and FM 23-1. The first part was a feasibility test, where acoustical signature data

were collected and analyzed. The test data were used to determine if acoustic signal discrimination between projectile data at the extreme firing ranges of the 7th ATC interest array were possible. The second part of the program extended the data collection effort for projectile discrimination by collecting data on projectiles within the extremes investigated in part 1. During the third part, a brassboard RDS was constructed and tested at APG. This test included all the projectiles used on the live-fire gunnery range. Subsequent to verification of the brassboard system's ability to discriminate effectively and efficiently, the system was to be demonstrated at the 7th ATC.

The projectiles fired during parts 1 and 2 of the test program are those actually fired on live-fire gunnery ranges and are listed in Table 1. The projectile's in-flight caliber determined its band group. No large-caliber service rounds were considered in the test program due to cost and because they are not used in live-fire training exercises. However, large-caliber service rounds could be added to the acoustic database at a later date.

3.1 Acoustic Round Discrimination Technique.

3.1.1 Background. As a supersonic projectile travels, several shocks from the projectile are propagated to the surrounding air. These shocks are created from the projectile's bow, surface features on the projectile's body, and the tail. A sensitive air pressure gauge placed in the path of the shock waves will register what is typically referred to as the N-Wave. The characteristics of the N-Wave are directly dependent on the geometry of the projectile, the projectile's velocity, the location of the shock origination relative to the pressure gauge, and the condition of the ambient air. Other discontinuous features of the projectile, such as fins or threads, will contribute to additional characteristic features on the N-Wave. Figure 2 graphically depicts the shock cone formed from supersonic projectiles, while Figure 3 shows the characteristic N-Wave pressure profile.

3.1.2 Theory and Formulation. A body traveling through the air faster than the ambient speed of sound will generate a conic shock profile. The shock pressure profile shape is directly dependent on the object's form. Air is compressed against the leading part of the object. Since the object is traveling faster than the time required for the air to re-expand ahead of the object, a conic shock front is generated. A sensitive pressure gauge some distance away from the object's trajectory will register the lead shock as a time-pressure discontinuity. As the body passes, the compressed air expands, and the local pressure

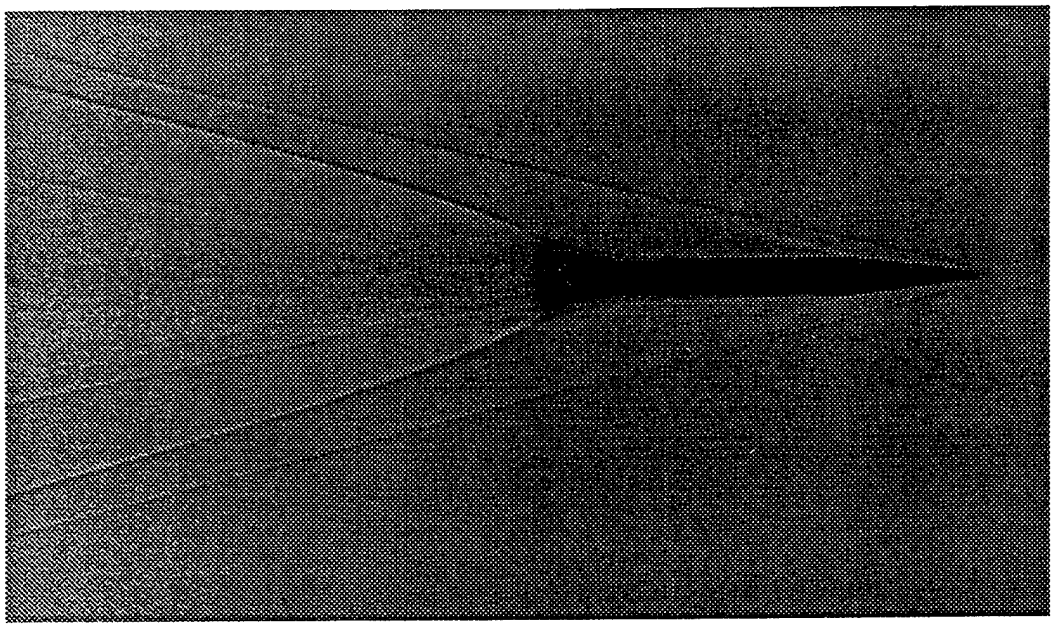

Figure 2. M865 shock cone shadow-shlieren photograph.

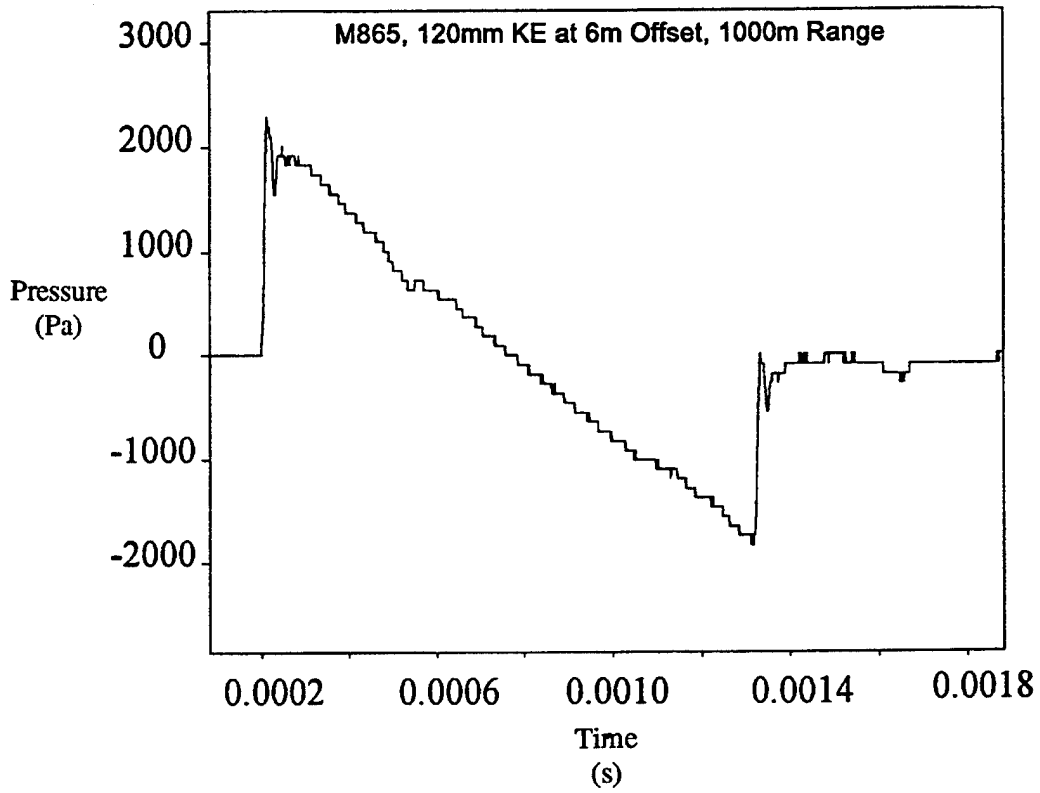

Figure 3. M865 N-Wave pressure profile.

decreases. As surface features on the object create shocks, the profile sensed by the pressure gauge register these as small positive discontinuities. As the local pressure decreases towards the tail of the object, the local pressure reaches a neutral pressure area that is equivalent to the ambient pressure. Pressure aft of the neutral area continues to decrease below ambient. If the object has surface features in the aft region, the shock also appears as positive discontinuities in the pressure profile.

On the tail, the object wake is made to fall back into the area previously occupied by the object. Turbulent eddies are created by the air viscosity interaction with the object surface. These eddies trail into the wake core and support a region of low pressure. As the energy in the eddies dissipates in the wake, the region collapses, showing up as the final shock in the pressure profile. This is called the tail shock, where the low pressure changes to ambient. Other eddies trailing off the object may show up after the tail shock as strong variations in pressure. In some cases, the objects shape could generate second and third generations of low pressure wake cores, resulting in what appears as several tail shocks.

The magnitude, duration, and shape of the N-Wave for an ogive body of revolution, small-caliber shaped projectile, traveling at or faster than the speed of sound, were calculated (Whitham 1952). Expressed for large distances, in general terms, the shock overpressure is,

$$\frac{p}{p_o} = 2^{1/4}\gamma(\gamma+1)^{-1/2}(M^2-1)^{1/8}\left[\int_0^{y} F(y)dy\right]^{1/2} O^{-3/4}, \qquad (1)$$

where

p = overpressure,

p_o = ambient pressure,

γ = ratio of specific heats of air (1.4),

M = Mach number,

y = a characteristic curve relationship between x and O,

x = distance along the axis from the bow,

O = offset distance,

F(y) = a function used to solve the differential equation determining the flow past the body of revolution.

This equation formed the basis of the theory for acoustic round discrimination. By simplifying the generalized results into simple equations (Skochko 1966), one can calculate the pressure and total duration of the N-Wave by:

$$\frac{p}{p_o} \approx \frac{(.53)(M^2-1)^{1/8}}{O^{3/4}}\left(\frac{D}{L^{1/4}}\right)$$

$$T = \frac{(1.82)O^{1/4}M}{a(M^2-1)^{3/8}}\left(\frac{D}{L^{1/4}}\right), \qquad (2)$$

where

a = ambient air speed of sound (meters/second),

D = projectile diameter (meters),

L = projectile length (meters),

T = total duration (seconds).

Theoretically, a properly emplaced sensitive pressure gauge can measure the N-Wave of passing projectiles. Additionally, if the ambient air conditions, the projectile location, and velocity relative to the pressure gauge, were known, the projectile could be identified. A system, constructed to gather data and perform analysis for projectile identification.

3.2 Acoustic Location and Velocity Technique.

3.2.1 Background. Determination of the projectile's location and final velocity was performed with a proven acoustical technique constructed of simple pressure sensitive devices that were linked to a clock. This technology was developed by the ARL Human Research and Engineering Directorate (HRED) for small-caliber projectiles (Kalb, unpublished). Three microphones were arranged in a line in front of a target and placed perpendicular to the projectiles flight path (see Figure 4). It allowed the projectile's location above the microphone array to be determined. On HRED ranges, the projectile and range are known prior to firing, enabling the projectile's velocity to be derived from ballistic firing tables. Three additional microphones were added to the HRED setup to create the RDS microphone setup (see Figure 5). The additional microphones were placed directly in front of the original three microphones, yielding a second location for redundancy in case a microphone was damaged or failed. The two center microphones

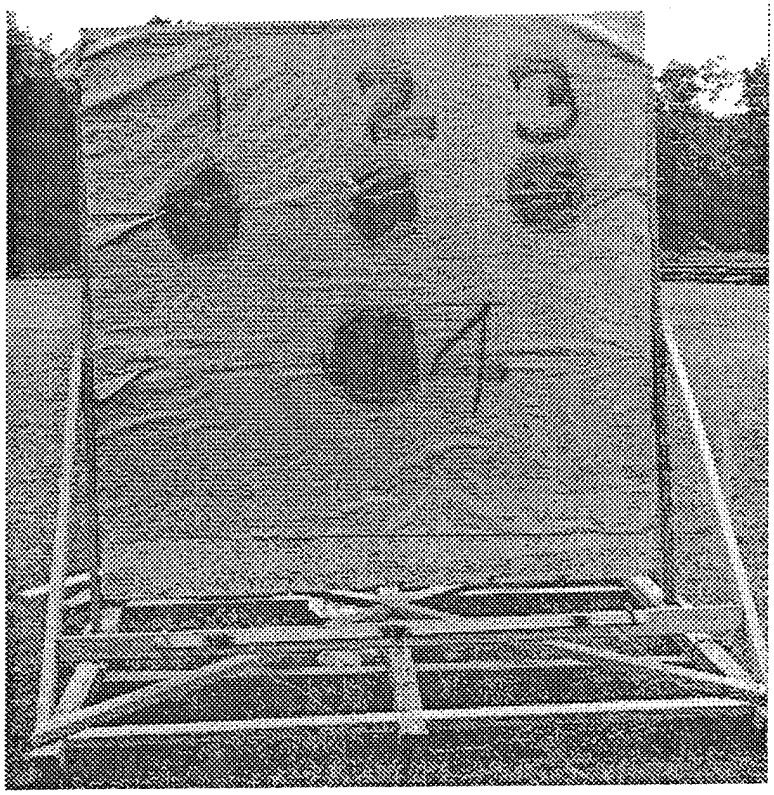

Figure 4. HRED microphone array.

provided the projectile's velocity. Knowing the spatial position of each sensor and measuring the time each was triggered by the passing projectile's supersonic shock wave, one can closely approximate the location and velocity at the target.

3.2.2 Theory and Formulation. The projectile's shock wave can be visualized as an infinite cone traveling with the projectile. The ambient speed of sound and the projectile's velocity result in the classic shock angle expression:

$$\alpha = \sin^{-1}\left(\frac{a}{v}\right) = \sin^{-1}\left(\frac{1}{M}\right), \quad M = \frac{v}{a}, \tag{3}$$

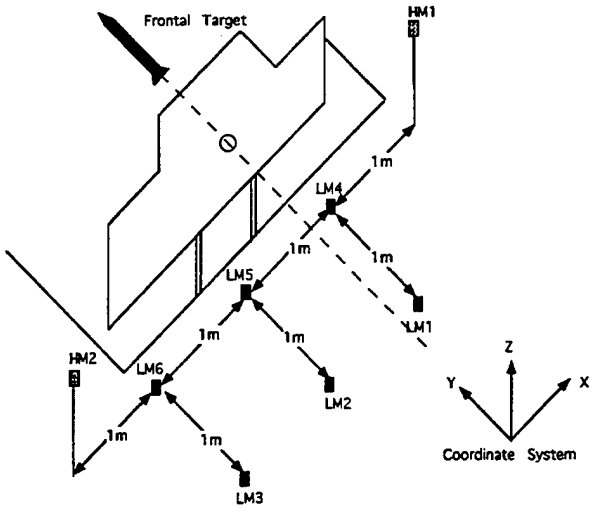

Figure 5. Microphone array and target setup.

where

α = shock angle (°)

M = Mach number,

v = projectile velocity (meters/second),

a = ambient speed of sound (meters/second).

This relationship assumes that the cone form is maintained, subsequent to its time of arrival, throughout the distance of the shock wave propagation.

The projectile is assumed to be traveling parallel to the Y-axis striking the target at coordinates (X,Y,Z). Microphones 1, 2, and 3 are placed in the front right, front center, and front left, respectively. Microphones 4, 5, and 6 are placed in the back right, back center, and back left. These location microphones (LM) are referred to as LM1–LM6. The microphone centers for microphones 1–6 are located at (X+1, Y,Z), (X,Y,Z), (X-1,Y,Z), (X+1,Y+1,Z), (X, Y+1,Z), and (X-1,Y+1,Z), respectively. Figure 5 shows the microphone placement relative to the target and the coordinate system used.

On the arrival of the shock cone at each microphone, a total of five time differences (T_1,T_2,T_3,T_4, and T_5) are recorded. Two time differences are needed for each location array and one time difference for the velocity determination. T_1–T_5 are defined as follows:

T_1 = Time difference between LM2 and LM1,
T_2 = Time difference between LM3 and LM2,
T_3 = Time difference between LM5 and LM2,
T_4 = Time difference between LM5 and LM4,
T_5 = Time difference between LM6 and LM5.

The time differences T_1 and T_2 are measured from a moving sound source and can be related to a hypothetical source that originates from a point in a vertical plane defined by LM1, LM2, and LM3. The transformed time difference from each microphone pair defines a hyperbola of ambiguity, which is the set of all point sources which produce this same arrival time difference. The intersection of these hyperbolas locates the point source through which the projectile traveled (X,Z). Figure 6 is an example of the hyperbolas of ambiguity.

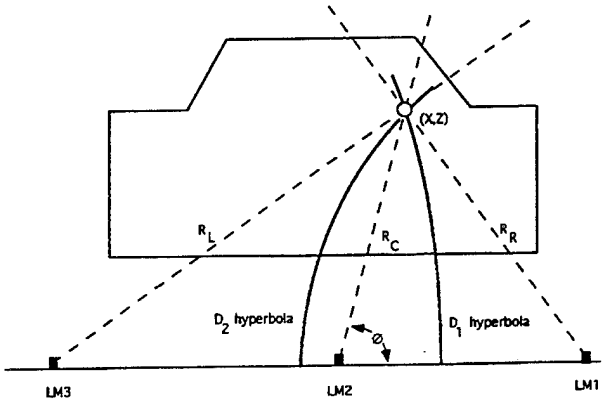

Figure 6. Projectile location by intersection of hyperbolas of ambiguity.

The altered difference in arrival time between the center and right microphone pair, D_1, can be determined from the following equation:

$$D_1 = \frac{(R_C - R_R)}{a} = \frac{T_1}{\cos(\alpha)}, \quad (4)$$

where

R_C = in-plane distance from center microphone to projectile location (meters),

R_R = in-plane distance from right microphone to projectile location (meters),

and the difference in arrival time between the left and center microphone pair, D_2, is:

$$D_2 = \frac{(R_L - R_C)}{a} = \frac{T_2}{\cos(\alpha)}, \tag{5}$$

where

R_L = in-plane distance from left microphone to projectile location (meters).

It is useful to note that a positive time indicates that the source is to the right of the midpoint of a microphone pair and that a negative time indicates that the source is to the left.

The sound source location is related to the microphone positions by using the law of cosines. On the right side triangle:

$$R_R^2 = R_C^2 + A^2 - 2R_C A\cos\theta = (R_C - aD_1)^2 = R_C^2 - 2R_C aD_1 + a^2 D_1^2, \tag{6}$$

where

A = microphone separation distance (1 m),

θ = angle from microphone array axis to R_C.

Similarly for the left side triangle:

$$R_L^2 = R_C^2 + A^2 - 2R_C A\cos(\pi-\theta) = (R_C + aD_2)^2 = R_C^2 + 2R_C aD_2 + a^2 D_2^2, \tag{7}$$

where $\cos(\pi - \theta) = -\cos(\theta)$.

Subtracting equation 6 from 7 yields:

$$4R_C A\cos\theta = 2R_C a(D_2+D_1) + a^2(D_2^2-D_1^2). \tag{8}$$

From geometry, the offset distance of the projectile from the center microphone is:

$$R_C = \sqrt{Z^2 + X^2}\ . \tag{9}$$

Solving equations 8 and 9 for Z yields:

$$Z = R_C\cos\theta = a(D_2+D_1)\left(\frac{R_C + \frac{a(D_2 - D_1)}{2}}{2A}\right). \tag{10}$$

Rearranging equation 9 for X yields:

$$X = \sqrt{R_C^2 - Z^2}\ . \tag{11}$$

The projectile location for microphones 4, 5, and 6 can be solved using the same equations with the substitution of D_4 and D_5.

Knowing that the position of the microphones are fixed and the projectile is assumed to be perpendicular to the array, one can approximate the velocity. The velocity is determined by taking the difference in position of the center microphones and dividing by the difference in arrival times of the center microphones.

$$v_P = \frac{\left(Y_{LM2} - Y_{LM5}\right)}{T_5}, \tag{12}$$

where

V_P = predicted projectile velocity (meters/second),

Y_{LM2} = y position of LM2 (meters),

Y_{LM5} = y position of LM5 (meters).

3.2.3 Alternate Acoustic Location and Velocity Technique. Another location and velocity prediction algorithm based on microphone detection of supersonic shock waves was developed and used on Yuma Proving Ground (YPG) test ranges (Stallings 1992). Stallings' technique does not require any special microphone placement. The only requirement to locate projectiles and determine velocity is to have at least 4 noncoplanar microphones. Three of the microphones form a triangle in the target plane, and the other microphone is placed in front of the others. Generally, the more microphones used, the better the location accuracy that can be provided. Better location accuracy is also accomplished when the microphones lie close to the target plane and the hits lie in or near the center of the microphone array. The input variables for accurate round location are meteorological data (to include temperature, humidity, wind speed, and wind direction), a velocity estimate, fall angle estimate, target position, gun position, microphone positions, and microphone trigger times. Location errors magnify when input values are not precisely known. Stallings showed, through YPG tests, that errors as small as 2–3 cm are common.

Stallings' technique first assumes that the projectile hits the target at the center of mass. The theoretical times that the shock wave was detected by each microphone are then calculated. The actual microphone times are compared to the calculated times. The output variables, projectile location, and velocity are incrementally adjusted around the initial guess until the difference between calculated and actual times is within a predetermined tolerance. This is a time-intensive algorithm that converges to the solution in approximately 30 s on a fast personal computer. The algorithm could be optimized to reduce inefficiencies in the program. There are two iterative nested processes within the algorithm. Stallings believes that one of these can be eliminated to accelerate the program.

The Stallings algorithm cannot predict location in real time. Real time results are essential for proper integration with RETS. Since this technique was developed for test ranges, many of the input variables are known to a large accuracy at the testing range. There is no knowledge of the gun firing position on the training range. For the purpose of RDS, the gun position represents the greatest source of error for this technique and would significantly impact scoring accuracy.

4. LIVE-FIRE TESTING

A series of live-fire tests was designed to investigate the hypothesis that acoustic signatures could be used to discriminate round types. The smallest and largest projectiles within the test matrix were selected for the initial test of the feasibility of the hypothesis. The logic was that if the data obtained during the initial testing showed that the characteristics of the respective N-Waves permitted discrimination between the projectile extremes, then, and only then, would a second live-fire test be conducted. The second live-fire test would be a data collection effort to compile the N-Wave data of the remaining projectiles at different intervals of velocity. Once the data were collected and analyzed, an algorithm would be developed to produce round discrimination. Subsequently, the algorithm would be integrated with a computer/breadboard. A third live-fire test would be conducted to validate the algorithm and the RDS breadboard's performance. Needless to say, the success of this last test series was highly dependent on the results obtained within the feasibility and data collection tests.

These tests were formally described as the feasibility test, data collection test, and verification/validation test. The breakdown of rounds and ranges used within each test series is given in Table 2.

The data collected during the first two parts of the live-fire program were used to standardize the method of collecting the N-Wave data and the specific parameters used in the N-Wave calculation. To increase the amount of data acquired, several sensors were used for each shot. The parameters considered for the N-Wave calculations were: ambient air temperature, projectile velocity, caliber, length, and offset distance. Each live-fire test setup consisted of a fixed reference target and five high-fidelity microphones arranged such that the projected distance form the target center was 1, 3, 6, 9, and 12 m, respectively, to the microphones. Each projectile hit on the target was scored using a video scoring system, and the offset distance from the projectile to the microphones was calculated, generating one parameter for consideration. The projectile's velocity was measured with a Weibel radar system, designed specifically for projectile velocity measurement. The dimensions of each round were known, and meteorological data were measured.

To ensure that there was no unintentional biasing of the data, the order of fire was randomized to the extent practical. Theoretically, if an experiment involving different round types is conducted, the test

Table 2. Proposed Round and Firing Range Breakdown for Each Test

Test Type	Round Type	Range (m)		
Feasibility	120-mm M865	400		2,500
	120-mm M831	400		2,500
	105-mm M724	400		2,500
	105-mm M490	400		2,500
	25-mm M910	400		2,000
	25-mm M793	400		2,000
Data Collection	120-mm M865		1,250	
	120-mm M831		1,250	
	105-mm M724		1,250	
	105-mm M490		1,250	
	35-mm DM18	400	1,250	
	35-mm DM68	400	1,250	
	25-mm M910		1,250	2,500
	25-mm M793		1,250	2,500
	12.7-mm M33	400	900	
	7.62-mm M59	400	900	
Verification/Validation	120-mm M865			
	120-mm M831			
	105-mm M724			
	105-mm M490			
	35-mm DM18			
	35-mm DM68			
	25-mm M910	TBD[a]		
	25-mm M793			
	12.7-mm M33			
	7.62-mm M59			

[a] To be determined.

conditions should be identical for all round types so that the round differences can be detected. Since reality dictates that the process of extracting data is never the same each time, randomization reduces the average effect of any irrelevant factors, and the errors in the response are independently and randomly distributed over the population. Conversely, if rounds are systematically tested, i.e., all of a particular round are tested at one time, then the true response of that round cannot be separated from the extraneous factors such as weather conditions that contributed to the response.

4.1 Feasibility Test. The first part of the live-fire program was intended to be a small effort. Originally, the 120-mm HEAT and KE training projectiles were scheduled to be fired at the closest and farthest engagement distances, and the data were compared to the 25-mm armor-piercing (AP) and HE training projectiles at their extreme engagement distances. The extremes of the test matrix were designed to envelop the velocity expected in real use. According to the simplified N-Wave calculations, the N-Wave pressure and time duration produced from the largest projectile at its slowest velocity, far from the microphone, was expected to approach the N-Wave pressure and time duration of the smallest projectile at its fastest velocity, close to the microphone. If the round type of these two projectiles could be discriminated, round discrimination using N-Wave data would be considered feasible.

4.1.1 Test Purpose. The purpose of this test was to determine if the N-Wave data collected with a particular configuration of high-fidelity microphones could be used to discriminate the round types fired. The largest projectile, the 120-mm M831, at its slowest velocity was to be compared to the 25-mm M910 at its fastest velocity. If the N-Wave data from the same offset distance were separable, then these N-Waves of supersonic projectiles could be used to perform round discrimination at the target.

Due to the extremely high operational cost of M1/M1A1 tanks, and the prospect of incurring prohibitively high maintenance costs at the turn of the fiscal year, it was decided to advance a portion of the data collection effort into the feasibility study. Consequently, all 120-mm, 105-mm, and 25-mm projectiles were fired during the feasibility test. The 120-mm rounds were fired from an M1A1 Abrams tank, the 105-mm projectiles were fired from a M60A3 tank, and all the 25-mm rounds were fired from an M2 BFV. Table 3 describes the actual rounds fired during the feasibility test. With the modification of the test schedule, the sample set increased by 50% and would provide better parameter estimates in the statistical analysis for this phase of the test program.

Table 3. Actual Round and Firing Range Breakdown for the Feasibility Test

Round Type	Range (m)		
120-mm M865	400	1,000	1,700
120-mm M831	400	1,000	1,700
25-mm M910	400	1,000	1,400
25-mm M793	400	1,000	1,400
105-mm M724	400	1,000	1,700
105-mm M490	400	1,000	1,700

4.1.2 N-Wave Characteristics. The acoustic signature for each projectile was studied specifically for seven different characteristics. These were positive peak pressure, negative peak pressure, positive phase duration, negative phase duration, total duration, peak net pressure impulse, and peak absolute pressure impulse. The variables are illustrated in Figure 7. The data were compared to N-Wave formulas and analyzed using advanced statistical methods. Shadowgraphs of the projectiles in midflight from previous tests were compared to the N-Wave data to relate the signature features to the surface features of the projectiles. This comparison helped determine if certain N-Wave features were truly dependent on the projectile geometry or were the results of an environmental influence, such as a ground reflection.

The seven characteristics of the acoustic signature were essential to the N-Wave data comparisons. The N-Wave formulae were used as a theoretical guide to help test the hypothesis of round discrimination. The real N-Wave data were used to empirically refine the N-Wave formulae. These formulae provided an engineering basis for the round discrimination algorithm used on the breadboard.

4.1.3 Data Acquisition and Reduction. The data acquisition system consisted of two systems for recording and one system for sensing. The sensors were high-fidelity microphones able to operate in the range of overpressures encountered. These sensors were high-value items and were not intended as an all-weather solution to a fielded RDS. The priority lay in obtaining high-fidelity signals to accurately record the N-Wave phenomenon. The N-Wave data from several projectiles, at several offset distances, traveling at various velocities, had to be studied and analyzed. The two recording systems served a dual purpose. Each system had a specific deficiency—poor resolution in either time or voltage levels. Each was able to complement the other in that respect. The secondary purpose was to provide a backup recording system in the event of a malfunction during the live-fire test.

Reduction of the data was performed on a personal computer (PC). The data from each channel were converted into ASCII files. These files were read into a data processing program called DADisp (DSP Development Corporation 1991). This software had the capability to read the data, convert them into engineering units, and perform a series of calculations. Among those were the calculation of net pressure impulse and absolute pressure impulse. Along with these calculations and plots, DADisp helped to determine the pressure peaks and durations. At times, the signals were clipped. In an effort to maximize the resolution in the ordinate, the recording window was set as small as possible. At times, the recording devices were preset on low. As a result, hard data on the maximum levels were lost. DADisp software helped curve-fit the peaks, restoring the data with at least ±10% accuracy.

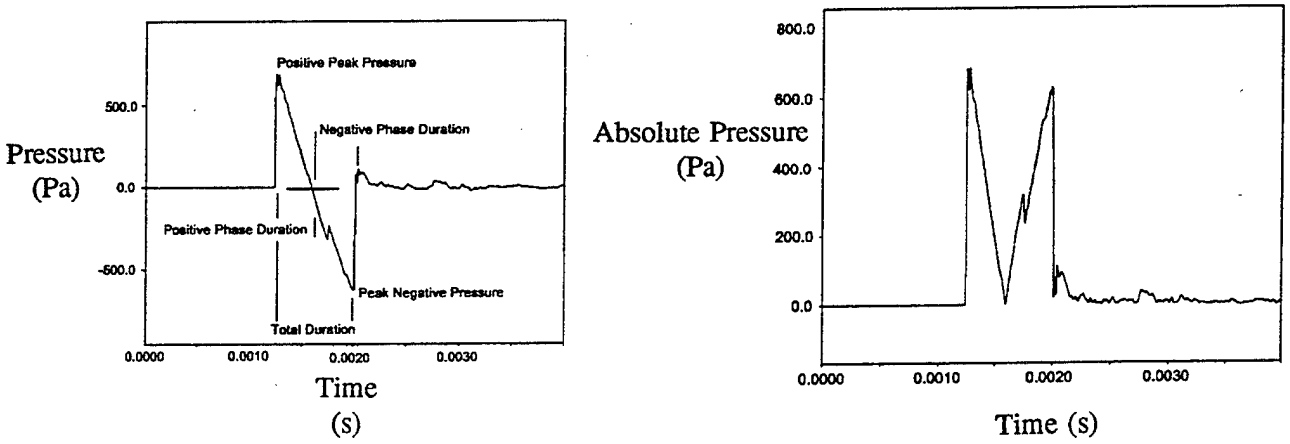

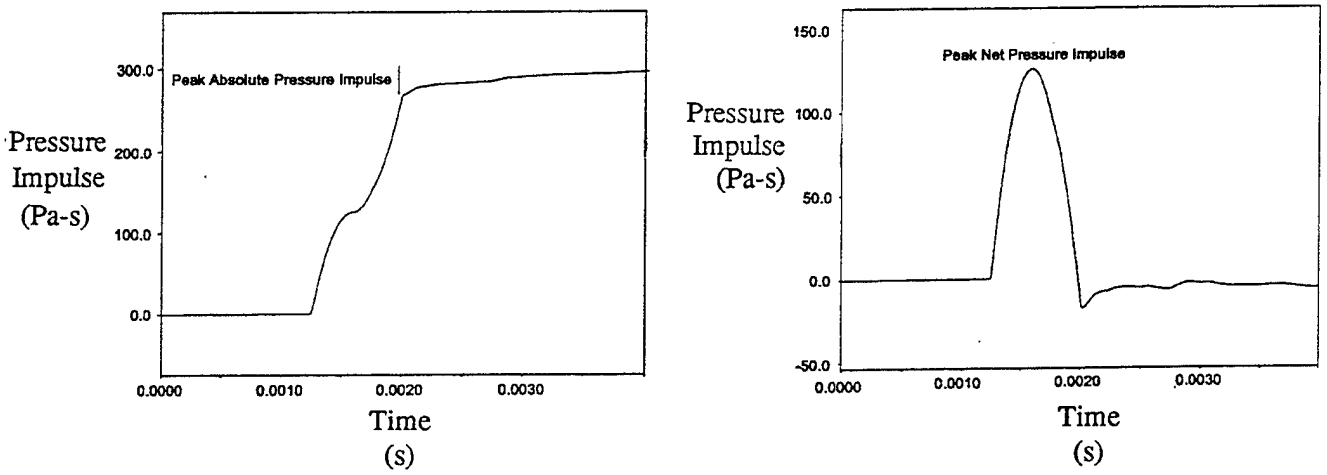

Figure 7. Seven parametric features of the N-Wave.

4.1.4 Instrumentation. B&K microphones are high-grade laboratory instruments with the following specifications: sensitivity of -56-dB sound pressure level (SPL), flat frequency response from less than 5 Hz to 50 kHz, and dynamic range up to 178 dB SPL with 3% distortion. Each B&K microphone unit is comprised of a type 4136 1/4-in microphone, a type 2639 preamplifier, and a type 2801 AC or a type 2804 DC power supply. The cost per unit is $3.5k–$4k in small quantities.

The outputs of the microphones were connected by 150-ft BNC cables to three TEAC digital audio tape (DAT) recorders and a Hewlett-Packard (HP) digital oscilloscope, model no. HP 54112D, controlled by a PC located behind a berm. The three DAT recorders had a total of six wide-band channels (two channels per DAT) with 48-kHz sampling rate and 14-bit resolution per channel. The HP digital oscilloscope had four input channels with 1-MHz sampling rate per channel and 8-bit resolution per channel. The PC communicated with the oscilloscope through the IEEE port. A data acquisition program written in C language was developed to automatically dump 64 kB of data per channel onto the PC's hard disk when the scope was triggered and to reset the scope to wait for the next trigger. Both types of recording instruments were used to provide both time resolution and amplitude resolution.

4.1.5 Acoustic Signatures. Live-fire tests were conducted at the H-field facility at APG, Edgewood Area (EA). Data collected during the feasibility test are summarized in Appendix A. The target was positioned up on top of a berm at the end of the field. The firing platform was moved to each firing station. After some calibration rounds were fired, the testing for each projectile type was performed. A cursory look at the data, while still on the field, indicated that the signals for each round type was distinct. Qualitatively, it was surmised that round discrimination was feasible. A subsequent closer look, within the laboratory confirmed this fact, quantitatively, and is discussed in section 5.

The M831 and M490 rounds possessed distinctly different N-Wave shapes. The M490 round produced the classic N-Wave, as seen in Figure 8, while the M831 round had several interval shocks on the negative phase of the N-Wave. As the offset distance varied, the level and occurrence of the shocks changed. This indicated that the shock was produced from a surface feature and was merging with the tail shock. The time relation of shock travel and the distance to the ground disputed the idea that it was a ground reflection (Ritzel and Gottlieb 1982). These observations were distinct to the M831 round and not the M865.

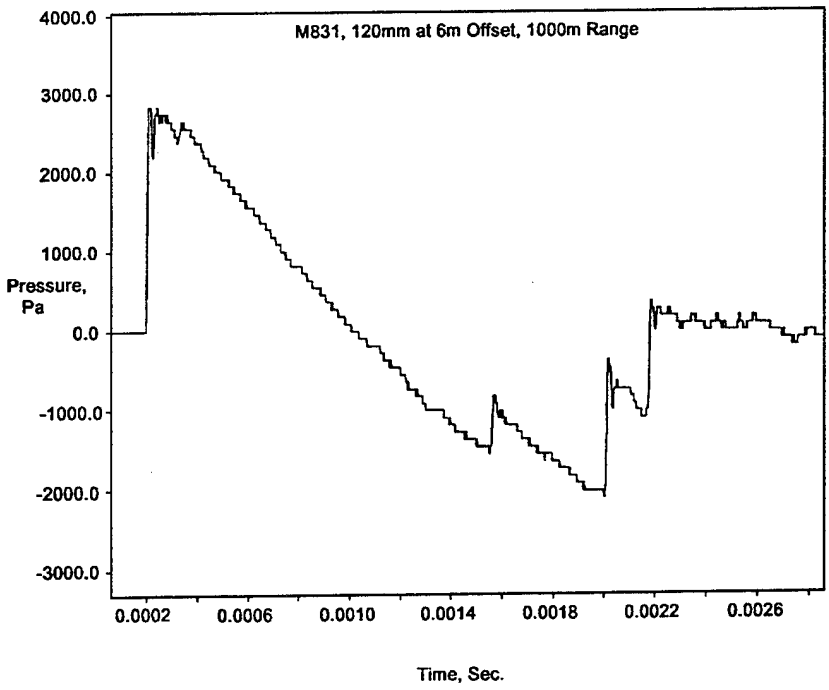

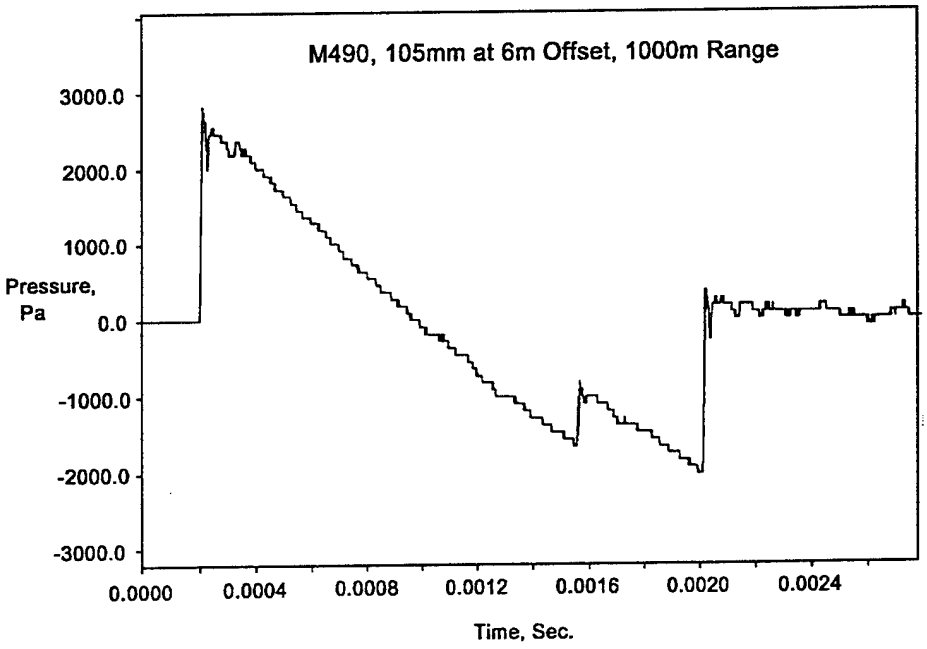

Figure 8. M831 and M490 comparisons.

It was speculated that these pressure differences are due to shock interaction with the fins, and the nonogival geometry of the M831 round. The M831 round has the stand-off fuse and the concave taper to the body, as opposed to the convex taper of the ogive. The body slims down aft of the body for aerodynamic flight. The bottle nose feature may create a separation, causing a shock, unless it is isentropically ramped. If the surface aft of the body turning away from the flow is of sufficient gradient, another separation would occur, creating more shocks. A detailed summary of the resultant data is included in Appendix B. Figure 9 shows the same comparison between the M793 and M910 fired from a BFV. The slimmer AP rounds shows the classic N-Wave while the HE round has the secondary tail shock.

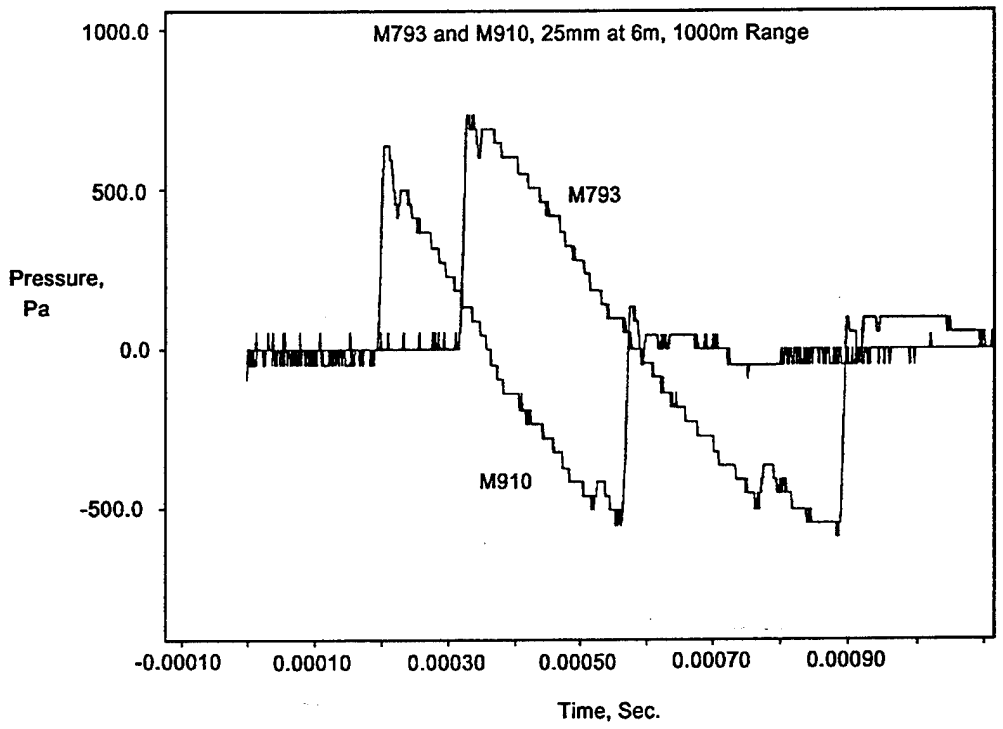

Figure 9. M793 and M910 signature comparisons.

4.1.6 Round Location and Velocity Determination Data. The RDS acoustic location system consisted of six electret microphones. Each microphone was connected so that it acted as a variable resistor when exposed to sound. In response to the acoustic shock wave, the current in the microphone wires increased.

The current was converted to a voltage signal by a signal conditioning card. The six pulses were recorded on two DATs. LM1, LM2, and LM3 were recorded on DAT 1, and LM4, LM5, LM6, and LM2 were recorded on DAT 2. LM2 was recorded on both DATs so that all six microphone trigger times could be related to one time base. The DAT clock was synchronized to the Weibel radar clock. Each channel was played back through a Nicolet digital oscilloscope and manually reduced for the time passed until shock detection (see Appendix C). The accuracy of these times was within ±21 μs. The time difference pulses T_1–T_5 were then calculated.

4.2 Data Collection Test. The result of the feasibility test suggested that round discrimination using acoustic signatures was possible and the data collection test should proceed. The ammunition used in the data collection test is shown in Table 4. This portion of the project was originally intended to be the major data collection effort. However, since all of the main gun data needed for the M60A3, M1/A1, and M2 were collected during the feasibility test, all that remained were the TPGID and small arms.

Table 4. Actual Breakdown of Rounds and Ranges for Data Collection Test

Round Type	Range (m)		
35-mm DM18	400	1,000	1,700
35-mm DM68	400	1,000	1,700
35-mm TPL-T	400	1,000	1,400
12.7-mm M33	400	1,000	
12.7-mm M17	400	1,000	
7.62-mm M59	400	600	800
7.62-mm M62	400	600	800

The small arms ammunition used on a training range is either ball or tracer. The tracer ammunition was studied as an independent round type since the effect of the tracer was postulated to have an effect on the N-Wave. It was theorized that the pyrotechnic material would increase the duration since it would add energy to the wake. The degree of effect was pure conjecture. Only one type of 35-mm TPGID was supposed to be tested. Before the data collection test occurred, two new types of TPGID rounds, DM68 and the TPL-T, were obtained for testing. These were surplus obtained from a lot which had just undergone proof-testing with the U.S. Army's Combat Systems Test Activity (CSTA). These rounds were tested independently of the DM18. Their diameter and length were unchanged, but the surface features

were different. The DM68 and the TPL-T have a sharp pointed cone attached to a cylinder body, as opposed to the DM18, which has an ogive shape. It was speculated that there would be a slight change in the N-Wave but that the change would not be significant.

The purpose of the data collection test was to complete the database of projectile signatures expected on a U.S. Army training range. These signatures were needed to develop the RDS algorithm and form the basis of all assumptions and work. Once the data were collected and reduced, a major milestone in the project would have been reached.

To perform the test, an M1A1 Abrams tank was needed to fire the TPGID ammunition. A Mann barrel, a device constructed for precise single-shot testing of small arms ammunition, was used to perform the 7.62-mm and 12.7-mm shots. The Mann barrel consisted of a towed gun carriage and two barrel assemblies, one for each caliber.

The effort to field a calibrated pressure sensor was deemed impractical after considering the number of sensors needed to cover all the U.S. Army live-fire gunnery ranges. This made any parameter not dependent on the pressure levels very attractive. The total duration was one parameter that seemed to be most consistent, and discriminating. The same seven variables examined in the feasibility test were studied in the data collection effort, in the likelihood that the total duration failed as a discriminator with inclusion of the additional data.

The same two recording systems used during the feasibility test were employed for the data collection test. A third recorder was added. This was a digital transient data recorder card mounted in a PC. It had 12-bit resolution in the ordinate, with a 250-kHz sampling rate. This was deemed sufficient response for the 7.62-mm rounds. The resultant plots were much smoother in appearance, and the accuracy of the data was enhanced.

Five B&K high-fidelity microphones were set up at 1 m, 3 m, 6 m, 9 m, and 12 m, respectively, to the left of the bull's-eye in front of the target. In addition, three low-cost ($150.00 each) high-fidelity microphones from Countryman were set up next to the B&K microphones at 3 m, 6 m, and 9 m. The Countryman microphones were much more ruggedized and rain resistant than the B&Ks.

A new data collection system was used. The system consisted of a 486 Extended Industry Standard Architecture (EISA) computer, two four-channel 1-MHz EISA data acquisition cards, and a graphical programming software tool called LabView for Windows. The system emulated an eight-channel high-speed (250 kHz per channel) digital oscilloscope with the programming capabilities of a PC. The acoustic signatures of the microphones were automatically captured and displayed on the monitor, scaled, truncated, and stored on the hard disk after each tank round was fired. This new system greatly reduced the data processing and reduction time. The same four-channel 1-MHz HP digital oscilloscope was used as a backup system.

Post-test data analysis showed that the Countryman microphones did not have the 65-dB dynamic range necessary to capture the supersonic shock wave of large projectiles. For small rounds such as 12.7 mm and the 7.62 mm, the Countryman microphones responded well.

A second series of live-fire tests was also conducted at H-Field facility at the APG, EA. Data from these tests are compiled in Appendix D. The same equipment used during the feasibility test was employed during the data collection test. The target was positioned on top of the same berm used during the feasibility tests. The firing platforms were moved to specific firing stations. After some calibration rounds were fired, the testing for each projectile type was performed. An immediate look at the data on the field indicated that the signals for the small-caliber rounds were different from the main gun rounds. This observation was subsequently verified during the detailed analysis.

The bulk of the data considered was from the transient data recorders. The resolution in the abscissa and ordinate made the data optimal when performing data reduction. Figure 10 shows the typical plot of a 35-mm DM18 projectile raw data, fired from 1,700 m at the 9-m offset distance.* See Appendix E for details. Appendix F summarizes the microphone positions and associated shock detection times.

*The N-wave appears upside down because the signal from the microphone was increased by an inverting amplifier.

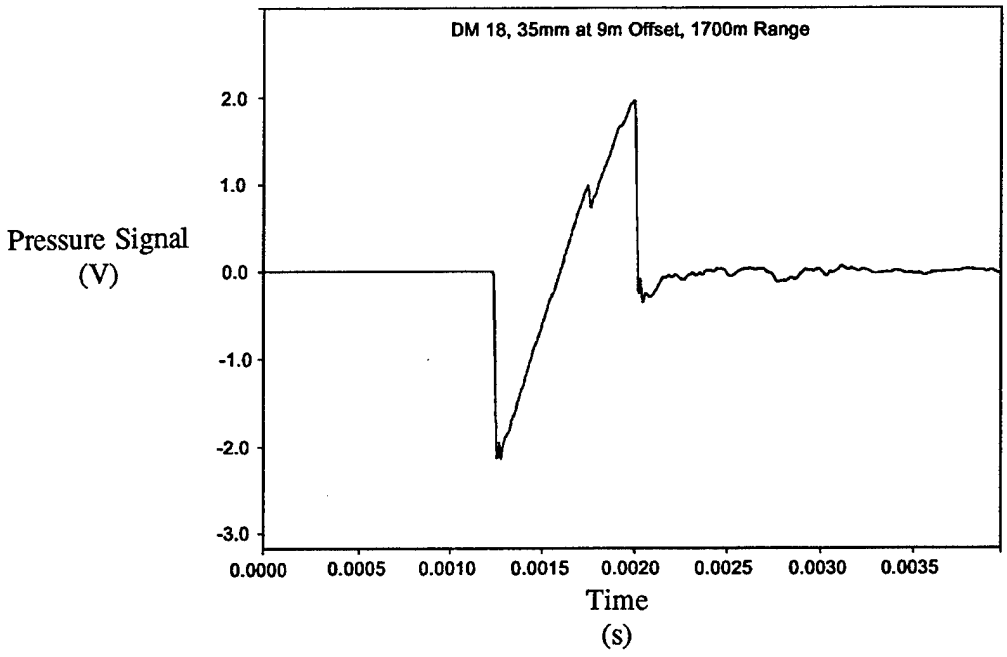

Figure 10. Raw data of 35-mm DM18 at 9-m offset, fired from 1,700 m.

5. ANALYSIS OF LIVE-FIRE DATA

The live-fire data was analyzed using two distinct approaches. The first was an engineering approach, based on Whithams formula, that described a mathematical model which related the physical properties and events. This model was thought to be adequate for predicting occurrences within and beyond the test matrix. The second approach used advanced statistical analysis. By analyzing the data on the variables, a empirical model was constructed to predict within the test matrix.

5.1 Variables Investigated. The seven variables investigated were as follows: positive peak pressure, negative peak pressure, positive phase duration, negative phase duration, total duration, peak net pressure impulse, and peak absolute pressure impulse. It was hypothesized that the positive peak pressure and negative peak pressure generated from the main gun rounds would be so much stronger than the BFV rounds that merely sensing the levels would provide discrimination. Subsequent calculations negated this hypothesis. A small round close to the sensor would appear stronger than a large round far from the sensor. The drop in peak pressure with distance was estimated to be roughly to the power of 1/5th.

The predictions of time durations were greatly varied over round type. According to the time duration formula, the total duration is strongly related to the diameter of the projectile. Since the rounds all have distinct diameters, and the other variables of the time duration formula can be quantified, time duration should be a pronounced discriminator. Time duration does not require any calibration. All that is needed is an accurate, high-speed clock. The intervals of positive and negative pressure phase time durations can also be used to identify the originator of an N-Wave.

There was much speculation that the environment would significantly influence the variables mentioned. The temperature of the ambient air, humidity, air density, wind, and dust were thought to be capable of distorting the perfect N-Wave such that the N-Wave of a small round fired on a cold day at sea level might appear the same as a large projectile N-Wave fired at high altitude on a hot day. To attempt to evaluate the N-Wave, a measure of the energy imparted to the atmosphere was used. The total duration pressure impulse is simply the integral of the entire N-Wave pressure curve. The value of the pressure impulse at some point in time along the N-Wave is the net value of energy contributed to the local environment. As the projectile flies through space, the KE is transferred by the viscous effects of the surrounding fluid. The majority of the energy transfer is performed in the nearly isentropic compression of the local air, thus the bow and tail shock. A small percentage of the energy is consumed in viscous losses, such as the trailing wake eddies, flow separation, friction heating of the projectile, and the losses incurred by a not perfectly isentropic compression of the air.

The total duration pressure impulse shows the entire amount of net energy imparted to the surrounding fluid. The negative value at the end of the total duration pressure impulse curve is due to energy loss to the surrounding fluid. The projectile passes through a point in space and momentarily displaces the air. The energy transferred to the nearly isentropic bow shock radiates from the bow. The air moves a little, but the energy in the shock travels at the local speed of sound. As the projectile passes, the local energy state of the air returns to the original level, plus any energy imparted to it by projectile kinetic losses. The air shocks back into the wake as the wake eddies dissipate energy and collapse. This marks the end of the energy transference. The net effect is a negative value. The value should be approximately equal to the losses imparted to the air, which result in local heating of the air.

The peak value of the total duration pressure impulse curve demonstrates the total duration energy transferred from the travelling projectile to the local air, at that instant in time. The energy transfer of the projectile is strictly a function of speed and projectile shape. Ambient air conditions have a negligible

effect on this value. As a result, a projectile could be discriminated by this feature without regard to the environmental conditions. Another method of using this variable is to consider the absolute contribution of energy transference.

The absolute pressure impulse is taken when considering all the values of the N-Wave as positive only. In this manner, the absolute total duration of energy transfer is considered. This works such that any losses in the projectile's flight are included into this value and can further separate the groups of projectiles for discrimination.

Three different engineering methods of analyzing the data were pursued. The first method was the use of the seven variables in conjunction with the time duration and the overpressure formulations. This method would provide the discriminant algorithm with a theoretically derived mathematical model that employed thermodynamic relationships. This model could be used to discriminate rounds if the live-fire data matched the calculated results. If not, a modification of this formulation could be performed, resulting in quasi-empirical formulation.

The other two methods were similar to each other in process. A Fourier transform of the data could produce key frequency features that could be used to discriminate the projectiles. Another method of transfer analysis is called Wavelet analysis. Using this method, the signal is transferred into the domain of a discrete function, rather than the continuous function of the frequency domain. By picking a discrete function, the signal is transferred by taking the convolution integral. This method works if there is a specific shape to each N-Wave when normalized in the abscissa and ordinate.

The results from the live-fire data collection efforts were N-Waves that were extremely similar in shape. The Wavelet theory would not work since the normalized shape of the N-Waves were so closely matched. A Fourier analysis was initially performed (Hulet 1992), showing extremely promising results (see Figures 11–14). The peak frequency for the 12.7 mm was 3.58 kHz; the 7.62 mm was 4.15 kHz. Unfortunately the data had undergone some smoothing process, and the resulting Fourier analysis yielded artificial suppressing frequency peaks. When the ARL live-fire data were transformed, the results did not yield adequate discriminants. The Fourier transform was shown to relate only to the duration intervals.

Since the durations were strongly related to a rounds specific dimensions and the transformation techniques were clearly influenced by the durations, the time duration formula was selected as the best

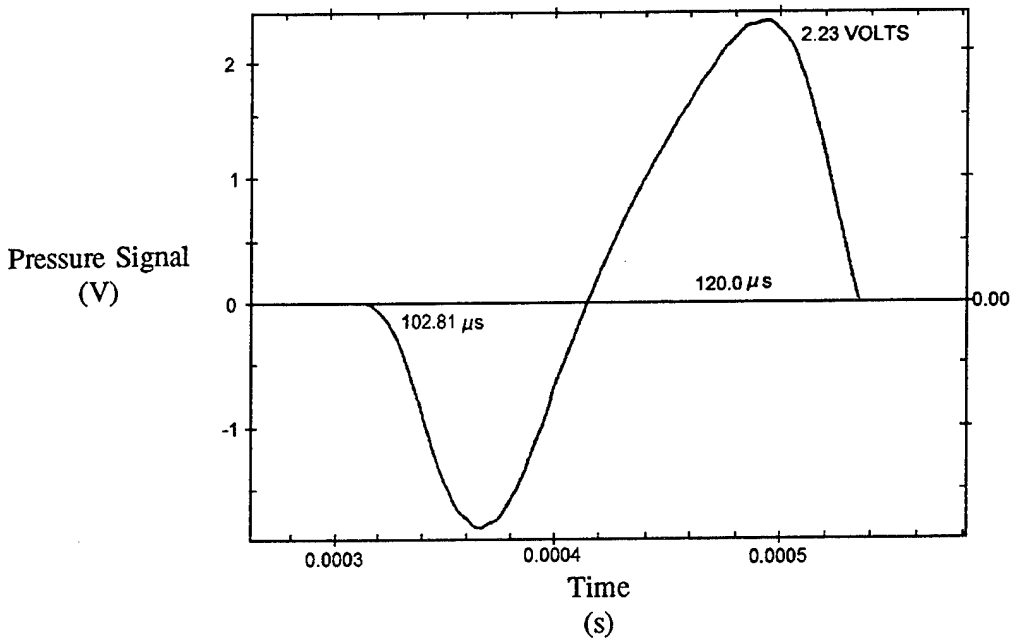

Figure 11. 7.62-mm projectile at 1,500 m.

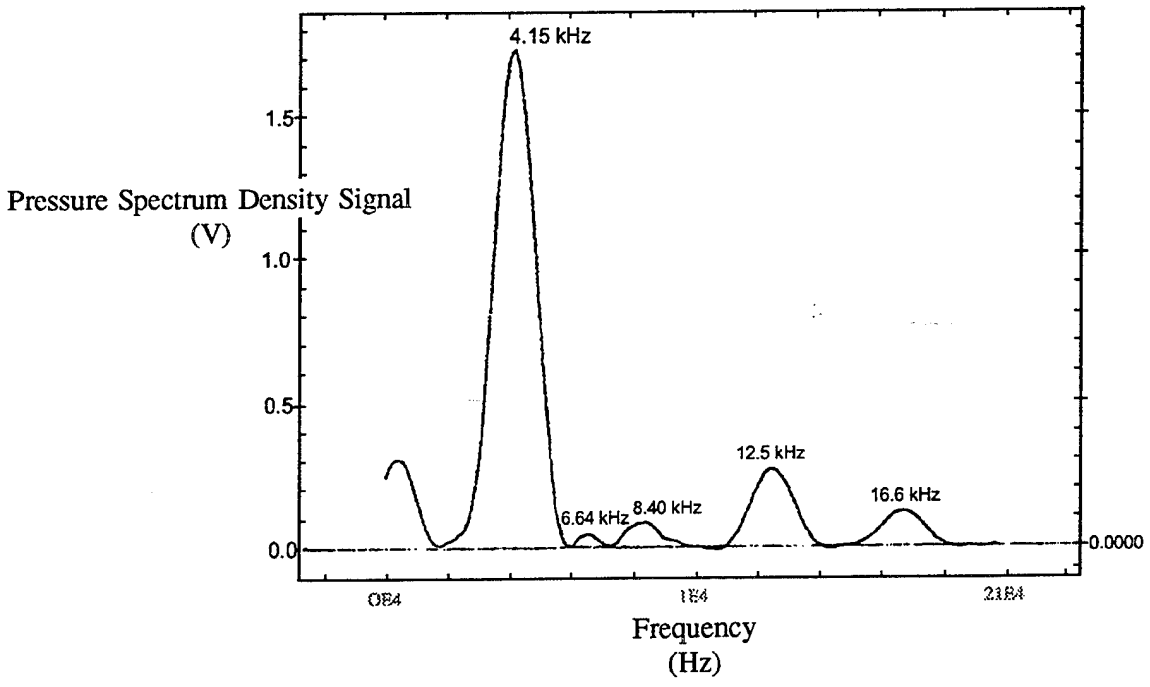

Figure 12. FFT of 7.62-mm projectile at 1,500 m.

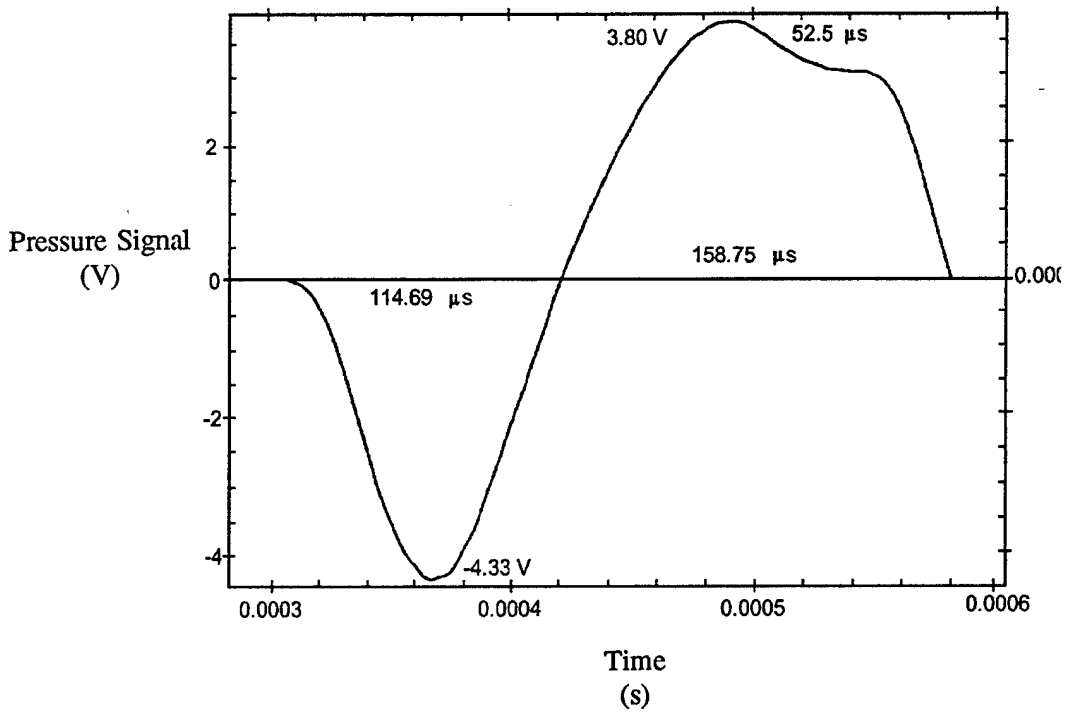

Figure 13. 12.7-mm projectile at 1,500 m.

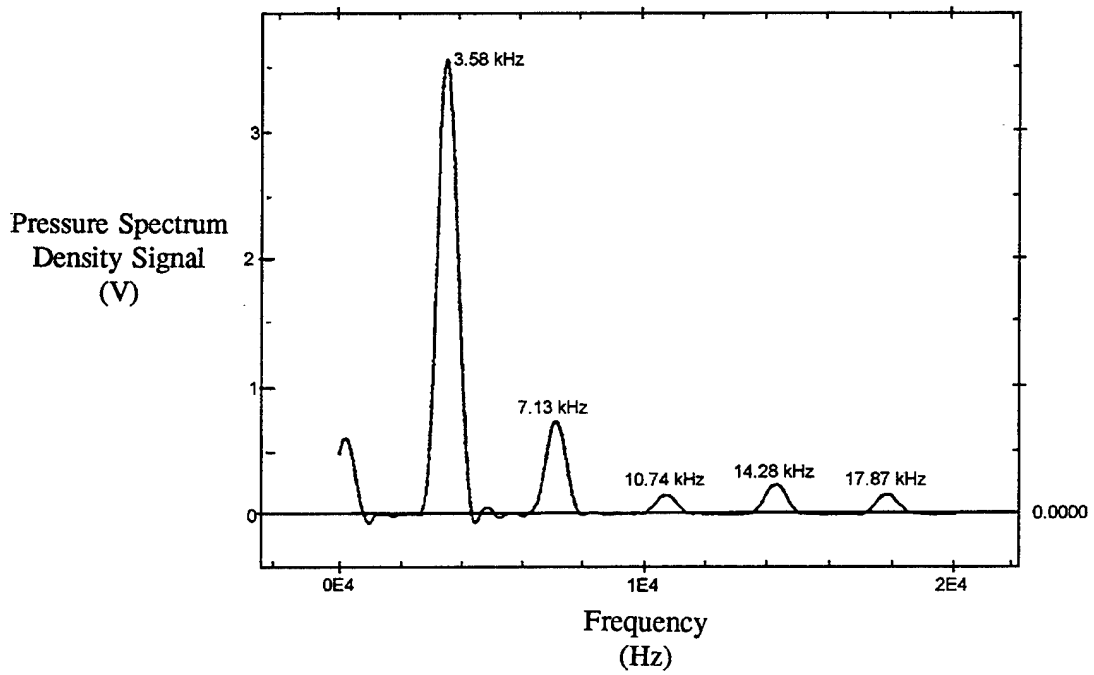

Figure 14. FFT of 12.7-mm projectile at 1,500 m.

possible, practical method of discrimination. The need to calibrate sensitive pressure gauges for a mass production item was impractical. Therefore, all the variables that required pressure levels, such as positive and negative pressure, peak value of total duration pressure impulse, total duration, and absolute pressure impulse, were disregarded. These data were retained for use in the event that the time durations could not be used to perform a high rate of round discrimination.

The total time duration was compared to the data and found to compare well. The resulting computed durations were constantly proportional to the data. This indicates that the earlier assumption, that the formula could be applied to large-caliber, non-ogival-shaped projectiles was good. The fairly constant proportionality for each projectile resulted in a stochastic modification of the duration formula with a shape constant.

5.2 Feasibility Study.

5.2.1 Live-Fire Data. An empirical model was developed from the feasibility test data to determine the feasibility of round discrimination. The following sections describe the data analyzed and statistical tests implemented. The analysis begins with examination of the 1,000-m data and ends with three models developed using a statistical tool known as discriminant analysis. The number of rounds in the analysis from each round type is listed in Table 5. As described earlier, for each round fired, five signatures were collected from microphones placed 1, 3, 6, 9, and 12 m, respectively, from the center of the target.

Table 5. Number of Rounds Analyzed in Feasibility Study

Distance (m)	25 mm		105 mm		120 mm	
	M793	M910	M490	M724	M831	M865
400	4	3	3	2	3	3
1,000	3	3	3	3	3	3
1,400	3	3	–	–	–	–
1,700	–	–	3	3	3	2

The 7th ATC's original minimum requirement was to distinguish between rounds <30 mm from those >30 mm. A more ambitious task was undertaken to try to distinguish among all the round types. This goal produced six categories for discrimination: 25-mm KE, 25-mm HEI, 105-mm KE, 105-mm HEAT,

120-mm KE, and 120-mm HEAT. The data collected from the signatures, location study, and Weibel radar were all candidates for inclusion in the models for discrimination.

5.2.2 1,000-m Data. Preliminary analyses to determine the feasibility of discriminating different round types were initially performed on the 1,000-m data. Statistical tests were performed on each variable, and at each microphone separately. These tests sought to determine if one of the variables could be used to discriminate the six round types. These tests also sought to determine the optimal microphone distance for future implementation.

The 1-m microphone often produced saturated signals. The actual offset distance fell into four regions. Region 1, data collected from both the 1-m and 3-m microphones, had offset distances less than 4 m. Region 2, data collected from the 6-m microphone, had offset distances from 4 m to 7 m. Region 3 has offset distances >7 m and up to 10 m. Region 4 offset distances were >10 m.

The Kruskal-Wallis test was used to test the hypothesis that the six round types have equivalent mean values in comparison to the alternative, which is that at least two round types differ. This nonparametric test performed an analysis on the ranks of the data rather than the actual data values. The ranks started with 1 for the smallest value among the six round types. The largest value from all six round types received a rank of N, the number of test data from the six populations. The advantage of the nonparametric test was that the test did not require assumptions of normality of the data or homogeneity of variances (HOV)—that is, equality of variance among the groups. Appendix M provides an example of implementing the Kruskal-Wallis test and provides detailed results of the test for each variable.

The results of the Kruskal-Wallis test performed on each variable indicate that at least two round types differed from each other in each of the four regions. To determine exactly which round types differed, the corresponding multiple comparison test was implemented. In summary, most of the variables distinguished between the small and large-caliber rounds—that is, <30 mm vs. >30 mm—satisfying the 7th ATC's minimum requirement. The only variable that did not was negative phase duration in regions 3 and 4.

All the other variables in each region distinguished between large HEAT and large KE rounds. The 105-mm and 120-mm training HEAT rounds were not statistically different from each other, nor were the

105-mm and 120-mm training KE rounds. But the 105-mm and 120-mm training HEAT rounds were statistically different from the 105-mm and 120-mm training KE rounds.

For some variables, the two smaller-caliber rounds were distinguishable from each other. These results are summarized with the following notation:

$$25\ K \neq 25\ H \neq (105\ K = 120\ K) \neq (105\ H = 120\ H).$$

The round types are listed in order from lowest average rank to the highest. Parentheses around two round types indicate there is no significant difference between the rounds. What the nonparametric analyses indicated was that many of the variables under consideration were good candidates for discriminating at least the small-caliber rounds from the large-caliber rounds for 1,000-m data. The duration and pressure impulse values were good for discriminating the rounds in the four categories grouped previously (i.e., small KE, small HEAT, large KE, and large HEAT). The first region (offset distance <4 m), representing data collected close to the flight of the round, was the hardest region in which to discriminate. The facts provided a guide to the placement of the microphones for future tests.

5.2.3 Analysis of Data From All Ranges. The preliminary analysis of the data at the 1,000-m range indicated that several of the variables were independently able to separate the round types. The goal was to find one or more variables that could separate the round types and was insensitive to range. As mentioned in the previous analyses, it was difficult in some cases to separate the M724 from the M865 rounds and difficult to separate the M490 and the M831 rounds from each other. Therefore, in the next analyses, the discrimination was among 4 groups (not 6): M910, M793, M724/M865, and M490/M831.

• *Visual Inspections.* Various plots of the signature variables of interest vs. microphone distance were examined to determine if there were obvious trends in the data that separated the round types, independent of the range. Positive peak pressure was plotted in Figure 15. Some separation in the data between the large-caliber rounds and the small-caliber rounds was observed. However, among the large-caliber rounds, separating the HEAT from the KE rounds over all the distances is not easy. This indicated that positive peak pressure is sensitive to range and would not be a good candidate for discrimination.

Upon examining the plots of total duration vs. microphone offset distance for each firing position (range), little change in the shape of the curves was observed. Figure 16 shows all the ranges together

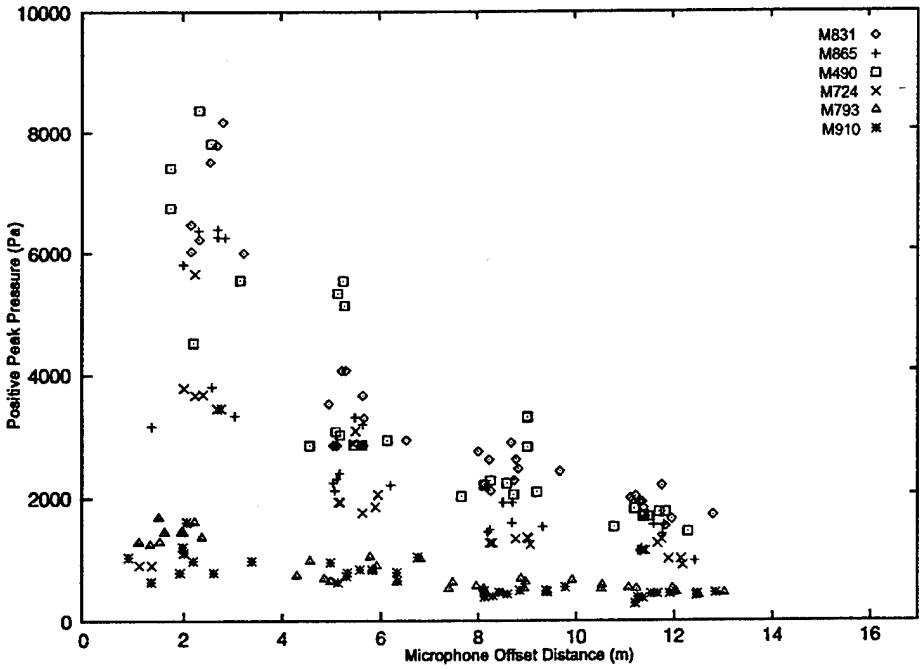

Figure 15. Positive peak pressure vs. microphone distance for all firing positions.

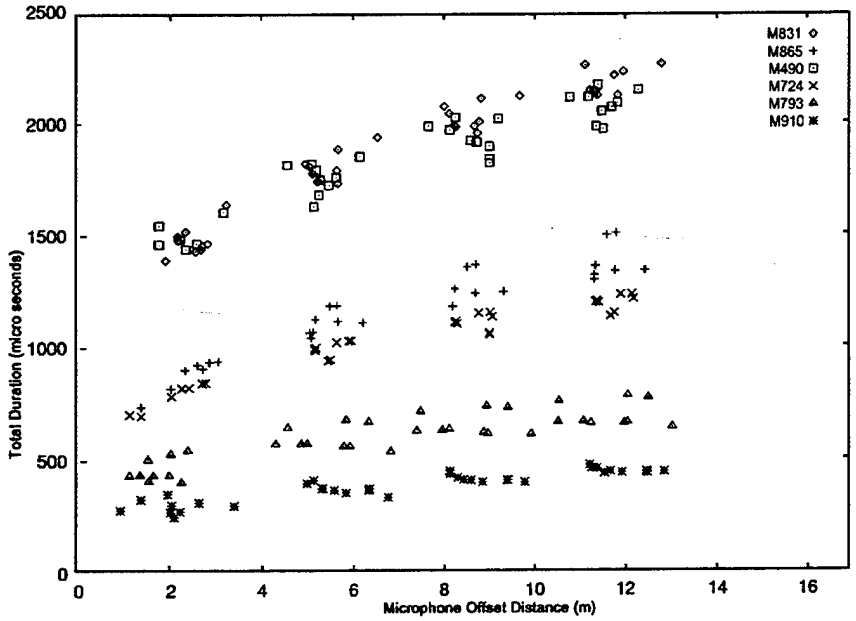

Figure 16. Total duration vs. microphone distance for all firing positions.

on one graph. This plot suggested that total duration is not sensitive to range and is a good candidate for discriminating round types. If microphone offset distance is known, the type of round can be determined based on the magnitude of the total duration. In some cases, the round can be determined independent of the microphone offset distance. For instance, if the total duration were >1,500 μs, the round would be a large HEAT round (M831 or M490), independent of the microphone offset distance. However, if the total duration were 600 μs, one could not be certain if it were a large HEAT round with a microphone offset distance <2 m, or a small HEAT round, M793, with a microphone offset distance of approximately 12 m. These observations led to conclude that total duration alone cannot be use to discriminate among the rounds, and a more objective and quantifiable way to combine variables and separate the groups was needed.

5.2.4 Discriminant Analysis for All Ranges.

• *General.* Discriminant analysis is a statistical technique which uses linear combinations of variables to determine if one or more variables will categorize the populations (round types), and it is described by Marriott (1990) in the following way:

> *Given a set of multivariate observations on samples, known with certainty to come from two or more populations, the problem is to set up some rule which will allocate further individuals to the correct population of origin with minimal probability of misclassification. This problem and sundry elaboration of it give rise to discriminatory analysis.*

In linear regression, one develops a linear model with one or more explanatory (independent) variables x_i's to describe the response (dependent) variable y. A linear equation is of the form:

$$y = B_0+B_1x_1+B_2x_2+B_3x_3+B_4x_4+\ldots\ldots,$$

where the coefficients B_i's are linear. The x_i's can take a nonlinear form such as x raised to a power or a functional form as the natural logarithm or exponent.

In the application of categorizing (or classifying) the round into the four groups (M910, M793, M724/M865, and M490/M831), round type is not a measurable response; therefore, univariate regression

analysis is not appropriate. The multivariate tool, discriminant analysis, allows us to form one or more functions, where the value of the function(s), in combination, categorizes the round types.

$$f_1 = a_0 + a_1x_1 + a_2x_2 + a_3x_3 + a_4x_4 + \ldots.$$
$$f_2 = b_0 + b_1x_1 + b_2x_2 + b_3x_3 + b_4x_4 + \ldots.$$
$$f_3 = c_0 + c_1x_1 + c_2x_2 + c_3x_3 + c_4x_4 + \ldots.$$
$$\vdots$$
$$f_n = z_0 + z_1x_1 + z_2x_2 + z_3x_3 + z_4x_4 + \ldots.$$

Only variables that are not highly correlated with one another and contribute significantly are selected into the model. Forming the functions is performed in a stepwise fashion, with the most "significant variable" that most separates (and therefore discriminates) among the round types entering the model first. Given that this first variable is in the model, the next variable, which is not highly correlated with the variable(s) already in the model and would contribute most from the remaining significant variables, is entered into the model. This process continues until no variable can satisfy the two aforementioned conditions.

Several criteria are available for entering significant variables into the model (SPSS Inc. 1990a). Wilk's Lambda was used in this analysis. Wilk's Lambda is the ratio of the within-groups sum of squares to the total sum of squares when the discriminant scores (the f_i's) are the dependent variables, and the group is the independent variable.

The tolerance for correlation of variables was set at 0.1. Tolerance is the amount of linear association between the incoming variable and the variable(s) already in the model. It is equal to $1-R_i^2$, where R_i^2 is the squared multiple correlation coefficient. Variables with small tolerance values (and therefore large R_i^2 values) are not entered into the model.

These analyses were performed using a statistical software package called SPSS. With a set of functions to characterize the discrimination, a territorial map of the categories of at most two dimensions is provided. This procedure is explained in more detail, with actual data from the test program, in the next paragraph.

• *Discriminatory Functions for Live Fire Data Set.* Wilk's Lambda criterion was implemented for the model development of the live fire data set. Total duration was the first variable to enter the model and is the one variable that best separates the round types into their appropriate groups. As described earlier, total duration alone cannot guarantee correct classification of all the rounds. The stepwise process continued with the following variables:

1. Total Duration
2. Peak of Absolute Pressure Impulse
3. Velocity
4. Microphonic Off-Set Distance
5. Negative Peak Pressure
6. Positive Peak Pressure
7. Subtotal Duration (addition of positive and negative phases).

These 7 variables were able to correctly classify 99.50% of the round types. As shown in Table 6. There was one misclassification: M793 classified as M910.

Table 6. Classification Result for Original Seven Variables

Actual Group	No. of Cases	Predicted Group Membership			
		1 M910	2 M793	3 M724/M865	4 M490/M831
1. M910	36	36 100%			
2. M793	36	1 2.8%	35 97.2%		
3. M724/M865	61			61 100%	
4. M490/M83	69				69 100%

If one looks back at Figure 16 (total duration vs. microphone distance), some curvature in the data is seen. The natural logarithm (ln) of total duration will linearize the plot as shown in Figure 17. Repeating the discriminant analysis process, the natural logarithm of total duration is the first variable to enter the model. Continuing the analysis, the model contains the following variables:

1. ln(Total Duration)
2. Offset Distance
3. Velocity
4. Total Duration
5. Peak of Absolute Pressure Impulse
6. Negative Peak Pressure
7. Peak of Pressure Impulse.

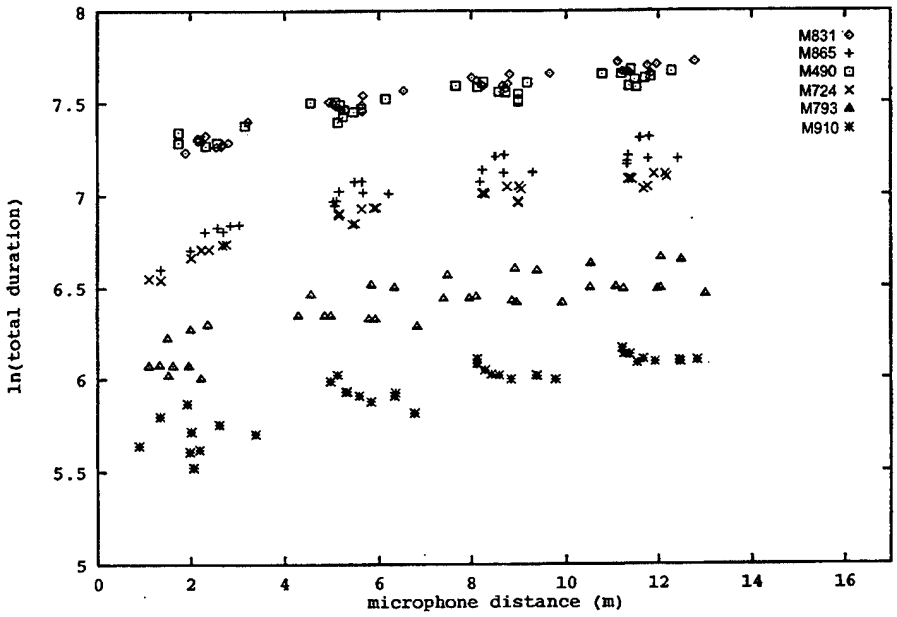

Figure 17. ln(total duration) vs. microphone distance.

These variables produced all correct classification results. Note that both the natural logarithm and raw units of total duration entered into the model. Although the two are not independent of one another, they pass the tolerance criterion. However, the pooled within-groups correlation between the two is 0.88. To avoid problems with multicollinearity, an unstable model as a result of highly correlated explanatory variables, it was not advisable to keep both of these variables in the model.

From the seven variables listed previously, subsets of variables were formed in search of smaller models that may be equally successful. Three reduced models will be explained in the following sections.

• *Reduced Model A.* From the set of variables produced in the aforementioned model, ln(total duration) and microphone offset distance were used to form a discriminating model that requires just one function:

$$f_1 = -84.059 + 12.774 \ln(\text{Total Duration}) - 0.523 \text{ Microphone Distance}. \quad (15)$$

When the frequency of the f_1-values are plotted in histogram form, as shown in Figure 18, four clusters are produced, which represent the four groups of interest. The histograms do not overlap, indicating correct classifications for all the groups were achieved. The values on the abscissa are the f_1-values. Below that, the class centriod is provided in two forms. The relative location of the centroid compared to the group histogram is given first. Each group is numbered as 1 for 25-mm KE, 2 for 25-mm HEI, 3 for Large KE, and 4 for Large HEAT. The f-value of the centriod is provided next. The limit values are the greatest value of the group starting from the left. These limits provide the following functional mapping:

$$\begin{aligned} f_1 &\leq -9.02 \quad \text{M910 (25 KE)} \\ -9.02 < f_1 &\leq -2.39 \quad \text{M793 (25 HEI)} \\ -2.39 < f_1 &\leq 4.78 \quad \text{M724, M865 (Large KE)} \\ f_1 &> 4.78 \quad \text{M490, M831 (Large HEAT).} \end{aligned} \quad (16)$$

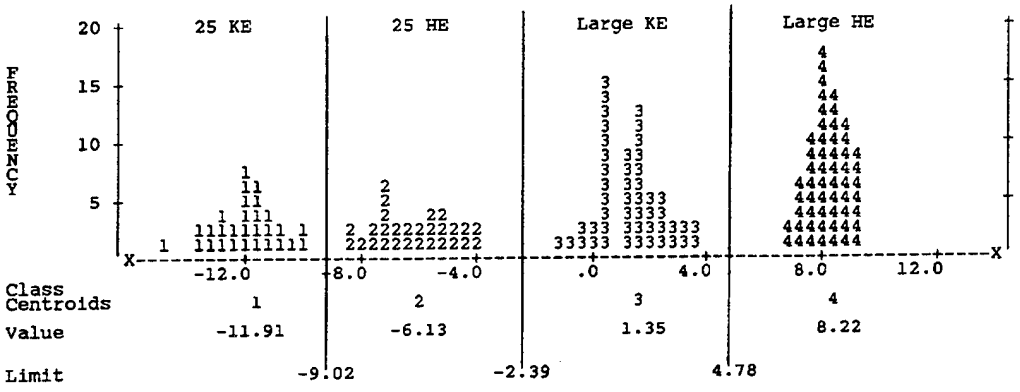

Figure 18. Feasibility phase model A: histogram of group classes.

• *Reduced Model B.* Referring back to the set of seven variables that include ln(total duration), other combinations of variables were considered that would classify all the rounds correctly. Consider the variables ln(total duration) and velocity. The discriminant analysis requires two functions as shown in equation 17, resulting in 98.03% of the data correctly classified. Of the misclassified data, one M910 round was classified as an M793, and three M793 rounds were predicted as M910's (see Table 7).

$$f_1 = -42.451 + 5.994 \ln(\text{Total Duration}) + 0.00129 \text{ Velocity}$$
$$f_2 = -2.800 + 0.529 \ln(\text{Total Duration}) + 0.00650 \text{ Velocity}. \quad (17)$$

Table 7. Classification Result for ln(Total Duration) and Velocity.

Actual Group	No. of Cases	Predicted Group Membership			
		1 M910	2 M793	3 M724/M865	4 M490/M831
1. M910	36	35 97.2%	1 2.8%		
2. M793	36	3 8.3%	33 91.7%		
3. M724/M865	61			61 100%	
4. M490/M831	69				69 100%

• *Limitations on Model B.* As mentioned earlier, the data gathered from the 1-m microphone to the target was not reliable. Therefore, only the data collected from a distance >3 m was considered in the analysis. With the same variables ln(total duration) and velocity, 100% correct classification was achieved with the model.

$$f_1 = -68.539 + 9.719 \ln(\text{Total Duration}) + 0.000994 \text{ Velocity}$$
$$f_2 = -3.652 - 0.397 \ln(\text{Total Duration}) + 0.00650 \text{ Velocity}. \quad (18)$$

The data plotted in (f1, f2) space is shown in a scatterplot in Figure 19. The data point is denoted with the group number. The "*" indicates the group centroid. Because of the graphics output from SPSS, overlapping points are not shown. The number of points indicated on the scatterplot may not add up to the number of cases actually analyzed, and misclassified cases may be difficult to visualize. Classification results are provided in the table for models where misclassification occurs.

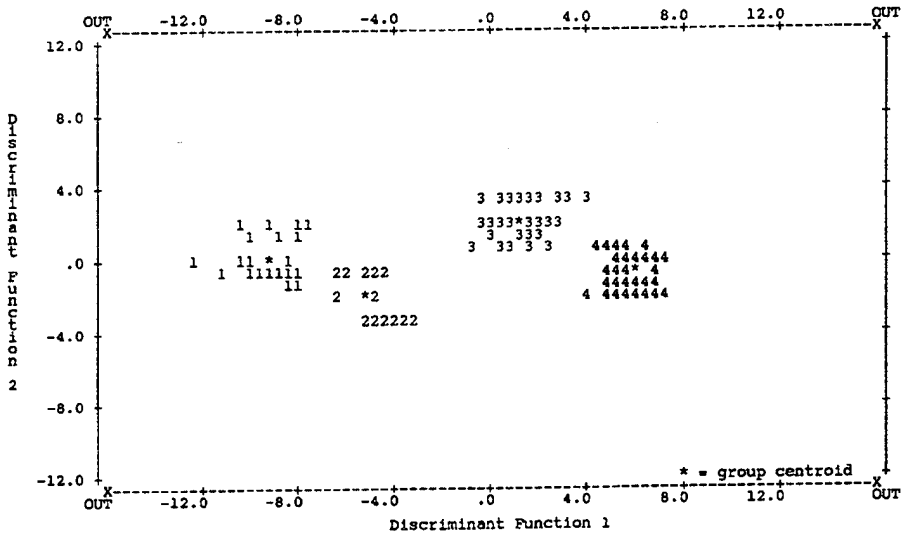

Figure 19. Feasibility phase model B: scatterplot.

The territorial map in Figure 20 shows the boundaries for each group in (f_1, f_2) space. These boundaries are constructed such that any point in a group in the f_1-f_2 plane would be closer to that group centroid than any other group centroid. This is useful for predicting the group membership of an unknown round.

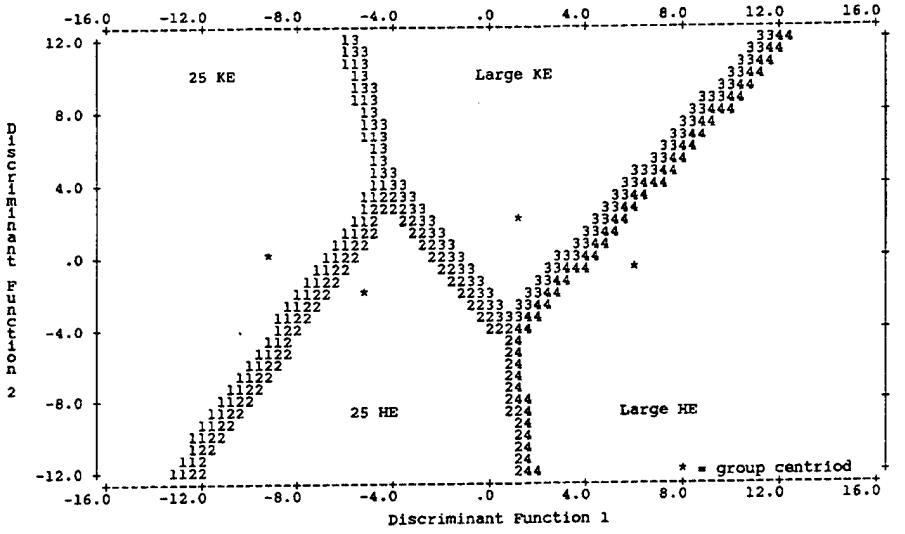

Figure 20. Feasibility phase model B: territorial map.

The process of selecting subsets of variables from the base set continues. The remaining variables: peak of absolute pressure impulse, negative peak, and peak of pressure impulse are difficult to obtain in the field because the microphone would have to be more finely calibrated.

• *Reduced Model C.* A third and quite different reduced model was considered. Total duration is the single variable that best discriminates among the groups of rounds. If this variable were collected from a microphone placed on each side of the target, collectively the rounds should be identified uniquely. Although our test array of five microphones was on the same side of the target, the data from two microphones were carefully selected to determine if discrimination were possible with nothing more than two total durations. A two-function discrimination model was developed from the 6- and 12-m microphones:

$$\begin{aligned} f_1 &= -17.186 + 0.0115 \text{ Total Duration } 6 + 0.00331 \text{ Total Duration } 12 \\ f_2 &= -0.0887 - 0.0317 \text{ Total Duration } 6 + 0.02651 \text{ Total Duration } 12. \end{aligned} \quad (19)$$

The assumptions for an optimal model is normality of the independent variables and equal covariance matrices of each group. Box's M test was used to check the equality of covariance matrices based on the determinants of the matrices. Box's M test is also sensitive to the normality assumption. Of the three models developed previously, only Model C did not pass Box's M test for equality of covariance matrices. This indicates that the model is not statistically optimal, and problems may arise in predicting rounds. In spite of this, the model predicted all correctly, as shown in Table 8, and the scatterplot and territorial map in Figures 21 and 22, respectively, show good separation among the groups.

• *Verification of the Feasibility Models.* Each of the three models described in the previous section represents the best classification rate since all of the data was used to develop the model. Often, live fire tests are conducted to verify that the model is truly adequate. This verification was expected to be performed later in the program when all round types had been incorporated into the final model(s). To check the adequacy of the current feasibility models, a portion of the data was taken for model development. The remaining data were reserved for testing the model, a form of goodness-of-fit. Stratified random sampling of two-thirds of data was implemented for adjusting the coefficients associated with the variables in each of the three models listed previously. Stratification was performed by randomly selecting one round from each round type at each range to be reserved for testing the model adequacy. The other rounds were used for the model development.

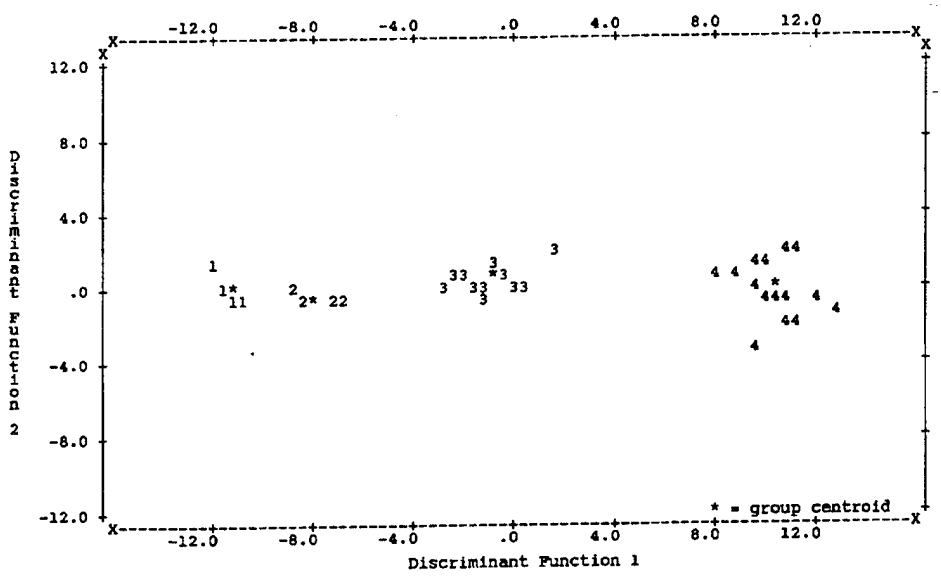

Figure 21. Feasibility phase model C: scatterplot.

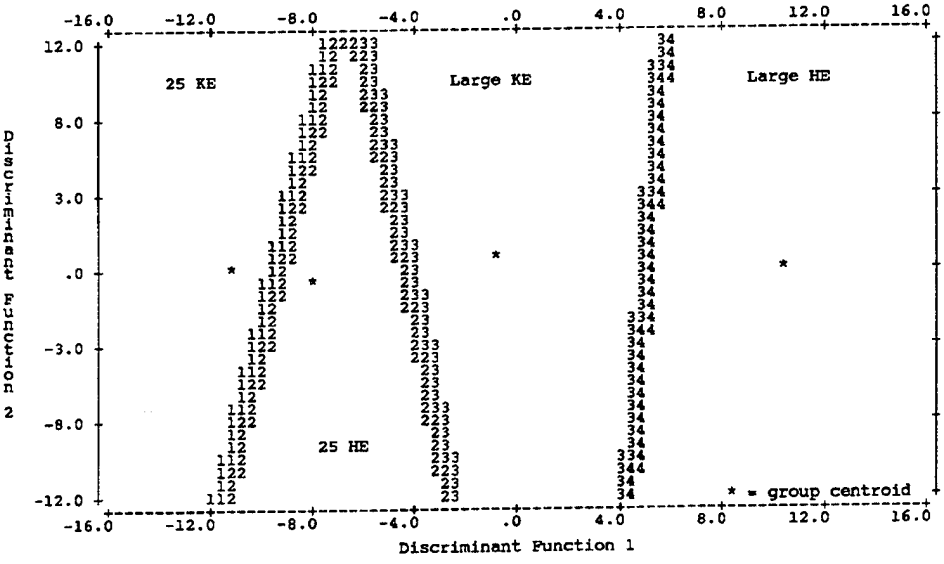

Figure 22. Feasibility phase model C: territorial map.

All three resulting models performed well. Each adjusted model correctly predicted all of the rounds used to develop the model, and each model correctly predicted each of the reserved rounds. Additionally, a set of theoretical data was created in a blind study to test the adequacy of Model C with two total durations. Twelve theoretical total duration values were computed for the various round types as if the microphones collecting acoustical signatures were placed on each side of the target. These values were placed in the discriminatory function. The resulting discriminant values correctly predicted the group membership for each round type, as seen in Table 9.

Table 8. Classification Result for Two Total Durations

Actual Group	No. of Cases	Predicted Group Membership			
		1 M910	2 M793	3 M724/M865	4 M490/M831
1. M910	9	9 100%			
2. M793	9		9 100%		
3. M724/M865	15			15 100%	
4. M490/M831	18				18 100%

Table 9. Verification Results

Actual Group	No. of Cases	Predicted Group Membership			
		1 M910	2 M793	3 M724/M865	4 M490/M831
1. M910	3	3 100%			
2. M793	4		4 100%		
3. M724/M865	3			3 100%	
4. M490/M831	2				2 100%

• *Feasibility Test Conclusion.* Acoustical signatures, particularly total duration of the N-Wave curve, can be used to discriminate between the following round types:

- small- and large-caliber rounds
- large (105- or 120-mm) HE and large KE training rounds
- 25-mm HEI and KE training rounds.

With the use of discriminant analysis, three models that correctly classify 100% of the rounds have been developed. These models contain the following variables:

- total duration and microphone offset distance
- total duration and velocity (>3 m)
- two total durations.

5.2.5 Location and Velocity Data. During the feasibility test, the six microphones were set up in two triangular arrays as shown in Figure 23 (see Appendix C for exact microphone locations). The time differences, microphone and target locations, and meteorological data were processed through the Stallings algorithm discussed in 3.2.3. The data were first reduced for velocity prediction. The Stallings algorithm predicted the velocity, on the average, within 2% of the actual velocity verified by radar. The locations were, on the average 20 cm from the actual video scored locations (see Appendix G). The error was mostly due to microphone placement. The projectile hits did not go through the center of the microphone array. The microphones were purposely placed low to the ground to keep them from being hit and to see what errors would be generated.

Six M831 projectiles, fired from the 1,000 m position, were analyzed to study the effects of input data on the accuracy of the predicted location. Table 10 shows how a change in each input value of meteorological data, fall angle, and gun position affects the projectile location.

The error associated with the microphone positions depends on the contribution of that microphone when determining the location. If the projectile flies close to a microphone, the algorithm weights that microphone's data such that it provides a larger contribution to the output location. Generally, the average survey error of all the microphones will be close to the average scoring error. The survey error was typically around 1 mm for each microphone with the use of a precision theodolite and an experienced

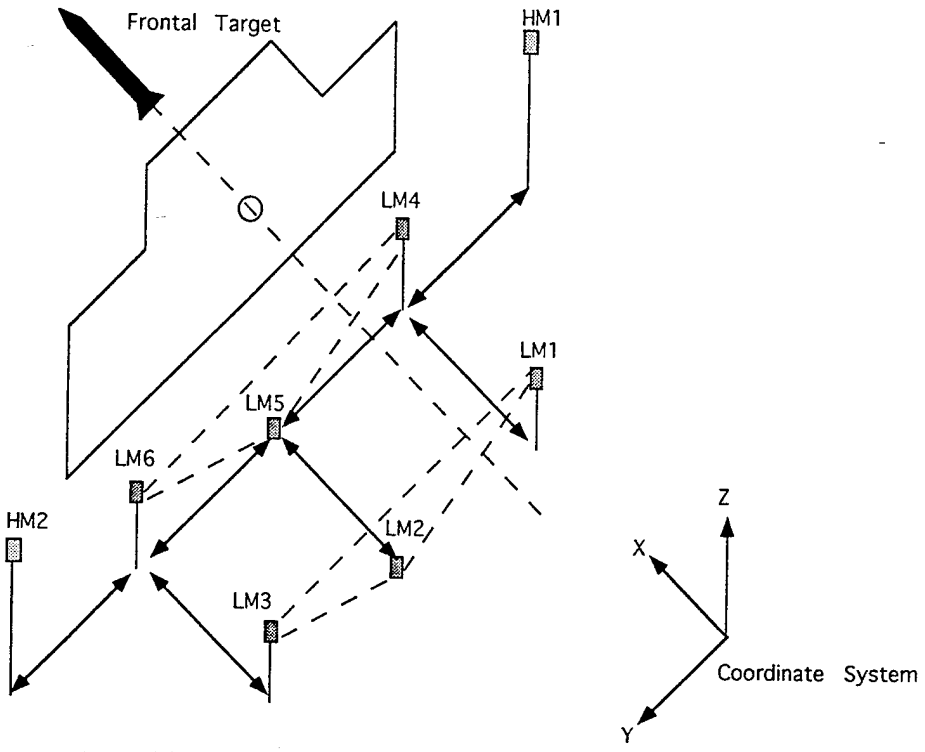

Figure 23. Feasibility test microphone array and target setup.

Table 10. Input Values Effect on Location

Input Values	Change for Each	Additional Change in Location (mm)
Meteorological Data		
Temperature Wind Humidity	1° 1 m/s Any Humidity	3 4 3 max
Ballistics		
Fall Angle	1 mil	3.6
Gun Position		
X Y Z	1 m 1 m 1 m	5 0.5 4

surveyor. Errors associated with microphone times also depended on that microphone's contribution. There is more of an effect on location for slower projectiles since their shock waves are more oblique. The errors associated with meteorological data and fall angle are considered relatively small. The major downfall with the Stallings technique is the dependence on knowing the gun's position. Elevation changes, Z, are not that great on a training range. The major errors come from not knowing an accurate range and deflection of the gun position relative to the target. The Stallings technique was eliminated as a candidate for RDS location algorithm because it was slow and had large potential gun position errors.

5.3 Collection Phase.

5.3.1 Live-Fire Data. The next phase of testing began with the purpose of expanding the existing data set to include: 7.62-mm ball (M59) and tracer (M62) rounds, 12.7-mm ball (M33) and tracer (M17) rounds, and three 35-mm TPGID (old HEAT DM18, new HEAT DM68, and KE simulator) rounds. This phase is designated as the collection phase. Randomization of rounds for testing took place as much as possible with the tight test schedule and small budget.

Since changing the firing platform for each round at each range was time-consuming, several rounds of the same size were fired at one range before moving the platform to another range. The goal was to divide the sample in half so that two groups of rounds of the same type were fired on two different days to average out any effects due to weather conditions. This was not always accomplished. The DM18 and DM68 round were late arriving. The DM68 and the TPGID KE simulators had not been type classified. The 7.62-mm and 12.7-mm rounds were fired first. Ball and tracer rounds were completely randomized. When the 35-mm KE was type classified, it was randomized with the DM18. The DM68 was tested with the DM18 on the last two days. However, the duration data for the last two days was not available for the analyses. Table 14 lists the number of rounds reduced that were included from each type in the analysis.

The ball and tracer rounds are listed separately in Table 11, but there was little interest in discriminating between them in this study. There were some differences in total duration and velocity. The average velocity of the tracer rounds at each range was greater than the ball rounds for both 7.62 mm and 12.7 mm. The average total duration of the tracer rounds was approximately 13 μs greater than the

Table 11. Number of Rounds Analyzed in Collection Phase

Distance (m)	7.62 mm		12.7 mm		35 mm	
	M59	M62	M33	M17	DM68	KE Simulator
400	3	4	5	4	3	3
600	3	4	—	—	—	—
800	3	3	—	—	—	—
1,000	—	—	4	4	4	3
1,700	—	—	—	—	3	3

ball rounds for both 7.62 mm and 12.7 mm with the exception of the 7.62 mm at 800 m. For this combination, the average ball round was 230 μs greater than the tracer round. More investigation is required to determine what caused this large difference at 800 m. See Appendix E for tables of total duration and velocity values. For the remaining analyses, the ball and tracer rounds of 7.62 mm will be treated as one group as well as the 12.7-mm rounds.

5.3.2 Discriminate Analysis for Empirical Model Formation. The entire data set, from both the feasibility and collection phases, had a total of 8 groups: 7.62 mm, 12.7 mm, M910, M793, 35-mm TPGID KE simulator, DM18 and DM68, M724 and M865, and M490 and M831. A cursory analysis performed on the data before the complete data set was reduced indicated that prediction would be good overall. However, within the TPGID groups, only 66% of the rounds could be classified correctly.

A total of 34% of the DM18/DM68 rounds were predicted as TPGID KE simulator rounds. Likewise, 34% of the TPGID KE simulator rounds were predicted as DM18/DM68 rounds. An encouraging point was that these rounds were still classified as 35-mm TPGID. Upon examination of these two round types, we found that the velocities of KE training rounds at each range were on the average 250 m/s slower than the 120-mm KE training rounds. To continue the analysis, the 35-mm TPGID rounds were combined into one group resulting in seven groups for discrimination.

• *Model I: Total Duration, Microphone Distance, and Velocity.* Based on the three models developed during the feasibility phase, discriminant functions were formed first with variables ln(total duration) and microphone distance. Unlike the one-function model formed for the four groups in that phase, the model

for seven groups required two functions. However, misclassification was high, particularly between the M910 group and 12.7 mm. The misclassification rate was 17%.

The next attempt was to form a model with variables ln(total duration) and velocity, as in Model B. This model produced 88% correct classification of the groups. Only the M490/M831 rounds were without misclassification. TPGID was the most difficult of all the groups to classify correctly.

Finally, all three variables—ln(total duration), microphone offset distance, and velocity—were included to produce a two-function model (see equation 20). This resulted in a good classification rate of 97.85% as shown in Table 12. From the scatterplot of the data in (f_1, f_2) space (Figure 24), one can see why several 7.62-mm rounds (group 1) were classified as 12.7 mm (group 2); the functional values were closer to the centroid of group 2. Likewise, several M910 rounds (group 3) were misclassified as 12.7 mm (group 2) since their values were closer to that centroid. The misclassified rounds could be easily identified by overlaying the territorial map (Figure 25) on the scatterplot (Figure 24). (The pattern numbers in the territorial map form the border lines between the groups.)

$$\begin{aligned} f_1 &= -87.510 + 13.594 \ln(\text{Total Duration}) \\ &\quad + 0.00413 \text{ Velocity} - 0.529 \text{ Microphone Offset Distance} \\ f_2 &= 6.592 - 1.928 \ln(\text{Total Duration}) \\ &\quad + 0.00650 \text{ Velocity} + 0.0671 \text{ Microphone Offset Distance}. \end{aligned} \tag{20}$$

This model was tested with data collected during the verification/validation phase. The groups' centroids listed in Table 13 are necessary for determining the group membership of the unknown rounds fired. The boundary conditions are set at $f_1(-20, 20)$ and $f_2(-4, 4)$. Any rounds producing values of f_1 and f_2 outside these boundaries were classified as an unknown round.

• *Model II: Three Variables at 6 m.* As discussed earlier, the field equipment array had two high-fidelity microphones placed 6 m from the center of the target. The same variables used in the previous model were considered, but the coefficients were based on the 6-m microphone data only. The classification rate for this model (see equation 21) was close to the Model I with 97.12% correct as shown in Table 14. The centroids, scatterplot, and territorial map are provided (see Table 15 and Figures 26 and 27, respectively). The boundary conditions are $f_1(-20, 20)$, $f_2(-4, 4)$, and $f_3(-4,4)$. This model was denoted as Empirical Model II and tested in the verification/validation phase.

$$
\begin{aligned}
f_1 &= -95.122 + 14.681 \ln(\text{Total Duration}) \\
&\quad + 0.00432\ \text{Velocity} - 0.5122\ \text{Microphone Offset Distance} \\
f_2 &= 5.512 - 1.878 \ln(\text{Total Duration}) \\
&\quad + 0.00618\ \text{Velocity} + 0.258\ \text{Microphone Offset Distance} \\
f_3 &= -9.133 - 0.202 \ln(\text{Total Duration}) \\
&\quad - 0.00041\ \text{Velocity} + 1.987\ \text{Microphone Offset Distance}.
\end{aligned} \tag{21}
$$

Table 12. Classification Results for ln(Total Duration), Microphone Offset Distance and Velocity

Actual Group	No. of Cases	Predicted Group Membership						
		1 7.62 mm	2 12.7 mm	3 M910	4 M793	5 TPGID	6 M724/ M865	7 M490/ M831
1. 7.62 mm	59	54 91.5%	5 8.5%					
2. 12.7 mm	65		65 100.0%					
3. M910	29		3 10.3%	26 89.7%				
4. M793	29				29 100.0%			
5. TPGID	29					29 100.0%		
6. M724/M865	56						56 100.0%	
7. M490/M831	65							65 100.0%

NOTE: Cases correctly classified: 97.85%.

Table 13. Discriminant Functions Group Centroids

Group	f_1	f_2
M62/M59	−13.170	−0.621
M17/M33	−8.676	−0.609
M910	−6.346	2.030
M793	−1.686	−0.990
DM18/DM68/TPL-T	1.800	0.581
M724/M865	9.119	2.207
M490/M831	14.447	−1.810

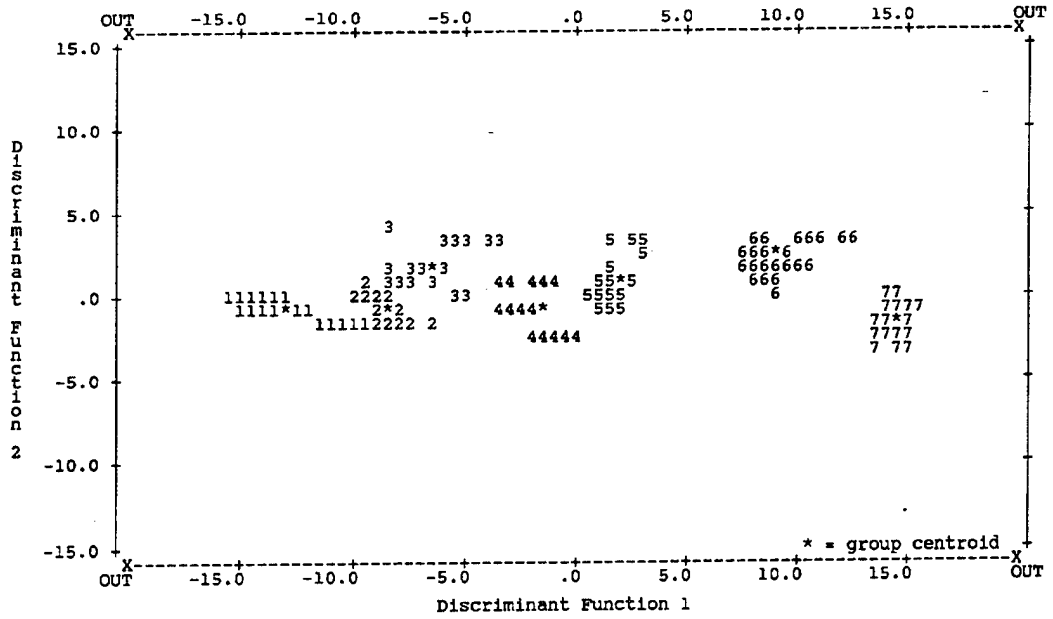

Figure 24. Model I: scatterplot.

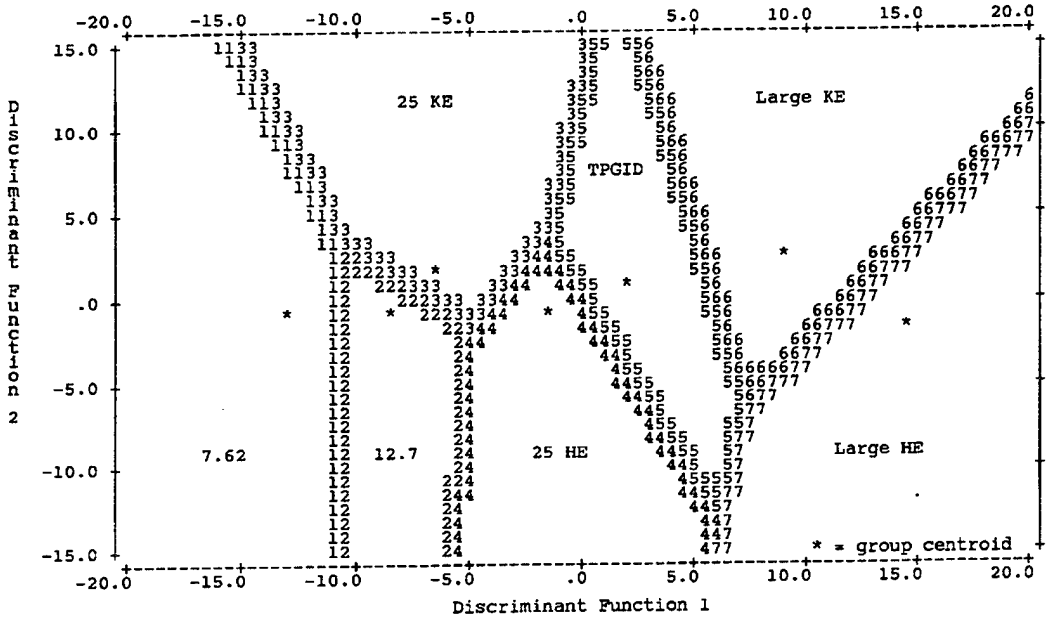

Figure 25. Model I: territorial map.

Table 14. Model II Classification Results

Actual Group	No. of Cases	Predicted Group Membership						
		1 7.62 mm	2 12.7 mm	3 M910	4 M793	5 TPGID	6 M724/ M865	7 M490/ M831
1. 7.62 mm	17	15 88.2%	2 11.8%					
2. 12.7 mm	17		17 100.0%					
3. M910	9		1 11.1%	8 88.9%				
4. M793	9				9 100.0%			
5. TPGID	18					18 100.0%		
6. M724/M865	16						16 100.0%	
7. M490/M831	18							18 100.0%

NOTE: Cases correctly classified: 97.12%.

Table 15. Model II Group of Centroids

Group	f_1	f_2	f_3
7.62	−14.276	−0.582	-0.191
12.7	−9.323	−0.583	0.011
M910	−6.790	1.826	0.145
M793	−1.598	−0.893	1.060
TPGID	2.035	0.474	-0.474
M724/M865	9.811	2.089	0.160
M490/M831	15.726	−1.697	-0.100

• *Model III: Two Total Durations.* The final empirical model, equation 22, includes two total duration variables as constructed in the feasibility phase (Model C). The data from the 9-m microphone were the most discriminating, and the 3-m microphone data were the second most discriminating. Although an effort was made to use the data measured at 6 m, the data at 3 m and 9 m were the least correlated as well as the most discriminating. The correlation between the total duration values at 9 m

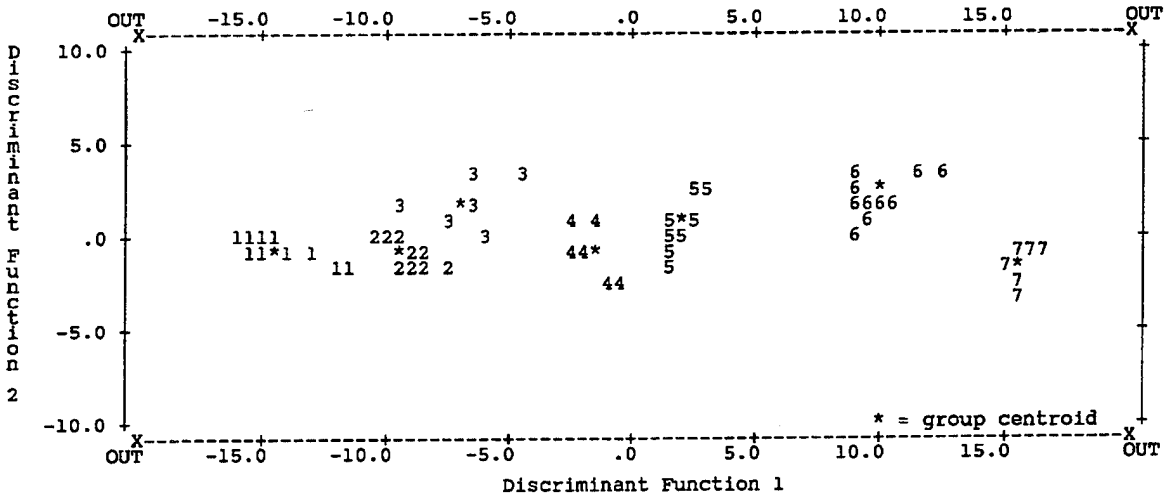

Figure 26. Model II: scatterplot.

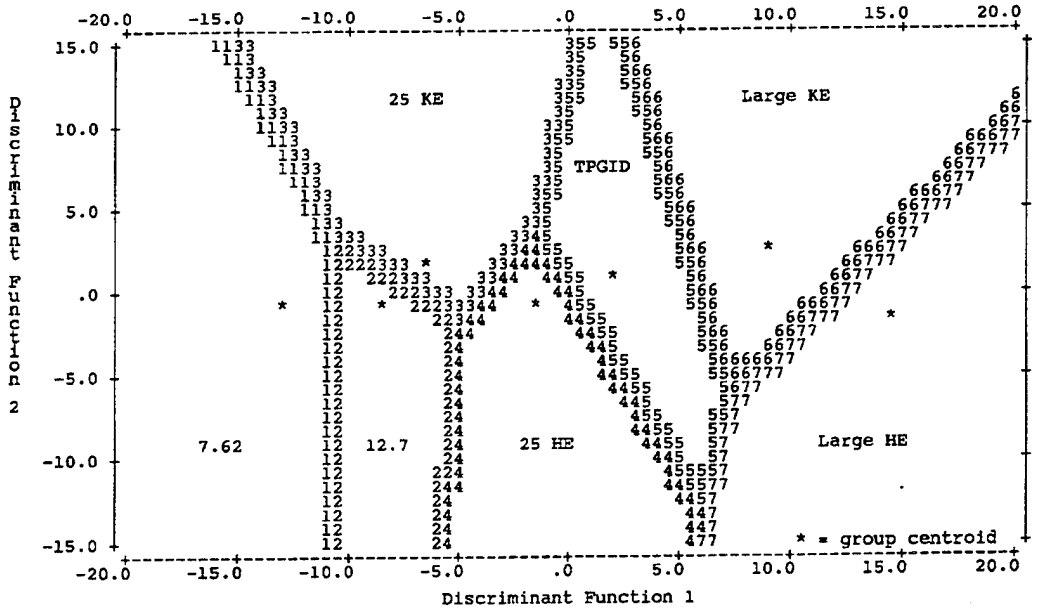

Figure 27. Model II: territorial map.

and 6 m is 0.94. This high correlation between explanatory variables can cause a problem known as multicollinearity in which the coefficients are very sensitive. The goal is to obtain coefficients that are robust so that the model will be valid under various conditions.

$$
\begin{aligned}
f_1 &= -16.158 - 0.000608 \text{ Total Duration (3-m Mic)} \\
&\quad + 0.0199 \text{ Total Duration (9-m Mic)} \\
f_2 &= 0.200 + 0.0316 \text{ Total Duration (3-m Mic)} \\
&\quad - 0.0233 \text{ Total Duration (9-m Mic)}.
\end{aligned} \tag{22}
$$

The correct classification rate for this model was lower than the other two models at 89.69% (see Table 16). The difficulty in discriminating occurred for rounds 35 mm and smaller. The scatterplot and territorial map (Figures 28 and 29) respectively show this from the location of the group centroids. The centroids of three smallest rounds—7.62 mm, 12.7 mm, and M910 are very close as are the centroids of M793 and TPGID. The boundary values for the discriminant functions below are $f_1(-15,25)$ and $f_2(-4,4)$. The group centroids are provided in Table 17.

The three models developed in this collection phase were tested against a new set of data during the verification/validation test along with the brassboard system. Those results are given in section 9.

5.3.3 Location and Velocity Data Reduction. The microphones were placed in the H configuration, two lines of three microphones each (Figure 30). For this study, the intersection of Hyperbolas of Ambiguity method was used to calculate offset distance. The predicted locations were on average 24 cm away from the actual video scored locations, and the predicted velocities were within 3% (see Appendix H). Errors in location and velocity are mostly due to the projectile's incoming angle. The projectile must travel parallel to the centerline connecting the two center microphones for the calculation to be accurate. As this incoming angle increases, the calculated errors increase quadratically.

6. RDS ALGORITHM DEVELOPMENT

6.1 Theoretical Formulation Technique. The total duration formula described in equation 2 was based on test data with small-caliber projectiles fired from M14 and AR15 rifles (Kalb, unpublished). The constant value of 1.82 was used in the formula for small-caliber ogival bodies. A new variable was created for this constant and named the acoustic shape constant, K. During phase I and II of the data collection testing, each K was solved for by rearranging Schochko's (1966) formula for K and plugging in the known values.

Table 16. Model III Classification Results

Actual Group	No. of Cases	Predicted Group Membership						
		1 7.62 mm	2 12.7 mm	3 M910	4 M793	5 TPGID	6 M724/ M865	7 M490/ M831
1. 7.62 mm	17	15 88.2%	2 11.8%					
2. 12.7 mm	15		12 80.0%	3 20.0%				
3. M910	9			2 22.2%	7 77.8%			
4. M793	9				6 66.7%	3 33.3%		
5. TPGID	18					18 100.0%		
6. M724/M865	14						14 100.0%	
7. M490/M831	15							15 100.0%

NOTE: Cases correctly classified: 89.69%.

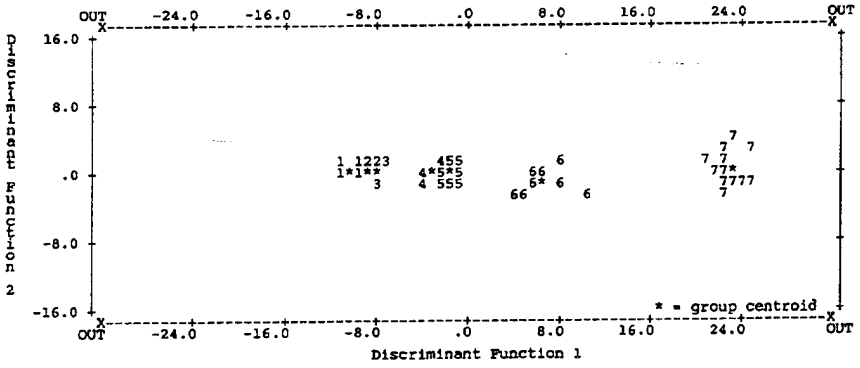

Figure 28. Model III: scatterplot.

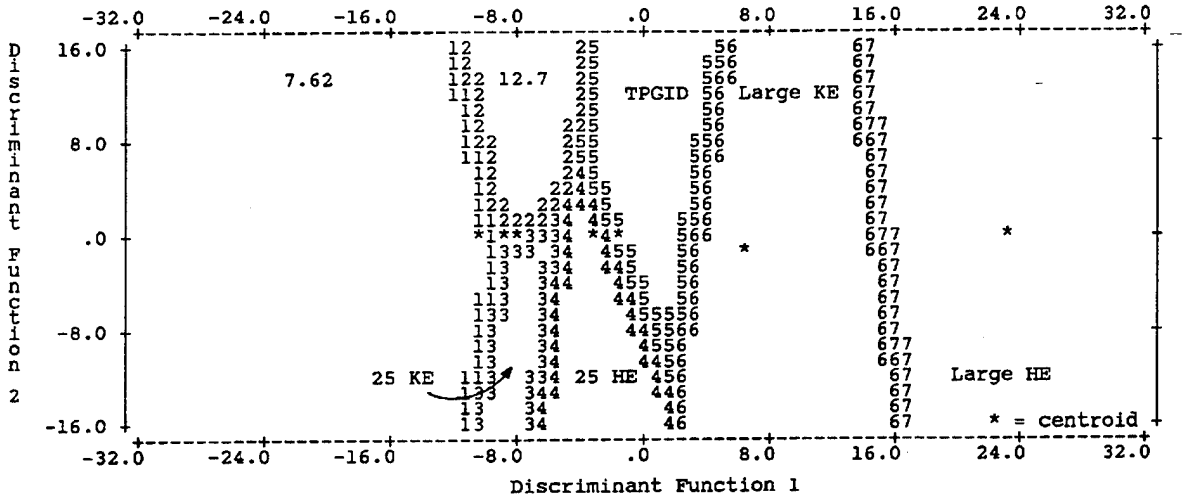

Figure 29. Model III: territorial map.

Table 17. Model III Group of Centroids

Group	f_1	f_2
7.62	−10.574	0.198
12.7	−8.561	0.515
M910	−8.036	−0.132
M793	−3.415	−0.581
TPGID	−1.444	0.037
M724/M865	6.787	−0.878
M490/M831	22.815	0.464

$$K = \frac{T\ a(M^2-1)^{3/8}\ L^{1/4}}{O^{1/4}\ M\ D}. \tag{23}$$

An averaged K value was then determined over the velocities and offset distances tested. Since each projectile has unique physical properties (diameter and length) and K value, equation 23 was rearranged to equate the projectile physical dependents on one side with the measured values on the other. The projectile dependents were grouped together and labeled the projectile shape value (PSV). The formula becomes

$$PSV = \frac{D}{L^{1/4}}K = \frac{T\ a(M^2-1)^{3/8}}{(O)^{1/4}M}. \tag{24}$$

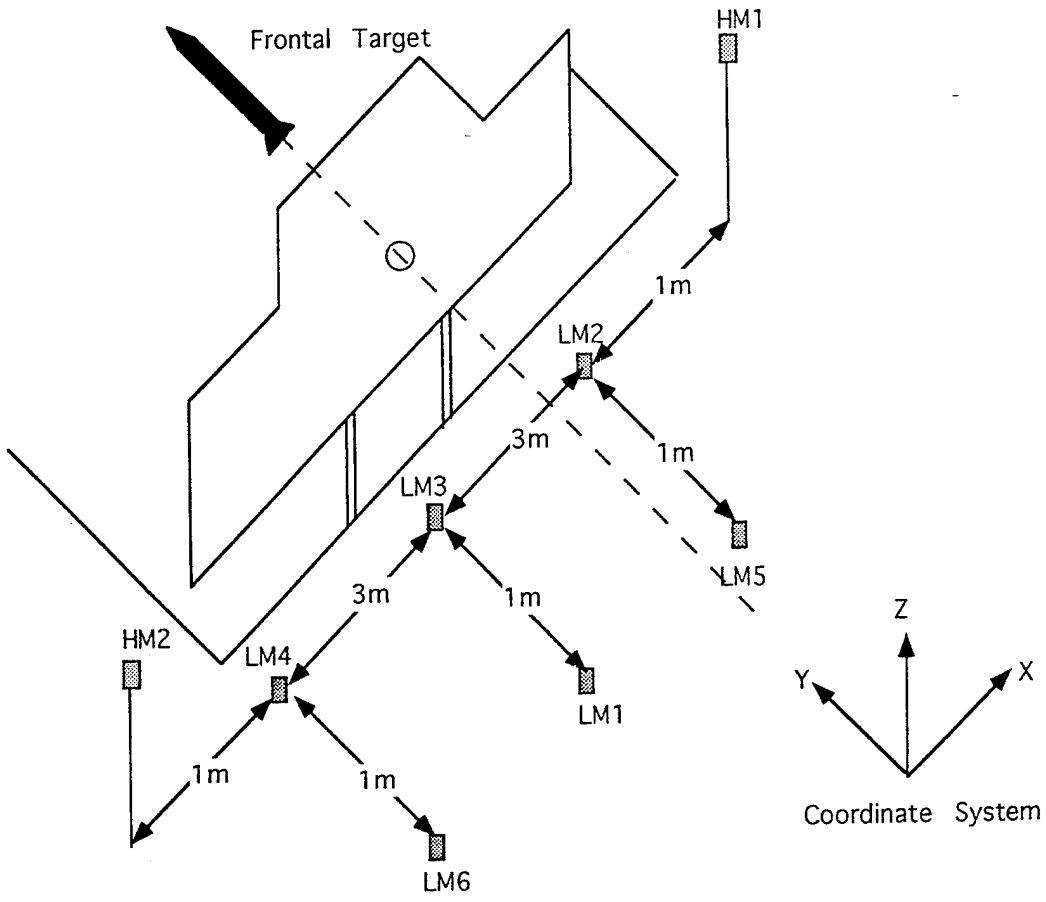

Figure 30. Data collection test microphone array and target setup.

Table 18 contains the empirical PSV and category for each projectile type tested. The measured values were input into equation 3 after the raw analysis. Next, the measured were compared to the empirical values. The system identifies the projectile type by calculating the smallest measured empirical PSV differential.

After the data were analyzed and the measured values were input into equation 24, the next step was to check to see how these values compared with tabular values. This was accomplished by finding the difference of the measured PSV from microphone 1 and the theoretical PSV and selecting the projectile type that best agrees.

$$PSV1 = \frac{D}{L^{1/4}}K = \frac{(T\ Mic\ 1)a(M^2-1)^{3/8}}{(O\ Mic\ 1)^{1/4}M}, \tag{25}$$

Table 18. Average Projectile Shape Values

Gun Caliber (mm)	Projectile Type	Diameter (mm)	Length (m)	Average K	Average PSV	Projectile Category (mm)
7.62	M59 (ball)	7.82	0.032	2.08	0.038	7.62
7.62	M62 (tracer)	7.82	0.034	2.16	0.039	7.62
12.7	M33 (ball)	12.95	0.059	2.11	0.056	12.7
12.7	M17 (tracer)	12.95	0.059	2.21	0.058	12.7
25	M910 (KE-TP)	16.20	0.076	1.99	0.062	25 KE
25	M793 (HEI-TP)	25.00	0.115	2.18	0.093	25 KE
35	TPL (KE-TPGID)	35.00	0.180	2.04	0.110	35
35	DM18 (HE-TPGID)	35.00	0.180	2.12	0.114	35
35	DM68 (HE-TPGID)	35.00	0.180			35
105	M724 (KE-TP)	63.50	0.256	1.72	0.154	105/120 KE
120	M865 (KE-TP)	38.00	0.468	3.71	0.170	105/120 KE
105	M490 (HEAT-TP)	105.00	0.654	2.50	0.291	105/120 KE
120	M831 (HEAT-TP)	120.00	0.844	2.37	0.296	105/120 KE

PSV1 = PSV for HM1

Remainder1 = abs (PSV1- PSV).

The remainders were ranked from the smallest to the largest. In the same manner, the PSV for microphone 2 is solved for

$$PSV2 = \frac{D}{L^{1/4}}K = \frac{(T\ Mic\ 2)a(M^2-1)^{3/8}}{(O\ Mic\ 2)^{1/4}M}, \tag{26}$$

PSV2 = PSV for HM2

Remainder2 = abs(PSV2- PSV).

The remainders are ranked from smallest to largest.

If both rankings agree, that is the projectile type predicted. If not, there are three possible cases where the ranks are different. In case 1, PSV1 is closer and greater than round type A, and PSV2 is closer and lesser than round type B. This yields two positive remainders for round type A and two negative remainders for round type B. Round type B is selected. In case 2, PSV1 is closer and greater than round

type A, and PSV2 is closer and lesser than round type B. Round type A is selected. In case 3, PSV1 is closer and lesser than round type A, and PSV2 is closer and greater than round type B. Take the average of PSV1 and PSV2 and reevaluate the remainder to find the round type.

Figure 31 shows the projectile terminal velocity plotted against PSV. It can be seen that some PSV's from different round types overlap at extreme conditions. All of the projectiles fired have well-defined velocities at known ranges (see Table 2). If a PSV is computed and there are two possibilities, the correct round type can be selected if referenced to the velocity axis. For instance, the 12.7-mm and 25-mm KE rounds have similar PSV's. If the terminal velocity of the projectile fired was greater than 850 m/s, the 12.7-mm round could be ruled out as a possible choice since it cannot achieve that velocity. This model was called the theoretical model.

6.2 Hybrid.

6.2.1 Discriminatory Analysis for PSV. The quasi-empirical formulation for PSV is a function of the same significant variables used in the empirical model, total duration, microphone offset distance, and velocity. The theoretical and the empirical results were combined to form a "hybrid" model. The PSV will be used in the discriminant analysis.

From the data collected in the feasibility phase and data collection phase, the projectile shape was tested to determine if it could serve as a discriminator of the seven groups. Discriminant analysis was implemented with the model based on the data collected from the 6-m microphone. This distance was chosen since this was the same location for the high-fidelity microphones as planned for the live-fire validation test. The classification of the remaining data was performed for a sensitivity check of the model.

The model with projectile shape alone resulted in 8 misclassifications and 94 correct classifications for a success rate of 92.16%. The shape variable was added to the database of variables to determine if it were a superior discriminant variable when compared to the other variables. Using the discriminant analysis models, PSV was found to improve the performance of the classifications. PSV's were first to enter the model with ln(total duration) following. The correct classification rate dropped to 85.29%. Although total duration was allowed to enter the model based on the tolerance criterion, the pooled group correlation between shape and ln(total duration) was 0.814.

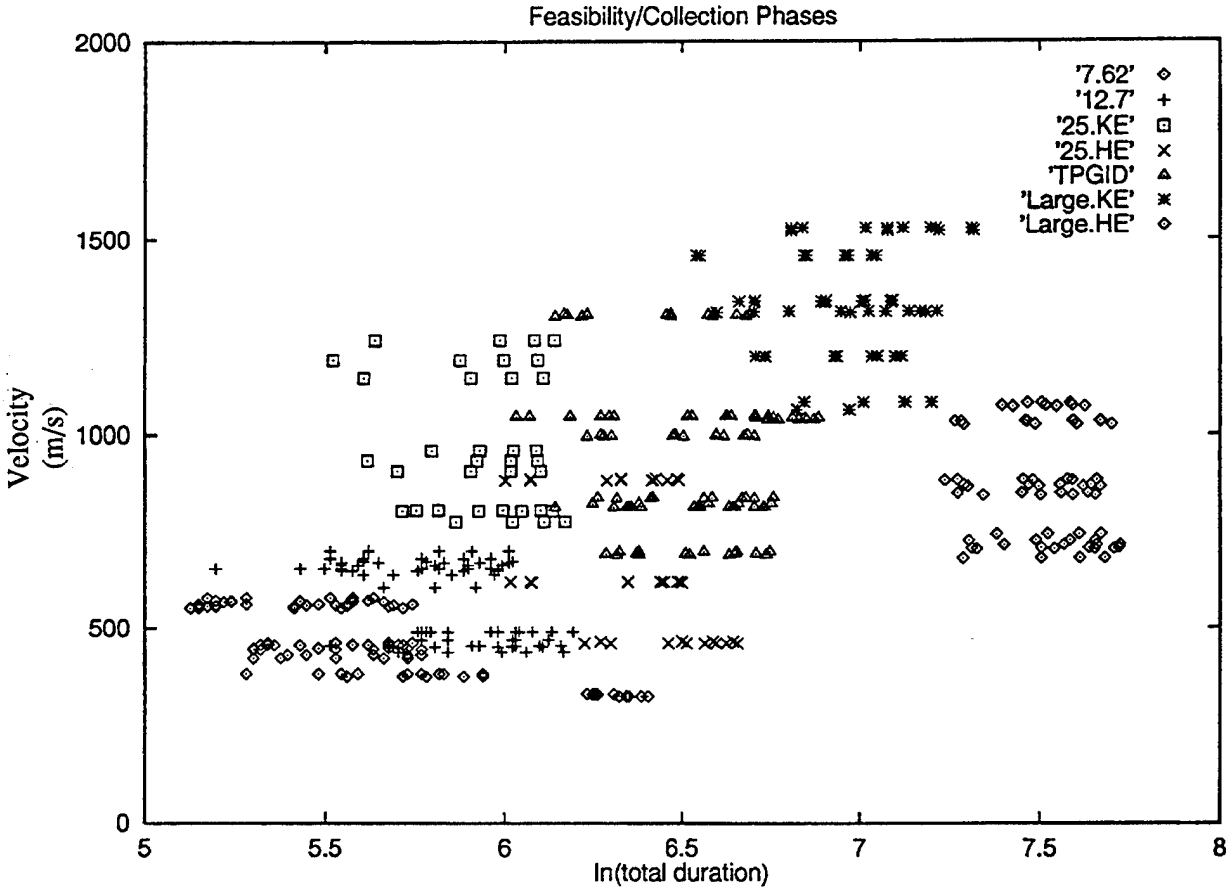

Figure 31. ln(total duration) vs. velocity.

Velocity became the variable to enter the model after PSV. This was intuitively appealing, since PSV was basically replacing ln(total duration) in the earlier model formed with ln(total duration) and velocity. If we compare plots of ln(total duration) vs. velocity (Figure 31) with PSV vs. velocity (Figure 32), we notice that the relative positions of the round groups are similar. The plot with PSV forms tighter groupings.

The two-function model with variables PSV and velocity, equation 27, provided a 99.02% correct classification rate from the 6-m data, with one 25-mm KE misclassified as a 12.7-mm round. The discriminatory functions F_1 and F_2 plotted in Figure 33 resembles the data in the original units of PSV vs. velocity Figure 32.

$$\begin{aligned} F_1 &= -22.757 + 144.233\ \text{PSV} + 0.00500\ \text{Velocity} \\ F_2 &= -3.904 - 10.733\ \text{PSV} + 0.00632\ \text{Velocity}. \end{aligned} \tag{27}$$

6.2.2 Model Implementation for Prediction. A model was developed that separated the seven types of rounds with good success. The true test of the adequacy of the model would come when additional rounds were fired in the verification/validation phase (section 9). How is the two-function model implemented once the data are collected? First, the centroids of each group were calculated for both functions as provided in Table 19.

Table 19. Group Centroids

Group	F_1	F_2
7.62	−14.765	−1.296
12.7	−11.495	−0.909
M910	−8.781	1.716
M793	−5.610	−0.787
TPGID	−1.338	0.848
M724/M865	7.800	2.678
M490/M831	25.093	−1.586

Second, boundary conditions for F_1 and F_2 were determined to guard against signals outside of the target area of interest. This is not really necessary since the round location method would not allow the

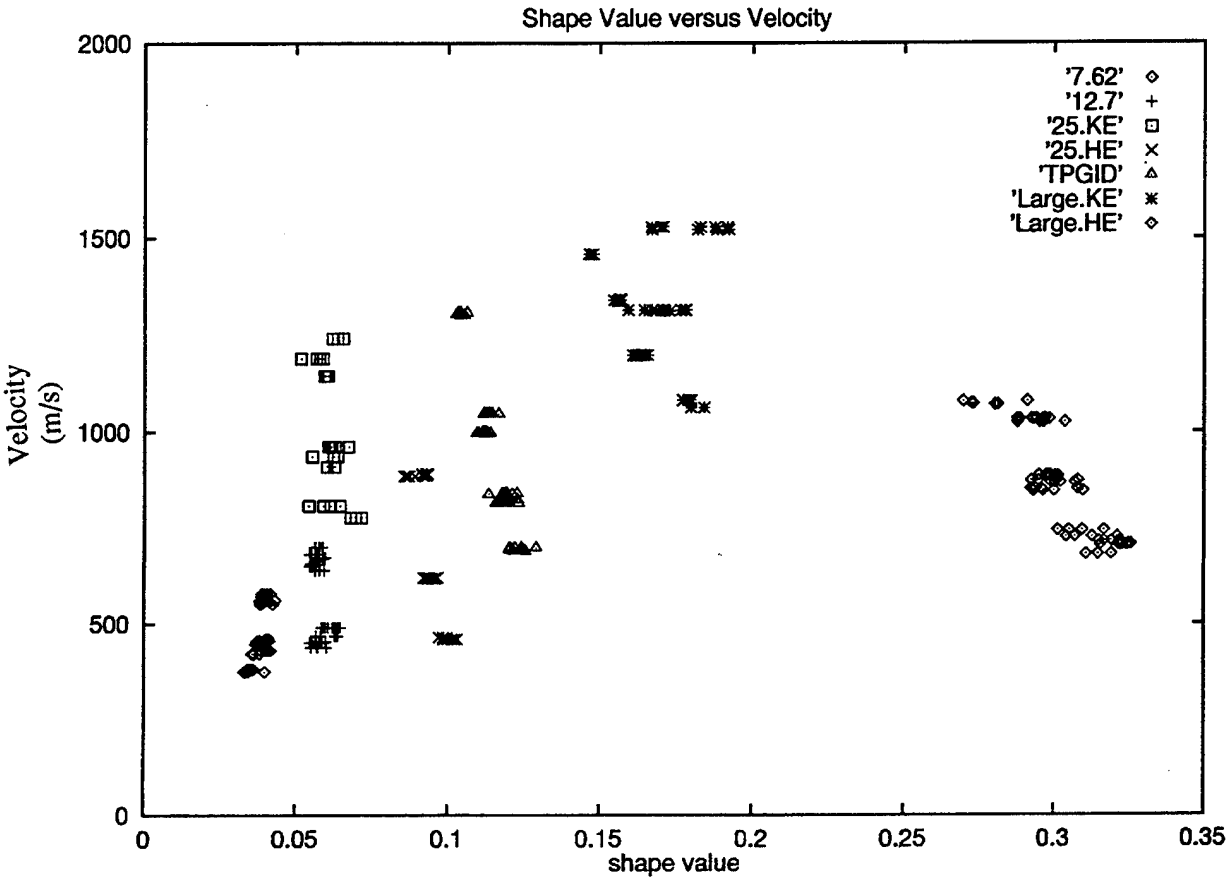

Figure 32. PSV value vs. velocity.

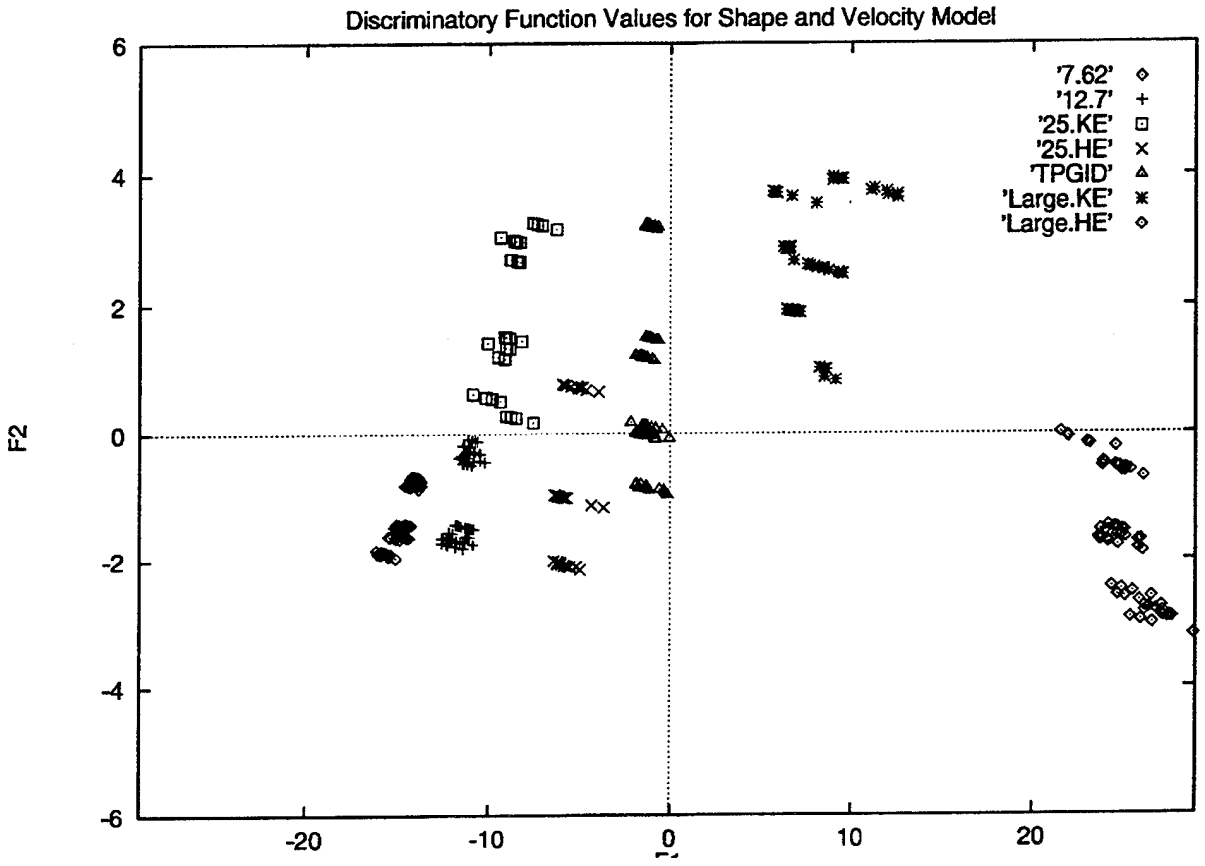

Figure 33. Discriminatory functions F1 and F2.

target to drop if the round did not hit the target. But to implement the round discrimination method independently of the round location method, boundary conditions are necessary. The boundary area is a simple rectangular area in F_1 and F_2 space. The minimum and maximum values for each function is: F_1 (–17.0, 29.0) and F_2 (–4.5, 5.5).

When an unknown round is fired at the target, the total duration, microphone offset distance, and velocity will be collected, and the PSV will be computed. Then values of F_1 and F_2 are computed for this round. The distance is calculated between the unknown round and each group centroid. The minimum distance will dictate the classification of the unknown round.

Because two microphones will be placed on each side of the target in the verification/validation test to collect total duration data, two pair of discriminant scores will be computed, one for the left microphone and one for the right. It is possible that the minimum distance of the discriminant score for the left microphone classifies the unknown round into a different group as the right. In that case, the final group assignment would be the smallest of those two minimum distances.

7. SOFTWARE DEVELOPMENT

A microprocessor was determined to be the most effective way to process the input data using the model, perform decisions, and execute commands. The RDS needed to take the data developed by the sensors after a round was sensed. The signals for location and acoustic signature were to be processed, and the values of that process utilized by the prediction model. Once a prediction was made as to round type and location of hit, commands based on a decision of "kill," "hit but no kill," and "no hit" would command the RETS system. A 486 PC/104 embedded computer was selected as the microprocessor due to the ease of programming, ability to use peripherals (disk drives, monitors, and keyboards), and accessibility to remote sites. Additional hardware consisted of power supplies, a floppy drive, a hard drive, and three electronic interface boards. The boards were designed and fabricated at ARL. They were the location interface board, the sensor interface board, and the A/D board. To control the computer, special software was generated.

The software for the RDS system was developed in Microsoft C to run under an IBM PC or compatible platform. The I/O devices used to collect the signal wave forms and counter values were memory-mapped devices which enabled a high rate of data transfer. Two data files were created to run

the program. The first file is called "locate.dat" and contained microphone and target coordinates needed to calculate round location. The second file was called "shapes.dat," and it contained "shape values" needed to categorize rounds for identification.

The program began with a series of questions to initialize the system. The first question asked whether or not results will be transmitted back to a remote location. The second question asked whether or not raw data and results will be saved onto the hard disk. If data and results are to be saved, a file name was specified. Finally, the program asked what type of target was being used for the training exercise.

The system waited for a hardware trigger signal from any one of the location microphones. The trigger was caused by the shock from a projectile flying by any of the location microphones. While the system polled the trigger line, a 2,000-point circular buffer was being continuously filled with data collected through the high-fidelity microphones and into the dual-channel analog-to-digital board at a rate of 250 kHz per channel.

When triggered, 1,000 points of shock wave data were collected from each high-fidelity microphone. A total of 12,000 points of shock wave data were collected from each high-fidelity microphone when the circular buffer data were added. The circular buffer contained pretrigger data which ensured the entire wave form of the shock wave was preserved in case the shock wave reached the high-fidelity microphones before the location microphones which triggered the collection.

Counter values were next read in from the quartz counter board. There were five counters, and each measured the relative delay of the shock wave as it passed between adjacent location microphones. Figure 34 shows how the counters were set up in relation to the location microphones. Each counter was controlled by a pair of location microphones; Counter 0 by LM1 and LM2, Counter 1 by LM2 and LM3, Counter 2 by LM2 and LM5, Counter 3 by LM4 and LM5, and Counter 4 by LM5 and LM6. Counters started counting when either one of its controlling microphones encountered the shock wave and stopped when its other controlling microphone encountered the shock wave (both controlling microphones could start or stop the counter). Knowing the rate at which the counters counted and the counter values when they stopped, the time delays of the shock wave between microphones are then determined. In addition to the counters, four data bits were read to determine which of the microphones in each pair started each counter counting. The sign of the counters was adjusted accordingly from these four data bits to show if the round came from the left or the right.

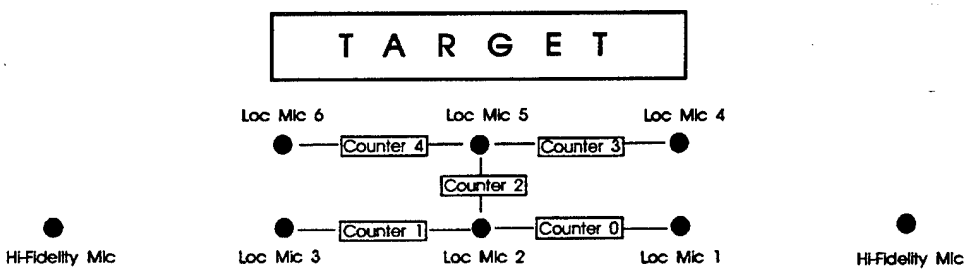

Figure 34. Location microphones.

Using the counter values, the location of the round on the target, the offset distances of the round from the high-fidelity microphones, and the round velocity were calculated. The round velocity was calculated first using Counter 2. The location and offset distances were calculated using velocity and Counters 0, 1, 3, and 4.

Using the shock wave length, round velocity, and round offset distance from the high-fidelity microphones, the round type was determined. To calculate the shock wave length, the wave form data was first passed through a five-point moving average smoothing filter to eliminate random noise. Next, the data was truncated to 500 points to eliminate the data points before and after the shock wave. The shock wave length was found by performing a point-by-point differentiation of the remaining 500-point wave form, picking out the two peaks. The separation between the two peaks corresponded to the shock wave length. Figures 35a through 35d graphically illustrate the process of finding the shock wave length.

After the round location and type had been determined, the program checked if the round hit inside the kill area and if the round type could kill the target type. If both of these conditions were true, the program would signal the RETS to lower the target. The RDS would accept a signal from the RETS vibration sensor, which indicates a round striking the target. The round type, location, and velocity was radioed back to a remote site via a modem and hand-held radio. The system was reset to the initial values.

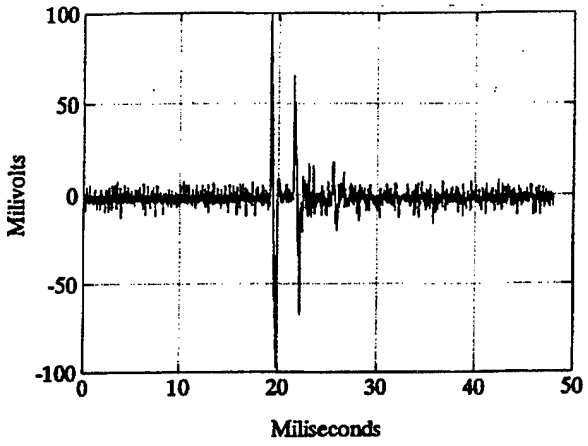

Figure 35a. N-wave (12,000 pts).

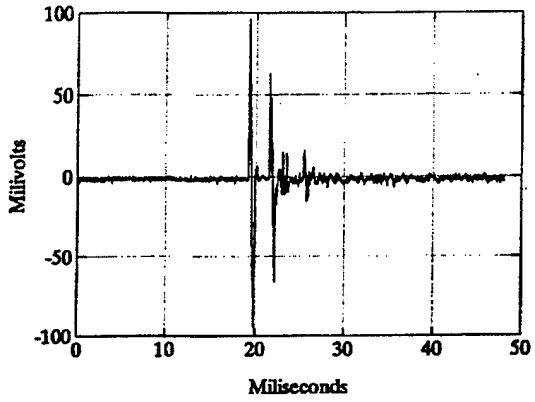

Figure 35b. Filtered N-wave (12,000 pts).

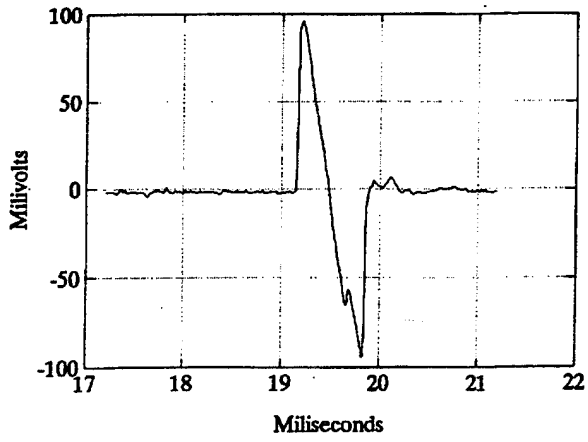

Figure 35c. Truncated filtered N-wave (1,000 pts).

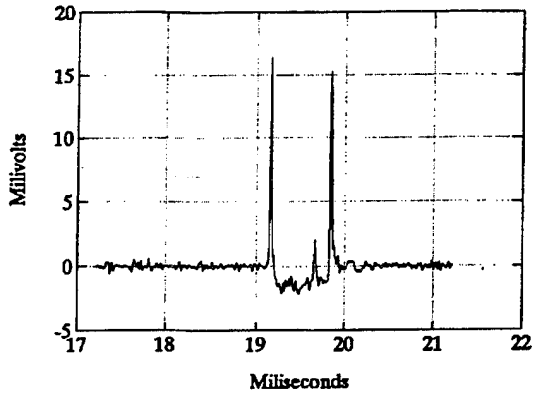

Figure 35d. Point-by-point differentiation (1,000 pts).

8. BRASSBOARD

8.1 Theory of Operation. The RDS brassboard was a stand-alone system that directly interfaced with the RETS. The RDS sent a kill signal to the RETS when the system discriminates the round. It is a modular PC-based system, and it has its own radio communication link to the range control tower. The RDS brassboard was made of off-the-shelf components except for the two electronic interface boards. The system operates on 110-V/60-Hz or 220-V/50-Hz AC power.

Prior to running the RDS, software initialization was required with each power up. Temperature, target type, microphone positions relative to the target, and kill zone information must be entered by the user. There was a storage option where all raw data could be stored on the hard disk for post-test analysis. After initialization, the system established radio communication with the tower. When this connection was established, the RDS was set. As a round flew through the sensor array, the RDS was triggered by shock wave impinging on one of the location microphones. The two high-fidelity microphones captured the shock wave. The RDS computer calculated the durations, the Cartesian position of the round, and the velocity of the round.

With the durations, the microphone offset distances (derived from the location information), and the velocity, the RDS identified a round type. If that round satisfied the kill criteria for that particular target type and it was within the kill zone, the RDS sent a "target down" signal to the ECU of the RETS. The RETS lowered the target as if it received a target down signal from the vibration sensors. The round identification, location, and velocity information was transmitted back to the tower. Another PC in the tower displayed a picture identification of the round, an "X" on a tank silhouette target, and the velocity (see Figure 37). The RDS transmitted results to the tower each time the system was triggered, regardless if the kill criteria was satisfied. It took 2 s for the RDS to process and transmit data, but it took 10–15 s if the storage option was enabled. During the processing time, any other incoming round would be ignored. The RDS brassboard logged the vibration input. It was not part of an algorithmic decision. The RDS was PC compatible. This enabled the designers to use DOS and Windows application software and hardware to develop the discrimination algorithms (Figure 36) and the communication system.

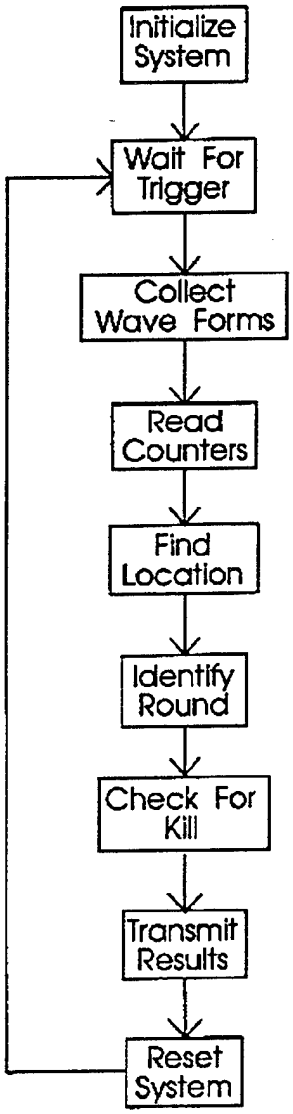

Figure 36. Algorithm flow chart.

8.2 Construction.

8.2.1 Location Interface Board. The location interface board (LIB) was a 6-in × 6-in printed circuit board (PCB) that incorporated a similar circuit designed by Dr. Joel Kalb of the Human Research and Engineering Directorate (HRED) for his round location system. The RDS's version had six electret microphone inputs instead of four. The additional inputs were the right front and left front microphones. The microphone front-end electronics, threshold comparator, debouncing latches, and time difference gates were identical to Dr. Kalb's (Kalb, unpublished).

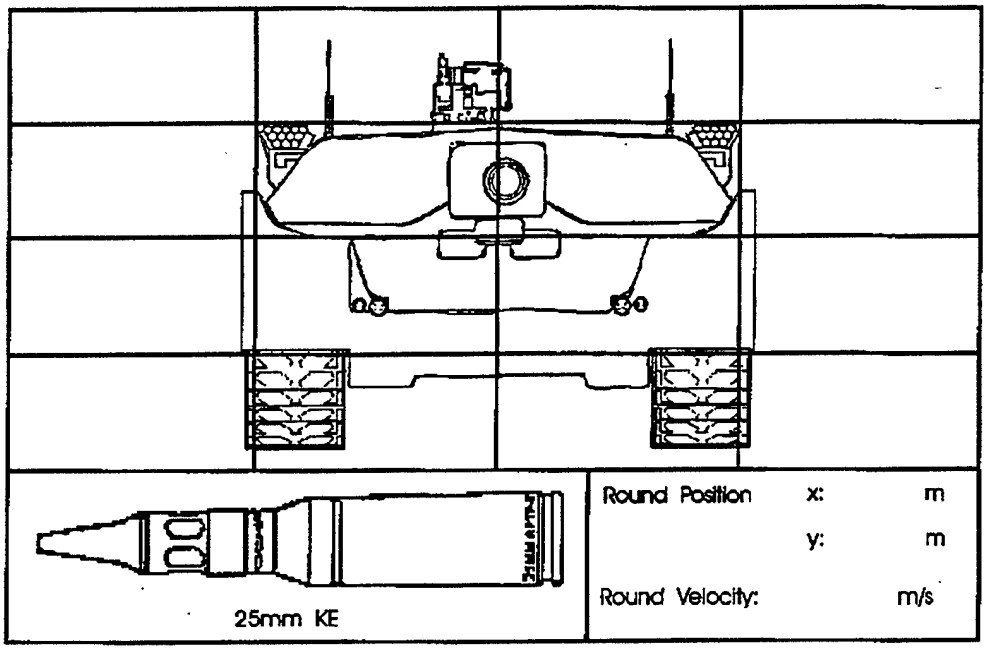

Figure 37. Tank silhouette.

The LIB provided power to the six-electrode microphones and measured the time delays between location microphones. The board had outputs from five time difference gates and four direction registers. The gates measured the time delays between pairs of microphones: front left and front center, front right and front center, back left and back center, back right and back center, and front center and back center. Each gate sent a pulse when one of the two microphones was triggered, and it sent another pulse when the second microphone was triggered. Each direction register associated a negative or a positive sign to each time difference gate except for the two center microphones. It was assumed that the shock wave would impinge upon the front row of the array before the back row. The outputs of the LIB fed directly into the PC/104 computer through the counters and I/O's mini-module. The time duration and direction of fire calculations were done by software.

In addition, the LIB had a NPN transistor circuit for the target down signal. When the discrimination algorithm determined that the target should be lowered, the computer sent a 5-ms pulse to the circuit. The circuit acted as a driver and sent an inverted pulse (HIT SIG) to the ECU of the RETS to lower the target. Refer to LIB circuit diagrams for further details (Figure 38).

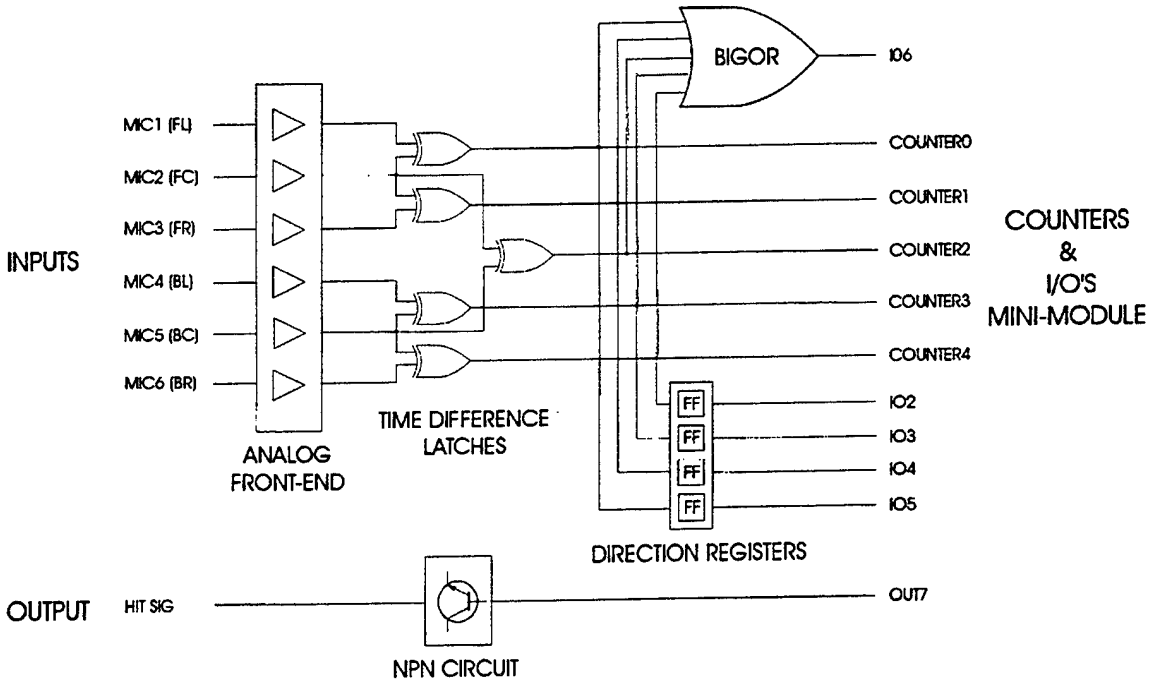

Figure 38. Location interface board circuits.

8.2.2 Sensors Interface Board. The sensors interface board (SIB) was also a 6-in × 6-in PCB. It contained circuits for the high-fidelity microphones (B&K's and Countrymans), the vibration sensors, and additional electronics for future use such as the switches and LED's. Only the circuits for the B&K microphones and the vibration sensors were used. The RDS brassboard used two high-fidelity B&K microphones to capture the supersonic shock waves. The interfacing circuit was a simple voltage divider with gain of 1/4 and impedance buffer. The two outputs were fed directly into the A/D's.

The SIB had two vibration sensor inputs. The vibration circuit was identical to the one in the RETS ECU except for the hit sensor failure circuit (TM9-6920-442-14&P). As soon as one of the two vibration sensors was triggered, the circuit produced a 5-V, 1–10-ms output, signifying a tagged hit. This HIT signal was fed into the computer by a register on the A/D board. Refer to SIB circuit diagrams for further details (Figure 39).

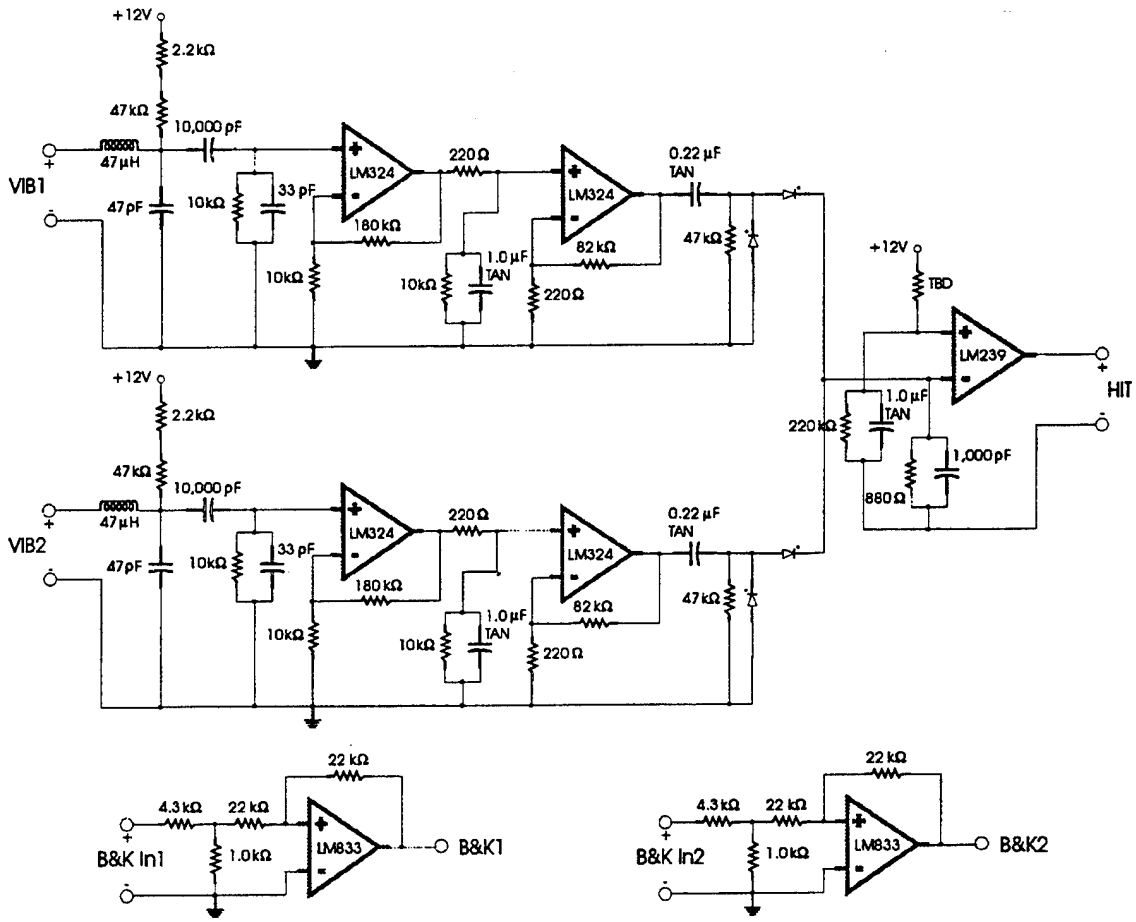

Figure 39. Sensor interface board circuits.

8.2.3 A/D Board. The A/D board was a 4-in × 4-in PCB with a PC/104 bus connector that stacks onto the PC/104 computer. It had two 12-bit analog-to-digital converters (ADC) with track and hold. The ADC's, part no. MAX120 from Maxim Integrated Products, ran on a 4-MHz clock and sampled at a 250-kHz rate. The A/D board had encoding and decoding logic that enabled the data bus from the ADC's to interface directly with the PC/104 bus. The digitized data from the ADC's were continuously being dumped on the bus. The computer took the data and stored them in a circular buffer. When one of the location microphone was triggered by the shock wave, the BIGOR gate from the LIB sent a pulse to the computer through a register on the A/D board to collect 10,000 more data points. After the 10,000th point, the computer stopped the ADC's from dumping anymore data onto the bus. The ADC's remained in this state until the computer finished with the discrimination algorithm. The A/D board also accepted the HIT signal from the SIB. The software logged the HIT signal, but it did not use the signal in any decision process. Refer to the A/D board circuit diagrams for future details (Figure 40).

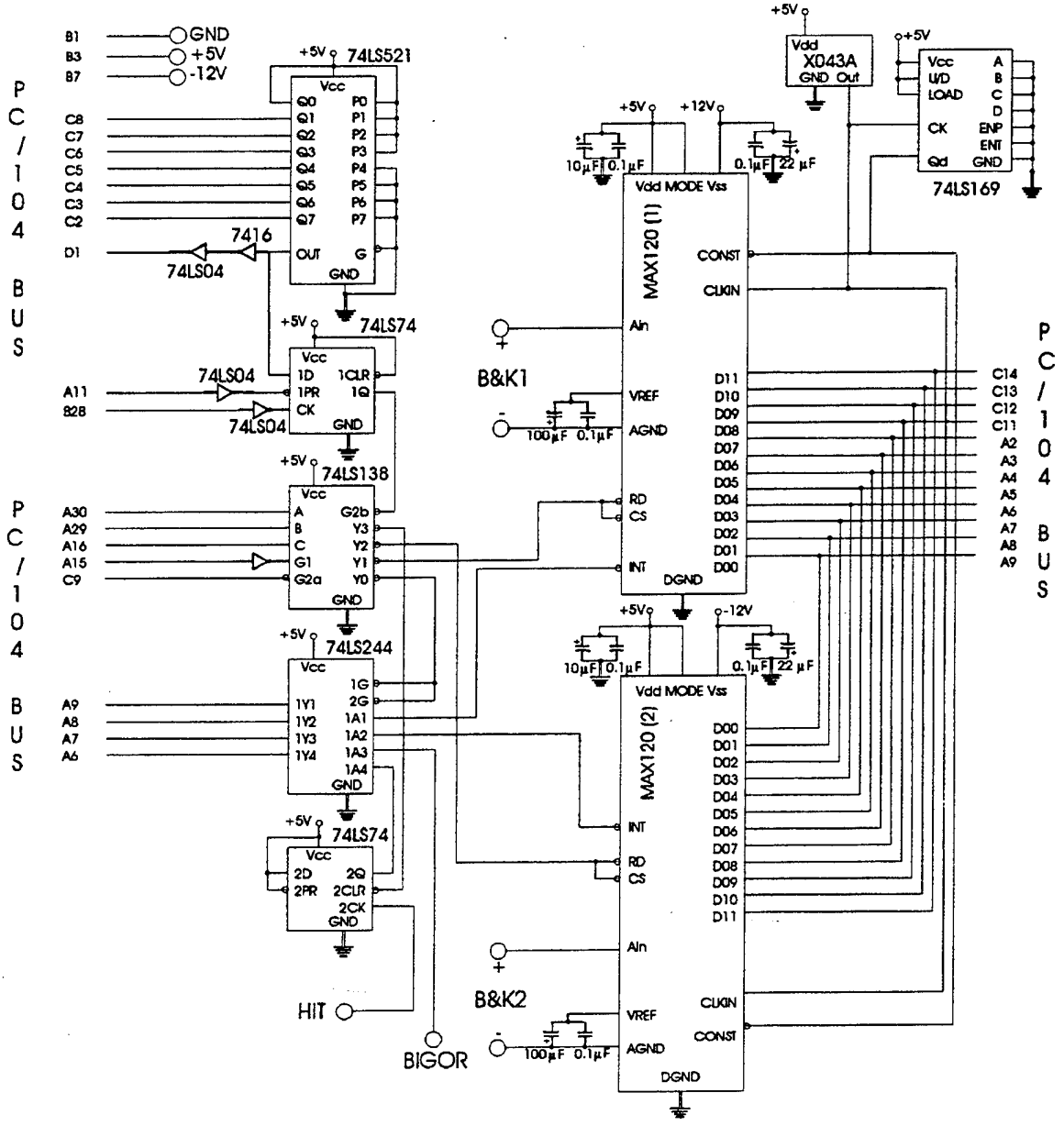

Figure 40. A/D board circuit diagram.

9. RDS INTEGRATION WITH RETS.

9.1 Electronics Packaging. The RDS brassboard system architecture is shown in Figure 41. The system was housed in a 24-in × 20-in × 12-in stainless steel box with a sealed lid. The box will protect the electronics from rain and fragment debris. On the outside of the box, there were six location microphone input connectors (MIC1 to MIC6), two high-fidelity microphone input connectors (B&K1 and B&K2), two vibration sensor input connectors (VIB1 and VIB2), one target signal down output connector (HIT SIG), a parallel port, a serial port, a VGA monitor input, and a keyboard input. Eight 40-ft-long, shielded, twisted pair cables connected the microphones to the RDS unit. A 20-ft cable connects the HIT SIG output to the RETS's ECU.

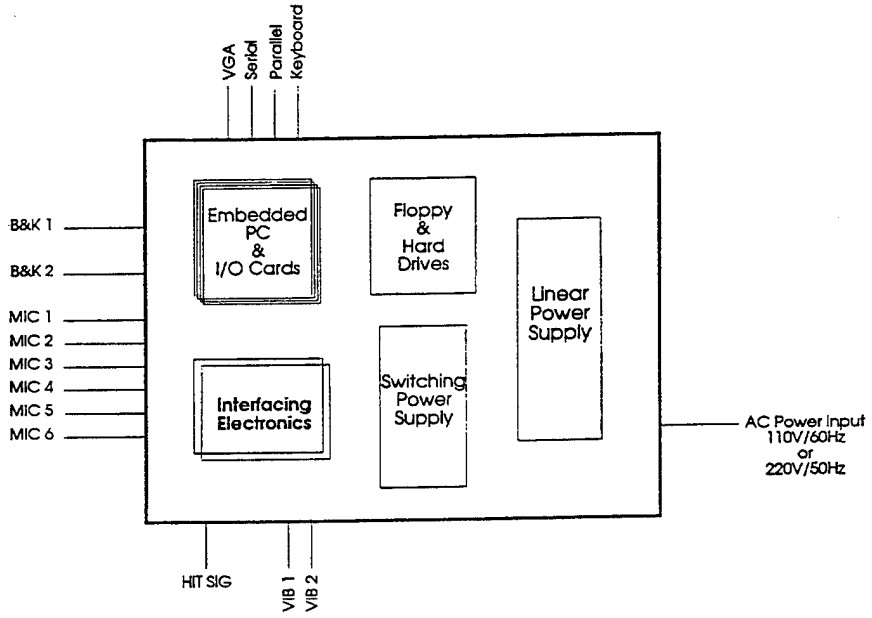

Figure 41. RDS system diagram.

The core of the RDS brassboard was the PC/104 embedded computer. The computer was composed of four 4-in × 4-in stackable modules: a 486-25SX CPU core module with a math coprocessor, a hard/floppy disk controller mini-module, a SVGA mini-module and a counter, and a I/O's mini-module. The embedded computer only required a single +5-V, 750-mA power supply for operation. The PC/104 embedded architecture was chosen because it is compact and modular. During the development phase, a more sophisticated computer system could be assembled by stacking more mini-modules. A mini-module can be a flash memory card, a data acquisition card, an I/O card, or a communication card. The RDS brassboard only used four modules. Only the 486-25SX core module and the counters and I/O's mini-module were needed for operation after system initialization.

9.2 ECU Connection. The RDS brassboard interfaces with the RETS with no modification. Due to time, budget and proprietary RETS hardware constraints it was impossible to incorporate the RDS outputs into the RETS's communication system without working and consulting with Paramax System Corp., the main RETS contractor. Instead, a separate radio communication subsystem for the RDS was designed and used. In the future, however, the RDS outputs would be incorporated into the RETS's CCU, and the results would be displayed in the control tower.

The RDS interfaced with the RETS through the ECU of the RETS. It hooked up to the RETS by disconnecting all vibration sensors from the ECU. Then, connecting two of those vibration sensors to the RDS vibration sensor inputs, VIB1 and VIB2, and connecting the RDS's target down signal output, HIT SIG, to one of the hit sensor inputs on the ECU, the hardware connection was then complete.

9.3 Radio Communication to Tower. In addition to the program written for the RDS hardware, a second program was written for the RDS system to interpret results sent to a remote site from the target area. As mentioned earlier, the target area and remote site communicated through a modem and hand-held radio at each site. The RDS computer communicated with the modem through a serial port. The modem was a Kantronics modem running at 9,600 baud while the radio was a Motorola GP300 VHF radio with an operating range of 146 MHz to 174 MHz. The radio frequency used was dependent on the usable frequency bands at each test site.

10. VERIFICATION/VALIDATION TEST

10.1 Purpose. The primary purpose of the test was to verify the performance of the RDS brassboard and validate the system's operational capabilities within the spectrum of live-fire conditions expected on a U.S. Army training range. A secondary purpose was to allow private contractors the opportunity to verify/validate their own round identification systems and/or collect data that may assist in the future development of RDS for use on U.S. Army training ranges.

The verification test was conducted from 23 Jun–1 Jul 1993 at the high velocity range, APG, MD. A RETS lifter was used. Two 6-ft × 6-ft × 2-ft concrete blocks were placed to the left of the target to protect the RDS brassboard and radio communication system. The RDS was connected to the RETS ECU. The 7th ATC training environment was replicated as best as possible. A berm was built around the lifter to simulate the target pit. Discrimination microphones were attached to 1-m-long stakes. Location array

microphones were attached to stakes and located 20 cm above ground level. Support data for the test included Weibel radar velocity data, video scoring on the target, local meteorological data, and survey data. The test plan called for all training projectile types fired in the feasibility and data collection tests to be fired. The verification/validation test firing matrix and test results are presented in Appendix K. Average velocity errors of 3% and average location errors of 9 cm were observed.

10.2 Statistical Summary of Data at APG. Five models were constructed in sections 4 and 5, and each was evaluated against its ability to predict the rounds fired during the validation test. The five models include PSV formulation with equation 25 (Whitham's theoretical model), the three empirical models, and the Hybrid model.

The three empirical models and the Hybrid model that used discriminant analysis were not statistically optimal since the assumption of equality covariances for all the groups was not met. This indicated that the estimate of pooled covariance matrix was a biased estimate of the true but unknown covariance matrix. It was not surprising that Model III, with two total durations as variables in the model, did not have equal covariance matrices, since the covariances were not equal when only four groups were considered during the feasibility phase. Attempting to achieve this for seven groups to discriminate makes it even harder for all the models considered. Model II came closest to having equal convariances. However, it should be noted that due to these inequalities, some of the coefficients may be unstable. Nevertheless, using pooled estimates of the covariance matrix for each analysis resulted in robust algorithms for most of the models, based on the results from this phase of testing.

Table 20 summarizes the number of rounds correctly classified by each model. Four of the models performed comparably at around 90%; however, empirical Model III performed the worse. One problem with Model III stemmed from the microphone array. Two total durations were selected from the five microphones collecting the signatures. This change in configuration made the coefficients for the algorithm unreliable. The model resulted in poor prediction especially for the 25-mm rounds. The model predicted a 12.7-mm round in each case.

Model I used data from all the microphones. This fact made it appear that there were five times more independent shots than there actually were. The five duration values obtained from one shot were not independent outcomes, and the velocities paired with each of the five durations were the same.

Table 20. Model Comparison—Number of Correct Classifications

Round	No. of Rounds	Theoretical	Empirical			
			I	II	III	Hybrid
7.62 mm	3	3	1	1	1	3
12.7 mm	9	9	9	9	6	9
M910	9	9	8	9	0	9
M793	5	5	4	3	0	4
TPGID	15	15	15	15	14	15
M724/M865	10	8	9	9	4	9
M490/M831	11	6	10	9	5	7
Total	62	55	56	55	30	56
Percent Correct		89%	90%	89%	48%	90%

Model II has the greatest appeal of the three empirical models. The algorithm was developed from the 6-m microphone which is suited for the final microphone array. One data set of duration, microphone distance, and velocity corresponds to one round tested.

The theoretical model and the Hybrid model are favored, since they have a theoretical basis and provide prediction results equal to or greater than the other models. Although equation 25 was derived from smaller-caliber rounds, the model performed quite well, as did the Hybrid. Both models (as well as Models I and II) have redundancy incorporated in them. They only require one high-fidelity microphone for discrimination. The other microphone acts as a check and as a backup system if the other microphone malfunctions during training exercises.

Unusually high duration signatures measured for the large-caliber rounds became a problem during testing. These readings were at least 50% higher than expected, and they did not occur consistently on the same microphone. This affected Model III more than the other models because both microphones are required for round classification. It was hypothesized that the large durations were due to reflections off the concrete block protecting the instrumentation. If this were true, one would expect the effect to be greatest for the microphone closest to the concrete wall; however, this did not explain the high signal received from the microphone on the far side when the microphone closest to the wall recorded values as expected. The source of the reflection is unlikely to be from the ground. The problem was not resolved in this phase of the program.

11. DEMONSTRATION RESULTS AT 7TH ATC

The RDS brassboard and a backup system were transported to Grafenwoehr, Germany, for a live fire demonstration. On 14 July 1993, the RDS was set up in front of target V-16 on Range 117. Target V-16 was located approximately 1,500 m from the initial firing line. This target was chosen in order to get the best engagement ranges for both small-caliber and large-caliber weapons. The microphones and target locations were surveyed in the same manner as in previous tests (see Figure 30). Five different projectile types were fired from an M1A1, an M1A1 outfitted with TPGID, and an M2. Each vehicle was fired from a random location on the range. An orange kill zone was painted on the target. Thermal blankets were placed in the same area (see Figure 42). If projectiles were determined to be in that area, the RETS would be sent information to lower the target. During the pre-test, 9 out of 12 projectiles were identified correctly by the theoretical model, and the RETS system lowered the target when signaled by the RDS. The stored data was analyzed on-site to determine why the three projectiles were not identified. On-site data reduction revealed that acoustic reflections were being captured within the prescribed window being analyzed. These reflections were assumed to be only ground reflections.

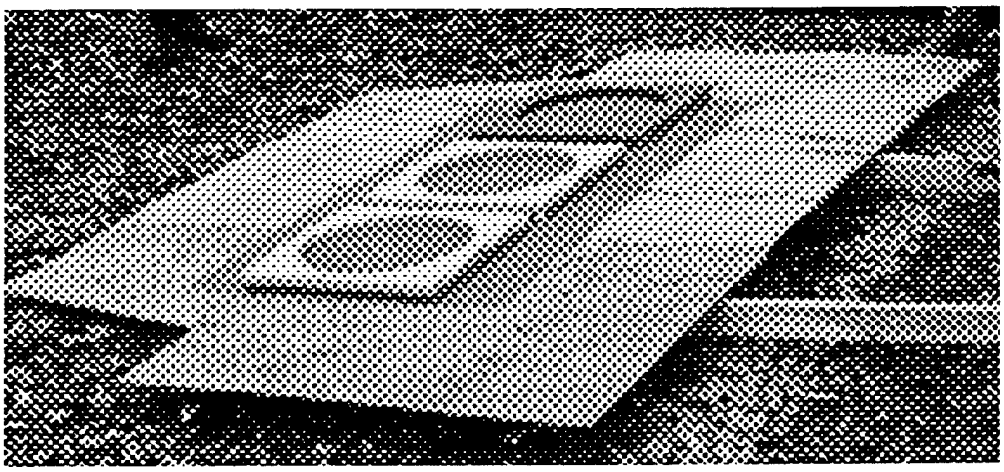

Figure 42. Kill zone.

These reflections sometimes caused an error in the total duration pulse period. A longer determination of total duration pulse period caused the algorithm to incorrectly identify the projectile. The predemonstration test matrix and results are located in Appendix L.

In an effort to separate any ground reflection from the N-Wave, the target was raised approximately 0.5 m for the demonstration test on 15 July 1993. The store mode was turned off so the RDS would compute real-time data reduction. The M1A1 with TPGID fired 10 projectiles. Only 3 of 10 TPGID rounds were identified as TPGID's. Similar results were recorded with the other projectile types fired. Problems were also encountered with the RETS interface. The RETS shorted during the demonstration and did not respond to the RDS communication. At that time, it was not known why the RDS performed so poorly. It was thought that ground reflections seen from the previous day caused the problems.

On the following day, the RDS was set up again with the store mode activated. Many projectiles were fired to gather data in the field. Due to rain, most of the data were not useful. Upon our return to APG, the pretest data were analyzed. It was determined that reflections were coming from the ground and from the top of the microphone stake. When the projectiles were fired around the microphone height or higher, the reflections were very close in time to the original N-Wave or even superimposed on the N-wave (see Figure 43). These reflections were mathematically determined to initiate from the flat surface on top of the microphone support stake (see Figure 44).

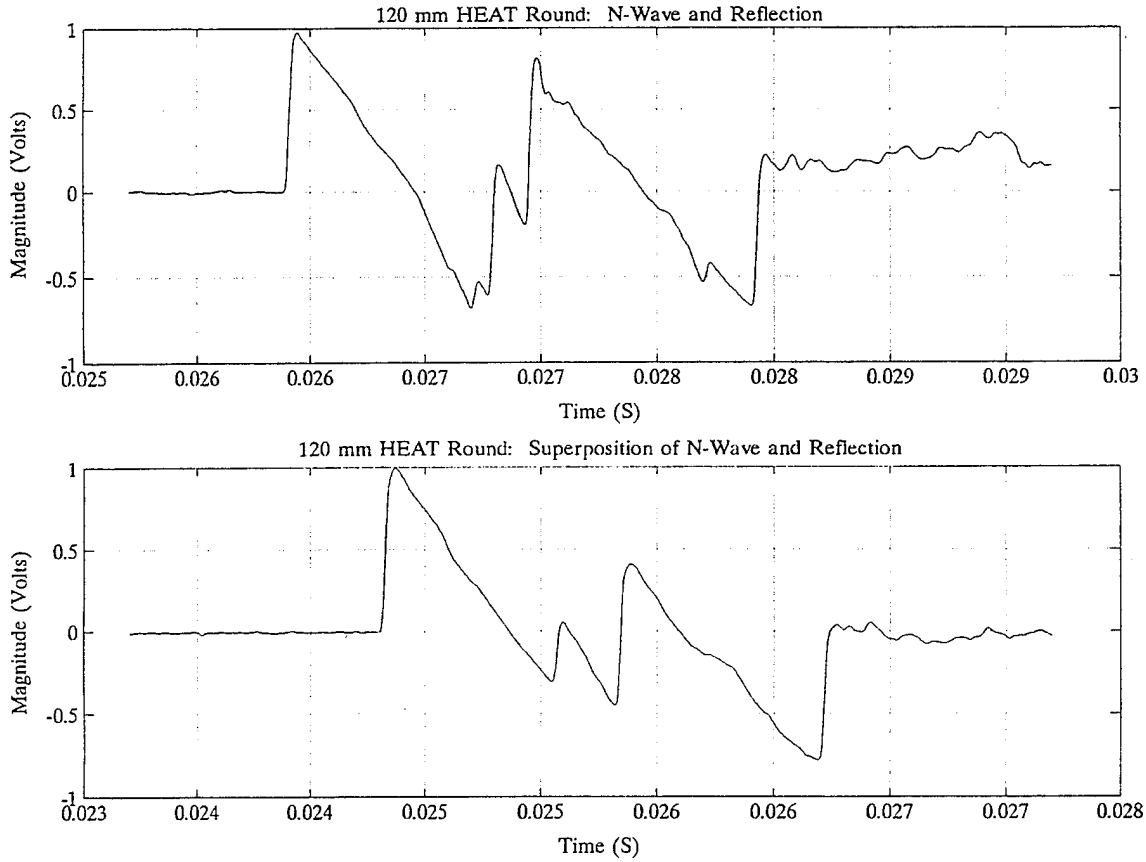

Figure 43. Microphone output due to a reflected N-Wave.

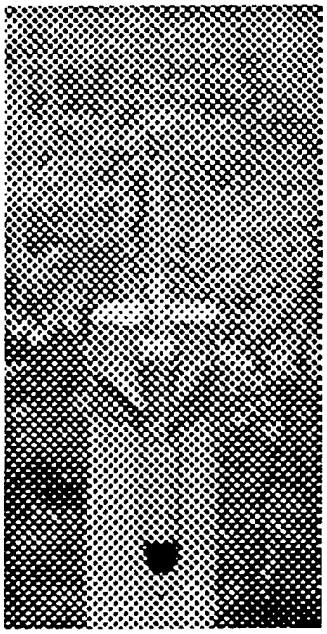

Figure 44. Microphone support stake.

The microphone location relative to the stake and ground surface was measured during this test. The shock's speed, projectile's speed, and, therefore, the Mach angle were also measured. The location of the projectile was hand scored at the conclusion of the test. The pressure time history of the N-Waves was recorded. Therefore, the distance that the shock wave traveled over time could be calculated. This value is represented as DIST1 and DIST2 for high-fidelity microphones 1 and 2. This distance was compared with the actual distance the shock wave would have traveled if reflected from the ground or the stake. The stake reflection represents the actual distance the shock wave traveled from the projectile to the microphone using the stake as a reflecting surface. By comparing the calculated reflection distance with those due to the ground or stake it can be shown in Table 21 that at least five of the projectiles had their N-Waves reflected off of the stake. Only those projectiles fired above the microphones had their shock waves reflected off of the stake. Only three of the five caused algorithm problems when computing N-Wave duration.

As a consequence of raising the target in the demonstration test, the projectiles were fired higher relative to the ground level. This separated the time between N-Wave and ground reflections but caused the problem of stake reflections. They were even more prevalent than during the pretest and resulted in the poor demonstration results. The problem could have been resolved by using a tripod to hold the microphone or angling the top of the stakes.

Table 21. 7th ATC Demonstration Results Analysis

Round No.	Mach Angle (rad)	Time diff 1 (μs)	Time diff 2 (μs)	Dist1 (m)	Dist2 (m)	Hand Scored Locations		Ground refl (m)	Stake refl (m)
						X (m)	Z (m)		
1	0.27	4,092		1.3		0.552	0.229	1.2	
2	0.37	1,000	1,000	0.3	0.3	0.305	0.686	1.7	0.3
3	0.48	516	476	0.2	0.1				
4	0.61	1,004	1,316	0.3	0.4				
5	0.58								
6	0.38	2,364		0.7		0.641	1.842	2.8	1.2
7	0.38	1,828	1,616	0.6	0.5	0.787	1.334	2.3	0.7
8	0.31	4,112	3,900	1.3	1.2	1.029	0.203	1.0	
9	0.31	3,724	4,428	1.2	1.4	0.457	0.210	1.2	
10	0.66	928		0.2		1.422	0.734	1.7	0.3
11	0.56	2,940	2,228	0.8	0.6	1.168	1.524	2.5	0.5
12	0.60		6,176		1.7				

12. CONCLUSIONS/RECOMMENDATIONS/FUTURE PLANS

The goal of this project was to determine if round discrimination were feasible using acoustic signatures. If it were, the secondary goal was to build a RDS to perform on a live-fire gunnery range. The first goal was achieved without any doubt. The models created, both theoretical and empirical, worked very well. The sensors used were excellent laboratory instruments. The data recording and analysis equipment was well chosen for this endeavor and produced an excellent database. The extent of the database was more than sufficient for the analyses. The intellectual contribution from outside agencies was tremendous and directly impacted the success of the program.

The secondary goal was only partially achieved. Hampered by technical problems, the final demonstration at the 7th ATC was not the great success desired. Although the RDS performed extremely well on the last days of the validation/verification test, the weather and unforeseen technical problems precluded a favorable result at Grafenwoehr. This can be most likely attributed to the urgent nature of having to demonstrate the RDS before the planned development date. The models were incorporated into a powerful, flexible system that allowed for easy modification. The instrumentation was extremely reliable laboratory equipment but was severely affected by the outdoor environment. Because of the time devoted to hardware performance after the verification test, little attention was given to the reflection phenomenon discovered during the verification test. Ultimately, this problem manifested itself into a significant major technical problem during the final demonstration.

A retrospective analysis sheds new light on these problems. Apparently, the shock incident to the wood microphone stand was reflected. The reflection was actually returning to the microphone before the N-Wave duration was completed. In differentiating the signal, additional peaks were encountered, and incorrect durations were calculated. This is the primary reason smaller rounds were being calculated as large tank training rounds. The RETS equipment failed to perform due to the electronic short in the RETS, affecting the testing on the third day. If these small problems are allowed to be worked out, there is a high degree of confidence that a working RDS could be used on a live-fire gunnery range.

A test plan has been developed to continue the RDS development. Future modifications include employing different microphone setups. A possible setup involves discrimination microphones that reside on ground level so only one N-Wave signature will be analyzed. Improvements to the data acquisition and reduction program will be made. The N-Wave period can be better determined by using maximum and minimum peaks, zero crossings, as well as the slopes. Ruggedizing the microphone hardware will greatly enhance the survivability in the rain and snow. These concepts will be field tested on a U.S. Army training range, such as Fort Knox or Fort Stewart, that closely resembles the terrain of Grafenwoehr. The data will be analyzed and correlated with the N-Wave signatures that already reside in the data base.

For a future demonstration of the proof-of-concept, the same RDS brassboard should be used with a new high-fidelity four-microphone system. Two low-cost high-fidelity microphones with high sensitivity should be used to process the N-Waves of small rounds, and two pressure transducers with high-dynamic range should be used to process the N-Waves of large tank rounds. Both microphones and transducers must be environment-resistant and ruggedized. The current RDS hardware must be modified to

accommodate two additional transducer inputs. The signal processing algorithm must be modified to isolate the N-Wave from its reflection. The discrimination algorithm should incorporate durations from the transducers. Several more field tests are needed to characterize the responses of the pressure transducers. There is a high degree of confidence that these improvements to the hardware and the algorithm will allow the RDS to perform at its potential and permit total achievement of the goals of this project.

13. REFERENCES

Conover, W. J. Practical Nonparametric Statistics, 2nd Ed.., John Wiley & Sons, Inc., New York, 1980.

DSP Development Corporation. DADiSP Version 3.0. Cambridge, MA, September 1991.

FM17-12-1, Tank Gunnery, U.S. Army Armor School, Ft. Knox, KY, 20 November 1992.

FM23-1, Bradley Fighting Vehicle Gunnery, U.S. Army Infantry School, Ft. Benning, GA, July 1994.

Heintz, R. M., C. M. Steele, and H. T. Albachten. "Live-Fire Scoring System Study." U.S. Army Combat Developments Command Experimentation Command, Ft. Ord, CA, Contract DA-04-200-AMC-1173(X), September 1966.

Hulet, B. Private conversation regarding FFT plots of projectiles used in U.S. Navy's Remote Strafe Scoring System, Systems Engineering (SE-40). Naval Warfare Assessment Center, Corona, CA, May 1992.

Kalb, J. "A Bullet Miss-Distance Indicator for Small Arms Ranges." U.S. Army Research Laboratory, Aberdeen Proving Ground, MD, unpublished.

Marriott, F. F. C. A Dictionary of Statistical Terms. Fifth Edition, Longman Scientific & Technical, New York: John Wiley and Sons, Inc., 1990.

Morrison, D. F. Multivariate Statistical Methods, 2nd Ed., McGraw-Hill Book Company, New York, 1976.

Ritzel, D. V., and J. J. Gottlieb. "Measurements of Overpressure Signatures from Supersonic Projectiles, Part II: The 3-Inch/70 MK 34 Projectile." Defence Research Establishment, Suffield, CA, 1982.

Schochko, W. Leonard, "Sound Analysis of Ballistic Shock Waves." U.S. Army Frankford Arsenal, Report No. 1798, January 1966.

SPSS Inc. Statistical Package for the Social Sciences, SPSS Reference Guide, Chicago, IL, 1990.

SPSS Inc. Advanced Statistics User's Guide. (Marija J. Norusis/SPSS Inc.), Chicago, IL, 1990.

Stallings, R. Private communication. U.S. Army Research Laboratory, Aberdeen Proving Ground, MD, May 1992.

"Target Holding Mechanism." Tank Gunnery, TM9-6920-442-14&P.

Whitham, G. B. "The Flow Pattern of a Super Sonic Projectile." Communications on Pure and Applied Mathematics, vol. V, pp. 301–348, 1952.

INTENTIONALLY LEFT BLANK.

APPENDIX A:

FEASIBILITY TEST RANGE DATA

INTENTIONALLY LEFT BLANK.

RD.	GUN	RD.	DATE	TIME	MET CONDITIONS				TERMINAL	IMPACT LOCATION	
#	TYPE	TYPE			TEMP	REL. HUM.	WINDS		MACH NO.	Y	Z
	(mm)			H:M:S	(C)	%	WD(deg)	WS(m/s)		(m)	(m)
1	105	M724	9/22/92	10:37:00	27.0	87	238.	6.0	ND	0.585	6.563
2	"	"	9/22/92	14:15:12	27.0	87	238.	6.0	4.22	0.235	7.073
3	"	"	9/22/92	14:20:08	27.2	87	231.	5.7	4.20	0.135	7.053
4	"	"	9/22/92	14:24:00	26.9	87	238.	4.8	4.20	0.005	6.793
5	"	M490	9/22/92	14:31:01	26.9	87	236.	4.9	3.11	0.435	7.273
6	"	"	9/22/92	14:32:40	27.0	87	235.	5.5	3.09	0.435	6.973
7	"	"	9/22/92	14:35:14	26.9	87	220.	4.8	3.11	0.275	6.933
8	"	"	9/22/92	14:38:41	27.5	85	235.	4.0	3.08	0.305	6.933
9	120	M865	9/22/92	15:07:51	27.4	85	230.	5.2	4.53	0.115	7.043
10	"	"	9/22/92	15:09:33	27.3	85	230.	6.1	4.47	0.405	6.903
11	"	"	9/22/92	15:11:07	27.3	85	231.	6.6	4.45	-0.115	6.723
12	"	"	9/22/92	15:13:40	27.4	85	220.	6.2	4.51	0.275	6.913
13	"	M831	9/22/92	15:15:55	27.5	85	230.	5.2	2.99	0.255	6.833
14	"	"	9/22/92	15:17:15	27.4	85	230.	5.7	3.02	0.125	6.793
15	"	"	9/22/92	15:18:18	27.5	85	229.	5.8	3.01	0.365	6.633
16	"	"	9/22/92	15:19:15	27.6	85	220.	5.8	3.01	0.245	6.623
17	25	M793	9/23/92	10:35:57	15.6	63	51.	8.8	2.58	-0.485	6.053
18	"	"	9/23/92	10:39:13	15.6	63	51.	8.8	2.61	-0.715	5.693
19	"	"	9/23/92	10:43:24	15.6	63	51.	8.8	2.63	0.565	6.813
20	"	"	9/23/92	10:46:44	15.6	63	51.	8.8	2.59	-0.035	7.383
21	"	"	9/23/92	10:47:43	15.6	63	51.	8.8	2.59	0.405	6.993
22	"	"	9/23/92	11:17:08	15.6	63	51.	8.8	2.61	0.245	7.503
23	"	"	9/23/92	11:19:30	15.6	64	59.	6.4	2.63	0.375	6.543
24	"	"	9/23/92	11:22:32	15.6	64	61.	8.0	2.61	0.055	6.733
25	"	"	9/23/92	11:23:16	15.8	64	59.	7.5	2.62	-0.135	6.813
26	"	"	9/23/92	11:24:06	15.8	64	56.	7.6	2.64	0.255	6.593
27	"	"	9/23/92	11:26:48	15.9	64	38.	8.9	2.61	1.335	6.913
28	"	"	9/23/92	11:28:55	15.7	64	41.	8.7	2.62	1.285	6.993

RD.	GUN	RD.	DATE	TIME	MET CONDITIONS				TERMINAL	IMPACT LOCATION	
#	TYPE	TYPE			TEMP	REL. HUM.	WINDS		MACH NO.	Y	Z
	(mm)			H:M:S	(C)	%	WD(deg)	WS(m/s)		(m)	(m)
29	25	M793	9/23/92	11:32:32	15.8	63	50.	7.8	2.61	0.965	7.733
30	"	"	9/23/92	11:33:17	16.0	64	43.	8.5	2.61	0.785	7.873
31	"	"	9/23/92	11:33:51	16.0	64	38.	8.2	2.61	0.505	7.713
32	"	M910	9/23/92	11:39:06	16.1	64	23.	8.2	3.43	ND	ND
33	"	"	9/23/92	11:40:43	15.9	63	34.	9.4	3.27	ND	ND
34	"	"	9/23/92	11:43:53	16.2	62	46.	9.2	3.21	ND	ND
35	"	"	9/23/92	11:45:01	16.2	62	50.	8.5	3.36	0.285	7.423
36	"	"	9/23/92	11:46:06	16.2	64	55.	7.6	3.34	0.425	7.603
37	"	"	9/23/92	12:18:09	17.2	62	41.	10.4	3.41	0.175	6.813
38	"	"	9/23/92	12:18:55	17.1	62	48.	7.4	3.39	0.675	6.913
39	"	"	9/23/92	12:19:33	17.2	62	41.	7.0	3.51	0.185	7.273
40	"	"	9/23/92	12:20:11	17.3	62	55.	7.7	3.37	0.455	6.333
41	"	"	9/23/92	12:20:51	17.3	62	55.	7.7	3.39	0.625	6.903
42	120	M865	9/25/92	9:43:36	11.4	84	72.	8.7	3.83	ND	ND
43	"	"	9/25/92	9:46:32	11.4	85	67.	7.5	3.85	ND	ND
44	"	"	9/25/92	9:50:39	11.4	84	74.	6.2	3.83	ND	ND
45	"	"	9/28/92	10:27:00	15.0	98	8.	0.8	ND	ND	ND
46	"	"	9/28/92	10:22:00	15.2	98	358.	0.9	ND	ND	ND
47	"	"	9/28/92	10:32:36	15.1	98	21.	1.1	3.85	-0.163	6.867
48	"	"	9/28/92	10:57:42	15.0	98	359.	1.1	3.86	-0.173	7.057
49	"	"	9/28/92	10:58:51	15.1	98	30.	0.7	3.86	-0.133	6.657
50	"	"	9/28/92	11:01:02	15.1	98	18.	1.3	3.84	0.257	6.817
51	"	M831	9/28/92	11:01:00	15.1	98	15.	1.0	ND	ND	ND
52	"	"	9/28/92	11:05:52	15.1	98	24.	1.6	2.58	0.327	6.297
53	"	"	9/28/92	11:07:14	15.2	98	30.	1.6	2.60	-0.023	6.407
54	"	"	9/28/92	11:08:59	15.3	98	29.	1.5	2.55	-0.273	6.947
55	"	"	9/28/92	11:10:16	15.4	98	28.	1.6	2.60	0.317	7.137
56	105	M724	9/28/92	14:23:00	16.4	98	187.	0.9	ND	ND	ND

RD.	GUN	RD.	DATE	TIME	MET CONDITIONS				TERMINAL	IMPACT LOCATION	
#	TYPE	TYPE			TEMP	REL. HUM.	WINDS		MACH NO.	Y	Z
	(mm)			H:M:S	(C)	%	WD(deg)	WS(m/s)		(m)	(m)
57	105	M724	9/28/92	14:30:00	16.5	98	200.	1.4	ND	ND	ND
58	"	"	9/28/92	14:35:55	16.5	98	221.	0.6	3.93	-0.113	6.937
59	"	"	9/28/92	14:58:58	17.3	97	166.	1.9	3.91	-0.153	6.957
60	"	"	9/28/92	14:59:56	17.1	97	165.	2.9	3.92	-0.013	6.567
61	"	M490	9/28/92	15:01:00	16.9	97	219.	2.3	ND	ND	ND
62	"	"	9/28/92	15:06:00	17.3	98	213.	1.4	ND	ND	ND
63	"	"	9/28/92	15:11:39	17.6	98	199.	2.2	2.49	0.247	6.757
64	"	"	9/28/92	15:12:47	17.2	98	204.	2.4	2.55	0.337	6.997
65	"	"	9/28/92	15:13:58	17.6	98	202.	2.5	2.48	-0.683	6.697
66	25	M910	9/28/92	15:50:00	18.5	98	205.	2.6	ND	ND	ND
67	"	"	9/28/92	15:52:00	18.5	98	205.	2.6	ND	ND	ND
68	"	"	9/28/92	15:56:00	18.5	98	205.	2.6	ND	ND	ND
69	"	"	9/28/92	15:56:30	18.5	98	205.	2.6	ND	ND	ND
70	"	"	9/28/92	15:57:00	18.5	98	205.	2.6	ND	ND	ND
71	"	"	9/28/92	16:03:57	18.5	98	205.	2.6	2.66	0.847	7.637
72	"	"	9/28/92	16:05:26	18.5	98	205.	2.6	2.73	0.877	7.617
73	"	"	9/28/92	16:19:42	18.7	98	227.	1.7	2.81	0.057	6.887
74	"	"	9/28/92	16:20:26	18.6	99	260.	2.5	2.83	ND	ND
75	"	"	9/28/92	16:21:21	19.2	98	259.	2.6	2.76	ND	ND
76	"	"	9/28/92	16:22:26	19.5	98	244.	2.8	2.66	ND	ND
77	"	"	9/28/92	16:23:18	19.3	98	241.	2.1	2.67	ND	ND
78	"	"	9/28/92	16:24:53	19.3	98	258.	2.1	2.77	ND	ND
79	"	M793	9/28/92	16:25:00	19.3	98	264.	2.2	ND	ND	ND
80	"	"	9/28/92	16:25:30	19.2	98	262.	2.6	ND	ND	ND
81	"	"	9/28/92	16:26:00	19.3	98	269.	2.8	ND	ND	ND
82	"	"	9/28/92	16:30:17	19.4	98	272.	2.4	1.81	-0.203	6.587
83	"	"	9/28/92	16:30:50	19.3	98	275.	2.6	1.82	-0.933	6.607
84	"	"	9/28/92	16:31:20	19.2	98	272.	2.2	1.81	-0.393	6.757

RD.	GUN	RD.	DATE	TIME	MET CONDITIONS				TERMINAL	IMPACT LOCATION	
#	TYPE	TYPE			TEMP	REL. HUM.	WINDS		MACH NO.	Y	Z
	(mm)			H:M:S	(C)	%	WD(deg)	WS(m/s)		(m)	(m)
85	25	M793	9/28/92	16:32:00	19.3	98	364.	1.8	ND	ND	ND
86	"	"	9/28/92	16:33:16	19.2	98	255.	2.4	1.82	-0.443	7.097
87	"	"	9/28/92	16:33:57	19.1	98	246.	2.5	1.81	1.137	7.797
88	"	"	9/28/92	16:34:26	19.1	98	250.	2.3	1.81	-0.343	7.027
89	"	"	9/28/92	16:34:55	19.1	98	255.	2.4	1.82	-1.213	6.777
90	"	"	9/28/92	16:35:27	19.2	98	257.	2.1	1.83	0.957	7.347
91	"	"	9/28/92	16:36:20	19.2	98	263.	1.6	1.84	-0.543	6.917
92	"	"	9/28/92	16:36:49	19.2	98	251.	2.3	1.81	-0.373	6.337
93	"	"	9/28/92	16:37:20	19.1	98	248.	2.5	1.81	ND	ND
94	105	M490	9/29/92	9:35:00	12.7	75	3.	5.8	ND	ND	ND
95	"	"	9/29/92	9:36:10	12.9	76	1.	5.8	2.15	0.767	7.661
96	"	"	9/29/92	9:56:55	14.3	70	13.	8.9	1.89	ND	ND
97	"	"	9/29/92	9:59:24	14.5	71	10.	8.1	2.19	-0.403	7.441
98	"	"	9/29/92	10:01:12	14.6	69	15.	7.2	2.01	0.297	6.131
99	"	M724	9/29/92	10:02:00	14.8	69	11.	6.2	ND	ND	ND
100	"	"	9/29/92	10:09:39	14.9	69	18.	6.2	3.51	-0.783	7.071
101	"	"	9/29/92	10:28:22	16.3	69	27.	4.7	3.51	-0.393	6.891
102	"	"	9/29/92	10:30:24	16.4	70	4.	5.3	3.51	-0.373	6.791
103	"	"	9/29/92	10:32:06	16.5	70	11.	4.8	3.51	-0.143	6.621
104	120	M831	9/29/92	11:21:00	18.0	66	357.	5.8	ND	ND	ND
105	"	"	9/29/92	11:26:48	17.5	64	9.	3.6	2.10	-1.023	6.811
106	"	"	9/29/92	11:46:44	16.6	62	351.	6.6	2.07	-0.243	6.361
107	"	"	9/29/92	11:49:37	16.7	62	26.	6.2	2.09	1.457	7.041
108	"	"	9/29/92	11:59:03	16.4	62	350.	5.9	2.08	0.707	7.001
109	"	M865	9/29/92	11:59:00	16.2	61	6.	5.2	ND	ND	ND
110	"	"	9/29/92	12:05:50	16.2	62	351.	6.1	3.17	-0.613	7.061
111	"	"	9/29/92	12:21:39	16.2	62	30.	4.9	3.11	0.857	7.521
112	"	"	9/29/92	12:23:04	16.4	61	28.	5.7	3.13	-0.223	6.531

RD.	GUN	RD.	DATE	TIME	MET CONDITIONS				TERMINAL	IMPACT LOCATION	
#	TYPE	TYPE			TEMP	REL. HUM.	WINDS		MACH NO.	Y	Z
	(mm)			H:M:S	(C)	%	WD(deg)	WS(m/s)		(m)	(m)
113	120	M865	9/29/92	12:24:35	15.9	61	35.	5.8	3.13	0.487	6.751
114	25	M793	9/29/92	14:49:00	18.3	50	351.	8.0	ND	ND	ND
115	"	"	9/29/92	14:49:30	18.3	50	351.	8.0	ND	ND	ND
116	"	"	9/29/92	14:50:00	18.4	49	355.	6.1	ND	ND	ND
117	"	"	9/29/92	14:52:30	18.4	51	335.	7.2	1.36	-0.923	6.161
118	"	"	9/29/92	14:54:42	18.1	50	352.	9.5	1.38	-0.193	7.151
119	"	"	9/29/92	14:56:27	18.1	49	342.	7.4	1.37	1.097	8.021
120	"	"	9/29/92	15:18:48	18.1	48	1.	7.6	1.34	ND	ND
121	"	"	9/29/92	15:20:56	18.4	50	15.	8.6	1.35	-1.643	6.041
122	"	"	9/29/92	15:22:22	18.2	49	16.	8.8	1.38	1.097	7.331
123	"	"	9/29/92	15:39:53	17.9	46	16.	7.9	1.36	-0.633	7.371
124	"	"	9/29/92	15:40:50	18.0	47	23.	8.1	1.35	1.417	7.541
125	"	"	9/29/92	15:41:44	17.9	46	11.	6.4	1.35	-0.243	6.991
126	"	"	9/29/92	15:41:44	18.1	46	25.	8.2	ND	0.047	7.861
127	"	"	9/29/92	15:41:44	18.1	46	25.	8.2	ND	ND	ND
128	"	"	9/29/92	15:41:44	18.1	46	25.	8.2	ND	-0.893	7.121
129	"	"	9/29/92	15:41:44	18.1	46	25.	8.2	ND	1.627	7.751
130	"	"	9/29/92	15:41:44	18.1	46	25.	8.2	ND	0.407	7.891
131	"	"	9/29/92	15:41:44	18.1	46	25.	8.2	ND	-0.873	6.821
132	"	"	9/29/92	15:41:44	18.1	46	25.	8.2	ND	0.267	7.251
133	"	"	9/29/92	15:41:44	18.1	46	25.	8.2	ND	1.827	7.461
134	"	M910	9/29/92	15:54:00	18.2	45	32.	9.4	ND	ND	ND
135	"	"	9/29/92	15:54:30	18.2	45	32.	9.4	ND	ND	ND
136	"	"	9/29/92	15:55:00	18.2	45	32.	8.5	ND	ND	ND
137	"	"	9/29/92	15:56:00	18.1	44	18.	6.6	ND	ND	ND
138	"	"	9/29/92	15:56:30	18.3	44	5.	6.4	ND	ND	ND
139	"	"	9/29/92	15:57:00	18.3	45	23.	6.6	ND	ND	ND
140	"	"	9/29/92	16:02:12	18.1	45	17.	6.6	2.37	ND	ND

RD.	GUN	RD.	DATE	TIME	MET CONDITIONS				TERMINAL	IMPACT LOCATION	
#	TYPE	TYPE			TEMP	REL. HUM.	WINDS		MACH NO.	Y	Z
	(mm)			H:M:S	(C)	%	WD(deg)	WS(m/s)		(m)	(m)
141	25	M910	9/29/92	16:04:01	18.1	45	29.	8.2	2.38	ND	ND
142	"	"	9/29/92	16:05:04	18.2	45	18.	7.5	2.27	ND	ND
143	"	"	9/29/92	16:20:57	18.3	45	22.	8.8	2.25	ND	ND
144	"	"	9/29/92	16:21:57	18.3	45	24.	9.0	2.36	ND	ND
145	"	"	9/29/92	16:22:39	18.5	46	5.	8.0	2.27	0.687	7.391
146	"	"	9/29/92	16:23:11	18.5	45	21.	7.8	2.35	ND	ND
147	"	"	9/29/92	16:23:53	18.5	45	21.	7.8	2.41	ND	ND
148	"	"	9/29/92	16:24:43	18.0	45	17.	7.2	2.36	-0.863	7.941
149	"	"	9/29/92	16:26:09	18.1	45	23.	7.3	2.39	ND	ND
150	"	"	9/29/92	16:26:43	18.1	45	21.	6.9	2.27	ND	ND
151	"	"	9/29/92	16:27:12	18.2	46	20.	5.6	2.31	ND	ND
152	"	"	9/29/92	16:27:47	18.2	46	20.	5.6	2.31	ND	ND
153	"	"	9/29/92	16:28:24	1.2	46	20.	5.6	2.28	ND	ND
154	120	M831	9/30/92	10:45:53	14.1	67	44.	5.2	3.03	0.367	7.437
155	"	"	9/30/92	11:02:00	13.9	62	44.	4.0	3.04	0.567	7.547
156	"	"	9/30/92	11:04:18	13.6	62	51.	4.0	3.05	0.587	7.397
157	"	"	9/30/92	11:05:53	13.6	62	47.	3.7	3.02	0.137	7.437
158	"	"	9/30/92	11:06:48	13.6	62	47.	3.7	3.04	0.007	7.347
159	"	"	9/30/92	11:07:50	13.6	62	53.	5.2	3.03	0.047	7.137
160	"	M865	9/30/92	11:15:28	13.3	61	34.	4.9	4.51	0.127	7.477
161	"	"	9/30/92	11:34:05	13.0	59	29.	5.2	4.49	0.057	7.247
162	"	"	9/30/92	11:36:56	13.5	60	32.	6.9	4.50	0.297	7.407
163	"	"	9/30/92	11:39:49	13.3	59	34.	4.7	4.50	0.207	7.517
164	"	"	9/30/92	11:40:56	13.3	59	32.	5.2	4.48	0.347	7.217
165	"	"	9/30/92	11:43:21	13.2	59	35.	6.3	4.48	0.247	7.277
166	25	M910	9/30/92	13:29:00	14.2	53	16.	6.2	ND	ND	ND
167	"	"	9/30/92	13:33:21	14.4	54	39.	7.4	3.49	0.007	7.607
168	"	"	9/30/92	13:48:20	14.6	52	43.	6.3	3.65	0.467	6.387

RD. #	GUN TYPE (mm)	RD. TYPE	DATE	TIME H:M:S	MET CONDITIONS TEMP (C)	REL. HUM. %	WINDS WD(deg)	WINDS WS(m/s)	TERMINAL MACH NO.	IMPACT LOCATION Y (m)	IMPACT LOCATION Z (m)
169	25	M910	9/30/92	13:49:44	14.3	53	37.	8.7	3.36	0.247	7.527
170	"	"	9/30/92	13:50:32	14.4	53	40.	7.1	3.60	0.187	7.197
171	"	"	9/30/92	13:51:18	14.4	53	35.	6.9	3.62	-0.253	6.917
172	"	"	9/30/92	13:52:04	14.4	53	40.	7.2	3.55	1.177	7.107
173	"	"	9/30/92	13:53:47	14.4	54	31.	7.0	3.53	0.697	7.197
174	"	"	9/30/92	13:54:15	14.4	53	20.	7.1	3.44	0.047	7.417
175	"	"	9/30/92	13:55:00	14.3	53	10.	5.9	ND	0.737	6.847
176	"	"	9/30/92	13:55:00	14.3	53	10.	5.9	ND	1.327	7.607
177	"	"	9/30/92	13:55:00	14.3	53	10.	5.9	ND	0.877	8.157
178	"	"	9/30/92	13:55:00	14.3	53	10.	5.9	ND	0.957	8.027
179	"	"	9/30/92	13:56:00	14.3	53	19.	5.1	ND	0.327	7.187
180	"	"	9/30/92	13:56:00	14.3	53	19.	5.1	ND	0.447	7.657
181	"	"	9/30/92	13:56:00	14.3	53	19.	5.1	ND	-0.033	8.287
182	"	"	9/30/92	13:56:00	14.3	53	19.	5.1	ND	0.987	7.197
183	"	M793	9/30/92	14:00:00	14.1	54	24.	5.9	ND	-2.303	2.167
184	"	"	9/30/92	14:06:49	14.7	52	27.	7.2	2.61	-0.153	7.477
185	"	"	9/30/92	14:20:34	15.3	54	4.	4.4	2.60	-1.173	7.327
186	"	"	9/30/92	14:21:05	15.6	54	9.	6.1	2.61	-0.143	7.137
187	"	"	9/30/92	14:21:33	15.6	54	9.	6.1	2.61	-0.473	7.627
188	"	"	9/30/92	14:21:57	15.6	53	30.	7.6	2.60	-0.853	7.407
189	"	"	9/30/92	14:22:24	15.6	53	30.	7.6	2.61	0.657	7.357
190	"	"	9/30/92	14:23:15	15.4	52	37.	7.1	2.61	-0.233	7.217
191	"	"	9/30/92	14:23:40	15.4	52	37.	7.1	2.60	-0.463	7.517
192	"	"	9/30/92	14:24:32	15.6	53	23.	6.9	2.59	-0.723	7.327

INTENTIONALLY LEFT BLANK.

APPENDIX B:

PROJECTILE CHARACTERISTICS DATA FROM FEASIBILITY TEST PHASE

INTENTIONALLY LEFT BLANK.

400 meter Data

shot	Round	mic	Pos P	Neg P1	Neg P2	A1	A2	A3	Atot	Peak	ABS	cal
	type		Pa	Pa	Pa	msec	msec	msec	msec	mPa-s	mPa-s	Pa/V
160	M865	3	6251.0	3254.5	-	477	456	-	933	1332.0	2138.0	192.802
		6	2831.8	2225.0	-	541	573	-	1114	661.0	1289.0	809.08
		9	1565.1	1537.7	-	655	583	-	1238	595.0	1012.0	2745.83
		12	1384.7	1282.9	-	606	730	-	1336	427.0	895.0	2036.37
161	M865	3	6389.0	3254.5	-	473	431	-	904	1343.0	2122.0	192.802
		6	3163.5	2152.2	-	618	566	-	1184	878.0	1490.0	809.08
		9	1894.6	1620.0	-	690	676	-	1366	735.0	1296.0	2745.83
		12	1527.3	1201.5	-	776	728	-	1504	683.0	1138.0	2036.37
162	M865	3	6262.0	3254.5	-	467	437	-	904	1311.0	2066.0	192.802
		6	3284.9	2022.7	-	613	570	-	1183	888.0	1494.0	809.08
		9	1894.6	1537.7	-	720	635	-	1355	714.0	1241.0	2745.83
		12	1527.3	1262.6	-	761	735	-	1496	617.0	1133.0	2036.37
155	M831	3	7775.9	2651.0	4100.0	656	369	429	1454	2380.3	4154.7	192.802
		6	4045.4	2225.0	2831.8	758	589	401	1748	1451.6	3105.8	809.08
		9	2581.1	1537.7	2059.4	971	578	439	1988	1346.6	2554.0	2745.83
		12	1893.8	1282.9	1547.6	129	717	393	2139	1003.9	2003.6	2036.37
156	M831	3	7499.2	2651.0	4000.0	645	372	413	1430	2340.1	4182.1	192.802
		6	4045.4	2427.2	2831.8	752	654	333	1739	1476.1	3103.0	809.08
		9	2855.7	2059.4	2059.4	952	742	291	1985	1413.4	2758.2	2745.83
		12	1893.8	1547.6	1669.8	135	857	250	2142	1048.6	2166.0	2036.37
157	M831	3	8167.8	1808.5	5811.0	676	254	534	1464	2519.7	3809.0	192.802
		6	3640.9	1618.2	2629.5	782	457	548	1787	1423.5	2927.8	809.08
		9	2581.1	1016.0	2059.4	992	450	563	2005	1306.7	2414.8	2745.83
		12	2158.6	1282.9	1669.8	132	730	446	2208	1071.5	2207.0	2036.37

400 meter Data

shot	Round type	mic	Pos P Pa	Neg P1 Pa	Neg P2 Pa	A1 msec	A2 msec	A3 msec	Atot msec	Peak mPa-s	ABS mPa-s	cal Pa/V
3	M724	1	909.8	3200.0	-	107	587	-	694	52.6	1646.0	365.39
		6	2857.3	1632.7	-	455	483	-	938	442.4	925.1	816.357
		9	1332.6	1243.8	-	509	544	-	1053	365.3	723.0	177.68
		12	1231.0	957.5	-	542	592	-	1134	281.6	586.7	854.877
4	M724	1	913.5	3197.2	-	123	577	-	700	57.0	1644.0	365.39
		6	3061.3	1836.8	-	459	484	-	943	453.8	942.0	816.357
		9	1332.6	1243.8	-	506	554	-	1060	362.8	731.4	177.68
		12	1293.5	1017.3	-	543	604	-	1147	301.3	627.2	854.877
6	M490	1										365.39
		6	5306.3	3061.3	-	731	897	-	1628	1329.0	2575.0	816.357
		9	2785.3	1915.5	-	853	986	-	1839	1132.8	1990.8	177.68
		12	1658.5	1547.3	-	897	1084	-	1981	810.2	1629.3	854.877
7	M490	1										365.39
		6	5102.2	2857.3	-	727	1020	-	1747	1267.8	2523.0	816.357
		9	3282.9	3000.0	-	839	980	-	1819	1236.7	2086.7	177.68
		12	1658.5	1547.3	-	906	1063	-	1969	779.2	1581.5	854.877
8	M490	1										365.39
		6	5510.4	3061.3	-	805	874	-	1679	1425.1	2776.0	816.357
		9	3260.6	2872.2	-	927	968	-	1895	1456.6	2330.6	177.68
		12	1658.5	1709.8	-	973	1076	-	2049	856.0	1745.0	854.877

400 meter Data

shot	Round type	mic	Pos P Pa	Neg P1 Pa	Neg P2 Pa	A1 msec	A2 msec	A3 msec	Atot msec	Peak mPa-s	ABS mPa-s	cal Pa/V
167	M910	1	1607.2	2479.1	-	104	146	-	250	111.5	304.3	854.877
		6	817.2	760.5	-	168	188	-	356	61.0	148.1	809.08
		9	466.8	466.8	-	213	189	-	402	67.1	112.9	2745.83
		12	407.3	448.0	-	218	224	-	442	54.2	109.5	2036.37
168	M910	1	1043.0	1282.3	-	126	155	-	281	76.1	193.5	854.877
		6	946.6	639.2	-	174	224	-	398	73.1	142.8	809.08
		9	466.8	466.8	-	217	221	-	438	68.3	116.8	2745.83
		12	346.2	285.1	-	220	243	-	463	43.2	78.1	2036.37
169	M910	1	1205.4	1521.7	-	119	153	-	272	88.8	227.0	854.877
		6	825.3	639.2	-	171	196	-	367	68.3	138.7	809.08
		9	411.8	411.8	-	219	192	-	411	62.7	101.1	2745.83
		12	407.3	346.2	-	210	239	-	449	47.5	93.1	2036.37
184	M793	1	1444.7	957.5	1521.7	179	113	141	433	159.3	383.0	854.877
		6	881.9	493.5	744.4	270	170	119	559	102.1	216.7	809.08
		9	604.1	411.9	549.2	289	209	114	612	94.8	19.3	2745.83
		12	427.6	346.2	386.9	330	228	102	660	81.2	155.9	2036.37
185	M793	1	1607.2	1196.8	2000.4	164	101	139	404	167.9	435.0	854.877
		6	995.2	493.5	776.7	249	152	136	537	111.5	236.7	809.08
		9	631.5	439.3	631.5	291	193	126	610	104.5	213.1	2745.83
		12	407.3	285.1	448.0	337	182	119	638	85.8	153.8	2036.37
186	M793	1	1444.7	957.5	1598.6	176	117	140	433	156.6	382.5	854.877
		6	1027.5	493.5	776.7	258	180	121	559	108.3	238.0	809.08
		9	659.0	439.3	631.5	282	218	118	618	99.3	210.3	2745.83
		12	488.7	325.8	427.6	319	231	106	656	85.0	165.4	2036.37

1000 meter Data

shot	Round type	mic	Pos P Pa	Neg P1 Pa	Neg P2 Pa	A1 msec	A2 msec	A3 msec	Atot msec	Peak mPa-s	ABS mPa-s	cal Pa/V
47	M865	1										202.27
		1	3151.0	-5210.0	-	334	339	-	733	646.7	1791.3	686.49
		6	2287.0	-1827.0	-	518	549	-	1067	512.5	1022.7	730.78
		12	1088.0	-996.5	-	669	648	-	1317	390.7	731.0	257.43
48	M865	3	6374.2	-3871.7	-	456	443	-	899	1369.6	2307.2	188.79
		6	2375.0	-1739.3	-	590	533	-	1123	643.9	1106.4	730.78
		9	1459.2	-1352.6	-	627	631	-	1258	494.0	919.5	333.15
		12	1145.0	-1088.0	-	689	670	-	1359	439.4	796.4	257.43
49	M865	3	5800.7	-4014.0	-	408	406	-	814	1253.7	2106.7	188.79
		6	2097.3	-1739.3	-	524	516	-	1040	503.2	963.1	730.78
		9	1421.2	-1352.6	-	581	598	-	1179	437.0	837.3	333.15
		12	1109.5	-1063.2	-	651	643	-	1297	396.4	750.0	257.43
53	M831	3	11425.0	-4220.0	-5424.0	601	397	391	1389	3239.0	5637.8	188.79
		6	2828.1	-1651.6	-2104.6	803	558	413	1774	1241.6	2489.0	730.78
		9	2082.2	-1459.2	-1665.8	928	669	385	1982	1050.2	2155.0	333.15
		12	1800.0	-1194.0	-1387.0	1005	748	367	2120	925.5	1803.0	257.43
54	M831	3	6022.4	-2441.9	-4195.0	666	476	335	1480	1877.5	3439.7	188.79
		6	2828.1	-1556.6	-2104.6	805	554	447	1806	1219.0	2377.4	730.78
		9	2185.5	-1146.0	-1769.0	947	563	531	2041	1054.8	2092.3	333.15
		12	1987.0	-745.0	-1352.0	991	513	638	2142	911.8	1717.5	257.43
55	M831	3	10428.0	-4020.1	-6881.1	639	426	373	1438	3116.2	5440.4	188.79
		6	2828.1	-2104.6	-2104.6	782	657	290	1729	1239.5	2469.1	730.78
		9	2248.8	-1709.1	-1709.1	932	738	284	1954	1026.4	2147.4	333.15
		12	1508.3	-1351.5	-1305.2	1016	856	248	2120	909.5	1804.6	257.43

1000 meter Data

shot	Round type	mic	Pos P Pa	Neg P1 Pa	Neg P2 Pa	A1 msec	A2 msec	A3 msec	Atot msec	Peak mPa-s	ABS mPa-s	cal Pa/V
58	M724	3	5645.4	-3658.8	-	377	440	-	817	995.9	1893.6	188.79
		6	1914.6	-1556.6	-	465	532	-	997	388.6	835.9	730.78
		9	1249.3	-1166.0	-	556	557	-	1113	356.5	701.6	333.15
		12	1112.0	-947.0	-	562	639	-	1201	306.6	641.5	257.43
59	M724	3	3658.8	-3186.0	-	375	441	-	816	758.6	1515.9	188.79
		6	1914.6	-1556.6	-	471	522	-	993	386.9	827.1	730.78
		9	1249.3	-1186.0	-	531	578	-	1109	355.5	707.1	333.15
		12	1109.0	-943.0	-	565	632	-	1197	301.0	630.4	257.43
60	M724	3	3775.8	-3422.1	-	359	422	-	781	803.7	1599.5	188.79
		6	1914.6	-1468.9	-	453	531	-	984	388.3	828.9	730.78
		9	1249.3	-1186.0	-	535	568	-	1103	361.3	721.9	333.15
		12	1109.5	-965.4	-	557	638	-	1195	297.3	622.6	257.43
63	M490	3	8374.6	-3961.5	-4018.0	569	458	412	1439	1597.7	3711.6	188.79
		6	2828.1	-1921.9	-2016.5	740	573	409	1722	1090.9	2326.6	730.78
		9	2203.3	-1435.9	-1499.2	898	616	406	1920	969.2	1664.4	333.15
		12	1735.0	-1112.0	-1256.0	963	701	403	2067	824.7	1667.4	257.43
64	M490	3	7807.4	-2142.9	-4538.8	585	219	661	1465	2187.0	4125.4	188.79
		6	2828.1	-1556.6	-2382.3	716	445	594	1755	1090.2	2288.9	730.78
		9	2018.5	-1186.0	-1625.8	868	511	564	1914	941.3	1885.3	333.15
		12	1733.0	-1011.0	-1351.0	953	598	535	2086	811.5	1651.3	257.43
65	M490	3	6745.4	-2595.9	-3801.0	642	366	537	1545	2062.8	3997.5	188.79
		6	2828.1	-1651.6	-2016.9	759	600	454	1813	1034.6	2204.1	730.78
		9	1998.9	-1312.6	-1499.2	918	651	416	1985	936.5	1864.3	333.15
		12	1495.7	-1063.2	-1207.4	979	727	405	2111	766.6	1583.3	257.43

1000 meter Data

shot	Round type	mic	Pos P Pa	Neg P1 Pa	Neg P2 Pa	A1 msec	A2 msec	A3 msec	Atot msec	Peak mPa-s	ABS mPa-s	cal Pa/V
71	M910	3	976.5	-976.5	-	137	169	-	299	74.5	177.3	781.18
		6	774.6	-555.4	-	170	197	-	367	51.7	118.4	730.78
		9	459.8	-425.0	-	196	214	-	410	47.4	95.2	333.15
		12	376.0	-414.0	-	208	238	-	446	41.0	93.3	257.43
72	M910	1	981.7	-1380.0	-	113	162	-	275	66.6	198.2	686.49
		6	635.8	-555.4	-	159	214	-	373	49.4	117.1	730.78
		9	439.8	-353.1	-	196	214	-	410	46.5	92.6	333.15
		12	401.6	-339.0	-	195	247	-	442	37.6	83.3	257.43
73	M910	1	638.4	-693.3	-	147	182	-	329	51.0	122.8	686.49
		6	781.9	-453.1	-	182	194	-	376	57.3	110.0	730.78
		9	439.8	-393.1	-	200	213	-	413	46.9	92.4	333.15
		12	404.2	-306.3	-	211	229	-	440	39.8	79.1	257.43
82	M793	1	1284.0	-1037.0	-1421.0	171	109	153	433	135.9	373.0	686.49
		6	635.8	-504.2	-599.2	251	204	115	570	88.0	207.5	730.78
		9	499.7	-353.1	-416.4	300	232	100	632	82.5	161.2	333.15
		12	484.0	-337.2	-370.7	318	265	74	657	73.6	150.7	257.43
83	M793	1	1287.0	-1119.0	-1421.0	154	109	147	410	135.5	377.4	686.49
		6	730.7	-504.2	-591.9	262	187	121	570	106.5	212.7	730.78
		9	499.7	-419.8	-479.7	291	226	109	626	80.6	174.4	333.15
		12	481.4	-339.8	-388.7	300	272	91	663	68.4	147.8	257.43
84	M793	1	1242.5	-1036.6	-1421.0	167	127	141	435	128.6	343.0	686.49
		6	679.6	-555.4	-643.1	259	195	116	570	93.2	209.2	730.78
		9	539.7	-419.2	-479.7	287	241	99	627	78.3	175.2	333.15
		12	499.4	-337.2	-370.7	312	276	77	665	71.9	146.3	257.43

1700 meter Data

shot	Round type	mic	Pos P Pa	Neg P1 Pa	Neg P2 Pa	A1 msec	A2 msec	A3 msec	Atot msec	Peak mPa-s	ABS mPa-s	cal Pa/V
110	M865	3	3317.6	2843.6	-	477	460	-	937	881.1	1578.7	189.575
		6	2176.3	1696.1	-	576	532	-	1108	561.2	1026.7	774.493
		9	1497.8	1310.6	-	635	609	-	1244	519.5	943.5	374.45
		12	943.9	943.9	-	685	653	-	1338	381.4	701.8	269.693
111	M865	3	3791.5	3200.0	-	480	441	-	921	945.5	1691.7	189.575
		6	222.8	1843.3	-	540	524	-	1064	575.5	1091.1	774.493
		9	-	-	-	-	-	-	-	-	-	774.493
		12	-	-	-	-	-	-	-	-	-	269.693
105	M831	3	5987.1	2737.6	3213.5	711	531	395	1637	2041.0	3530.0	189.575
		6	2904.4	2129.9	1936.2	859	780	297	1936	1156.5	2500.0	774.493
		9	2389.0	1965.9	1546.5	932	966	220	2118	1167.5	2404.8	374.45
		12	1685.6	1483.3	1078.8	1062	1064	134	2260	987.1	1977.1	269.693
106	M831	3	6224.5	1895.8	3674.0	664	311	543	1518	2068.0	3810.0	189.575
		6	3268.4	1572.2	2176.3	890	498	495	1883	1415.8	2622.3	774.493
		9	2433.9	1497.8	1685.0	958	731	419	2108	1283.6	2407.2	374.45
		12	1618.2	1213.6	1146.2	1056	880	288	2224	987.2	1835.4	269.693
108	M831	3	6471.5	4377.6	3673.9	626	546	325	149.7	2204.7	4144.4	189.575
		6	3508.5	2176.3	2176.3	819	646	353	1818	1541.4	2906.6	774.493
		9	2714.8	1404.2	1872.3	979	629	465	2073	1348.5	2489.8	374.45
		12	1955.8	1011.3	1415.9	1040	640	575	2255	1053.7	2047.6	269.693

1700 meter Data

shot	Round type	mic	Pos P Pa	Neg P1 Pa	Neg P2 Pa	A1 msec	A2 msec	A3 msec	Atot msec	Peak mPa-s	ABS mPa-s	cal Pa/V
101	M724	3	3440.0	2843.6	-	334	457	-	841	708.8	1411.8	189.575
		6	2029.2	1649.7	-	473	555	-	1028	422.0	908.0	774.493
		9	1217.0	1265.6	-	540	594	-	1134	369.1	766.2	374.45
		12	876.5	879.2	-	594	617	1211	302.5	597.8	269.7	
102	M724	3	3437.0	2843.6	-	384	455	-	839	718.4	1416.0	189.575
		6	1835.6	1556.7	-	492	534	-	1626	407.6	855.4	774.493
		9	1310.6	1265.6	-	547	605	-	1152	383.1	795.2	374.45
		12	976.3	946.6	-	592	639	-	1231	316.9	639.1	269.693
103	M724	3	3674.0	2963.0		373	445		818	746.1	1473.3	189.575
		6	1742.6	1649.7		486	535		1021	423.7	900.0	774.493
		9	1310.6	1314.3		533	616		1149	396.0	831.4	374.45
		12	976.3	979.0		611	619		1230	334.1	676.2	269.693
95	M490	1	4507.5	3949.1	4508.5	513	475	497	1485	1191.1	3651.1	901.668
		6	2997.3	2036.9	2137.6	746	608	436	1790	1114.3	2421.0	774.493
		9	2175.6	1613.9	1613.9	901	657	410	1968	1043.5	2101.0	374.45
		12	1786.9	1340.0	1264.9	962	778	372	2112	841.8	1784.5	269.693
97	M490	3	5532.6	2489.1	3200.0	648	442	513	1603	1676.8	3339.4	189.575
		6	2904.4	1595.5	1889.8	782	560	508	1850	1094.7	2249.0	774.493
		9	2059.5	1217.0	1591.4	926	588	504	2018	987.5	1934.7	374.45
		12	1415.9	1011.3	1213.6	1008	649	486	2143	781.1	1596.2	269.693
98	M490	3	7400.0	3437.0	5000.0	544	356	561	1461	1972.4	6252.8	189.575
		6	3051.5	2036.9	2176.3	755	576	487	1818	1195.8	2492.4	774.493
		9	2246.7	1497.8	1591.4	900	689	434	2023	1066.6	2134.3	374.45
		12	1685.6	1213.6	1213.6	983	782	401	2166	860.0	1777.0	269.693

1700 meter Data

shot	Round type	mic	Pos P Pa	Neg P1 Pa	Neg P2 Pa	A1 msec	A2 msec	A3 msec	Atot msec	Peak mPa-s	ABS mPa-s	cal Pa/V
145	M910	1	791.3	799.8	-	157	195	-	352	687.0	161.1	850.87
		6	617.8	428.4	-	207	205	-	412	54.7	105.0	823.791
		9	363.2	349.3	-	211	239	-	450	44.4	92.4	345.866
		12	242.7	269.7	-	239	238	-	477	36.7	72.6	269.693
146	M910	1	1114.6	1284.8	-	127	176	-	303	78.5	210.7	850.87
		6	716.7	551.9	-	185	190	-	375	63.6	123.9	823.791
		9	377.0	377.0	-	205	218	-	423	45.5	94.7	345.866
		12	337.1	323.6	-	206	255	-	461	42.2	90.1	269.693
148	M910	1	791.3	961.5	-	143	172	-	315	66.8	199.4	850.87
		6	1021.5	799.1	-	149	186	-	335	84.3	170.0	823.791
		9	520.6	486.7	-	189	212	-	401	56.9	120.5	345.866
		12	418.0	431.5		201	245		446	53.0	120.3	269.693
123	M793	1	1438.0	1191.2	1352.9	206	167	155	528	178.0	432.7	850.87
		6	617.8	469.6	568.4	323	218	124	665	104.5	222.4	823.791
		9	453.1	411.6	411.6	343	282	101	726	83.6	183.2	345.866
		12	364.1	377.6	364.1	370	325	73	768	78.0	165.8	269.693
124	M793	1	1361.4	1038.1	1191.2	222	176	145	543	168.4	398.9	850.87
		6	972.1	626.1	675.5	288	212	140	640	128.0	276.4	823.791
		9	605.3	453.1	473.8	341	255	114	710	110.4	220.0	345.866
		12	548.9	431.5	404.5	368	320	66	754	89.9	187.6	269.693
125	M793	1	1676.2	1429.5	1676.2	196	150	158	504	196.0	504.0	850.87
		6	823.8	676.1	676.1	304	267	103	674	119.8	269.1	823.791
		9	494.6	477.3	477.3	330	312	91	733	941.0	211.2	345.866
		12	418.0	364.1	364.1	344	357	78	778	81.3	174.4	269.693

INTENTIONALLY LEFT BLANK.

APPENDIX C:

MICROPHONE DATA FROM FEASIBILITY TEST PHASE

INTENTIONALLY LEFT BLANK.

FEASIBILITY TEST HIGH FIDELITY MICROPHONE POSITIONS:

All coordinates are in meters.

22SEP92

1m microphone	x: 1700.104	y: 0.157	z: 5.694
6m microphone	x: 1697.448	y: 5.284	z: 5.282
12m microphone	x:1696.780	y: 11.641	z: 5.109

23SEP92

1m microphone	x: 1700.104	y: 0.157	z: 5.523
3m microphone	x: 1697.835	y: 1.702	z: 4.072
6m microphone	x: 1697.448	y: 5.284	z: 5.118
9m microphone	x:1697.044	y: 8.485	z: 5.054
12m microphone	x:1696.780	y: 11.641	z: 4.944

24SEP92

1m microphone	x: 1700.104	y: 0.157	z: 5.548
3m microphone	x: 1697.835	y: 1.702	z: 5.109
6m microphone	x: 1697.448	y: 5.284	z: 5.139
9m microphone	x:1697.044	y: 8.485	z: 5.078
12m microphone	x:1696.780	y: 11.641	z: 5.023

25SEP92

1m microphone	x: 1700.104	y: 0.157	z: 5.551
3m microphone	x: 1697.835	y: 1.702	z: 5.112
6m microphone	x: 1697.448	y: 5.284	z: 5.115
9m microphone	x:1697.044	y: 8.485	z: 5.075
12m microphone	x:1696.780	y: 11.641	z: 5.039

28SEP92

1m microphone	x: 1700.104	y: 0.157	z: 5.547
3m microphone	x: 1697.835	y: 1.702	z: 5.096
6m microphone	x: 1697.448	y: 5.284	z: 5.139
9m microphone	x:1697.044	y: 8.485	z: 5.066
12m microphone	x:1696.780	y: 11.641	z: 5.014

29SEP92

1m microphone	x: 1700.104	y: 0.157	z: 5.541
3m microphone	x: 1697.835	y: 1.702	z: 5.090
6m microphone	x: 1697.448	y: 5.284	z: 5.121
9m microphone	x:1697.044	y: 8.485	z: 5.087
12m microphone	x:1696.780	y: 11.641	z: 5.008

30SEP92

1m microphone	x: 1700.104	y: 0.157	z: 5.547
3m microphone	x: 1697.835	y: 1.702	z: 5.108
6m microphone	x: 1697.448	y: 5.284	z: 5.136
9m microphone	x:1697.044	y: 8.485	z: 5.084
12m microphone	x:1696.780	y: 11.641	z: 5.026

FEASIBILITY TEST ROUND LOCATION MICROPHONE POSITIONS:

All coordinates are in meters.

Array 1

21SEP92

sensor 1	x: 1697.846	y: -4.458	z: 3.385
sensor 2	x: 1697.151	y: 0.128	z: 4.691
sensor 3	x: 1696.569	y: 4.278	z: 5.226
sensor 4	x: 1699.552	y: -5.346	z: 5.976
sensor 5	x: 1699.348	y: 0.009	z: 4.949
sensor 6	x: 1699.222	y: 5.276	z: 5.977

Array 2

28SEP92

sensor 1	x: 1697.852	y: -4.444	z: 3.382
sensor 2	x: 1697.108	y: 0.125	z: 4.468
sensor 3	x: 1696.554	y: 4.277	z: 5.222
sensor 4	x: 1699.520	y: -5.323	z: 5.969
sensor 5	x: 1699.475	y: 0.056	z: 4.901
sensor 6	x: 1699.238	y: 5.273	z: 5.972

Change during testing

sensor 1	Δx: 0.006	Δy: 0.014	Δz: -0.003
sensor 2	Δx: -0.043	Δy: -0.003	Δz: -0.223
sensor 3	Δx: -0.015	Δy: -0.001	Δz: -0.004
sensor 4	Δx: -0.032	Δy: 0.023	Δz: 0.002
sensor 5	Δx: 0.127	Δy: 0.047	Δz: -0.048
sensor 6	Δx: 0.016	Δy: -0.003	Δz: -0.025

FEASIBILITY TEST GUN POSITIONS:

All coordinates are in meters.

400 meter Range

22SEP92

M60	x: 1299.993	y: 24.205	z: 3.735
M1A1	x: 1299.666	y: 24.539	z: 3.558

23SEP92

M2	x: 1299.901	y: 23.715	z: 4.023

1000 meter Range

28SEP92

M1A1	x: 700.059	y: 6.717	z:2.335
M60	x: 700.017	y:9.122	x: 4.282
M2	x: 699.711	y: 9.160	x: 4.617

1700 meter Range

29SEP92

M60	x: 0.024	y: 1.739	z: 4.007
M1A1	x: 0.033	y: 2.299	z: 3.723

1400 meter Range

29SEP92

M2	x: 299.572	y: 4.877	z: 4.510

400 meter Range

30SEP92

M1A1	x: 1299.639	y: 24.031	z: 3.489
M2	x: 1300.034	y: 24.603	x: 4.012

RD.		Offset Distance					Arrival Time				
NO.	HMic1	HMic2	HMic3	HMic4	HMic5	LMic1	LMic2	LMic3	LMic4	LMic5	LMic6
Consec.	(m)	(m)	(m)	(m)	(m)	(msec)	(msec)	(msec)	(msec)	(msec)	(msec)
1	0.969	ND	4.870	ND	11.151	DNA	DNA	DNA	DNA	DNA	DNA
2	1.381	ND	5.357	ND	11.574	8.560	0.000	4.080	11.400	0.864	7.840
3	1.359	ND	5.445	ND	11.669	8.400	0.000	4.240	11.200	0.832	8.160
4	1.109	ND	5.491	ND	11.757	8.560	0.000	4.960	11.400	0.816	9.040
5	1.603	ND	5.242	ND	11.413	8.480	0.000	2.560	11.400	1.340	7.120
6	1.309	ND	5.135	ND	11.360	8.960	0.000	2.960	12.200	1.420	7.600
7	1.245	ND	5.274	ND	11.511	8.640	0.000	3.640	12.000	1.340	8.240
8	1.248	ND	5.246	ND	11.482	8.720	0.000	3.480	12.100	1.340	8.080
9	1.350	ND	5.461	ND	11.687	8.360	0.000	4.290	11.250	0.730	8.190
10	1.234	ND	5.141	ND	11.378	9.040	0.000	3.440	11.900	0.808	7.360
11	1.064	ND	5.588	ND	11.866	8.160	0.000	5.360	11.100	0.744	9.680
12	1.225	ND	5.268	ND	11.508	9.040	0.000	3.600	12.000	0.768	7.440
13	1.143	ND	5.263	ND	11.516	8.880	0.000	3.640	12.200	1.520	8.400
14	1.099	ND	5.376	ND	11.638	8.640	0.000	4.080	12.200	1.460	8.960
15	0.962	ND	5.101	ND	11.379	9.440	0.000	3.760	13.000	1.520	8.640
16	0.933	ND	5.214	ND	11.496	9.280	0.000	4.040	12.800	1.480	8.960
17	0.833	2.951	5.844	9.025	12.177	8.000	0.000	7.550	11.860	1.875	13.400
18	0.888	2.910	6.026	9.222	12.379	7.920	0.000	8.760	11.870	1.930	14.720
19	1.353	2.967	5.014	8.113	11.233	9.120	0.000	3.680	12.600	1.820	9.000
20	1.870	3.739	5.781	8.833	11.928	6.960	0.000	4.240	10.500	1.680	9.360
21	1.491	3.196	5.227	8.309	11.421	8.640	0.000	3.600	11.900	1.760	8.800
22	1.982	3.728	5.575	8.596	11.680	7.520	0.000	3.440	10.700	1.840	8.320
23	1.043	2.805	5.112	8.246	11.379	9.360	0.000	4.560	12.900	1.800	9.920
24	1.214	3.129	5.473	8.596	11.723	8.160	0.000	4.880	11.800	1.760	10.500
25	1.323	3.300	5.678	8.798	11.923	7.680	0.000	5.360	11.100	1.680	10.600
26	1.074	2.907	5.241	8.373	11.505	8.880	0.000	4.800	12.500	1.760	10.100
27	1.822	2.865	4.338	7.388	10.492	10.200	0.000	0.700	13.800	1.920	5.680
28	1.853	2.951	4.417	7.457	10.557	10.100	0.000	0.880	13.600	1.880	5.800

RD.		Offset Distance					Arrival Time				
NO.	HMic1	HMic2	HMic3	HMic4	HMic5	LMic1	LMic2	LMic3	LMic4	LMic5	LMic6
Consec.	(m)	(m)	(m)	(m)	(m)	(msec)	(msec)	(msec)	(msec)	(msec)	(msec)
29	2.353	3.734	5.049	7.983	11.034	8.400	0.000	1.200	11.600	1.840	5.680
30	2.432	3.910	5.276	8.200	11.244	7.920	0.000	1.630	11.000	1.760	6.240
31	2.217	3.833	5.438	8.411	11.475	7.760	0.000	2.440	10.800	1.800	7.040
32	ND	ND	ND	ND	ND	6.320	0.000	0.760	8.400	1.240	3.840
33	ND	ND	ND	ND	ND	5.280	0.000	-0.640	7.200	1.280	1.600
34	ND	ND	ND	ND	ND	9.600	0.000	-1.560	12.600	1.480	1.960
35	1.904	3.638	5.505	8.535	11.623	7.600	0.000	3.640	10.400	1.200	8.000
36	2.097	3.755	5.458	8.453	11.527	7.680	0.000	3.200	10.400	1.280	7.400
37	1.290	3.138	5.383	8.494	11.617	8.320	0.000	5.000	11.470	1.225	9.790
38	1.483	3.021	4.946	8.028	11.141	9.680	0.000	3.600	13.070	1.290	8.380
39	1.750	3.542	5.536	8.592	11.690	9.440	0.000	5.840	12.700	1.160	10.780
40	0.863	2.582	4.980	8.131	11.272	10.000	0.000	4.880	13.430	1.275	9.910
41	1.457	3.029	4.989	8.075	11.189	9.360	0.000	3.520	12.470	1.315	8.120
42	ND	ND	ND	ND	ND	DNA	DNA	DNA	DNA	DNA	DNA
43	ND	ND	ND	ND	ND	DNA	DNA	DNA	DNA	DNA	DNA
44	ND	ND	ND	ND	ND	DNA	DNA	DNA	DNA	DNA	DNA
45	ND	ND	ND	ND	ND	DNA	DNA	DNA	DNA	DNA	DNA
46	ND	ND	ND	ND	ND	DNA	DNA	DNA	DNA	DNA	DNA
47	1.358	2.572	5.715	8.834	11.949	6.590	0.000	5.810	9.850	0.605	9.970
48	1.546	2.713	5.784	8.884	11.989	6.160	0.000	5.440	9.310	0.615	9.540
49	1.147	2.409	5.626	8.764	11.888	7.040	0.000	6.030	10.330	0.450	10.200
50	1.274	2.247	5.300	8.412	11.526	7.730	0.000	4.700	11.070	0.645	9.010
51	ND	ND	ND	ND	ND	DNA	DNA	DNA	DNA	DNA	DNA
52	0.769	1.826	5.090	8.250	11.387	8.820	0.000	5.030	12.760	1.625	10.350
53	0.879	2.167	5.456	8.613	11.747	7.740	0.000	5.770	11.550	1.525	11.100
54	1.465	2.707	5.844	8.958	12.070	6.000	0.000	5.200	9.710	1.625	10.360
55	1.598	2.467	5.354	8.426	11.521	7.120	0.000	3.600	10.840	1.560	8.480
56	ND	ND	ND	ND	ND	DNA	DNA	DNA	DNA	DNA	DNA

RD.		Offset Distance					Arrival Time					
NO.	HMic1	HMic2	HMic3	HMic4	HMic5	LMic1	LMic2	LMic3	LMic4	LMic5	LMic6
Consec.	(m)	(m)	(m)	(m)	(m)	(msec)	(msec)	(msec)	(msec)	(msec)	(msec)
57	ND	ND	ND	ND	ND	DNA	DNA	DNA	DNA	DNA	DNA
58	1.416	2.585	5.689	8.799	11.910	6.530	0.000	5.560	9.730	0.530	9.670
59	1.444	2.628	5.733	8.843	11.953	6.695	0.000	5.465	9.850	0.520	9.530
60	1.034	2.259	5.486	8.630	11.757	7.685	0.000	5.880	11.020	0.640	10.210
61	ND	ND	ND	ND	ND	DNA	DNA	DNA	DNA	DNA	DNA
62	ND	ND	ND	ND	ND	DNA	DNA	DNA	DNA	DNA	DNA
63	1.213	2.208	5.290	8.410	11.527	8.000	0.000	4.215	11.890	1.690	9.370
64	1.461	2.340	5.284	8.374	11.477	7.665	0.000	3.615	11.390	1.615	8.500
65	1.424	2.873	6.167	9.312	12.438	5.360	0.000	6.315	9.210	1.640	11.620
66	ND	ND	ND	ND	ND	DNA	DNA	DNA	DNA	DNA	DNA
67	ND	ND	ND	ND	ND	DNA	DNA	DNA	DNA	DNA	DNA
68	ND	ND	ND	ND	ND	DNA	DNA	DNA	DNA	DNA	DNA
69	ND	ND	ND	ND	ND	DNA	DNA	DNA	DNA	DNA	DNA
70	ND	ND	ND	ND	ND	DNA	DNA	DNA	DNA	DNA	DNA
71	2.201	2.681	5.092	8.059	11.108	7.765	0.000	1.615	11.310	1.520	5.910
72	2.192	2.653	5.056	8.024	11.074	7.965	0.000	1.190	11.430	1.430	5.740
73	1.344	2.432	5.512	8.622	11.734	7.460	0.000	4.825	11.070	1.275	9.580
74	ND	ND	ND	ND	ND	DNA	DNA	DNA	DNA	DNA	DNA
75	ND	ND	ND	ND	ND	DNA	DNA	DNA	DNA	DNA	DNA
76	ND	ND	ND	ND	ND	DNA	DNA	DNA	DNA	DNA	DNA
77	ND	ND	ND	ND	ND	11.890	0.000	3.410	16.060	2.010	8.970
78	ND	ND	ND	ND	ND	DNA	DNA	DNA	DNA	DNA	DNA
79	ND	ND	ND	ND	ND	DNA	DNA	DNA	DNA	DNA	DNA
80	ND	ND	ND	ND	ND	DNA	DNA	DNA	DNA	DNA	DNA
81	ND	ND	ND	ND	ND	DNA	DNA	DNA	DNA	DNA	DNA
82	1.101	2.419	5.675	8.820	11.948	6.920	0.000	4.930	11.350	2.715	11.140
83	1.520	3.037	6.388	9.543	12.675	4.720	0.000	6.105	9.100	2.745	12.370
84	1.329	2.674	5.903	9.038	12.160	6.130	0.000	5.025	10.500	2.755	11.130

RD.		Offset Distance					Arrival Time				
NO.	HMic1	HMic2	HMic3	HMic4	HMic5	LMic1	LMic2	LMic3	LMic4	LMic5	LMic6
Consec.	(m)	(m)	(m)	(m)	(m)	(msec)	(msec)	(msec)	(msec)	(msec)	(msec)
85	ND	ND	ND	ND	ND	DNA	DNA	DNA	DNA	DNA	DNA
86	1.662	2.933	6.052	9.156	12.262	5.465	0.000	4.610	9.670	2.730	10.640
87	2.454	2.759	4.926	7.839	10.866	7.670	0.000	0.180	11.820	2.885	5.480
88	1.562	2.813	5.935	9.043	12.152	5.855	0.000	4.485	10.070	2.735	10.560
89	1.841	3.365	6.700	9.848	12.974	3.550	0.000	6.285	7.780	2.780	12.500
90	1.970	2.371	4.858	7.866	10.936	8.010	0.000	1.025	12.280	2.785	6.650
91	1.538	2.891	6.092	9.216	12.332	5.490	0.000	5.080	9.740	2.680	11.180
92	0.951	2.418	5.782	8.949	12.087	6.885	0.000	5.690	11.440	2.735	12.010
93	ND	ND	ND	ND	ND	9.390	0.000	7.190	14.220	2.720	13.940
94	ND	ND	ND	ND	ND	DNA	DNA	DNA	DNA	DNA	DNA
95	2.206	2.736	5.182	8.136	11.193	7.090	0.000	1.680	10.880	2.105	6.570
96	ND	ND	ND	ND	ND	10.100	0.000	5.050	14.590	2.775	11.550
97	1.981	3.156	6.142	9.194	12.287	4.860	0.000	4.630	8.390	1.965	9.900
98	0.606	1.749	5.088	8.254	11.399	8.800	0.000	4.940	13.150	2.420	11.030
99	ND	ND	ND	ND	ND	DNA	DNA	DNA	DNA	DNA	DNA
100	1.796	3.178	6.373	9.478	12.594	4.160	0.000	6.780	7.250	0.545	11.170
101	1.458	2.763	5.947	9.059	12.180	5.940	0.000	6.230	9.140	0.825	10.710
102	1.358	2.683	5.898	9.020	12.146	6.010	0.000	6.420	9.200	0.705	10.960
103	1.121	2.397	5.630	8.763	11.894	6.930	0.000	6.420	10.270	0.740	10.890
104	ND	ND	ND	ND	ND	DNA	DNA	DNA	DNA	DNA	DNA
105	1.734	3.223	6.529	9.663	12.792	3.680	0.000	6.510	7.530	2.140	12.310
106	0.912	2.323	5.664	8.820	11.961	6.990	0.000	5.920	11.110	2.190	11.840
107	1.985	1.966	4.282	7.295	10.385	8.980	0.000	0.340	13.120	2.335	5.550
108	1.560	2.155	4.948	8.010	11.114	7.920	0.000	2.550	11.980	2.210	7.980
109	ND	ND	ND	ND	ND	DNA	DNA	DNA	DNA	DNA	DNA
110	1.704	3.040	6.208	9.310	12.425	4.800	0.000	6.370	8.130	0.965	10.910
111	2.100	2.574	5.036	8.007	11.073	7.800	0.000	2.180	10.940	1.090	6.180
112	1.060	2.405	5.685	8.827	11.961	6.990	0.000	6.720	10.510	0.960	11.430

RD.		Offset Distance					Arrival Time				
NO.	HMic1	HMic2	HMic3	HMic4	HMic5	LMic1	LMic2	LMic3	LMic4	LMic5	LMic6
Consec.	(m)	(m)	(m)	(m)	(m)	(msec)	(msec)	(msec)	(msec)	(msec)	(msec)
113	1.254	2.058	5.066	8.169	11.289	8.360	0.000	4.620	11.770	1.100	9.290
114	ND	ND	ND	ND	ND	DNA	DNA	DNA	DNA	DNA	DNA
115	ND	ND	ND	ND	ND	DNA	DNA	DNA	DNA	DNA	DNA
116	ND	ND	ND	ND	ND	DNA	DNA	DNA	DNA	DNA	DNA
117	1.245	2.835	6.294	9.469	12.617	4.840	0.000	5.030	9.820	4.225	12.440
118	1.648	2.800	5.841	8.920	12.026	5.295	0.000	3.025	9.930	4.030	10.080
119	2.652	2.993	5.093	7.949	10.966	6.465	0.000	-0.160	10.990	4.125	6.280
120	ND	ND	ND	ND	ND	DNA	DNA	DNA	DNA	DNA	DNA
121	1.868	3.478	6.988	10.173	13.324	2.635	0.000	5.895	7.600	4.400	13.540
122	2.022	2.321	4.734	7.721	10.797	7.155	0.000	0.370	11.930	4.110	7.060
123	1.993	3.264	6.330	9.400	12.499	4.175	0.000	3.230	8.820	4.155	10.330
124	2.364	2.468	4.562	7.482	10.533	7.060	0.000	-0.350	11.840	4.335	6.410
125	1.504	2.720	5.835	8.933	12.048	5.335	0.000	3.155	10.140	4.185	10.320
126	2.323	3.228	5.910	8.882	11.940	DNA	DNA	DNA	DNA	DNA	DNA
127	ND	ND	ND	ND	ND	DNA	DNA	DNA	DNA	DNA	DNA
128	1.897	3.295	6.493	9.596	12.711	DNA	DNA	DNA	DNA	DNA	DNA
129	2.654	2.662	4.505	7.357	10.383	DNA	DNA	DNA	DNA	DNA	DNA
130	2.363	3.086	5.609	8.551	11.598	DNA	DNA	DNA	DNA	DNA	DNA
131	1.643	3.103	6.387	9.517	12.645	DNA	DNA	DNA	DNA	DNA	DNA
132	1.714	2.594	5.450	8.498	11.593	DNA	DNA	DNA	DNA	DNA	DNA
133	2.545	2.374	4.174	7.069	10.116	DNA	DNA	DNA	DNA	DNA	DNA
134	ND	ND	ND	ND	ND	DNA	DNA	DNA	DNA	DNA	DNA
135	ND	ND	ND	ND	ND	DNA	DNA	DNA	DNA	DNA	DNA
136	ND	ND	ND	ND	ND	DNA	DNA	DNA	DNA	DNA	DNA
137	ND	ND	ND	ND	ND	DNA	DNA	DNA	DNA	DNA	DNA
138	ND	ND	ND	ND	ND	DNA	DNA	DNA	DNA	DNA	DNA
139	ND	ND	ND	ND	ND	DNA	DNA	DNA	DNA	DNA	DNA
140	ND	ND	ND	ND	ND	DNA	DNA	DNA	DNA	DNA	DNA

RD.		Offset Distance					Arrival Time				
NO.	HMic1	HMic2	HMic3	HMic4	HMic5	LMic1	LMic2	LMic3	LMic4	LMic5	LMic6
Consec.	(m)	(m)	(m)	(m)	(m)	(msec)	(msec)	(msec)	(msec)	(msec)	(msec)
141	ND	ND	ND	ND	ND	DNA	DNA	DNA	DNA	DNA	DNA
142	ND	ND	ND	ND	ND	DNA	DNA	DNA	DNA	DNA	DNA
143	ND	ND	ND	ND	ND	DNA	DNA	DNA	DNA	DNA	DNA
144	ND	ND	ND	ND	ND	DNA	DNA	DNA	DNA	DNA	DNA
145	1.924	2.515	5.127	8.131	11.210	2.200	0.000	4.110	5.060	1.850	8.790
146	ND	ND	ND	ND	ND	DNA	DNA	DNA	11.200	1.850	7.290
147	ND	ND	ND	ND	ND	DNA	DNA	DNA	13.530	2.220	-4.180
148	2.608	3.835	6.763	9.774	12.843	13.120	0.000	-1.090	17.620	3.485	5.550
149	ND	ND	ND	ND	ND	DNA	DNA	DNA	DNA	DNA	DNA
150	ND	ND	ND	ND	ND	DNA	DNA	DNA	DNA	DNA	DNA
151	ND	ND	ND	ND	ND	DNA	DNA	DNA	DNA	DNA	DNA
152	ND	ND	ND	ND	ND	DNA	DNA	DNA	DNA	DNA	DNA
153	ND	ND	ND	ND	ND	DNA	DNA	DNA	DNA	DNA	DNA
154	1.902	2.684	5.429	8.452	11.529	7.550	0.000	2.570	10.870	1.200	7.210
155	2.042	2.690	5.297	8.292	11.357	7.950	0.000	2.065	10.970	1.185	6.500
156	1.899	2.546	5.213	8.230	11.305	8.170	0.000	1.985	11.460	1.180	6.560
157	1.890	2.806	5.638	8.673	11.754	7.080	0.000	3.225	10.190	1.125	7.950
158	1.806	2.808	5.721	8.775	11.863	6.970	0.000	3.480	10.150	1.150	8.210
159	1.594	2.618	5.606	8.684	11.785	7.540	0.000	3.980	10.640	1.205	8.740
160	1.930	2.845	5.663	8.694	11.772	7.000	0.000	3.745	9.560	0.425	7.510
161	1.703	2.698	5.637	8.701	11.795	7.220	0.000	3.930	9.970	0.395	8.000
162	1.865	2.694	5.480	8.511	11.591	7.320	0.000	3.175	10.080	0.430	7.150
163	1.971	2.835	5.608	8.628	11.702	6.710	0.000	3.435	9.360	0.365	7.300
164	1.681	2.507	5.358	8.413	11.505	7.540	0.000	3.400	10.270	0.290	7.550
165	1.732	2.612	5.473	8.525	11.614	7.345	0.000	3.465	10.050	0.335	7.465
166	ND	ND	ND	ND	ND	DNA	DNA	DNA	DNA	DNA	DNA
167	2.065	3.020	5.827	8.845	11.917	6.490	0.000	3.610	9.390	0.885	7.920
168	0.895	1.778	4.977	8.123	11.257	9.820	0.000	4.400	13.180	0.700	9.250

RD.		Offset Distance					Arrival Time				
NO.	HMic1	HMic2	HMic3	HMic4	HMic5	LMic1	LMic2	LMic3	LMic4	LMic5	LMic6
Consec.	(m)	(m)	(m)	(m)	(m)	(msec)	(msec)	(msec)	(msec)	(msec)	(msec)
169	1.982	2.823	5.576	8.593	11.665	7.220	0.000	3.070	10.200	0.910	7.480
170	1.650	2.581	5.498	8.563	11.658	7.580	0.000	3.830	10.570	0.755	8.310
171	1.430	2.664	5.816	8.928	12.043	6.925	0.000	5.575	10.010	0.790	7.700
172	1.864	2.067	4.555	7.583	10.669	9.580	0.000	0.910	12.700	0.830	5.220
173	1.736	2.318	5.029	8.070	11.157	8.740	0.000	2.080	11.770	0.810	6.460
174	1.873	2.841	5.712	8.755	11.838	6.870	0.000	3.810	9.820	0.860	8.290
175	1.424	1.989	4.858	7.946	11.055	DNA	DNA	DNA	DNA	DNA	DNA
176	2.369	2.527	4.665	7.590	10.632	DNA	DNA	DNA	DNA	DNA	DNA
177	2.707	3.159	5.343	8.205	11.210	DNA	DNA	DNA	DNA	DNA	DNA
178	2.606	3.013	5.204	8.083	11.097	DNA	DNA	DNA	DNA	DNA	DNA
179	1.649	2.493	5.365	8.425	11.519	DNA	DNA	DNA	DNA	DNA	DNA
180	2.130	2.841	5.455	8.440	11.499	DNA	DNA	DNA	DNA	DNA	DNA
181	2.747	3.622	6.181	9.100	12.121	DNA	DNA	DNA	DNA	DNA	DNA
182	1.847	2.208	4.766	7.790	10.873	DNA	DNA	DNA	DNA	DNA	DNA
183	4.180	4.969	8.147	11.175	14.234	DNA	DNA	DNA	DNA	DNA	DNA
184	1.955	3.009	5.920	8.963	12.046	DNA	DNA	DNA	DNA	DNA	DNA
185	2.222	3.632	6.819	9.915	13.019	3.670	0.000	5.860	6.880	1.685	11.210
186	1.618	2.742	5.784	8.869	11.972	7.015	0.000	4.120	10.470	1.530	9.300
187	2.173	3.328	6.273	9.312	12.390	5.390	0.000	4.205	8.600	1.580	9.200
188	2.117	3.437	6.544	9.623	12.719	4.595	0.000	5.195	7.850	1.645	10.540
189	1.878	2.480	5.132	8.151	11.229	8.295	0.000	1.655	11.740	1.555	6.520
190	1.715	2.862	5.896	8.975	12.074	6.535	0.000	4.475	10.020	1.615	9.630
191	2.065	3.239	6.221	9.273	12.358	4.485	0.000	4.490	8.740	1.620	9.680
192	1.986	3.287	6.394	9.477	12.576	5.145	0.000	5.160	8.440	1.655	10.450

APPENDIX D:

DATA COLLECTION TEST RANGE DATA

INTENTIONALLY LEFT BLANK.

RD.	GUN	RD.	DATE	TIME	MET CONDITIONS				TERMINAL	IMPACT LOCATION	
#	TYPE	TYPE			TEMP	REL. HUM.	WINDS		MACH NO.	Y	Z
	(mm)			H:M:S	(C)	%	WD(deg)	WS(m/s)		(m)	(m)
1	7.62	M62	3/31/93	10:35:00	14.6	80	130.	1.2	ND	ND	ND
2	Mann	"	3/31/93	10:43:00	14.6	80	130.	1.2	ND	ND	ND
3	"	M59	3/31/93	10:50:00	14.6	80	130.	1.2	ND	ND	ND
4	"	"	3/31/93	10:50:30	14.6	80	130.	1.2	ND	ND	ND
5	"	M62	3/31/93	11:20:49	14.6	80	130.	1.2	1.7	-0.2229	4.291
6	"	"	3/31/93	11:27:03	14.8	80	178.	0.8	1.7	-0.1802	4.174
7	"	"	3/31/93	11:28:40	14.8	79	165.	0.9	1.7	-0.0729	4.578
8	"	M59	3/31/93	11:30:16	14.7	79	177.	2.6	1.7	-0.173	4.160
9	"	"	3/31/93	11:32:58	14.9	80	180.	1.8	1.7	-0.0692	4.215
10	"	"	3/31/93	11:34:47	15.0	79	183.	2.1	1.7	-0.046	4.275
11	"	M62	3/31/93	13:21:45	13.5	85	213.	5.3	1.7	-0.1133	4.182
12	"	"	3/31/93	13:28:00	13.4	84	211.	6.4	1.7	-0.4088	4.161
13	"	"	3/31/93	13:33:02	12.9	84	199.	6.1	1.6	-0.6101	3.882
14	"	"	3/31/93	13:35:38	12.9	84	199.	6.1	1.7	-0.4175	4.281
15	"	M59	3/31/93	13:41:58	12.7	86	208.	6.2	1.7	0.1123	4.020
16	"	"	3/31/93	13:47:34	12.7	86	208.	6.2	1.7	0.1364	4.012
17	"	"	3/31/93	13:51:06	12.7	86	208.	6.2	1.7	0.1477	4.051
18	7.62	M62	4/5/93	10:49:54	6.2	65	62.	4.4	1.1	ND	ND
19	Mann	"	4/5/93	11:01:46	6.2	65	62.	4.4	1.1	ND	ND
20	"	"	4/5/93	11:08:09	6.2	65	62.	4.4	1.1	0.3222	4.658
21	"	M59	4/5/93	11:21:55	6.2	65	62.	4.4	1.0	0.2011	4.379
22	"	M62	4/5/93	11:25:05	6.2	65	62.	4.4	1.1	0.0512	4.345
23	"	M59	4/5/93	11:28:36	6.2	65	62.	4.4	1.0	0.3186	4.453
24	"	M62	4/5/93	11:42:05	6.2	65	62.	4.4	ND	ND	ND
25	"	"	4/5/93	11:46:55	6.2	65	62.	4.4	1.1	-0.2676	3.849
26	"	M59	4/5/93	11:47:55	6.2	65	62.	4.4	1.0	0.2553	4.359
27	12.7	M17	4/5/93	13:44:51	6.2	65	62.	4.4	2.1	ND	ND
28	Mann	"	4/5/93	13:55:01	6.4	65	62.	4.2	2.0	-0.433	4.469

RD.	GUN	RD.	DATE	TIME	MET CONDITIONS				TERMINAL	IMPACT LOCATION	
#	TYPE	TYPE			TEMP	REL. HUM.	WINDS		MACH NO.	Y	Z
	(mm)			H:M:S	(C)	%	WD(deg)	WS(m/s)		(m)	(m)
29	"	"	4/5/93	14:12:19	6.6	64	53.	4.4	2.0	-0.2137	3.389
30	"	"	4/5/93	14:23:24	6.6	64	65.	4.6	2.0	0.5578	4.107
31	"	"	4/5/93	14:25:25	6.8	64	58.	4.3	2.1	0.2793	4.173
32	"	M33	4/5/93	14:27:25	6.8	64	63.	3.7	ND	ND	ND
33	"	"	4/5/93	14:32:32	6.8	64	65.	3.6	1.7	ND	ND
34	"	"	4/5/93	14:36:39	7.0	65	53.	4.0	1.8	ND	ND
35	"	"	4/5/93	14:42:57	6.8	63	58.	3.4	1.8	ND	ND
36	"	"	4/5/93	14:56:49	7.1	64	49.	4.3	2.0	0.3273	3.070
37	"	"	4/5/93	14:58:45	7.1	63	56.	3.9	1.7	ND	ND
38	"	"	4/5/93	15:02:38	7.0	64	57.	4.5	1.8	ND	ND
39	"	"	4/5/93	15:05:30	7.1	63	80.	4.0	2.0	-0.0799	4.581
40	"	"	4/5/93	15:09:13	7.2	64	71.	4.4	1.9	0.0749	4.325
41	"	"	4/5/93	15:10:51	7.3	64	63.	4.7	1.7	ND	ND
42	"	"	4/5/93	15:13:52	7.3	63	52.	4.4	1.7	ND	ND
43	"	"	4/5/93	15:16:16	7.3	64	62.	4.5	1.9	-1.5507	3.863
44	"	"	4/5/93	15:18:38	7.3	64	61.	5.6	2.0	0.263	4.375
45	7.62	M62	4/6/93	10:03:06	6.0	58	57.	7.3	1.4	0.3988	4.730
46	Mann	M59	4/6/93	10:16:50	6.4	57	63.	8.3	1.3	0.1527	4.151
47	"	"	4/6/93	10:18:51	6.5	56	62.	8.9	1.3	-0.2308	4.558
48	"	M62	4/6/93	10:20:43	6.8	56	69.	7.4	1.4	-0.2004	4.598
49	"	"	4/6/93	10:22:49	6.8	56	59.	7.7	1.3	0.0002	4.410
50	"	M59	4/6/93	10:25:10	7.1	56	54.	9.0	1.3	-0.5658	4.487
51	"	M62	4/6/93	10:26:54	7.3	56	59.	9.6	1.4	-0.5264	4.361
52	12.7	M17	4/6/93	13:33:45	10.7	47	60.	7.2	1.4	ND	ND
53	Mann	"	4/6/93	13:42:06	10.4	46	59.	8.0	1.4	0.5712	4.696
54	"	M33	4/6/93	13:44:17	10.5	45	65.	8.1	1.3	0.0318	3.439
55	"	"	4/6/93	13:46:45	10.8	47	71.	8.1	1.3	-0.186	3.188
56	"	"	4/6/93	14:05:38	10.6	46	69.	7.9	1.3	0.7876	4.176

RD.	GUN	RD.	DATE	TIME	MET CONDITIONS				TERMINAL	IMPACT LOCATION	
#	TYPE	TYPE			TEMP	REL. HUM.	WINDS		MACH NO.	Y	Z
	(mm)			H:M:S	(C)	%	WD(deg)	WS(m/s)		(m)	(m)
57	"	"	4/6/93	14:08:12	10.7	45	80.	9.0	1.3	1.0217	3.785
58	"	M17	4/6/93	14:11:57	10.6	44	64.	8.4	1.5	-1.3249	4.693
59	"	"	4/6/93	14:15:12	10.6	44	64.	9.9	1.5	1.0534	4.913
60	"	"	4/6/93	14:18:33	10.7	45	68.	8.3	1.5	0.5658	5.133
61	"	M33	4/6/93	14:21:08	10.9	44	50.	8.6	1.3	ND	ND
62	7.62	M62	4/6/93	15:08:53	10.8	42	73.	8.4	1.7	0.3539	4.294
63	Mann	"	4/6/93	15:19:33	11.1	43	66.	8.5	1.7	-0.062	4.112
64	"	M59	4/6/93	15:21:20	10.8	42	67.	8.6	1.7	-0.1317	4.238
65	"	M62	4/6/93	15:22:19	10.8	42	68.	8.8	1.7	0.3402	3.973
66	"	M59	4/6/93	15:23:28	10.8	42	70.	8.1	1.6	-0.1763	4.139
67	"	"	4/6/93	15:24:09	10.9	42	62.	7.6	1.7	-0.3942	4.123
68	"	M62	4/6/93	15:25:47	10.8	43	64.	8.3	1.7	-0.3049	4.280
69	35	DM18	4/7/93	10:48:00	9.9	47	352.	4.8	ND	ND	ND
70	TIPGID	"	4/7/93	10:53:43	10.1	46	0.	4.5	2.5	ND	ND
71	"	"	4/7/93	10:55:50	10.1	46	359.	4.5	2.5	ND	ND
72	"	"	4/7/93	10:58:43	10.1	46	2.	3.3	2.5	ND	ND
73	"	TPL-T	4/7/93	10:02:19	10.1	46	359.	4.5	3.1	ND	ND
74	"	"	4/7/93	11:04:40	10.3	46	1.	5.1	3.1	ND	ND
75	"	DM18	4/7/93	11:09:53	10.5	46	346.	5.2	2.4	0.6263	3.896
76	"	TPL-T	4/7/93	11:34:07	11.5	47	349.	3.9	3.1	0.1648	4.089
77	"	DM18	4/7/93	11:36:22	11.6	47	349.	4.5	2.5	0.7707	4.567
78	"	TPL-T	4/7/93	11:37:56	11.7	49	352.	3.6	3.1	0.0248	3.613
79	"	DM18	4/7/93	11:42:38	12.1	48	4.	4.4	2.5	1.0961	3.860
80	"	TPL-T	4/7/93	11:43:00	12.0	48	355.	3.9	3.1	0.3734	3.505
81	35	TPL-T	4/7/93	13:57:30	13.4	51	115.	1.6	3.8	ND	ND
82	TIPGID	"	4/7/93	14:01:54	13.3	51	102.	1.9	3.8	-0.0546	4.267
83	"	"	4/7/93	14:15:53	13.1	48	113.	2.4	3.8	0.0085	4.008
84	"	DM18	4/7/93	14:17:13	13.2	49	122.	2.3	2.9	-0.2	4.742

RD.	GUN	RD.	DATE	TIME	MET CONDITIONS				TERMINAL	IMPACT LOCATION	
#	TYPE	TYPE			TEMP	REL. HUM.	WINDS		MACH NO.	Y	Z
	(mm)			H:M:S	(C)	%	WD(deg)	WS(m/s)		(m)	(m)
85	"	"	4/7/93	14:19:58	13.5	49	128.	1.8	2.9	-0.0491	4.268
86	"	"	4/7/93	14:21:10	13.4	49	122.	1.5	2.9	-0.5449	4.430
87	"	TPL-T	4/7/93	14:22:38	13.3	49	123.	2.1	3.9	0.0302	4.112
88	35	TPL-T	4/7/93	15:07:32	14.1	48	104.	2.9	2.4	ND	ND
89	TIPGID	DM18	4/7/93	15:10:06	14.0	48	111.	3.5	2.1	ND	ND
90	"	TPL-T	4/7/93	15:12:40	14.2	48	112.	3.6	2.4	0.3719	3.673
91	"	DM18	4/7/93	15:24:49	13.6	49	127.	1.9	2.0	-1.1667	4.013
92	"	TPL-T	4/7/93	15:26:02	13.9	49	120.	1.9	2.4	-0.2488	5.227
93	"	DM18	4/7/93	15:27:42	13.7	50	121.	2.4	2.0	-1.0879	4.114
94	"	TPL-T	4/7/93	15:29:05	13.4	49	115.	2.2	2.4	0.0701	4.556
95	"	DM18	4/7/93	15:30:33	13.4	49	115.	2.0	2.1	-0.1515	4.288
96	12.7	M17	4/8/93	11:06:46	10.4	28	82.	3.3	2.0	-0.2146	4.602
97	Mann	M33	4/8/93	11:08:37	10.4	29	75.	3.6	2.1	0.3322	4.554
98	"	"	4/8/93	11:13:47	10.8	29	74.	3.1	2.0	0.0656	4.316
99	"	"	4/8/93	11:16:58	10.9	33	77.	2.8	2.0	0.1268	4.631
100	"	"	4/8/93	11:19:08	10.8	34	72.	2.9	2.1	0.1647	4.261
101	"	"	4/8/93	11:19:54	10.9	34	76.	2.7	2.1	0.1647	4.211
102	"	"	4/8/93	11:20:55	11.0	35	79.	2.4	2.0	0.3106	4.180
103	"	"	4/8/93	11:24:19	10.9	37	76.	2.3	2.1	-1.2304	4.346
104	"	"	4/8/93	11:26:01	11.0	37	75.	2.1	2.1	-1.2948	4.340
105	"	"	4/8/93	11:27:38	11.1	38	78.	1.9	2.1	-1.3645	4.395
106	"	"	4/8/93	11:30:25	11.3	39	83.	2.0	2.1	-1.4346	3.167
107	"	"	4/8/93	11:33:26	11.6	38	99.	1.7	2.1	-1.3139	3.541
108	"	"	4/8/93	11:34:18	11.6	38	99.	1.7	2.1	-1.3424	3.510
109	"	"	4/8/93	11:36:45	11.5	38	87.	1.9	2.1	0.9299	4.498
110	"	"	4/8/93	11:38:42	11.5	37	95.	1.7	2.1	1.1778	4.753
111	"	"	4/8/93	11:39:36	11.5	37	92.	1.7	2.1	1.1793	4.673
112	"	"	4/8/93	11:41:45	11.6	37	99.	1.6	2.1	1.2093	3.748

RD.	GUN	RD.	DATE	TIME	MET CONDITIONS				TERMINAL	IMPACT LOCATION	
#	TYPE	TYPE			TEMP	REL. HUM.	WINDS		MACH NO.	Y	Z
	(mm)			H:M:S	(C)	%	WD(deg)	WS(m/s)		(m)	(m)
113	"	"	4/8/93	11:43:02	11.6	37	102.	1.3	2.1	1.188	3.529
114	"	"	4/8/93	11:44:13	11.5	28	88.	2.1	2.1	0.9888	3.512
115	"	"	4/8/93	11:46:51	11.6	37	103.	1.8	2.0	1.195	3.630
116	"	"	4/8/93	11:48:22	11.7	38	121.	1.2	2.1	1.1598	3.727
117	"	"	4/8/93	11:49:46	11.8	38	121.	1.2	2.1	1.139	3.339
118	"	M17	4/8/93	11:50:50	11.8	38	102.	1.0	2.1	0.4572	3.711
119	12.7	M33	4/8/93	14:03:46	15.1	35	94.	2.2	2.1	0.0334	4.152
120	Mann	M17	4/8/93	14:15:09	15.0	33	78.	1.4	2.1	-0.1314	4.214
121	"	"	4/8/93	14:16:52	15.1	33	92.	1.6	2.1	-0.2068	3.736
122	"	"	4/8/93	14:18:13	15.1	32	92.	2.2	2.1	-0.4208	4.292
123	"	M33	4/8/93	14:19:23	15.3	32	90.	2.3	2.1	0.1546	3.897
124	"	"	4/8/93	14:21:14	15.4	31	96.	2.2	2.1	-0.135	3.693
125	35	DM18	4/8/93	15:05:20	16.7	31	86.	4.0	2.8	0.0246	4.372
126	TIPGID	DM68	4/8/93	15:16:03	16.3	34	87.	3.8	3.0	-0.1415	4.607
127	"	"	4/8/93	15:17:27	16.3	34	87.	3.8	3.0	-0.1808	4.429
128	"	"	4/8/93	15:18:19	16.3	33	85.	3.8	2.9	-0.1237	4.322
129	"	DM18	4/8/93	15:19:14	16.3	33	87.	3.5	2.9	-0.0951	4.226
130	35	DM68	4/9/92	9:19:37	8.6	100	71.	4.1	2.0	-0.4724	4.873
131	TIPGID	DM18	4/9/92	9:34:49	8.8	100	78.	3.6	2.0	0.1653	4.754
132	"	DM68	4/9/92	9:37:54	8.7	100	82.	3.5	2.0	0.0732	4.653
133	"	"	4/9/92	9:40:02	8.8	100	82.	3.1	2.0	0.2015	4.996
134	"	DM18	4/9/92	9:42:33	8.8	100	78.	3.6	2.0	-0.9863	3.644
135	"	"	4/9/92	9:46:11	8.9	100	78.	3.5	2.0	0.2626	4.081
136	35	DM68	4/9/92	10:16:39	9.1	100	92.	1.7	2.5	0.2093	4.224
137	TIPGID	"	4/9/92	10:31:41	9.5	100	75.	1.0	2.5	-0.401	4.220
138	"	DM18	4/9/92	10:33:21	9.6	100	76.	0.7	2.5	0.162	3.698
139	"	"	4/9/92	10:35:01	9.4	100	57.	0.7	2.5	0.412	3.565
140	"	DM68	4/9/92	10:37:15	9.4	100	61.	0.7	2.5	-0.5789	4.083

INTENTIONALLY LEFT BLANK.

APPENDIX E:

PROJECTILE CHARACTERISTICS DATA FROM COLLECTION TEST PHASE

INTENTIONALLY LEFT BLANK.

Shot	Round	Ch	Pos P	Neg P1	Neg P2	A1	A2	A3	ATot	Peak	ABS	Cal
	Type		Pa	Pa	Pa	msec	msec	msec	msec	mPa-sec	mPa-sec	Pa/Volt
20	M62	1				112	216		256			
		2				128	232		268			
		3				156	288		320			
		4				180			340			
		8				204			380			
21	M59	1				272			524			
		2				268			516			
		3				264			524			
		4				260			524			
		8				248			516			
22	M62	1				116	208		260			
		2				128			304			
		3				168			324			
		4				184			360			
		8				212			380			
23	M59	1				320			604			
		2				308			592			
		3				292			568			
		4				276			572			
		8				308			556			
25	M62	1				104			196			
		2				116			240			
		3				156			308			
		4				184			336			
		8				212			380			
26	M59	1				260			516			
		2				268			508			
		3				248			524			
		4				272			520			
		8				300			548			
28	M17	1				112	192	220	272			
		2				116	196	224	272			
		3				152	252		324			
		4										
		8				212	336		412			
29	M17	1				92	156	188	228			
		2				104	164		244			
		3				148	252		320			
		4				184	288		364			
		8				208			396			
30	M17	1				104	172	200	256			
		2				124	200		284			
		3				160	260		340			
		4				176	296		376			
		8				200			408			
31	M17	1				96	168	192	248			
		2				120	200		276			
		3				152	268		336			
		4				180	300		368			
		8				216			408			

Shot	Round	Ch	Pos P	Neg P1	Neg P2	A1	A2	A3	ATot	Peak	ABS	Cal
	Type		Pa	Pa	Pa	msec	msec	msec	msec	mPa-sec	mPa-sec	Pa/Volt
36	M33	1				52	116		180			
		2				116	196		256			
		3				164			336			
		4				184			364			
		8				216			388			
38	M33	1				132	252		288			
		2										
		3										
		4				172			332			
		8				204			372			
39	M33	1				108	188	216	256			
		2				116	204		268			
		3				152	272		332			
		4				184			364			
		8				208			400			
40	M33	1				108	180		256			
		2				116	196		264			
		3				152	264		316			
		4				172			360			
		8				220			396			
43	M33	1				124			272			
		2										
		3				144			296			
		4				168			348			
		8				212			392			
44	M33	1				100			248			
		2				120			272			
		3				164			320			
		4				176			360			
		8				204			388			
45	M62	1	868.74	-466.28	-578	96	164		212	34.58	77.14	693.88
		2	554.2	-365.29	-476.75	112	176		228	30.69	65.93	557.27
		3	259.07	-224.41	-224.41	124	228		264	18.64	39.29	357.35
		4	127.99	127.99	-141.64		148		276	13.99	27.46	324.86
		8	85.56	85.56	-110.81		164		304	9.82	20.13	107.47
46	M59	1	1102.56	-738.91	-857.62	92	168		200	45.76	101.51	693.88
		2	677.63	-503.25	-571.2	108	188		216	34.74	73.73	557.27
		3	218.34		-248.35	140			252	17.48	35.34	357.35
		4	191.46		-174.56	156			288	15.74	29.71	324.86
		8	85.42		-91.57	204			308	11.59	21.47	107.47
47	M59	1	879.14		-643.92	96	176		200	36.37	79.88	693.88
		2	749.25		-575.94	100			200	30.67	68.07	557.27
		3	197.26		-244.78	148			240	19.13	38.12	357.35
		4	209.21		-230	148			292	18.19	37.68	324.86
		8	125.42		-145.95	160			308	13.14	26.66	107.47
48	M62	1	867.35	-469.8	-573.14	92	150		204	34.71	76.42	693.88
		2	647.55	-373.93	-429.65	100	160		208	29.99	59.71	557.27
		3	275.16	-257.29	-286.95	136	212		264	22.18	46.4	357.35
		4	183.22		-175.43	152			292	16.63	31.48	324.86
		8	114.35		-129.61	164			300	11.78	22.25	107.47

Shot	Round	Ch	Pos P	Neg P1	Neg P2	A1	A2	A3	ATot	Peak	ABS	Cal
	Type		Pa	Pa	Pa	msec	msec	msec	msec	mPa-sec	mPa-sec	Pa/Volt
49	M62	1	814.61	-491.26	-650.86	104	164		220	40.37	86.55	693.88
		2	667.05	-429.65	-492.07	108	180		232	33.17	73.04	557.27
		3	303.03	-308.74	-273.01	128	240		280	23.05	54.99	357.35
		4	176.4		-194.92	156			308	16.81	36.17	324.86
		8	96.4		-110.4	192			320	12.31	22.15	107.47
50	M59	1	768.12		-618.24	100			204	37.19	75.93	693.88
		2	818.63		-663.15	96			200	33.44	75.75	557.27
		3	331.62		-355.92	120			252	23.08	48.56	357.35
		4	190.37		-159.18	140			280	13.47	26.27	324.86
		8	91.14		-107.8	184			320	11.22	20.37	107.47
51	M62	1	899.96	-473.92	-636.29	100	152		208	37.45	80.84	693.88
		2	818.07	-455.29	-534.42	96	156		208	34.07	78.18	557.27
		3	189.39		-198.68	140			252	17.74	36.19	357.35
		4	239.75		-215.71	136			292	17.83	40.74	324.86
		8	114.46		-159.5	196			312	17.31	37.94	107.47
53	M17	1	1600.08	-636.3	-880.53	136	220		320	69.94	166.96	693.88
		2	1121.22	-528.85	-655.35	144	244		344	55.45	137.09	557.27
		3	594.27		-472.77	172			416	56.61	141.02	357.35
		4	214.41		-159.18	184			412	24.96	57.05	324.86
		8	164		-154	228			456	25.33	48.62	107.47
54	M33	1	3244.57	-1350.9	-2178	104	168		248	118.58	313.22	693.88
		2	1207.04	-692.13	-959.06	128	224		296	69.21	161.19	557.27
		3	438.47	-401.66	-453.12	168	308		376	44.11	108.05	357.35
		4	322.59		-307.97	192			416	32.37	77.13	324.86
		8	150.36		-179.16	248			444	24.34	47.51	107.47
55	M33	1	3046.8	-1323.9	2427.18	104	160		248	132.13	329.48	693.88
		2	1263.33	-767.92	-1151.3	132	208		292	79.94	181.31	557.27
		3	373.07		-399.16	176			368	40.54	83.12	357.35
		4	295.3		-290.1	196			412	33.4	69.67	324.86
		8	250.52		-275.35	224			472	32.81	62.17	107.47
56	M33	1	1779.1	-754.9	-1165.2	132	216		296	80.31	189.8	693.88
		2	941.23	-580.12	-682.1	144	260		332	59.35	142.8	557.27
		3	352.34		-366.64	204			396	39.82	82.55	357.35
		4	191.34		-184.52	228			412	24.57	44.52	324.86
		8	143.26		-154.33	272			448	24.27	48.97	107.47
57	M33	1	1788.81	-864.6	-1230.2	132	216		300	88.87	217.68	693.88
		2	711.07	-468.7	-599.04	160	268		344	54.05	116.39	557.27
		3	369.14		-311.25	184			400	35.98	82.06	357.35
		4	306.18		-215.87	224			428	27.94	58.8	324.86
		8	181.52		-226.02	240			476	27.8	64.88	107.47
58	M17	1	1004.04	-498.2	-498.2	144	224		320	58.33	116.24	693.88
		2	1526.4	-730.57	-730.7	128	216		316	73.99	156.87	557.27
		3	326.6	-225.8	-225.8	172	248		344	38.77	73.22	357.35
		4	326.6	-273.7	-275.9	196	300		396	32.33	67.56	324.86
		8	183.4		-185.07	224			436	27.02	54.04	107.47
59	M17	1	1380.12	-571	-661.27	140	220		324	67.05	146.74	693.88
		2	664.26	-351.1	-466.43	156	244		344	48.77	98.89	557.27
		3	289.58		-267.3	180			388	29.84	62.91	357.35
		4	271.58		-220.91	188			420	28.37	61.7	324.86
		8	182.06		-199.15	236			460	25.84	56.6	107.47

Shot	Round	Ch	Pos P	Neg P1	Neg P2	A1	A2	A3	ATot	Peak	ABS	Cal
	Type		Pa	Pa	Pa	msec	msec	msec	msec	mPa-sec	mPa-sec	Pa/Volt
60	M17	1	1425.92	-562.7	-774.37	136	228		328	63.01	152.63	693.88
		2	891.07	-417.4	-557.83	148	240		344	52.39	117.98	557.27
		3	260.86		-266.98	184			388	32.29	63.66	357.35
		4	220.58		-241.7	216			416	31.55	64.01	324.86
		8	185.5		-184.7	216			488	25.07	52.11	107.47
62	M62	1	1741.63	-661.96	-807.67	72	128		176	39.48	100.93	693.88
		2	862.65	-396.77	-565.63	92	144		196	29.93	66.74	557.27
		3	335.91		-368.78	120			248	25.21	58.7	357.35
		4	165.03		-163.41	136			264	13.86	27.75	324.86
		8	130.9		-167.44	152			280	12.78	27.92	107.47
63	M62	1	1772.16	-597.43	-854.86	72	128		180	39.87	107.81	693.88
		2	755.66	-401.2	-571.2	92	140		188	31.18	65.47	557.27
		3	294.81		-255.5	116			228	16.73	34.67	357.35
		4	180.95		-167.3	148			264	15.8	30.12	324.86
		8	78.67		-81.57	172			276	9.03	17.61	107.47
64	M59	1	1602.16		-831.96	72			172	36.68	96.87	693.88
		2	967.42		-650.33	84			180	33.58	76.12	557.27
		3	291.13		-301.35	116			232	19.71	38.95	357.35
		4	255.99		-216.68	132			252	15.46	30.45	324.86
		8	113.92		-113.31	156			296	10.99	21.77	107.47
65	M62	1	2042.77	-686.2	-988.08	68	120		172	41.16	111.01	693.88
		2	797.45	-432.44	-545.57	84	144		196	29.55	66.79	557.27
		3	356.99		-291.95	104			240	19.88	48.48	357.35
		4	179.32		-165.03	136			260	13.6	26.16	324.86
		8	123.92		-146.6	176			312	14.5	28.45	107.47
66	M59	1	1613.26		-832.65	72			168	38.08	95.55	693.88
		2	980.79		-597.39	80			172	32.06	73.07	557.27
		3	350.56		-297.67	104			224	18.01	38.72	357.35
		4	187.77		-182.57	152			256	14.84	31.83	324.86
		8	133.05		-186.79	172			304	15.29	40.55	107.47
67	M59	1	1958.81		-1053.3	80			180	42.4	118.61	
		2	1175.3		-719.43	80			176	34.53	82.13	557.27
		3	376.29		-351.27	104			224	18.79	44.42	357.35
		4	250.14		-229.03	136			260	14.75	31.37	324.86
		8	105.97		-146.49	168			292	11.99	24.33	107.47
68	M62	1	1560.53		-727.88	76			184	353.29	92.75	693.88
		2	1102		-650.61	84			188	34.77	81.77	557.27
		3	237.28		-222.63	124			228	17.69	32.84	357.35
		4	215.71		-210.84	132			264	15.28	32.1	324.86
		8	130.04		-151.54	160			288	14.08	26.98	107.47
73	TPL-T	1	629.21	-403.58	-555.64	400	680		848	120.85	267.61	700.68
		2	725.22	-369.54	-492.48	392	705		872	110.47	239.03	554.026
		3	422.32		-393.2	420			924	91.431	205.91	350.769
		4	395.44		-359.34	436			944	94.485	201.32	319.416
		8	274.52		-347.99	504			964	85.586	176.83	105.102
74	TPL-T	1	602.55		-507.99	388			820	113.15	237.01	700.68
		2	501.67		-523.83	408			860	118.31	249.41	554.026
		3	434.95		-393.91	420			908	93.81	199.18	350.769
		4	486.79		-392.88	416			940	99.01	217.53	319.416
		8	282.34		-332.02	480			976	85.03	176.74	105.102

Shot	Round	Ch	Pos P	Neg P1	Neg P2	A1	A2	A3	ATot	Peak	ABS	Cal
	Type		Pa	Pa	Pa	msec	msec	msec	msec	mPa-sec	mPa-sec	Pa/Volt
75	DM18	1	3501.95		-3503.3	140	288	388	516	175.83	1186.95	700.68
		2	2411.68		-1853.2	252	352	476	588	244.21	563.95	554.026
		3	900.768		-900.74	320	456		716	155.46	348.85	350.769
		4	603.687		-573.97	368			780	119.12	244.29	319.416
		8	483.884		-479.37	392			856	111.21	221.53	105.102
76	TPL-T	1	3505.5		-3499.9	120			484	161.4	1112.27	700.68
		2	2772.62		-2178.1	232			548	286.78	645.11	554.026
		3	1139.65		-996.89	300			684	172.84	380.29	350.769
		4	780.66		-708.15	356			756	144.84	299.88	319.416
		8	513.74		-509.85	404			816	123.08	249.02	105.102
77	DM18	1	3505.5		-2454.4	232			552	293.44	725.2	700.68
		2	2251.8		-1621.9	268			608	235.02	525.04	554.026
		3	867.45		-807.82	332			708	142.65	300.05	350.769
		4	748.71		-658.96	364			788	132.24	286.73	319.416
		8	411.58		-426.19	412			816	102.94	198.63	105.102
78	TPL-T	1	3505.5		-3499.9	84			432	133.64	1192.5	700.68
		2	2772.6		-2470.1	220			528	313.76	714.9	554.026
		3	1096.85		-1038.9	304			676	177.85	394.76	350.769
		4	793.75		-703.35	352			752	146.31	299.39	319.416
		8	519.44		-524.79	416			848	127.89	260.38	105.102
79	DM18	1	3505.5		-3046.5	216			524	335.45	839.39	700.68
		2	2139.37		-1665.1	268			612	239.62	538.97	554.026
		3	864.65		-874.47	328			724	155.69	341.65	350.769
		4	705.91		-645.54	372			796	133.93	279.19	319.416
		8	501.65		-524.77	416			860	122.87	253.84	105.102
80	TPL-T	1	3505		-3500	76			416	129.8	1315.22	700.68
		2	2772.6		-2211.9	228			540	292.8	666.7	554.026
		3	1120.7		-990.2	296			684	173.92	394	350.769
		4	872		-746.2	352			764	151.85	321.3	319.416
		8	526		-524.8	400			820	125.82	258.83	105.102
82	TPL-T	1	3503.3	-2598.1	-3503.3	132	308		480	181.72	995.49	700.68
		2	2770.1	-1332.3	-2526.5	212	340		508	295.34	715.53	554.026
		3	1346.2	-686	-1093.7	280	472		636	179.5	393.72	350.769
		4	904.58	-538.2	-755.74	336	556		716	144.46	312.97	319.416
		8	526.5		-526.5	384	628		776	127.78	259.6	105.102
83	TPL-T	1	3505		-3500	104			464	148.54	1116.15	700.68
		2	2772.6		-2506.7	212			500	326.49	721.92	554.68
		3	1147.37		-1109.1	284			644	183.8	401.43	350.769
		4	826.01		-758.61	348			724	149.2	305.96	319.416
		8	526.03		-524.77	384			796	126.28	252.67	105.102
84	DM18	1	3503.3		-2360.5	228	316	448	532	294.83	685.26	700.68
		2	2672.6	-846.48	-2114.2	232	332	436	544	266.72	610.92	554.026
		3	1052.4	-458.15	-1065.3	300	420		648	172.35	374.4	350.769
		4	808.76	-331.24	-753.28	344	480		732	140.52	299.85	319.416
		8	525.51	-525.41	-525.41	380			792	123.26	248.85	105.102
85	DM18	1	3505		-2988.4	212			508	335.57	804.05	700.68
		2	2772.62		-2414.7	236			532	306.2	684.47	554.026
		3	1060.73		-1087.7	308			668	178	382.3	350.769
		4	793.75		-761.81	352			748	143.52	302.34	319.416
		8	526.77		-524.8	400			816	128.3	256.35	105.102

Shot	Round	Ch	Pos P	Neg P1	Neg P2	A1	A2	A3	ATot	Peak	ABS	Cal
	Type		Pa	Pa	Pa	msec	msec	msec	msec	mPa-sec	mPa-sec	Pa/Volt
86	DM18	1	3505.5		-2469.9	224			528	307.64	703.97	700.68
		2	2772.6		-2691.7	208			528	257.71	701.73	554.026
		3	1055.8		-1101.4	304			652	178.96	385.45	350.769
		4	825.05		-809.4	352			732	152.14	316.88	319.416
		8	513.21		-524.77	408			800	122.5	237.49	105.102
87	TPL-T	1	3505.5		-3500	132			476	191.48	1025.6	700.68
		2	2772.6		-2400.6	220			508	303.39	678.77	554.026
		3	1118.25		-1053.3	292			644	177.46	381.85	350.769
		4	899.16		-765	340			728	150.19	323.82	319.416
		8	508.06		-507.54	408			804	121.7	237.65	105.102
90	TPL-T	1	3505		-3500	56			464	81.27	1328.2	700.68
		2	2583.15		-2077.9	236			568	281.98	646.8	554.026
		3	1062.48		-948.13	300			696	171.07	391.58	350.769
		4	832.08		-652.57	336			772	133.89	293.7	319.416
		8	506.5		-468.2	392			836	115.25	232.6	105.102
91	DM18	1	3256		-2327.7	248			584	285.3	675.6	700.68
		2	2772.6		-2766.5	180			536	209.6	788.1	554.026
		3	1071.9		-1132.9	296			672	175.4	403.8	350.769
		4	832.1		-652.6	336			772	133.89	293.7	319.416
		8	425.45		-424.6	404			820	104.6	206.5	105.102
92	TPL-T	1	3505		-1915	232			576	266.9	611.4	700.68
		2	2346.6		-1731.6	244			592	243.1	565.6	554.026
		3	1102.1		-1003.9	296			688	169	382.7	350.769
		4	782.3		-708.8	356			760	138.2	295.5	319.416
		8	435.5		-451.6	416			816	112.4	223.7	105.102
93	DM18	1	3331		-2329.8	248			588	286.7	689.3	700.68
		2	2772.6		-2766.8	204			552	242.2	758.5	554.026
		3	1055.8		-1101.4	300			680	171.4	392.4	350.769
		4	739.5		-711	348			760	135.3	294.1	319.416
		8	485.5		-491.9	400			844	111	227.2	105.102
94	TPL-T	1	3505.5		-2492	220			548	314.9	771.5	700.68
		2	2511.9		-1900	236			572	257	590	554.026
		3	1042.84		-1006	308			700	171.2	380.8	350.769
		4	752.56		-658.9	356			768	136.7	281.8	319.416
		8	494.7		-457.5	392			840	113.2	226.8	105.102
95	DM18	1	3505.5		-2722.8	228			556	312.5	766.7	700.68
		2	2500		-1992.1	252			588	252.9	594.2	554.026
		3	878.3		-935.2	316			708	152.5	348.2	350.769
		4	683.9		-629.3	360			776	125.9	274.3	319.416
		8	439		-448.1	412			852	106.2	216.1	105.102

APPENDIX F:

MICROPHONE DATA FROM COLLECTION TEST PHASE

INTENTIONALLY LEFT BLANK.

DATA COLLECTION HIGH FIDELITY MICROPHONE POSITIONS:

All coordinates are in meters.

30 Mar 93

3-m hub	x: -1.512	y: 1697.509	z: 1.388
6-m hub	x: -5.022	y: 1697.238	z: 1.506
9-m hub	x:-8.270	y: 1697.001	z: 1.450
12-m hub	x:-11.432	y: 1696.818	z: 1.380

Microphone Elevations, top of microphone:

Hub Reference	31 Mar 93	5 Apr 93	6 Apr 93	7 Apr 93
3-m hub	2.723024	2.723024	2.726072	2.738264
6-m hub	2.86236	2.853216	2.86236	2.856264
9-m hub	2.80636	2.80636	2.812456	2.818552
12-m hub	2.7516	2.711976	2.699784	2.6754

DATA COLLECTION ROUND LOCATION MICROPHONE POSITIONS:

All coordinates in meters.

30 MARCH93

sensor 1	x: -.0242	y: 1697.945	z:1.516
sensor 2	x: 2.798	y: 1698.901	z:1.685
sensor 3	x: -0.192	y: 1698.927	z:1.692
sensor 4	x:-3.230	y: 1698.966	z:1.692
sensor 5	x: -1.796	y: 1698.902	z:1.692
sensor 6	x: -2.205	y: 1698.915	z:1.725

8 APR 93

10° Rotation, Counter Clockwise about sensor 3

sensor 1	x: -0.006	y: 1697.976	z:1.654
sensor 2	x: 2.772	y: 1699.465	z:1.719
sensor 3	x: -0.192	y: 1698.927	z:1.692
sensor 4	x:-3.150	y: 1698.448	z:1.607
sensor 5	x: 2.953	y: 1698.460	z:1.698
sensor 6	x: -2.974	y: 1697.498	z:1.666

DATA COLLECTION GUN POSITIONS:

All coordinates in meters.

References			
1700 M Position	x: 0	y: 0	z: 0
1000 M Position	x: -7.181	y: 700.252	z: 0.244
800 M Position	x: -8.530	y: 900.249	z: 0.801
600 M Position	x: -11.340	y: 1100.137	z: -0.175
400 M Position	x: -23.602	y: 1299.785	z: -0.534
30 MAR 93			
7.62 mm Muzzle	x: 22.583	y: 1299.923	z: 0.676
5 APR 93			
7.62 Muzzle	x: -6.296	y: 900.175	z: 1.990
6 APR 93			
.50 cal Muzzle	x: -5.230	y: 700.283	z: 1.490
7.62 Muzzle	x: -22.074	y: 1299.934	z: 0.737
7 APR 93			
35 mm Muzzle	x: -5.487	y: 698.197	z: 2.051
35 mm Muzzle	x: -22.813	y: 1298.062	z: 1.370
35 mm Muzzle	x: -1.967	y: 1.882	z: 1.778
8 APR 93			
0.50 cal Muzzle	x: -22.126	y: 1299.823	z: 0.736
35 mm Muzzle	x: -22840	y: 1297.942	z: 1.376
9 APR 93			
35 mm Muzzle	x: -1.900	y: -1.877	z: 1.819
35 mm Muzzle	x: -8.713	y: 698.340	z: 2.063

RD.		Offset Distance						Arrival Time			
NO.	HMic1	HMic2	HMic3	HMic4	HMic5	LMic1	LMic2	LMic3	LMic4	LMic5	LMic6
Consec.	(m)	(m)	(m)	(m)	(m)	(msec)	(msec)	(msec)	(msec)	(msec)	(msec)
1	ND	ND	ND	ND	ND	DNA	DNA	DNA	DNA	DNA	DNA
2	ND	ND	ND	ND	ND	DNA	DNA	DNA	DNA	DNA	DNA
3	ND	ND	ND	ND	ND	DNA	DNA	DNA	DNA	DNA	DNA
4	ND	ND	ND	ND	ND	DNA	DNA	DNA	DNA	DNA	DNA
5	1.590	2.030	5.007	8.183	11.340	-1.694	3.590	0.000	2.785	1.844	1.256
6	1.467	1.970	5.016	8.205	11.365	-1.650	3.150	0.000	3.020	1.516	1.454
7	1.840	2.348	5.238	8.386	11.535	-1.640	3.620	0.000	2.855	1.860	1.298
8	1.451	1.964	5.020	8.209	11.370	-1.688	3.600	0.000	2.985	1.838	1.396
9	1.481	2.076	5.134	8.321	11.481	-1.684	3.270	0.000	3.160	1.592	1.544
10	1.537	2.135	5.173	8.354	11.513	-1.672	3.380	0.000	3.120	1.656	1.520
11	1.458	2.021	5.083	8.272	11.433	-1.632	3.555	0.000	3.115	1.786	1.484
12	1.530	1.812	4.793	7.977	11.137	-1.626	4.055	0.000	2.590	2.194	1.060
13	1.387	1.468	4.528	7.735	10.901	-1.780	4.420	0.000	2.195	2.516	0.756
14	1.644	1.904	4.818	7.990	11.146	-1.616	3.975	0.000	2.505	2.140	1.014
15	1.264	2.079	5.263	8.470	11.635	DNA	DNA	DNA	DNA	DNA	DNA
16	1.254	2.092	5.285	8.492	11.658	DNA	DNA	DNA	DNA	DNA	DNA
17	1.293	2.126	5.305	8.509	11.674	DNA	DNA	DNA	DNA	DNA	DNA
18	ND	ND	ND	ND	ND	DNA	DNA	DNA	DNA	DNA	DNA
19	ND	ND	ND	ND	ND	DNA	DNA	DNA	DNA	DNA	DNA
20	1.903	2.666	5.641	8.790	11.914	DNA	DNA	DNA	DNA	DNA	DNA
21	1.620	2.383	5.441	8.616	11.752	0.000	3.515	2.840	3.635	3.130	3.215
22	1.593	2.252	5.288	8.462	11.599	0.000	4.265	2.530	4.660	3.265	3.605
23	1.698	2.519	5.575	8.745	11.879	0.000	3.395	2.860	3.660	3.060	3.245
24	ND	ND	ND	ND	ND	DNA	DNA	DNA	DNA	DNA	DNA
25	1.188	1.678	4.858	8.070	11.222	0.000	4.890	2.475	4.635	3.700	3.515
26	1.601	2.408	5.488	8.666	11.803	0.000	3.625	2.840	3.750	3.185	3.260
27	ND	ND	ND	ND	ND	DNA	DNA	DNA	DNA	DNA	DNA
28	1.825	2.052	4.865	8.011	11.138	DNA	DNA	DNA	DNA	DNA	DNA

RD.		Offset Distance						Arrival Time			
NO.	HMic1	HMic2	HMic3	HMic4	HMic5	LMic1	LMic2	LMic3	LMic4	LMic5	LMic6
Consec.	(m)	(m)	(m)	(m)	(m)	(msec)	(msec)	(msec)	(msec)	(msec)	(msec)
29	0.756	1.459	4.838	8.077	11.239	DNA	DNA	DNA	DNA	DNA	DNA
30	1.394	2.490	5.719	8.923	12.071	DNA	DNA	DNA	DNA	DNA	DNA
31	1.416	2.304	5.463	8.658	11.802	DNA	DNA	DNA	DNA	DNA	DNA
32	ND	ND	ND	ND	ND	DNA	DNA	DNA	DNA	DNA	DNA
33	ND	ND	ND	ND	ND	DNA	DNA	DNA	DNA	DNA	DNA
34	ND	ND	ND	ND	ND	DNA	DNA	DNA	DNA	DNA	DNA
35	ND	ND	ND	ND	ND	DNA	DNA	DNA	DNA	DNA	DNA
36	0.334	1.872	5.354	8.601	11.765	0.000	5.355	1.510	6.835	3.200	4.595
37	ND	ND	ND	ND	ND	0.000	2.105	1.695	4.360	1.580	3.185
38	ND	ND	ND	ND	ND	0.000	8.395	1.530	-1.670	5.970	-1.570
39	1.844	2.346	5.236	8.380	11.505	0.000	4.860	1.450	4.520	3.130	2.895
40	1.571	2.255	5.305	8.482	11.619	0.000	4.810	1.545	5.025	3.075	3.285
41	ND	ND	ND	ND	ND	0.000	4.365	1.745	2.475	3.155	1.855
42	ND	ND	ND	ND	ND	0.000	-0.760	1.755	6.975	-0.390	5.020
43	2.073	1.141	3.615	6.802	9.948	0.000	7.480	1.510	1.545	5.220	0.505
44	1.617	2.425	5.500	8.676	11.813	0.000	4.385	1.465	5.265	2.715	3.460
45	1.971	2.769	5.734	8.878	12.004	DNA	DNA	DNA	DNA	DNA	DNA
46	1.383	2.191	5.333	8.528	11.675	0.000	4.590	2.260	5.165	3.260	3.795
47	1.841	2.235	5.082	8.227	11.354	0.000	4.790	2.190	4.555	3.425	3.305
48	1.874	2.286	5.125	8.265	11.391	0.000	4.785	2.110	4.635	3.425	3.305
49	1.653	2.263	5.255	8.423	11.559	0.000	4.620	2.310	4.890	3.310	3.565
50	1.883	1.999	4.743	7.884	11.012	0.000	5.265	2.175	4.105	3.815	2.920
51	1.751	1.909	4.739	7.897	11.031	0.000	5.330	2.135	4.255	3.835	2.990
52	ND	ND	ND	ND	ND	DNA	DNA	DNA	DNA	DNA	DNA
53	1.961	2.867	5.886	9.040	12.168	DNA	DNA	DNA	DNA	DNA	DNA
54	0.692	1.700	5.087	8.325	11.488	DNA	DNA	DNA	DNA	DNA	DNA
55	0.572	1.404	4.847	8.093	11.257	DNA	DNA	DNA	DNA	DNA	DNA
56	1.523	2.719	5.956	9.160	12.308	0.000	3.190	2.185	6.070	2.195	4.425

RD.		Offset Distance						Arrival Time			
NO.	HMic1	HMic2	HMic3	HMic4	HMic5	LMic1	LMic2	LMic3	LMic4	LMic5	LMic6
Consec.	(m)	(m)	(m)	(m)	(m)	(msec)	(msec)	(msec)	(msec)	(msec)	(msec)
57	1.304	2.746	6.114	9.343	12.501	0.000	2.870	2.170	6.450	1.870	4.745
58	2.458	1.976	4.126	7.195	10.302	0.000	5.980	1.950	2.860	4.285	1.945
59	2.306	3.371	6.412	9.557	12.680	0.000	2.410	1.970	6.040	1.625	4.350
60	2.392	3.180	6.032	9.136	12.242	0.000	3.290	1.965	5.280	2.305	3.785
61	ND	ND	ND	ND	ND	DNA	DNA	DNA	DNA	DNA	DNA
62	1.532	2.437	5.563	8.750	11.893	DNA	DNA	DNA	DNA	DNA	DNA
63	1.369	2.006	5.115	8.310	11.457	0.000	5.220	1.725	4.955	3.480	3.335
64	1.507	2.048	5.080	8.262	11.405	0.000	5.290	1.710	4.750	3.525	3.155
65	1.212	2.233	5.476	8.688	11.841	0.000	4.630	1.770	5.725	2.980	3.905
66	1.422	1.944	5.011	8.202	11.347	0.000	5.435	1.805	4.765	3.665	3.165
67	1.481	1.789	4.797	7.984	11.129	0.000	5.840	1.785	4.295	3.975	2.810
68	1.594	1.968	4.926	8.099	11.239	0.000	5.510	1.755	4.360	3.750	2.835
69	ND	ND	ND	ND	ND	DNA	DNA	DNA	DNA	DNA	DNA
70	ND	ND	ND	ND	ND	DNA	DNA	DNA	DNA	DNA	DNA
71	ND	ND	ND	ND	ND	DNA	DNA	DNA	DNA	DNA	DNA
72	ND	ND	ND	ND	ND	DNA	DNA	DNA	DNA	DNA	DNA
73	ND	ND	ND	ND	ND	DNA	DNA	DNA	DNA	DNA	DNA
74	ND	ND	ND	ND	ND	DNA	DNA	DNA	DNA	DNA	DNA
75	1.201	2.432	5.743	8.961	12.120	DNA	DNA	DNA	DNA	DNA	DNA
76	1.317	2.153	5.331	8.530	11.683	0.000	3.840	0.905	5.795	2.050	3.585
77	1.882	2.925	6.040	9.208	12.349	0.000	2.215	1.120	6.305	1.015	4.125
78	0.860	1.768	5.103	8.333	11.495	0.000	4.625	0.895	6.180	2.560	3.775
79	1.407	2.839	6.200	9.424	12.584	0.000	1.545	1.120	7.395	0.310	4.950
80	0.752	2.035	5.434	8.671	11.835	0.000	3.780	0.890	6.850	1.800	4.380
81	ND	ND	ND	ND	ND	DNA	DNA	DNA	DNA	DNA	DNA
82	1.517	2.113	5.164	8.342	11.488	DNA	DNA	DNA	DNA	DNA	DNA
83	1.251	1.981	5.161	8.363	11.518	0.000	4.705	0.740	5.085	2.630	2.970
84	2.011	2.395	5.178	8.296	11.421	0.000	4.605	0.960	4.115	2.765	2.405

RD.		Offset Distance						Arrival Time			
NO.	HMic1	HMic2	HMic3	HMic4	HMic5	LMic1	LMic2	LMic3	LMic4	LMic5	LMic6
Consec.	(m)	(m)	(m)	(m)	(m)	(msec)	(msec)	(msec)	(msec)	(msec)	(msec)
85	1.517	2.117	5.169	8.348	11.494	0.000	4.895	0.965	4.675	2.910	2.760
86	1.819	1.949	4.746	7.891	11.028	0.000	5.455	0.955	3.640	3.400	1.985
87	1.351	2.065	5.206	8.400	11.552	0.000	4.515	0.730	4.960	2.495	2.900
88	ND	ND	ND	ND	ND	DNA	DNA	DNA	DNA	DNA	DNA
89	ND	ND	ND	ND	ND	DNA	DNA	DNA	DNA	DNA	DNA
90	0.916	2.103	5.455	8.684	11.846	DNA	DNA	DNA	DNA	DNA	DNA
91	1.849	1.321	4.025	7.203	10.352	0.000	6.560	1.365	3.020	4.420	1.565
92	2.496	2.791	5.329	8.375	11.471	0.000	4.125	1.150	4.065	2.560	2.510
93	1.863	1.440	4.130	7.298	10.444	0.000	6.390	1.370	3.120	4.300	1.670
94	1.789	2.410	5.369	8.519	11.655	0.000	3.900	1.155	5.120	2.285	3.225
95	1.558	2.063	5.077	8.250	11.395	0.000	4.635	1.340	5.010	2.890	3.175
96	1.878	2.271	5.115	8.250	11.382	0.000	5.785	1.395	3.245	4.675	1.455
97	1.786	2.588	5.617	8.775	11.913	0.000	4.835	1.485	4.385	3.725	2.530
98	1.550	2.232	5.293	8.469	11.614	0.000	5.485	1.410	4.015	4.385	2.140
99	1.860	2.503	5.446	8.590	11.723	0.000	5.210	1.455	3.880	4.100	2.040
100	1.490	2.265	5.374	8.557	11.705	0.000	5.400	1.425	4.350	4.345	2.535
101	1.439	2.232	5.361	8.549	11.698	0.000	5.355	1.440	4.315	4.305	2.475
102	1.412	2.324	5.494	8.688	11.839	0.000	6.015	1.365	3.670	4.920	1.815
103	2.129	1.632	4.074	7.203	10.337	0.000	7.220	1.160	1.025	6.190	-0.670
104	2.169	1.616	4.012	7.139	10.273	0.000	7.255	1.100	0.800	6.230	-0.850
105	2.257	1.663	3.968	7.083	10.213	0.000	7.260	1.065	0.615	6.275	-1.035
106	1.686	0.436	3.601	6.844	10.009	0.000	8.475	0.950	0.475	7.520	-1.295
107	1.702	0.827	3.771	6.993	10.155	0.000	8.045	1.015	0.820	7.110	-0.915
108	1.713	0.790	3.737	6.962	10.124	0.000	8.095	1.005	0.805	7.170	-0.935
109	1.873	3.010	6.174	9.352	12.496	0.000	3.695	1.565	5.310	2.585	3.485
110	2.208	3.361	6.484	9.644	12.780	0.000	3.090	1.580	5.430	1.955	3.595
111	2.137	3.315	6.462	9.629	12.769	0.000	3.130	1.580	5.545	2.005	3.725
112	1.401	2.903	6.295	9.525	12.687	0.000	3.445	1.740	7.080	2.445	5.170

RD.		Offset Distance						Arrival Time			
NO.	HMic1	HMic2	HMic3	HMic4	HMic5	LMic1	LMic2	LMic3	LMic4	LMic5	LMic6
Consec.	(m)	(m)	(m)	(m)	(m)	(msec)	(msec)	(msec)	(msec)	(msec)	(msec)
113	1.242	2.814	6.246	9.485	12.649	0.000	3.345	1.660	6.745	2.325	4.890
114	1.078	2.618	6.046	9.285	12.449	0.000	3.910	1.635	6.565	2.930	4.690
115	1.311	2.850	6.265	9.500	12.663	0.000	3.390	1.705	6.545	2.285	4.650
116	1.351	2.849	6.243	9.473	12.636	0.000	3.420	1.675	6.470	2.325	4.580
117	1.093	2.718	6.180	9.423	12.588	0.000	3.580	1.690	6.935	2.550	5.045
118	0.972	2.196	5.545	8.773	11.934	0.000	5.160	1.485	5.455	4.150	3.580
119	1.390	2.094	5.219	8.410	11.560	DNA	DNA	DNA	DNA	DNA	DNA
120	1.481	2.021	5.076	8.257	11.405	DNA	DNA	DNA	DNA	DNA	DNA
121	1.048	1.643	4.895	8.115	11.275	DNA	DNA	DNA	DNA	DNA	DNA
122	1.643	1.899	4.820	7.986	11.129	DNA	DNA	DNA	DNA	DNA	DNA
123	1.126	2.030	5.280	8.493	11.651	DNA	DNA	DNA	DNA	DNA	DNA
124	0.981	1.676	4.958	8.182	11.343	DNA	DNA	DNA	DNA	DNA	DNA
125	1.610	2.243	5.269	8.439	11.582	DNA	DNA	DNA	DNA	DNA	DNA
126	1.867	2.317	5.185	8.323	11.455	DNA	DNA	DNA	DNA	DNA	DNA
127	1.701	2.152	5.090	8.248	11.387	DNA	DNA	DNA	DNA	DNA	DNA
128	1.584	2.106	5.113	8.284	11.428	DNA	DNA	DNA	DNA	DNA	DNA
129	1.484	2.055	5.114	8.295	11.443	DNA	DNA	DNA	DNA	DNA	DNA
130	2.213	2.388	4.982	8.066	11.169	DNA	DNA	DNA	DNA	DNA	DNA
131	1.988	2.634	5.528	8.657	11.775	DNA	DNA	DNA	DNA	DNA	DNA
132	1.891	2.497	5.407	8.545	11.667	DNA	DNA	DNA	DNA	DNA	DNA
133	2.230	2.846	5.649	8.749	11.854	DNA	DNA	DNA	DNA	DNA	DNA
134	1.479	1.060	4.114	7.331	10.487	DNA	DNA	DNA	DNA	DNA	DNA
135	1.317	2.235	5.428	8.627	11.774	DNA	DNA	DNA	DNA	DNA	DNA
136	1.458	2.284	5.410	8.597	11.738	DNA	DNA	DNA	DNA	DNA	DNA
137	1.575	1.864	4.821	7.994	11.133	DNA	DNA	DNA	DNA	DNA	DNA
138	0.932	1.937	5.254	8.479	11.635	DNA	DNA	DNA	DNA	DNA	DNA
139	0.825	2.100	5.482	8.715	11.874	DNA	DNA	DNA	DNA	DNA	DNA
140	1.532	1.649	4.613	7.796	10.939	DNA	DNA	DNA	DNA	DNA	DNA

APPENDIX G:

LOCATION DATA FROM FEASIBILITY TEST PHASE

INTENTIONALLY LEFT BLANK.

RD.	PREDICTED IMPACT LOCATION ON TARGET			Error Analysis		Error Analysis	PREDICTED	Error Analysis	EA	Array
NO.	X	Y	Z	del Y	del Z	Offset Distance	Velocity	Δ Vel	ΔV	Config
Consec.	(m)	(m)	(m)	m	m	m	m/s	m/s	%	
1	DNA	DNA	DNA							
2	1701.13	0.443	7.210	-0.208	-0.137	0.249	1442	23	2	2,4,5,6
3	1701.13	0.349	7.196	-0.214	-0.143	0.257	1467	-10	1	2,4,5,6
4	1701.12	0.221	6.970	-0.216	-0.177	0.279	1476	-19	1	2,4,5,6
5	1701.14	0.569	7.506	-0.134	-0.233	0.269	1108	-29	3	2,4,5,6
6	1701.14	0.616	7.181	-0.181	-0.208	0.276	1068	6	1	2,4,5,6
7	1701.14	0.459	7.105	-0.184	-0.172	0.252	1104	-25	2	2,4,5,6
8	1701.14	0.508	7.104	-0.203	-0.171	0.265	1105	-36	3	2,4,5,6
9	1701.13	0.360	7.142	-0.245	-0.099	0.264	1608	-32	2	2,4,5,6
10	1701.15	0.640	7.108	-0.235	-0.205	0.312	1571	-17	1	2,4,5,6
11	1701.11	0.068	6.903	-0.183	-0.180	0.257	1505	40	3	2,4,5,6
12	1701.15	0.628	7.061	-0.353	-0.148	0.383	1615	-49	3	2,4,5,6
13	1701.14	0.462	7.063	-0.207	-0.230	0.310	1016	24	2	2,4,5,6
14	1701.13	0.357	6.946	-0.232	-0.153	0.278	1041	7	1	2,4,5,6
15	1701.14	0.563	6.779	-0.198	-0.146	0.246	1020	24	2	2,4,5,6
16	1701.14	0.466	6.778	-0.221	-0.155	0.270	1035	12	1	2,4,5,6
17	1701.07	-0.704	6.140	0.219	-0.087	0.236	890	-11	1	2,4,5,6
18	1701.05	-0.940	5.707	0.225	-0.014	0.225	919	-30	3	2,4,5,6
19	1701.12	0.283	6.978	0.282	-0.165	0.327	896	-2	0	2,4,5,6
20	1701.09	-0.226	7.426	0.191	-0.043	0.196	892	-10	1	2,4,5,6
21	1701.12	0.202	7.194	0.203	-0.201	0.286	916	-32	3	2,4,5,6
22	1701.11	0.046	7.663	0.199	-0.160	0.255	909	-21	2	2,4,5,6
23	1701.12	0.153	6.724	0.222	-0.181	0.286	916	-21	2	2,4,5,6
24	1701.10	-0.172	6.853	0.227	-0.120	0.257	862	25	3	2,4,5,6
25	1701.09	-0.315	6.963	0.180	-0.150	0.234	945	-51	5	2,4,5,6
26	1701.11	0.030	6.785	0.225	-0.192	0.296	917	-18	2	2,4,5,6
27	1701.17	1.142	7.164	0.193	-0.251	0.317	875	16	2	2,4,5,6
28	1701.17	1.087	7.210	0.198	-0.217	0.294	894	0	0	2,4,5,6

RD.	PREDICTED IMPACT LOCATION ON TARGET			Error Analysis		Error Analysis	PREDICTED	Error Analysis	EA	Array
NO.	X	Y	Z	del Y	del Z	Offset Distance	Velocity	Δ Vel	ΔV	Config
Consec.	(m)	(m)	(m)	m	m	m	m/s	m/s	%	
29	1701.15	0.758	7.999	0.207	-0.266	0.337	904	-15	2	2,4,5,6
30	1701.14	0.542	8.060	0.243	-0.187	0.307	907	-16	2	2,4,5,6
31	1701.13	0.333	7.938	0.172	-0.225	0.284	931	-42	4	2,4,5,6
32	DNA	DNA	DNA							
33	DNA	DNA	DNA							
34	DNA	DNA	DNA							
35	1701.11	0.068	7.647	0.217	-0.224	0.311	1178	-33	3	2,4,5,6
36	1701.12	0.180	7.821	0.245	-0.218	0.328	1133	6	1	2,4,5,6
37	1701.10	-0.072	6.975	0.247	-0.162	0.296	1156	8	1	2,4,5,6
38	1701.14	0.591	6.665	0.084	0.248	0.262	1137	20	2	2,4,5,6
39	1701.11	-0.025	6.492	0.210	0.781	0.809	1191	9	1	2,4,5,6
40	1701.12	0.260	6.502	0.195	-0.169	0.258	1129	23	2	2,4,5,6
41	1701.13	0.418	7.076	0.207	-0.173	0.270	1114	43	4	2,4,5,6
42	DNA	DNA	DNA							
43	DNA	DNA	DNA							
44	DNA	DNA	DNA							
45	DNA	DNA	DNA							
46	DNA	DNA	DNA							
47	1701.12	-0.124	6.979	-0.039	-0.112	0.118	1300	11	1	2,4,5,6
48	1701.12	-0.145	7.197	-0.028	-0.140	0.142	1295	19	1	2,4,5,6
49	1701.12	-0.074	6.792	-0.059	-0.135	0.147	1415	-102	7	2,4,5,6
50	1701.12	0.269	6.931	-0.012	-0.114	0.115	1291	14	1	2,4,5,6
51	DNA	DNA	DNA							
52	1701.12	0.319	6.455	0.008	-0.158	0.159	857	20	2	2,4,5,6
53	1701.12	-0.043	6.546	0.020	-0.139	0.140	875	10	1	2,4,5,6
54	1701.12	-0.266	7.124	-0.007	-0.177	0.178	847	22	3	2,4,5,6
55	1701.12	0.314	7.309	0.003	-0.172	0.172	874	13	1	2,4,5,6
56	DNA	DNA	DNA							

RD.	PREDICTED IMPACT LOCATION ON TARGET			Error Analysis		Error Analysis	PREDICTED	Error Analysis	EA	Array
NO.	X	Y	Z	del Y	del Z	Offset Distance	Velocity	Δ Vel	ΔV	Config
Consec.	(m)	(m)	(m)	m	m	m	m/s	m/s	%	
57	DNA	DNA	DNA							
58	1701.12	-0.052	7.034	-0.061	-0.097	0.114	1343	-2	0	2,4,5,6
59	1701.12	-0.005	7.038	-0.148	-0.081	0.169	1352	-16	1	2,4,5,6
60	1701.12	0.080	6.675	-0.093	-0.108	0.142	1270	68	5	2,4,5,6
61	DNA	DNA	DNA							
62	DNA	DNA	DNA							
63	1701.12	0.390	6.841	-0.143	-0.084	0.166	836	16	2	2,4,5,6
64	1701.12	0.466	7.135	-0.129	-0.138	0.189	859	13	2	2,4,5,6
65	1701.11	-0.548	6.856	-0.135	-0.159	0.209	844	3	0	2,4,5,6
66	DNA	DNA	DNA							
67	DNA	DNA	DNA							
68	DNA	DNA	DNA							
69	DNA	DNA	DNA							
70	DNA	DNA	DNA							
71	1701.13	0.945	7.670	-0.098	-0.033	0.103	908	1	0	2,4,5,6
72	1701.13	0.996	7.634	-0.119	-0.017	0.120	942	-6	1	2,4,5,6
73	1701.12	0.169	7.410	-0.112	-0.523	0.535	898	63	7	2,4,5,6
74	DNA	DNA	DNA							
75	DNA	DNA	DNA							
76	DNA	DNA	DNA							
77	1701.13	1.222	6.130				838	77	9	2,4,5,6
78	DNA	DNA	DNA							
79	DNA	DNA	DNA							
80	DNA	DNA	DNA							
81	DNA	DNA	DNA							
82	1701.12	-0.110	6.657	-0.093	-0.070	0.117	620	2	0	2,4,5,6
83	1701.11	-0.857	6.667	-0.076	-0.060	0.097	624	-2	0	2,4,5,6
84	1701.12	-0.288	6.844	-0.105	-0.087	0.136	614	6	1	2,4,5,6

RD.	PREDICTED IMPACT LOCATION ON TARGET			Error Analysis		Error Analysis	PREDICTED	Error Analysis	EA	Array
NO.	X	Y	Z	del Y	del Z	Offset Distance	Velocity	Δ Vel	ΔV	Config
Consec.	(m)	(m)	(m)	m	m	m	m/s	m/s	%	
85	DNA	DNA	DNA							
86	1701.12	-0.361	7.171	-0.082	-0.074	0.111	618	6	1	2,4,5,6
87	1701.13	1.239	7.857	-0.102	-0.060	0.118	613	6	1	2,4,5,6
88	1701.12	-0.259	7.105	-0.084	-0.078	0.115	617	2	0	2,4,5,6
89	1701.11	-1.139	6.860	-0.074	-0.083	0.112	623	0	0	2,4,5,6
90	1701.13	1.045	7.399	-0.088	-0.052	0.102	626	0	0	2,4,5,6
91	1701.11	-0.454	6.982	-0.089	-0.065	0.111	626	3	0	2,4,5,6
92	1701.12	-0.272	6.409	-0.101	-0.072	0.124	617	4	1	2,4,5,6
93	1701.118	-0.095	5.457				618	2	0	2,4,5,6
94	DNA	DNA	DNA							
95	1701.12	0.626	7.867	0.141	-0.206	0.249	729	-2	0	2,4,5,6
96	1701.12	0.349	5.865				617	26	4	2,4,5,6
97	1701.12	-0.554	7.556	0.151	-0.115	0.190	747	-2	0	2,4,5,6
98	1701.12	0.163	6.291	0.134	-0.160	0.209	663	19	3	2,4,5,6
99	DNA	DNA	DNA							
100	1701.12	-0.855	7.032	0.072	0.039	0.082	1337	-143	11	2,4,5,6
101	1701.12	-0.441	6.939	0.048	-0.048	0.068	1146	50	4	2,4,5,6
102	1701.12	-0.469	6.831	0.096	-0.040	0.104	1214	-16	1	2,4,5,6
103	1701.12	-0.264	6.677	0.121	-0.056	0.133	1190	7	1	2,4,5,6
104	DNA	DNA	DNA							
105	1701.12	-1.156	6.853	0.133	-0.042	0.140	728	-11	2	2,4,5,6
106	1701.12	-0.362	6.462	0.119	-0.101	0.156	703	3	0	2,4,5,6
107	1701.12	1.305	7.257	0.152	-0.216	0.265	712	2	0	2,4,5,6
108	1701.12	0.583	7.179	0.124	-0.178	0.217	711	-2	0	2,4,5,6
109	DNA	DNA	DNA							
110	1701.12	-0.671	7.077	0.058	-0.016	0.060	1085	-4	0	2,4,5,6
111	1701.12	0.742	7.638	0.115	-0.117	0.164	1059	2	0	2,4,5,6
112	1701.12	-0.323	6.538	0.100	-0.007	0.101	1080	-12	1	2,4,5,6

RD.	PREDICTED IMPACT LOCATION ON TARGET			Error Analysis		Error Analysis	PREDICTED	Error Analysis	EA	Array
NO.	X	Y	Z	del Y	del Z	Offset Distance	Velocity	Δ Vel	ΔV	Config
Consec.	(m)	(m)	(m)	m	m	m	m/s	m/s	%	
113	1701.12	0.296	6.788	0.191	-0.037	0.194	1034	32	3	2,4,5,6
114	DNA	DNA	DNA							
115	DNA	DNA	DNA							
116	DNA	DNA	DNA							
117	1701.12	-1.056	6.051	0.133	0.110	0.172	466	1	0	2,4,5,6
118	1701.12	-0.423	7.071	0.230	0.080	0.243	470	3	1	2,4,5,6
119	1701.12	0.896	8.027	0.201	-0.006	0.202	467	0	0	2,4,5,6
120	DNA	DNA	DNA							
121	1701.11	-1.871	5.657	0.228	0.384	0.446	474	-12	3	2,4,5,6
122	1701.12	0.897	7.352	0.200	-0.021	0.201	470	1	0	2,4,5,6
123	1701.12	-0.801	7.229	0.168	0.142	0.220	462	4	1	2,4,5,6
124	1701.12	1.097	7.539	0.320	0.002	0.320	455	6	1	2,4,5,6
125	1701.12	-0.445	6.888	0.202	0.103	0.226	458	2	0	2,4,5,6
126	DNA	DNA	DNA							
127	DNA	DNA	DNA							
128	DNA	DNA	DNA							
129	DNA	DNA	DNA							
130	DNA	DNA	DNA							
131	DNA	DNA	DNA							
132	DNA	DNA	DNA							
133	DNA	DNA	DNA							
134	DNA	DNA	DNA							
135	DNA	DNA	DNA							
136	DNA	DNA	DNA							
137	DNA	DNA	DNA							
138	DNA	DNA	DNA							
139	DNA	DNA	DNA							
140	DNA	DNA	DNA							

RD.	PREDICTED IMPACT LOCATION ON TARGET			Error Analysis		Error Analysis	PREDICTED	Error Analysis	EA	Array
NO.	X	Y	Z	del Y	del Z	Offset Distance	Velocity	Δ Vel	ΔV	Config
Consec.	(m)	(m)	(m)	m	m	m	m/s	m/s	%	
141	DNA	DNA	DNA							
142	DNA	DNA	DNA							
143	DNA	DNA	DNA							
144	DNA	DNA	DNA							
145	1701.12	-1.059	8.778	1.746	-1.387	2.230	791	-13	2	2,4,5,6
146	1701.121	0.549	7.510				799	6	1	2,4,5,6
147	1701.132	3.784	8.746				802	22	3	2,4,5,6
148	1701.13	2.216	4.874	-3.079	3.067	4.345	690	117	17	2,4,5,6
149	DNA	DNA	DNA							
150	DNA	DNA	DNA							
151	DNA	DNA	DNA							
152	DNA	DNA	DNA							
153	DNA	DNA	DNA							
154	1701.13	0.344	7.516	0.023	-0.079	0.083	1004	25	3	2,4,5,6
155	1701.14	0.503	7.636	0.064	-0.089	0.109	1011	21	2	2,4,5,6
156	1701.15	0.579	7.466	0.008	-0.069	0.069	1013	21	2	2,4,5,6
157	1701.12	0.079	7.516	0.058	-0.079	0.098	1038	-13	1	2,4,5,6
158	1701.11	0.020	7.471	-0.013	-0.124	0.124	1028	5	0	2,4,5,6
159	1701.11	0.008	7.236	0.039	-0.099	0.107	1004	26	3	2,4,5,6
160	1701.11	0.044	7.577	0.083	-0.100	0.130	1470	58	4	2,4,5,6
161	1701.11	0.030	7.351	0.027	-0.104	0.107	1494	27	2	2,4,5,6
162	1701.12	0.204	7.525	0.093	-0.118	0.150	1459	68	5	2,4,5,6
163	1701.11	0.050	7.658	0.157	-0.141	0.211	1526	0	0	2,4,5,6
164	1701.12	0.171	7.341	0.176	-0.124	0.215	1588	-69	4	2,4,5,6
165	1701.12	0.145	7.431	0.102	-0.154	0.184	1546	-27	2	2,4,5,6
166	DNA	DNA	DNA							
167	1701.10	-0.114	7.622	0.121	-0.015	0.122	1158	30	3	2,4,5,6
168	1701.16	0.335	6.722	0.132	-0.335	0.360	1138	102	9	2,4,5,6

RD.	PREDICTED IMPACT LOCATION ON TARGET			Error Analysis		Error Analysis	PREDICTED	Error Analysis	EA	Array
NO.	X	Y	Z	del Y	del Z	Offset Distance	Velocity	Δ Vel	ΔV	Config
Consec.	(m)	(m)	(m)	m	m	m	m/s	m/s	%	
169	1701.12	0.136	7.544	0.111	-0.017	0.112	1136	7	1	2,4,5,6
170	1701.11	0.059	7.212	0.128	-0.015	0.129	1221	3	0	2,4,5,6
171	1701.09	-0.412	6.876	0.159	0.041	0.164	1230	-1	0	2,4,5,6
172	1701.17	1.024	7.164	0.153	-0.057	0.163	1195	11	1	2,4,5,6
173	1701.15	0.632	7.257	0.065	-0.060	0.088	1188	11	1	2,4,5,6
174	1701.11	-0.081	7.433	0.128	-0.016	0.129	1168	-1	0	2,4,5,6
175	DNA	DNA	DNA							
176	DNA	DNA	DNA							
177	DNA	DNA	DNA							
178	DNA	DNA	DNA							
179	DNA	DNA	DNA							
180	DNA	DNA	DNA							
181	DNA	DNA	DNA							
182	DNA	DNA	DNA							
183	DNA	DNA	DNA							
184	DNA	DNA	DNA							
185	1701.004	-1.265	7.325	0.092	0.002	0.092	901	-16	2	2,4,5,6
186	1701.097	-0.222	7.193	0.079	-0.056	0.096	894	-4	0	2,4,5,6
187	1701.076	-0.572	7.658	0.099	-0.031	0.103	892	-3	0	2,4,5,6
188	1701.04	-0.945	7.412	0.092	-0.005	0.092	892	-6	1	2,4,5,6
189	1701.14	0.563	7.488	0.094	-0.131	0.161	879	9	1	2,4,5,6
190	1701.09	-0.377	7.223	0.144	-0.006	0.144	873	14	2	2,4,5,6
191	1701.07	-0.637	7.485	0.174	0.032	0.177	883	2	0	2,4,5,6
192	1701.06	-0.838	7.304	0.115	0.023	0.118	884	-1	0	2,4,5,6

INTENTIONALLY LEFT BLANK.

APPENDIX H:

ANGLE CORRECTION TECHNIQUE

INTENTIONALLY LEFT BLANK.

A method to theoretically correct the velocity is to employ a system of a family of hyperbolas, and solve for the speed. This is an iterative method, since more than one of the variables are unknown. Referring to Figure H-1, the following is defined:

where

D_{ST} = Distance between mic 1 and P1.
h = Elevation of projectile above ground plane.
M = Mach Number.
β = Azimuth Deviation.
y_f = Equation for Shock Front.
y_h = Equation for lead Hyperbola.
y_{h2} = Equation for succeeding Hyperbola.
y_s = Equation for line going through mic 1 and mic 2.
c = true distance for correct velocity calculation.

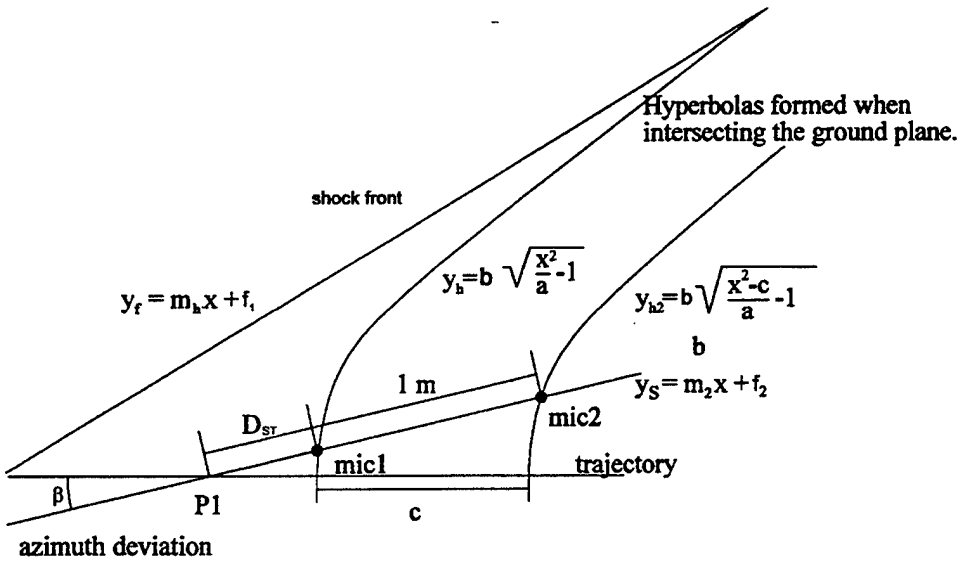

Figure H-1. Hyperbola created by cone intersecting ground plane.

First one must consider that the conic section that intersects a plane that is parallel to the conix axis will form a hyperbola of the following form:

$$y_h = b\sqrt{\frac{x^2}{a} - 1}. \tag{29}$$

The angle of the shock cone is $\Theta = \sin^{-1}1/M$. The slope of the shock cone can be written as

$$\lim_{x\to\infty}\frac{dy_h}{dx} = m_h. \tag{30}$$

Taking the derivative of the hyperbolic equation yields

$$\frac{dy_h}{d_x} = \frac{d(bU^{1/2})}{dx},$$

$$U = \frac{x^2}{a} - 1,$$

$$dy_h = \frac{b}{\sqrt{a - \frac{a^2}{x^2}}},$$

$$\lim_{x\to\infty}\frac{dy_h}{dx} = \lim_{x\to\infty}\frac{b}{\sqrt{a - \frac{a^2}{x^2}}} = \frac{b}{\sqrt{a}}. \tag{31}$$

The distance from the origin to where the hyperbola intersects the x-axis is where $x^2=a$. This is shown as

$$y = b\,\frac{\sqrt{x^2}}{a} - 1,$$

$$\frac{x^2}{a} - 1 = 0,$$

$$\frac{x^2}{a} = 1,$$

$$x^2 = a. \tag{32}$$

This is the point where the shock cone generated by the projectile intersects the microphone, as depicted in Figure H-2.

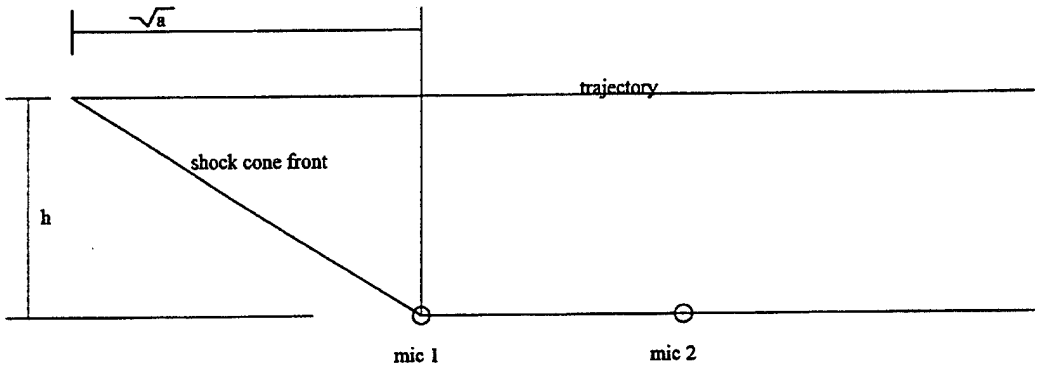

Figure H-2. Shock cone geometry.

Using Figure H-2, we are able to say that

$$\frac{\sqrt{a}}{h} = \sqrt{M^2 - 1}. \tag{33}$$

This implies a solution for the magnitude of a plus solving for d,

$$a = h^2 (M^2 - 1),$$

$$\frac{b}{\sqrt{a}} = \sqrt{M^2 - 1},$$

$$b = \sqrt{a(M^2 - 1)} = h(M^2 - 1). \tag{34}$$

By knowing the length of D, since it intersects the trajectory at P1, we know the y value at mic 1.

$$y_1 = D_{ST} \sin \beta. \tag{35}$$

The value of x also needs to be solved and can be done by substituting the result of y into the solution for x of the intersecting hyperbolic equation.

Now the point of mic 1 is known in Cartesian coordinates. Substituting cot β for m_f into the equation that describes the line of mic 1 and mic 2, we can define the intercept, f_2.

$$y_h = b\sqrt{\frac{x_h^2}{a}-1},$$

$$x_h^2 = a\left[\left(\frac{y_h}{b}\right)^2+1\right],$$

$$x_1 = \sqrt{a\left[\left(\frac{y_h}{b}\right)^2+1\right]}, \tag{36}$$

$$f = y_s - x_s \cot\beta, \tag{37}$$

or

$$f = y_1 - x_1\beta,$$

$$y_s = y_1 + (x_s - x_s)\cot\beta. \tag{38}$$

To find the Cartesian values for mic 2, we repeat the substitution, but for the second hyperbola.

$$y_2 = (D_{ST}+1m)\sin\beta,$$

$$y_2 = y_1 + (x_2 - x_1)\cot\beta,$$

$$x_2 = (Y_2 - Y_1)\tan\beta + x_1. \tag{39}$$

Knowing the values of x_2 and y_2 is the key to finding c. We write the equation for the hyperbola intersecting mic 2 at Dt = 0. This is identical to the first hyperbola except it is displaced along the x-axis by value c. Transforming x'=x+c,

$$y_{h2} = b\sqrt{\frac{(x_{h2} - c)^2}{a} - 1.} \tag{40}$$

Solving the equation for c,

$$y_2 = (D + 1m) \sin \beta,$$

$$x_2 = (y_2 - y_1) \tan \beta + x_1,$$

$$c = x_2\sqrt{a\left[\left(\frac{y_2}{b}\right)^2 + 1\right]}. \tag{41}$$

With c determined, the corrected velocity should be calculated as

$$V = \frac{c}{T_2}. \tag{42}$$

For this method to work, an initial guess must be made for the Mach number. On the first guess, we assume c is 1 m. For an increase in azimuth deviation, a, the true velocity length, c, is decreasing. As well, the further to the left or right of the centerline, c becomes even smaller. With any azimuth deviation, the predicted velocity will always be higher. The resulting c, based on the higher Mach number, will be calculated to slightly less than reality. The resultant updated velocity will be more accurate.

It can be shown geometrically that an iterative process of updating the velocity and Mach number and calculating a new value for **c** will eventually converge to the true velocity rapidly. For the purpose of the RDS, one, maybe two, iterations would be all that was necessary. The true test of this method lay in processing the data obtained from the data collection test.

Unfortunately, the method did not work. It was determined that the fault did not lay in the theory but in the assumptions. It was assumed that the azimuth deviation would be known. The method of finding the azimuth deviation was not accurate. The solution for the true velocity is strongly related to that angle. As a result, this method could not be used.

INTENTIONALLY LEFT BLANK.

APPENDIX I:

LOCATION DATA FROM DATA COLLECTION TEST

INTENTIONALLY LEFT BLANK.

RD.	PREDICTED IMPACT LOCATION ON TARGET			Error Analysis		Error Analysis	PREDICTED	Error Analysis	EA	Array
NO.	X	Y	Z	del X	del Z	miss distance	Velocity	del Vel	del V	Config
Consec.	(m)	(m)	(m)	m	m	m	m/s	m/s	%	
1	ND	ND	ND							
2	ND	ND	ND							
3	ND	ND	ND							
4	ND	ND	ND							
5	1700.948	-0.420	4.344	0.197	-0.053	0.204	580	-14.	2	1,2,3,4
6	1700.948	-0.230	4.575	0.049	-0.401	0.404	595	-8.	1	1,2,3,4
7	1700.948	-0.405	4.369	0.332	0.209	0.393	599	-9.	2	1,2,3,4
8	1700.948	-0.363	4.246	0.190	-0.086	0.208	582	-10.	2	1,2,3,4
9	1700.948	-0.223	4.361	0.154	-0.146	0.212	583	-8.	1	1,2,3,4
10	1700.948	-0.265	4.325	0.219	-0.050	0.224	587	-9.	2	1,2,3,4
11	1700.948	-0.312	4.283	0.199	-0.100	0.223	602	-10.	2	1,2,3,4
12	1700.948	-0.590	4.236	0.181	-0.075	0.196	604	-13.	2	1,2,3,4
13	1700.948	-0.803	3.930	0.193	-0.048	0.199	552	-18.	3	1,2,3,4
14	1700.948	-0.598	4.346	0.180	-0.064	0.192	608	-16.	3	1,2,3,4
15	ND	ND	ND							
16	ND	ND	ND							
17	ND	ND	ND							
18	ND	ND	ND							
19	ND	ND	ND							
20	ND	ND	ND							
21	ND	ND	ND				346	-18.	5	1,2,3,4
22	1700.948	-0.003	4.112	0.054	0.232	0.238	388	-13.	3	1,2,3,4
23	ND	ND	ND				343	-19.	6	1,2,3,4
24	ND	ND	ND							
25	1700.948	-0.300	3.721	0.032	0.128	0.132	397	-15.	4	1,2,3,4
26	ND	ND	ND				346	-15.	4	1,2,3,4
27	ND	ND	ND							
28	ND	ND	ND							

RD.	PREDICTED IMPACT LOCATION ON TARGET			Error Analysis		Error Analysis	PREDICTED	Error Analysis	EA	Array
NO.	X	Y	Z	del X	del Z	miss distance	Velocity	del Vel	del V	Config
Consec.	(m)	(m)	(m)	m	m	m	m/s	m/s	%	
29	ND	ND	ND							
30	ND	ND	ND							
31	ND	ND	ND							
32	ND	ND	ND							
33	ND	ND	ND							
34	ND	ND	ND							
35	ND	ND	ND							
36	1700.948	0.135	3.278	0.193	-0.208	0.283	650	6.	1	1,2,3,4
37	1700.948	0.936	8.308				579	3.	1	1,2,3,4
38	1700.948	-2.708	3.332				642	-35.	5	1,2,3,4
39	1700.948	-0.285	4.666	0.205	-0.085	0.222	677	-12.	2	1,2,3,4
40	1700.948	-0.135	4.468	0.210	-0.144	0.254	636	15.	2	1,2,3,4
41	1700.948	-1.073	7.683				563	5.	1	1,2,3,4
42	1700.948	3.068	6.288				560	24.	4	1,2,3,4
43	1700.948	-1.687	3.903	0.136	-0.039	0.142	650	-10.	1	1,2,3,4
44	1700.948	0.041	4.531	0.222	-0.156	0.271	670	13.	2	1,2,3,4
45	ND	ND	ND							
46	1700.783	0.011	4.096	0.142	0.055	0.152	435	-13.	3	1,2,3,4
47	1700.783	-0.276	4.684	0.045	-0.127	0.134	448	0.	0	1,2,3,4
48	1700.783	-0.243	4.587	0.043	0.011	0.044	465	-8.	2	1,2,3,4
49	1700.783	-0.093	4.520	0.093	-0.111	0.145	425	6.	1	1,2,3,4
50	1700.783	-0.600	4.534	0.034	-0.047	0.058	451	-6.	1	1,2,3,4
51	1700.783	-0.551	4.496	0.025	-0.136	0.138	460	3.	1	1,2,3,4
52	ND	ND	ND							
53	ND	ND	ND							
54	ND	ND	ND							
55	ND	ND	ND							
56	1700.783	0.794	4.323	-0.007	-0.147	0.147	449	2.	0	1,2,3,4

RD.	PREDICTED IMPACT LOCATION ON TARGET			Error Analysis		Error Analysis	PREDICTED	Error Analysis	EA	Array
NO.	X	Y	Z	del X	del Z	miss distance	Velocity	del Vel	del V	Config
Consec.	(m)	(m)	(m)	m	m	m	m/s	m/s	%	
57	1700.783	0.992	3.818	0.030	-0.033	0.044	453	-15.	3	1,2,3,4
58	1700.783	-1.227	4.668	-0.098	0.026	0.101	504	-13.	2	1,2,3,4
59	1700.783	1.073	4.915	-0.019	-0.002	0.019	498	-8.	2	1,2,3,4
60	1700.783	0.522	5.185	0.044	-0.051	0.067	500	-9.	2	1,2,3,4
61	ND	ND	ND							
62	ND	ND	ND							
63	1700.783	-0.264	4.213	0.202	-0.101	0.226	569	3.	1	1,2,3,4
64	1700.783	-0.341	4.225	0.210	0.013	0.210	574	-14.	2	1,2,3,4
65	1700.783	0.104	4.094	0.236	-0.121	0.266	555	8.	2	1,2,3,4
66	1700.783	-0.378	4.208	0.202	-0.069	0.213	544	9.	2	1,2,3,4
67	1700.783	-0.618	4.180	0.224	-0.057	0.231	550	8.	1	1,2,3,4
68	1700.783	-0.516	4.388	0.211	-0.108	0.237	560	10.	2	1,2,3,4
69	ND	ND	ND							
70	ND	ND	ND							
71	ND	ND	ND							
72	ND	ND	ND							
73	ND	ND	ND							
74	ND	ND	ND							
75	ND	ND	ND							
76	1700.823	0.260	4.156	-0.096	-0.067	0.117	1085	-39.	4	1,2,3,4
77	1700.823	0.873	4.588	-0.103	-0.021	0.105	877	-39.	4	1,2,3,4
78	1700.823	0.140	3.653	-0.115	-0.040	0.122	1097	-51.	5	1,2,3,4
79	1700.823	1.177	3.871	-0.081	-0.011	0.081	877	-37.	4	1,2,3,4
80	1700.823	0.458	3.565	-0.084	-0.060	0.104	1103	-57.	5	1,2,3,4
81	ND	ND	ND							
82	ND	ND	ND							
83	1700.823	-0.107	4.071	0.115	-0.063	0.132	1327	-27.	2	1,2,3,4
84	1700.823	-0.318	4.776	0.118	-0.035	0.123	1023	-26.	3	1,2,3,4

RD.	PREDICTED IMPACT LOCATION ON TARGET			Error Analysis		Error Analysis	PREDICTED	Error Analysis	EA	Array
NO.	X	Y	Z	del X	del Z	miss distance	Velocity	del Vel	del V	Config
Consec.	(m)	(m)	(m)	m	m	m	m/s	m/s	%	
85	1700.823	-0.244	4.295	0.195	-0.027	0.197	1018	-22.	2	1,2,3,4
86	1700.823	-0.639	4.472	0.094	-0.042	0.103	1028	-28.	3	1,2,3,4
87	1700.823	-0.090	4.210	0.120	-0.098	0.155	1345	-38.	3	1,2,3,4
88	ND	ND	ND							
89	ND	ND	ND							
90	ND	ND	ND							
91	1700.823	-1.082	4.097	-0.084	-0.083	0.119	719	-25.	3	1,2,3,4
92	1700.823	-0.209	5.271	-0.039	-0.045	0.060	854	-38.	4	1,2,3,4
93	1700.823	-1.027	4.184	-0.061	-0.070	0.093	717	-26.	4	1,2,3,4
94	1700.823	0.128	4.655	-0.058	-0.099	0.114	850	-36.	4	1,2,3,4
95	1700.823	-0.095	4.372	-0.057	-0.084	0.101	733	-34.	5	1,2,3,4
96	1700.975	-0.888	4.651	0.674	-0.048	0.675	704	-23.	3	1,2,3,4
97	1700.975	-0.318	4.854	0.650	-0.300	0.716	661	37.	6	1,2,3,4
98	1700.975	-0.583	4.471	0.648	-0.155	0.666	696	-20.	3	1,2,3,4
99	1700.975	-0.566	4.816	0.692	-0.186	0.717	675	5.	1	1,2,3,4
100	1700.975	-0.465	4.421	0.629	-0.160	0.649	689	16.	2	1,2,3,4
101	1700.975	-0.465	4.483	0.630	-0.272	0.686	682	22.	3	1,2,3,4
102	1700.975	-0.791	4.233	1.101	-0.054	1.102	719	-34.	5	1,2,3,4
103	1700.975	-1.746	3.986	0.516	0.359	0.629	847	-150.	18	1,2,3,4
104	1700.975	-1.803	3.959	0.509	0.381	0.635	893	-188.	21	1,2,3,4
105	1700.975	-1.856	3.988	0.492	0.407	0.638	922	-207.	22	1,2,3,4
106	1700.975	-1.802	2.460	0.367	0.707	0.797	1034	-332.	32	1,2,3,4
107	1700.975	-1.749	3.030	0.435	0.511	0.671	967	-262.	27	1,2,3,4
108	1700.975	-1.750	2.976	0.407	0.534	0.671	977	-269.	28	1,2,3,4
109	1700.975	0.276	5.057	0.653	-0.559	0.860	627	75.	12	1,2,3,4
110	1700.975	0.528	5.424	0.650	-0.671	0.934	622	92.	15	1,2,3,4
111	1700.975	0.533	5.288	0.646	-0.615	0.892	622	98.	16	1,2,3,4
112	1700.975	0.702	3.991	0.507	-0.243	0.562	564	131.	23	1,2,3,4

RD.	PREDICTED IMPACT LOCATION ON TARGET			Error Analysis		Error Analysis	PREDICTED	Error Analysis	EA	Array
NO.	X	Y	Z	del X	del Z	miss distance	Velocity	del Vel	del V	Config
Consec.	(m)	(m)	(m)	m	m	m	m/s	m/s	%	
113	1700.975	0.670	4.234	0.518	-0.705	0.875	592	125.	21	1,2,3,4
114	1700.975	0.464	4.103	0.524	-0.592	0.791	601	114.	19	1,2,3,4
115	1700.975	0.636	4.365	0.559	-0.735	0.924	576	110.	19	1,2,3,4
116	1700.975	0.608	4.394	0.552	-0.666	0.865	586	110.	19	1,2,3,4
117	1700.975	0.631	4.017	0.508	-0.678	0.847	581	127.	22	1,2,3,4
118	1700.975	-0.120	4.030	0.577	-0.319	0.660	661	42.	6	1,2,3,4
119	ND	ND	ND							
120	ND	ND	ND							
121	ND	ND	ND							
122	ND	ND	ND							
123	ND	ND	ND							
124	ND	ND	ND							
125	ND	ND	ND							
126	ND	ND	ND							
127	ND	ND	ND							
128	ND	ND	ND							
129	ND	ND	ND							
130	ND	ND	ND							
131	ND	ND	ND							
132	ND	ND	ND							
133	ND	ND	ND							
134	ND	ND	ND							
135	ND	ND	ND							
136	ND	ND	ND							
137	ND	ND	ND							
138	ND	ND	ND							
139	ND	ND	ND							
140	ND	ND	ND							

INTENTIONALLY LEFT BLANK.

APPENDIX J:

VERIFICATION/VALIDATION TEST DATA

INTENTIONALLY LEFT BLANK.

RD. #	PREDICTED Velocity m/s	PREDICTED Loc X (m)	Z (m)	PREDICTED ROUND TYPE Formulation	Statistical	PREDICTED OFFSET DISTANCE 1	2	HIT TARGET KZONE	TARGET WENT DOWN	VELOCITY ERROR %	LOCATION ERROR (m)
1	1158.08	0.081	3.870	35 TPGID	TPGID KE	6.405	6.505			-1.4	
2	1165.50	0.189	2.987	35 TPGID	TPGID KE	6.028	6.307	*	*	-.8	0.075
3	922.08	-0.349	2.564	35 TPGID	TPGID HEAT	6.475	5.706	*	?	-2.3	0.074
4	923.36	-0.039	3.007	35 TPGID	TPGID HEAT	6.257	6.100	*	*	-1.6	0.077
5	1030.13	-0.042	3.227	35 TPGID	TPGID KE	6.293	6.172	*	*		0.067
6	1016.00	1.004	3.080	35 TPGID	TPGID KE	5.256	7.150	*	*	-.3	0.082
7	834.90	-0.093	3.045	35 TPGID	TPGID HEAT	6.297	6.070	*	*	-1.1	0.050
8	848.54	-1.147	3.139	35 TPGID	TPGID HEAT	7.336	5.089	*	*	-2.8	0.076
9	849.62	0.556	3.257	35 TPGID	TPGID HEAT	5.764	6.721	*	*	-.8	0.096
10	718.26	0.107	2.899	35 TPGID	TPGID HEAT	6.090	6.231	*	*	-2.2	0.060
11	870.70	-0.747	2.125	35 TPGID	TPGID HEAT	6.802	5.269	*	*	-3.7	0.065
12	356.47	0.347	5.486	12.7	TPGID HEAT	6.013	7.098				
13	848.18	0.916	2.451	35 TPGID	TPGID HEAT	5.205	6.930	*	*	.1	0.094
14	723.33	-0.156	3.377	35 TPGID	TPGID HEAT	6.445	6.118	*	*	-2.3	0.067
15	724.77	-0.215	1.759	35 TPGID	TPGID HEAT	6.270	5.743	*	*	-2.8	0.096
16	718.65	0.363	2.203	35 TPGID	LARGE HE	5.732	6.349	*	*	-1.5	0.090
17	1430.62	-0.216	2.074	25 KE	TPGID KE	6.301	5.745	*	*	-3.5	0.094
18	951.25	0.215	2.080	LARGE HEAT	LARGE HE	5.883	6.171	*	*	-.8	0.134
19	1434.21	-0.548	2.120	LARGE KE	TPGID KE	6.610	5.444	*	*	-3.7	0.099
20	1454.55	-0.708	1.946	LARGE KE	TPGID KE	6.773	5.256			-4.9	0.110
21	845.85	0.255	1.984	LARGE KE	TPGID HEAT	5.836	6.202	*	*	-.7	0.155
22	1300.39	0.446	1.915	LARGE KE	LARGE KE	5.623	6.403	*	*	.0	0.081
23	1237.24	-0.489	1.404	LARGE HEAT	LARGE HE	6.552	5.455			-2.8	
24	1233.05	-0.624	3.512	LARGE KE	TPGID KE	6.922	5.705	*	*	-3.0	0.145
25	702.74	0.366	2.646	25 HE	TPGID HEAT	5.776	6.425	*	*	-1.2	0.058
26	743.08	-0.403	4.665	LARGE HEAT	LARGE HE	7.111	6.408			-2.5	
27	773.69	0.599	4.234	LARGE HEAT	LARGE HE	6.038	7.097			-1.4	
28	763.94	0.311	3.632	35 TPGID	LARGE HE	6.084	6.619	*	*	-1.3	0.082
29	669.46	0.445	1.432	12.7	7.62 OR 12.7	5.614	6.407				
30	683.64	0.437	2.906	12.7	7.62 OR 12.7	5.725	6.541	*	*		
31	730.99	0.762	3.393	12.7	7.62 OR 12.7	5.584	6.997				
32	603.59	-0.432	1.841	7.62	7.62 OR 12.7	6.469	5.546	*	?		
33	535.12	0.68	5.331	12.7	7.62 OR 12.7	6.436	7.538				
34	594.27	-2.295	5.991	12.7	7.62 OR 12.7	9.205	5.710				
35	564.10	-0.879	5.812	12.7	7.62 OR 12.7	7.959	6.582				
36	591.19	-0.408	4.055	12.7	7.62 OR 12.7	6.853	6.099				
37	597.55	-0.519	1.593	12.7	7.62 OR 12.7	6.588	5.412				
38	383.47	-0.051	2.269	7.62	7.62 OR 12.7	6.156	5.914				
39	364.37	0.647	3.302	7.62	7.62 OR 12.7	5.536	6.684				
40											
42	797.45	0.293	1.588	25 HE	7.62 OR 12.7	5.738	6.263				
43	805.96	-0.421	2.396	25 HE	7.62 OR 12.7	6.481	5.640	*	*		
44	1258.26	-0.985	2.748	25 KE	7.62 OR 12.7	7.060	5.182				
45	1249.61	0.072	2.516	25 KE	7.62 OR 12.7	6.020	6.135	*	*		
46	863.93	-1.301	4.278	25 KE	7.62 OR 12.7	7.760	5.451				
47	848.54	0.436	2.666	25 KE	7.62 OR 12.7	5.720	6.504	*	*		
48	863.93	0.141	3.710	25 KE	7.62 OR 12.7	6.261	6.509				
49											
50								*			
51											
52	1154.36	-1.670	1.000	25 KE	7.62 OR 12.7	7.678	4.334	*	*		
53	1150.06	-2.109	1.501	25 KE	7.62 OR 12.7	8.089	3.888		*		
54	1134.46	0.025	1.488	25 KE	7.62 OR 12.7	5.977	6.000	*	*		

55	1122.10	0.030	1.474	25 KE	7.62 OR 12.7	5.974	6.003				
56	629.76	1.185	0.943	25 HE	7.62 OR 12.7	4.861	7.163				
57	566.35	0.451	1.504	25 HE	7.62 OR 12.7	5.553	6.424	*	*		
58	1046.65	0.240	2.592	25 KE	7.62 OR 12.7	5.872	6.332	*	*		
59	1064.69	-0.770	1.324	25 KE	7.62 OR 12.7	6.768	5.209				
60	1056.84	-0.262	3.091	25 KE	7.62 OR 12.7	6.471	5.965	*	*		
61								*	*		
62								*	*		
63	955.96	-0.325	1.689	LARGE HEAT	LARGE HE	6.329	5.662	*	*		
64	1444.60	-0.124	1.596	LARGE HEAT	LARGE HE	6.118	5.865	*	*		
65	1426.14	-0.201	1.744	LARGE KE	7.62 OR 12.7	6.209	5.786	*	*		

RD. #	GUN POS. (m)	ROUND TYPE (mm)	DATE	TIME H:M:S	TERMINAL VELOCITY (m/sec)	VIDEO SCORING LOCATION HORIZ (m)	VIDEO SCORING LOCATION VERT (m)	OFFSET (m) 1	DISTANCE (m) 2
1	800	35 TPGID KE	6/23/93	13:23:55	1142.18				
2	"	35 TPGID KE	6/23/93	13:29:54	1156.61	0.118	3.012	6.042	6.276
3	"	35 OLD HEAT	6/23/93	14:42:50	901.42	-0.420	2.584	6.490	5.664
4	"	35 NEW HEAT	6/23/93	15:38:59	908.96	-0.099	3.056	6.263	6.075
5	1200	35 TPGID KE	6/23/93	16:10:17	NA	-0.090	3.273	6.308	6.139
6	"	35 TPGID KE	6/23/93	16:13:50	1013.41	0.951	3.143	5.270	7.118
7	"	35 OLD HEAT	6/23/93	16:21:56	825.50	-0.142	3.056	6.305	6.033
8	"	35 NEW HEAT	6/23/93	16:25:51	825.05	-1.218	3.164	7.379	5.028
9	1700	35 TPGID KE	6/23/93	17:09:16	843.22	0.465	3.288	5.777	6.679
10	"	35 NEW HEAT	6/23/93	17:13:16	702.55	0.049	2.910	6.087	6.187
11	"	35 TPGID KE	6/23/93	17:21:54	839.64	-0.810	2.141	6.829	5.217
12	"	35 TPGID KE	6/23/93	17:24:44	NA			6.218	6.213
13	"	35 TPGID KE	6/23/93	17:29:05	848.95	0.847	2.388	5.208	6.891
14	"	35 NEW HEAT	6/23/93	17:31:24	707.04	-0.220	3.397	6.466	6.049
15	"	35 NEW HEAT	6/23/93	17:40:09	705.15	-0.290	1.699	6.290	5.711
16	"	35 NEW HEAT	6/23/93	17:43:28	708.16	0.292	2.148	5.732	6.315
17	800	105 KE	6/24/93	10:58:24	1382.3	-0.285	2.010	6.296	5.729
18	"	105 HEAT	6/24/93	11:44:24	943.8	0.146	1.965	5.863	6.157
19	"	105 KE	6/24/93	11:51:11	1382.9	-0.593	2.032	6.605	5.423
20	"	105 KE	6/24/93	11:54:37	1387.2	-0.787	1.869	6.791	5.220
21	1200	105 HEAT	6/24/93	13:30:44	839.7	0.199	1.840	5.805	6.203
22	"	105 KE	6/24/93	13:35:08	1300.2	0.402	1.847	5.602	6.406
23	1800	105 KE	6/24/93	14:32:40	1203.0			6.218	6.213
24	"	105 KE	6/24/93	15:23:19	1196.7	-0.619	3.657	6.922	5.757
25	"	105 HEAT	6/24/93	15:29:07	694.6	0.411	2.608	5.674	6.488
26	"	105 HEAT	6/24/93	15:39:13	725.3			6.218	6.213
27	"	105 HEAT	6/24/93	15:45:08	762.9			6.218	6.213
28	"	105 HEAT	6/24/93	15:48:55	754.1	0.340	3.709	6.029	6.678
29	400	12.7	6/25/93	12:47:07	NA	NA	NA	NA	NA
30	"	12.7	6/25/93	12:50:22	NA	NA	NA	NA	NA
31	"	12.7	6/25/93	12:56:36	NA	NA	NA	NA	NA
32	"	7.62	6/25/93	13:10:13	NA	NA	NA	NA	NA
33	800	12.7	6/25/93	13:51:09	NA	NA	NA	NA	NA
34	"	12.7	6/25/93	13:55:19	NA	NA	NA	NA	NA
35	"	12.7	6/25/93	13:59:27	NA	NA	NA	NA	NA
36	"	12.7	6/25/93	14:01:44	NA	NA	NA	NA	NA
37	"	12.7	6/25/93	14:03:15	NA	NA	NA	NA	NA
38	"	7.62	6/25/93	14:10:50	NA	NA	NA	NA	NA
39	"	7.62	6/25/93	14:16:25	NA	NA	NA	NA	NA
40	"	7.62	6/25/93	14:19:12	NA	NA	NA	NA	NA
42	600	25 HE	7/1/93	10:54:00	NA	NA	NA	NA	NA
43	"	25 HE	7/1/93	10:55:00	NA	NA	NA	NA	NA
44	"	25 KE	7/1/93	11:15:00	NA	NA	NA	NA	NA
45	"	25 KE	7/1/93	11:18:00	NA	NA	NA	NA	NA
46	1700	25 KE	7/1/93	11:30:00	NA	NA	NA	NA	NA
47	"	25 KE	7/1/93	11:33:00	NA	NA	NA	NA	NA
48	"	25 KE	7/1/93	11:43:00	NA	NA	NA	NA	NA
49	"	25 HE	7/1/93	11:45:00	NA	NA	NA	NA	NA
50	"	25 HE	7/1/93	11:46:00	NA	NA	NA	NA	NA
51	"	25 HE	7/1/93	11:48:00	NA	NA	NA	NA	NA
52	1000	25 KE	7/1/93	14:15:00	NA	NA	NA	NA	NA
53	"	25 KE	7/1/93	14:20:00	NA	NA	NA	NA	NA
54	"	25 KE	7/1/93	14:22:00	NA	NA	NA	NA	NA

55	"	25 KE	7/1/93	14:27:00	NA	NA	NA	NA	NA
56	"	25 HE	7/1/93	14:29:00	NA	NA	NA	NA	NA
57	"	25 HE	7/1/93	14:53:00	NA	NA	NA	NA	NA
58	"	25 HE	7/1/93	14:55:00	NA	NA	NA	NA	NA
59	"	25 KE	7/1/93	14:56:00	NA	NA	NA	NA	NA
60	"	25 KE	7/1/93	14:58:00	NA	NA	NA	NA	NA
61	"	25 KE	7/1/93	15:01:00	NA	NA	NA	NA	NA
62	"	25 HE	7/1/93	15:04:00	NA	NA	NA	NA	NA
63	"	120 HE	7/1/93	16:28:00	NA	NA	NA	NA	NA
64	"	120 KE	7/1/93	16:36:00	NA	NA	NA	NA	NA
65	"	120 KE	7/1/93	16:38:00	NA	NA	NA	NA	NA

APPENDIX K:

STATISTICAL ANALYSIS OF 1,000-m DATA

INTENTIONALLY LEFT BLANK.

Implementing Kruskal-Wallis Test: An Example

The Kruskal-Wallis nonparametric test was implemented in the feasibility test phase for the 1,000-m data. An example of the test procedure is provided in this appendix. The null hypothesis (the hypothesis that is to be rejected) is that the six round types have identical distributions (and therefore equal means) vs. the alternative that at least two round types differ.

The advantage of a nonparametric test over a parametric test is that the test does not require the assumptions of normality of the data or homogeneity of variances among the groups. This test performs analysis of variance on the ranks of the data. The ranks start with 1 for the smallest value among all the six round types. If more than one response value is the same (that is, there are ties), then these tied values would be assigned the average rank. This test was performed on each variable separately and at four regions corresponding to the data collected from the microphones. The data from the 1- and 3-m microphones were grouped into one region since the 1-m microphone had incomplete data. The range of offset distances in meters for each region is as follows:

Region 1 ≤ 4

$4 <$ Region 2 ≤ 7

$7 <$ Region 3 ≤ 10

$10 <$ Region 4.

An example of the analysis provided for this test is for the positive peak pressures collected at the microphone stationed 12 m from the center of the target, region 4.

Table K-1. Example of Positive Peak Pressure From Region 4

25 mm		105 mm		120 mm	
HE (Pa)	KE (Pa)	HEAT (Pa)	KE (Pa)	HEAT (Pa)	KE (Pa)
481.40	376.00	1495.70	1109.00	1508.30	1088.00
483.98	401.60	1733.00	1109.50	1800.00	1109.50
499.41	404.20	1735.00	1112.00	1987.00	1145.00

Table K-2. Order Values and Ranks

Round (mm)	Ordered Values (Pa)	Rank	Rank with Ties
25 KE	376.00	1	1
25 KE	401.60	2	2
25 KE	404.20	3	3
25 HEI	481.40	4	4
25 HEI	483.98	5	5
25 HEI	499.41	6	6
120 KE	1088.00	7	7
105 KE	1109.00	8	8
105 KE	1109.50	9	9.5
120 KE	1109.50	10	9.5
105 KE	1112.00	11	11
120 KE	1145.00	12	12
105 HEAT	1495.70	13	13
120 HEAT	1508.30	14	14
105 HEAT	1733.00	15	15
105 HEAT	1735.00	16	16
120 HEAT	1800.00	17	17
120 HEAT	1987.00	18	18

All the positive peak pressure values from Table K-1 are ordered and then ranked. Table K-2 lists the ordered values and the corresponding rank. The two values with ranks 9 and 10 are the same and therefore should be given the same rank. The fourth column provides the rank correction by assigning the average of the two tied ranks, 9.5. These values become the data for which the analysis will be based (see Table K-3).

Table K-3. Ranks of Positive Peak Pressure

	25-mm M793	25-mm M910	105-mm M490	105-mm M724	120-mm M831	120-mm M865
	4	1	13	8	14	7
	5	2	15	9.5	17	9.5
	6	3	16	11	18	12
sum of ranks	15	6	44	28.5	49	28.5

The test statistic, T, for the Kruskal-Wallis test is computed the following way (Conover 1980):

$$T = \frac{1}{S^2}\left(\sum_{i=1}^{k=6}\frac{SR^2}{n_i} - \frac{N(N+1)^2}{4}\right),$$

where

SR = sum of the ranks as given in Table K-3, and

$$S^2 = \frac{1}{N-1}\left(\sum_{i=1}^{N} Rank_i^2 - \frac{N(N+1)^2}{4}\right).$$

The test statistic, is compared to the chi-square distribution with 5 (6 groups - 1) degrees of freedom at the $\alpha = 0.05$ level. (The chi-square test provided an approximate quantile since the exact distribution was not available.)

The calculated test statistic of 15.794 is significant at the alpha = 0.01 level. This indicates at least two groups differ in their average rank. To determine which ones differ, pairwise comparisons were performed. Two groups, i and j, would be statistically different if the following inequality is satisfied:

$$\left|\frac{SR_i}{n_i} - \frac{SR_j}{n_j}\right| > t\left[S^2\,\frac{N-1-T}{N-k}\right]^{1/2}\left[\frac{1}{n_i} - \frac{1}{n_j}\right]^{1/2}$$

The "t" is the t-distribution with N - k degrees of freedom at the 1 - $\alpha/2$ quantile. For this data set, if two average ranks differ more than 3.01, then the two groups are significantly different at the $\alpha = 0.05$ level. The ordered average rank for each group is listed in Table K-4.

Table K-4. Ordered by Average Rank

25-mm M910	2.00
25-mm M793	5.00
105-mm M724	9.50
120-mm M865	9.50
105-mm M490	14.67
120-mm M831	16.33

To summarize the results, the following notation is used for this example and for the other N-Wave variables in Table K-5. The round types are listed in order from lowest average rank to the highest. Parentheses around two or more round types indicate there is no significant difference between (or among) the rounds. The short-hand notation to summarize the results for positive peak pressures from region 4 is:

$$(25\ K = 25\ H) \neq (105\ \ H = 120\ \ H) \neq (105\ K = 120\ K).$$

To conserve space, H and K are abbreviated for HEI or HEAT and KE, respectively. The result for example tells us:

- 25-mm KE is not significantly different from 25-mm HEI in average rank.
- 25-mm KE and HE are significantly different from both round types of size 105 and 120 mm.
- 105-mm HE is not significantly different from 120-mm HE.
- 105-mm KE is not significantly different from 120-mm KE.
- The large HEAT rounds (105 mm and 120 mm) are significantly different from the large KE rounds (105 mm and 120 mm).

Table K-5. Multiple Comparison Results

Variable	Region	Notational Summary
Positive Peak Pressure	1	(25 K = 25 H) ≠ (105 K = 120 K) ≠ (105 H = 120 H)
	2	(25 H = 25 K) ≠ (105 K = 120 K) ≠ (105 H = 120 H)
	3	25 K ≠ 25 H ≠ (105 K = 120 K) ≠ (105 H = 120 H)
	4	(25 K = 25 H) ≠ (105 K = 120 K) ≠ (105 H = 120 H)
Negative Peak Pressure	1	(25 K = 25 H) ≠ (105 H = 105 K = 120 H = 120 K)
	2	(25 H = 25 K) ≠ (105 K = [105 H) = 120 H) = 120 K]
	3	(25 K = 25 H) ≠ (105 K = 105 H = 120 H = 120 K)
	4	(25 H = 25 K) ≠ (105 K = 120 K = 105 H = 120 H)
Positive Phase Duration	1	25 H ≠ 25 K ≠ (105 K = 120 K) ≠ (105 H = 120 H)
	2	25 H ≠ 25 K ≠ 105 K ≠ 120 K ≠ 105 H ≠120 H
	3	25 H ≠ 25 K ≠ 105 K ≠ 120 K ≠ 105 H ≠ 120 H
	4	25 H ≠ 25 K ≠ 105 K ≠ 120 K ≠ 105 H ≠ 120 H
Negative Phase Duration	1	(25 H = 25 K) ≠ (105 H = 120 K = 105 K = 120 H)
	2	(25 H = 25 K) ≠ (105 K = [120 K = 105 H) = 120 H]
	3	(25 K = [25 H) = {105 K] = 105 H = 120 K = 120 H}
	4	(25 K = [25 H) = {105 K] = 105 H = 120 K = 120 H}
Total Duration	1	(25 K = 25 H) ≠ (105 K = 120 K) ≠ 120 H = 105 H)
	2	25 K ≠ 25 H ≠ 105 K ≠ 120 K ≠ (105 H = 120 H)
	3	25 K ≠ 25 H ≠ (105 K = 120 K) ≠ (105 H = 120 H)
	4	25 K ≠ 25 H ≠105 K ≠ 120 K ≠ 105 H ≠ 120 H
Peak Pressure Impulse	1	25 K ≠ 25 H ≠ (105 K = 120 K) ≠ (105 H = 120 H)
	2	25 K ≠ 25 H ≠ 105 K ≠ 120 K ≠ 105 H ≠ 120 H
	3	25 K ≠ 25 H ≠105 K ≠ 120 K ≠ 105 H ≠ 120 H
	4	25 K ≠ 25 H ≠ 105 K ≠ 120 K ≠ 105 H ≠ 120 H
Peak of Absolute Pressure Impulse	1	25 K ≠ 25 H ≠ (105 K = 120 K) ≠ (105 H = 120 H)
	2	25 K ≠ 25 H ≠ 105 K ≠ 120 K ≠105 H ≠120 H
	3	25 K ≠ 25 H ≠ 105 K ≠ 120 K ≠ 105 H ≠ 120 H
	4	25 K ≠ 25 H ≠ 105 K ≠ 120 K ≠ 105 H ≠ 120 H
Negative Phase Pressure Impulse	1	25 K ≠ 25 H ≠ (105 K = 120 K) ≠ (105 H = 120 H)
	2	25 K ≠ 25 H ≠ 105 K ≠ 120 K ≠ (120 H = 105 H)
	3	25 K ≠ 25 H ≠ 105 K ≠ 120 K ≠ 105 H ≠ 120 H
	4	25 K ≠ 25 H ≠ 105 K ≠ 120 K ≠ (120 H = 105 H)

Most of the variables at each region can distinguish between large- and small-caliber rounds (25 mm vs. 105 mm or 120 mm). The only variable that cannot is negative phase duration in regions 3 and 4. The results of the pairwise multiple comparison tests for each region on each variable indicate that we can

not discriminate among all six round types. A general conservative result is the relationship as seen for the positive peak pressure:

$$(25\ K = 25\ H) \neq (105\ K = 120\ K) \neq (105\ H = 120).$$

For some variables in some of the regions, the two small-caliber rounds were distinguishable:

$$25\ K \neq 25\ H \neq (105\ K = 120\ K) \neq (105\ H = 120\ H).$$

For the most part, there is good agreement of the observed values with the statistical nonparametric results. However, on occasion, there are a few results that do not appear intuitive. Take for instance, negative phase duration plotted against offset distance in Figure K-1. In regions three and four, the 25-mm HE and KE rounds are not significantly different from each other by the Kruskal-Wallis test, as indicated by the parentheses ( ) around 25 K = 25 H, in Table K-5. Furthermore, all of the large-caliber rounds are not significantly different from each other, as indicated by the braces {}. These two results should be obvious from the plot. What is not intuitive is the nonparametric test indicating that 25-mm HEI and 105-mm KE are not significantly different. From the plot, one would think that they should be different. This result shows that by analyzing the data using the ranks, large differences in magnitude of the response variable in the original units may be masked.

Conversely, the nonparametric test can be very powerful in detecting small differences in magnitude if the ranks of the data within a round type are close together. This is illustrated in Figure K-2 for the peak net pressure impulse. The smallest ranks are the 25 KE rounds followed by the 25 HEI. Then, in order for regions 1–4, the ranking is as follows: 105 KE, 120 KE, 105 HEAT, and 120 HEAT.

What we have shown in these analyses is that many of the variables under consideration are good candidates to discriminate among at least the small-caliber rounds from the large-caliber rounds. In some regions for some variables, all the rounds are significantly different from each other. For the most part, the first region, representing data collected closes to the flight of the round (<4 m), is the hardest region to discriminate. This result is a guide to the placement of the microphones in future tests.

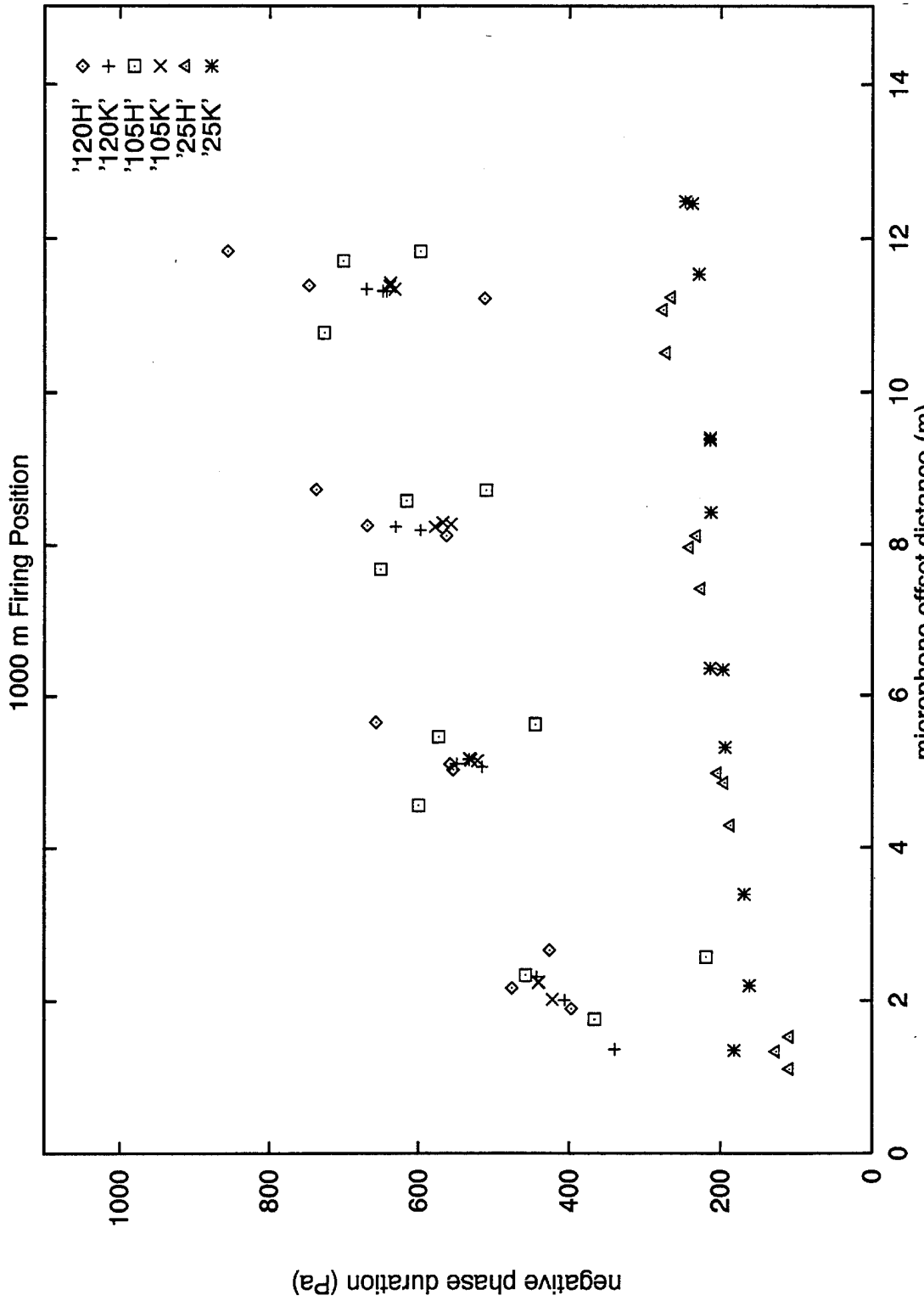

Figure K-1. Microphone offset distance vs. negative phase duration for rounds fired at 1,000 m.

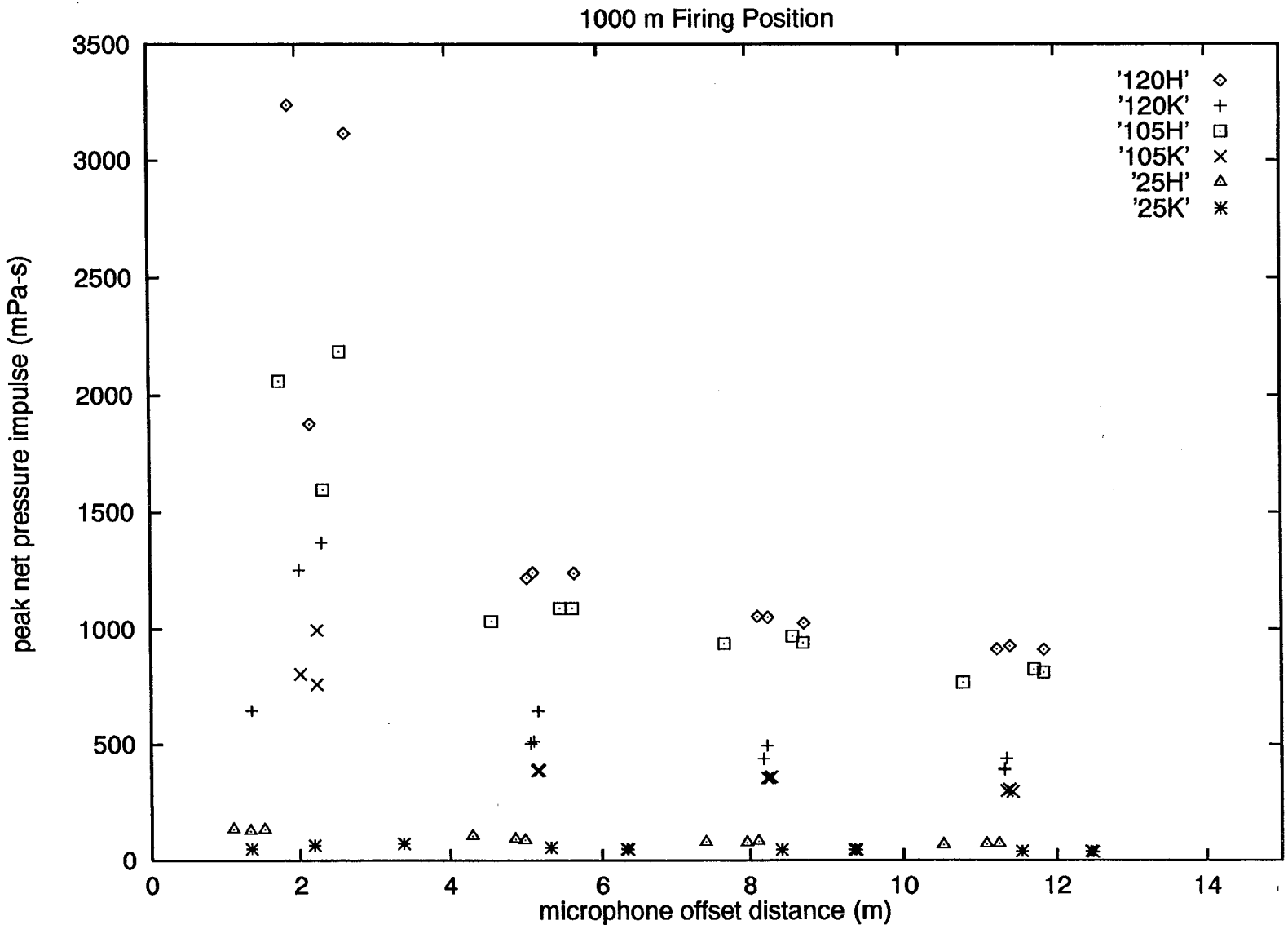

Figure K-2. Microphone offset distance vs. peak net pressure impulse for rounds fired at 1,000 m.

APPENDIX L:

PREDEMONSTRATION TEST DATA

INTENTIONALLY LEFT BLANK.

RD. #	GUN POS. (m)	ROUND TYPE (mm)	DATE	TIME H:M:S	TERMINAL VELOCITY (m/s)	HAND SCORED LOCATION HORIZ (m)	HAND SCORED LOCATION VERT (m)	OFFSET DISTANCE (m) 1	OFFSET DISTANCE (m) 2
1	1410	120(M865)	7/14/93	12:24:25	NA	0.552	1.229		
2	1130	120 (M831)	7/14/93	12:26:56	NA	0.305	1.686		
3	430	12.7 (M17)	7/14/93	12:31:16	NA				
4	430	7.62 (M62)	7/14/93	12:32:27	NA				
5	430	7.62 (M62)	7/14/93	12:32:41	NA				
6	960	35 (DM18)	7/14/93	12:44:43	NA	0.641	2.842		
7	960	35 (DM18)	7/14/93	12:46:15	NA	0.787	2.334		
8	1000	25 (M910)	7/14/93	12:54:27	NA	1.029	1.203		
9	1000	25 (M910)	7/14/93	12:56:39	NA	0.457	1.210		
10	1000	25 (M793)	7/14/93	12:57:13	NA	1.422	1.734		
11	1000	25 (M793)	7/14/93	12:57:55	NA	1.168	2.524		
12	1410	35 (DM18)	7/14/93	12:58:49	NA				

RD. #	PREDICTED Velocity (m/s)	PREDICTED LOC X (m)	Z (m)	PREDICTED ROUND TYPE			PREDICTED OD		HIT TARGET ZONE	TARGET WENT DOWN
				Formulation	Statistical	Hybrid	1	2		
1	1229.45	2.78	2.305	Large KE	***Large HE***	Large KE	3.466	8.545	no	no
2	902.73	-4.188	-8.289	**Large KE**	Large HE	**Large KE**	7.860	4.932	no	no
3	719.42	0.544	1.206	12.7	**7.62**	**25KE**	5.462	6.681	no	no
4	573.64	-0.489	2.014	7.62	7.62	**12.7**	6.451	5.563	yes	yes
5	601.69	-0.37	1.988	**12.7**	**35**	**25KE**	6.326	5.687	yes	yes
6	894.01	0.536	2.907	35	35	35	5.609	6.504	no	no
7	890.67	0.687	2.358	35	35	35	5.390	6.629	yes	yes
8	1093.20	0.511	4.652	25KE	**7.62**	25KE	6.155	6.950	no	no
9	1069.52	-0.436	4.792	25KE	**7.62**	25KE	7.093	6.097	no	no
10	536.48			**LargeKE**	**35**	**35**			no	no
11	624.71	1.307	3.370	25HE	**7.62**	25HE	4.903	7.398	no	no
12	585.65			35	35	35			no	no
				9 of 12	5 of 12	7 of 12				

BIBLIOGRAPHY

Conover, W. J. Practical Nonparametric Statistics. Second Edition, New York: John Wiley and Sons, Inc., 1980.

Establishment Suffield. Suffield Memorandum No. 1041, Ralston, Alberta Canada, June 1982.

Morrison, D. F. Multivariate Statistical Methods. Second Edition, New York: McGraw-Hill Book Company, 1976.

SPSS Inc. Statistical Package for the Social Sciences. SPSS Reference Guide, Chicago, IL, 1990b.

Tatsuoka, M. M. Multivariate Analysis, Techniques for Educational and Psychological Research. New York: John Wiley and Sons, Inc., 1971.

INTENTIONALLY LEFT BLANK.

LIST OF SYMBOLS

a	=	ambient speed of sound, meters/second
A	=	microphone separation distance, 1 meter
c	=	true distance for correct velocity calculation
D	=	projectile diameter, meters
D_i	=	arrival time difference, i = 1–4
$F(y)$	=	is a function used to solve the differential equation determining the flow past the body of revolution
h	=	elevation of projectile above ground plane
K	=	shape constant, 1.82
L	=	projectile length, meters
L_{Mi}	=	location microphone, i = 1–6
M	=	Mach number
O	=	offset distance, perpendicular distance from projectile trajectory to mic, meters
p	=	overpressure
p_o	=	ambient pressure
R_C	=	in-plane distance from center microphone to projectile location, meters
R_L	=	in-plane distance from left microphone to projectile location, meters
R_R	=	in-plane distance from right microphone to projectile location, meters
T	=	total duration pulse period, seconds
T_1	=	time difference between microphone 2 and 1
T_2	=	time difference between microphone 3 and 2
T_3	=	time difference between microphone 5 and 2
T_4	=	time difference between microphone 5 and 4
T_5	=	time difference between microphone 6 and 5
V	=	projectile velocity, meters/second
V_P	=	predicted projectile velocity, meters/second
x	=	distance along the axis from the bow
y	=	describes a characteristic curve relationship between x and O
y_f	=	equation for shock front
y_h	=	equation for lead hyperbola
y_{h2}	=	equation for succeeding hyperbola
Y_{LM2}	=	y position of microphone 2, meters
Y_{LM5}	=	y position of microphone 5, meters
Y_{LMi}	=	y position of microphone i
y_s	=	equation for line going through mic 1 and mic 2
α	=	shock angle, °
β	=	azimuth deviation
γ	=	ratio of specific heats of air (1.4)
θ	=	angle from microphone array axis to R_C

INTENTIONALLY LEFT BLANK.

NO. OF COPIES	ORGANIZATION
2	ADMINISTRATOR ATTN DTIC DDA DEFENSE TECHNICAL INFO CTR CAMERON STATION ALEXANDRIA VA 22304-6145
1	DIRECTOR ATTN AMSRL OP SD TA US ARMY RESEARCH LAB 2800 POWDER MILL RD ADELPHI MD 20783-1145
3	DIRECTOR ATTN AMSRL OP SD TL US ARMY RESEARCH LAB 2800 POWDER MILL RD ADELPHI MD 20783-1145
1	DIRECTOR ATTN AMSRL OP SD TP US ARMY RESEARCH LAB 2800 POWDER MILL RD ADELPHI MD 20783-1145
	ABERDEEN PROVING GROUND
5	DIR USARL ATTN AMSRL OP AP L (305)

NO. OF COPIES	ORGANIZATION
2	UNDER SECRETARY OF DEFNS FOR RSRCH AND ENGRG ATTN TWP OM T HITCHCOCK WASHINGTON DC 20301-3100
2	DIR ATTN TECH LIB T HAFNER DEFNS ADVNCD RSRCH PROJ AGCY 3701 N FAIRFAX DR ARLINGTON VA 22203-1714
1	DIR ATTN TECH LIB DEFNS INTLLGNC AGCY WASHINGTON DC 20301
7	CDR ATTN T KENNEDY C MCFARLAND C GALLAWAY E PATNAIK R ROHR G ULLRICH M HOLM DEFNS NUC AGCY WASHINGTON DC 20305-1000
1	HQDA ATTN DAEN RDZ A WASHINGTON DC 20310-1000
1	HQDA ATTN DAEN RDM WASHINGTON DC 20310-1000
1	HQDA ATTN SARD TR K KIMONOS WASHINGTON DC 20310-0103
1	HQDA ATTN SARD TR R CHAIT WASHINGTON DC 20310-1030
1	HQDA ATTN SARD TT C NASH WASHINGTON DC 20310-0103
1	HQDA ATTN SARD TT F MILTON WASHINGTON DC 20310-1030

NO. OF COPIES	ORGANIZATION
1	NATICK RD&E CTR ATTN F BISSETT PDS SATD STRNC YS KANSAS ST NATICK MA 01760-5020
2	CDR ATTN TECH LIB ATCD G M PASTEL US ARMY TRAINING & DOCTRINE CMND FT MONROE VA 23651
3	CDR ATTN SMCAR AEE WW PAI LU N SLAGG J PEARSON US ARMY ARMAMENT RD&E CTR PICATINNY ARSENAL NJ 07806-5000
10	CDR ATTN TECH LIB STRBE N HEBERLEIN STRBE NA WEAVER STRBE BLORE STRBE CFLO STRBE NE 3 CYS STRBE ND SPITZER STRBE NDM DILLON FT BELVOIR VA 22060-5606
14	DIR ATTN AMSRL SS FF J GERBER T PHAM M FONG K TRAN AMSRL WT N J GWALTNEY J INGRAM J MCGARRITY AMSRL WT NA R KEHS AMSRL WT NB M ABE AMSRL WT ND J MILETTA AMSRL WT NF L JASPER AMSRL WT NG T OLDHAM AMSRL WT HD J CORRIGAN AMSRL SL C J HUGHES US ARMY RESEARCH LABORATORY 2800 POWDER MILL RD ADELPHI MD 20783-1145

NO. OF COPIES	ORGANIZATION
3	DIR ATTN TECH LIB AMSRL MA PA W HASKELL E RIGAS US ARMY RESEARCH LABORATORY WATERTOWN MA 02172-0001
1	CDR ATTN STEW NED J MEASON US ARMY WSMR WSMR NM 88002
2	CDR ATTN TECH LIB AMFTA RSA T MEITZLER US ARMY TACOM WARREN MI 48397-5000
3	CDR ATTN TECH LIB G LONG D BACH US ARMY NUC AND CHEML AGCY 7150 HELLER LOOP STE 101 SPRINFIELD VA 22150-3198
2	COMMANDER ATTN TECH LIB M OGORZALEK US ARMY CONCEPTS ANALYSIS AGCY 8120 WOODMONT AVE BETHESDA MD 20814
1	CDR ATTN TECH LIB US ARMY RSRCH OFC PO BOX 12211 RSRCH TRI PK NC 27709
3	CDR ATTN T REEDER G GOODWIN TECH LIB US ARMY NGIC 220 7TH ST NE CHARLOTTESVILLE VA 22901-5396

NO. OF COPIES	ORGANIZATION
1	CDR ATTN TECH LIB US ARMY DUGWAY PROVING GROUND DUGWAY UT 84022
2	US ARMY CORPS OF ENGRS ATTN TECH LIB C HERRING CONST ENGRG RSRCH LAB PO BOX 9005 CHAMPAIGN IL 61826-9005
8	US ARMY ENGR WATERY EXPERMT STAT ATTN TECH LIB J STOUT J INGRAM R DINAN G MCMAHON P KING C JOACHIM B ARMSTRONG PO BOX 631 VICKSBURG MS 39180-0631
1	CMDT ATTN TECH LIB US ARMY ENGINEER SCHOOL FT LEONARD WOOD MO 65473
1	CDR ATTN TECH LIB US ARMY COLD REGIONS R&E LAB PO BOX 282 HANOVER NH 03755
2	CDR ATTN STEYT MT EA C HASTON STEYT MT AT A HOOPER US ARMY YUMA PROVING GROUND YUMA AZ 85365
1	CDR ATTN R FRANSEEN US AMCOM FIELD ASST IN SCI AND TECHLGY PROG FT BELVOIR VA 22060-5606

NO. OF COPIES	ORGANIZATION
1	US ARMY CORPS OF ENGINEERS ATTN D NEBUDA OMAHA DISTRICT MAIL CODE CEMRO ED SH 215 N 17TH ST OMAHA NE 68102-4978
8	OFFICER IN CHARGE ATTN TECH LIB F WARNOCK R FERGUSON K CHIEN J COLLINS CODE R 45 R PERSH M RUPPALT CODE R31 A LE NAVAL SURFACE WARFARE CTR 10901 NEW HAMPSHIRE RD SILVER SPRING MD 20903-5640
4	CDR ATTN TECH LIB L FONTENOT J BROWN CODE G72 J POWERS NAVAL SURFACE WARFARE CTR 17320 DAHLGREN RD DAHLGREN VA 22448-5000
2	CDR ATTN TECH LIB M ORR CODE 1101 NAVAL SURFACE WARFARE CTR PHILADELPHIA PA 19112-5083
2	CDR ATTN TECH LIB WILLIAM A SCHMIDT NAVAL RSRCH LAB WASHINGTON DC 20375
1	CDR ATTN TECH LIB NAVAL SURFACE WARFARE CTR SILVER SPRING MD 20903-5000

NO. OF COPIES	ORGANIZATION
1	CDR ATTN TECH LIB NAVAL SURFACE WARFARE CTR CHINA LAKE CA 93555-6001
1	OFFICER IN CHARGE ATTN TECH LIB NAVAL EOD FACILITY INDIAN HEAD MD 20640
3	CDR ATTN R DENTON MAJ CUTCHALL TECH LIB NAVAL COASTAL SYSTEMS CTR PANAMA CITY FL 32407
1	NAVAL WARARE ASSESSMENT CTR ATTN B HULET PO BOX 5000 NWAC CORONA CA 91718-5000
2	DIR ATTN TECH LIB J BRIONES NUCLEAR EFFECTS DIRECTORATE WSMR NM 88002
2	CDR ATTN D VAUGHN TECH LIB MARINE CORPS RD&E CMND QUANTICO VA 22134-5080
1	CDR ATTN AETT SA MR JEFF SMITH 7TH ARMY TRAINING COMMAND HQ 7TH ATC UNIT #28130 APO AE 09114
1	CDR ATTN AMXLS SA MR SCOTT KOHNKE US NATIONAL TRAINING CTR BLDG 502 FT IRWIN CA 92310

NO. OF COPIES	ORGANIZATION
1	CDR ATTN AMSTI RLO NTC HECTOR LOPEZ US ARMY STRICOM STRICOM LNO BLDG 130 PO BOX 10332 FT IRWIN CA 92310
1	CDR ATTN AFZF CS SA MR ROY J HOLLEY HQ III CORPS FT HOOD TX 76544-5056
1	DIR ATTN AMSRL SS SL JIM CHOPAK US ARMY RESEARCH LABORATORY 2800 POWDER MILL RD ADELPHI MD 20783-1197
2	US DEPT OF ENERGY ATTN TECH LIB KK 22 K SISSON WASHINGTON DC 20585
1	US MILITARY ACADEMY ATTN CAPT KEITH E MATTHEWS DEPT OF MATH SCI WEST POINT NY 10996
2	USIA WORLD NET ATTN TECH LIB J RYAN RM 2410 PATRICK HENRY BLDG 601 D ST NW WASHINGTON DC 20547
1	PHILLIPS LAB ATTN TECH LIB KIRTLAND AFB NM 87118-6008
5	FIELD COMMAND DNA ATTN LCDR Z MYERS CPT M SCOTT J RENICK E MARTINEZ 2 CYS KIRTLAND AFB NM 87115-5000
1	AFOSR ATTN TECH LIB BOLLING AFB DC 20332

NO. OF COPIES	ORGANIZATION
3	WL MNME ATTN G PARSONS J FOSTER TECH LIB EGLIN AFB FL 32542-5000
1	DIR NASA SCIENCE TECHL INTNAT FACLTY PO BOX 8754 BWI AIRPORT MD 21240
2	NOAA OCEANIC AND ATMOSPHERIC RSRCH ATTN CPT SMART W CALLENDER 1335 E W HWY SSMC3 MAILCODE R PDC SILVER SPRING MD 20910
1	OIR CSD CRB ATTN A M JONES RM 1413 OHB WASHINGTON DC 20505
1	DIR ATTN TECH LIB IDAHO NAT LAB PO BOX 1625 IDAHO FALLS ID 83415
1	DIR ATTN TECH LIB LOS ALAMOS NAT LAB PO BOX 1663 LOS ALAMOS NM 87545
4	DIR ATTN TECH LIB R OSTENSEN S SNYDER M SAGARTZ SANDIA NAT LABS PO BOX 5800 ALBUQUERQUE NM 87185

NO. OF COPIES	ORGANIZATION
2	DIR ATTN TECH LIB A KUHL LAWRENCE LIVERMORE NAT LAB PO BOX 808 LIVERMORE CA 94550
1	AAI CORPORATION ATTN TECH LIB PO BOX 126 HUNT VALLEY MD 21030-0126
2	ABERDEEN RESEARCH CENTER ATTN J KEEFER N ETHRIDGE PO BOX 548 ABERDEEN MD 21001
1	AEROSPACE CORPORATION ATTN TECH LIB PO BOX 92957 LOS ANGELES CA 90009
1	ALCAN POWDERS AND CHEMICALS ATTN TECH LIB PO BOX 290 ELIZABETH NJ 07207
3	ALLIED CONTRACTORS INC ATTN TECH LIB T CRAWFORD A SIMPSON 204 E PRESTON ST BALTIMORE MD 21202
1	ALUMINUM COMPANY OF AMERICA ATTN TECH LIB 1501 ALCOA BLDG PITTSBURG PA 15219
1	AMPAL ATTN TECH LIB PO BOX 31 FLEMINGTON NJ 08822

NO. OF COPIES	ORGANIZATION
2	ANSER MISSILE DIVISION ATTN TECH LIB R LEGINUS CRYSTAL GATEWAY 3 1215 JEFFERSON DAVIS HWY ARLINGTON VA 22202
1	APPLIED RESEARCH ASSOCIATES INC ATTN R FLOREY 2750 EISENHOWER AVE STE 104 ALEXANDRIA VA 22314
2	APPLIED RESEARCH ASSOCIATES INC ATTN R GUICE R HEYMAN 5941 S MIDDLEFIELD RD LITTLETON CO 80123
1	APPLIED RESEARCH ASSOCIATES INC ATTN J DRAKE 3202 WISCONSIN AVE VICKSBURG MS 39180
1	ATLANTIC RESEARCH CORPORATION ATTN TECH LIB 5390 CHEROKEE AVE ALEXANDRIA VA 22314
1	ATOMIZED METAL POWDERS INC ATTN TECH LIB 25 E 39TH ST NEW YORK NY 10016
1	BATTELE TWSTIAC 505 KING AVE COLUMBUS OH 43202-2093
1	BDM CORPORATION ATTN TECH LIB 7915 JONES BRANCH DR MCLEAN VA 22102
2	BOEING HELICOPTERS ATTN TECH LIB J COSGROVE PO BOX 16858 MS P30 07 PHILADELPHIA PA 19142-0858

NO. OF COPIES	ORGANIZATION
2	BOEING MILITARY AIRPLANE COMPANY ATTN TECH LIB R LORENZ PO BOX 7730 WICHITA KS 67277-7730
1	BOOZ ALLEN & HAMILTON INC ATTN TECH LIB CRTSTAL SQ 2 STE 1100 1725 JEFFERSON DAVIS HWY ARLINGTON VA 22202-4158
2	DENVER RESEARCH INSTITUTE ATTN TECH LIB L BROWN PO BOX 10127 DENVER CO 80210
2	DYNAMIC SCIENCE INC ATTN S ZARDAS P NEUMAN PO BOX N ABERDEEN MD 21001
2	ELECTROSPACE SYSTEMS INC ATTN TECH LIB S PAREKH PO BOX 831359 RICHARDSON TX 75083-1359
1	EMTEC SYSTEMS INC ATTN J LATTERY 4500 ANAHEIM AVE NE B6 ALBUQUERQUE NM 87113
1	ETHYL CORPORATION ATTN TECH LIB HOUSTON PLANT BOX 472 PASADENA TX 77501
1	FMC CORPORATION ATTN TECH LIB 1105 COLEMAN AVE SAN JOSE CA 95108
1	FRANKLIN RESEARCH CENTER ATTN TECH LIB BENJAMIN FRANKLIN PKY PHILADELPHIA PA 19103

NO. OF COPIES	ORGANIZATION
2	GENERAL SCIENCES INC ATTN TECH LIB M RILEY 655 S GRAVERS RD PLYMOUTH MEETING PA 19462
1	ITT RESEARCH INSTITUTE ATTN TECH LIB 10 W 35TH ST CHICAGO IL 60616
2	ITT AEROSPACE OPTICAL DIVISION ATTN TECH LIB K RUSTER 3700 E PONTIAC ST PO BOX 3700 FT WAYNE IN 46803
3	THE JOHNS HOPKINS UNIVERSITY ATTN TECH LIB T COUGHLIN J KOUROUPIS APPLIED PHYSICS LAB JOHNS HOPKINS RD LAUREL MD 20707
1	KAMAN SCIENCES CORPORATION ATTN F MCMULLAN 6400 UPTOWN BLVD STE 300E ALBUQUERQUE NM 87110
2	MARTIN MARIETTA AEROSPACE ATTN TECH LIB M BAUER PO BOX 179 DENVER CO 80201
2	MCDONNELL DOUGLAS CORPORATION ATTN TECH LIB C COREY BALLISTIC MISSILE DEFENSE 5301 BOLSA AVE HUNINGTON BEACH CA 92647
1	MEDTHERM CORPORATION ATTN LARRY JONES PO BOX 412 HUNTSVILLE AL 35804

NO. OF COPIES	ORGANIZATION
2	NEW MEXICO ENGRG RSRCH INST ATTN TECH LIB R ROBEY U OF NM ALBUQUERQUE NM 87131-1376
1	DEPARTMENT OF STATISTICS ATTN DR JAMES R THOMPSON RICE UNIVERSITY HOUSTON TX 77251-1892
2	OLIN ORDNANCE ATTN TECH LIB J KIBIGER PRODUCT MATERIAL CONTROL 10101 9TH ST N ST PETERSBURG FL 33716
1	PCI ATTN V SCHMIDT 900 19TH ST NW STE 600 WASHINGTON DC 20006
2	REYNOLDS METALS COMPANY ATTN TECH LIB N KOOPMAN PLANT #3 4101 CAMP GROUND RD LOUISVILLE KY 40211
3	S CUBED MAXWELL LABS ATTN TECH LIB C NEEDHAM K SCHNIEDER ALBUQUERQUE NM 87131
1	SI DIVISION OF SPECTRUM 39 ATTN W SCHUMAN 8831 SATYR HILL RD STE 312 BALTIMORE MD 21234
2	SCIENCE APPLICATIONS INTNL CORP ATTN TECH LIB J BRYARS 11526 SORRENTO VALLEY RD STE A SAN DIEGO CA 92121

NO. OF COPIES	ORGANIZATION
4	SCIENCE APPLICATIONS INTNL CORP ATTN J SIMMONS J GUEST J DISHON P VERSTEEGAN PO BOX 1303 1710 GOODRICH DR MCLEAN VA 22102
1	SCIENCE APPLICATIONS INTNL CORP ATTN S DOERR 2109 AIR PK RD SE ALBUQUERQUE NM 87106
1	SIBERLINE MANUFACTURING CO INC ATTN TECH LIB PO BOX A LANSFORD PA 18232
2	SIMULA GOVERNMENT PRODUCTS INC ATTN TECH LIB W PERCIBALLI 10016 S 51ST ST PHOENIX AZ 85044-5299
1	SOUTHWEST RESEARCH INSTITUTE ATTN TECH LIB PO DRAWER 28510 SAN ANTONIO TX 78284
1	SRI INTERNATIONAL ATTN TECH LIB 333 RAVENSWOOD AVE MENLO PK CA 94025
2	TECH REPS INC ATTN F MCMULLEN B COLLINS 5000 MARBLE NE STE 222 ALBUQUERQUE NM 87110
1	TELEDYNE MCCORMICK SELPH ATTN C GARRISON PO BOX 6 HOLLISTER CA 95023-0006
1	TERA ATTN TECH LIB NM INSTITUTE OF TECHLGY SOCORRO NM 87801

NO. OF COPIES ORGANIZATION

1 THERMOGAGE INC
ATTN CHARLES BROOKLY
330 ALLEGHANY ST
FROSTBURG MD 21532

1 TRANSMET CORPORATION
ATTN TECH LIB
4290 PERIMETER DR
COLUMBUS OH 43228

1 US BRONZ POWDERS INC
ATTN TECH LIB
PO BOX 31
RT 202
FLEMINGTON NJ 08822

1 UNYSIS CORPORATION
ATTN H ZADEH
A J FREDERICK
4000 S MEMORIAL PKY
HUNTSVILLE AL 35802

2 UNIVERSITY OF MD AT COLLEGE PK
DEPT OF MECHL ENGRG
ATTN ENME J WALLACE
U PIOMELLI
RM 2168
COLLEGE PK MD 20742-5121

1 UNIVERSITY OF MD AT COLLEGE PK
ATTN ENGRG AND PHYS SCI LIB
MATHEMATICS BLDG
COLLEGE PK MD 20742

1 VALIMET INC
ATTN TECH LIB
431 E SPERRY RD
STOCKTON CA 95206

5 WALCOFF AND ASSOCIATES INC
ATTN T TOYA
C PAQUETTE
C WALCOFF
W DEAL
R WALDEN
12015 LEE JACKSON MEM HWY
#500
FAIRFAX VA 22033-3300

NO. OF COPIES ORGANIZATION

1 STRICOM
ATTN AMSTI MC L LAWRENCE
2350 RESEARCH PKY
ORLANDO FL 32826-3276

ABERDEEN PROVING GROUND

1 CMD, AMCCOM
ATTN: SMCAR-ACW (E3516)
WEAPONS SYSTEMS CONCEPT TEAM

9 DIR, USAMSAA
ATTN: AMSXB-GB, ABEL
AMXSY-S, CARROLL
AMXSY-GC,
B BRAMWELL
C EISSNER
L MEREDITH
W WIDERMAN
A WONG
LTC HASSELL
JTCG-ME, LAGRANGE

5 CMD, USACSTA
ATTN: STECS-AE-CL,
R. SCUTTI
D. GRIFFEN
STECS-AE-TL, BINDEL
STECS-AE-TH, WILEY
STECS-LI, R. HENDRICKSEN

4 DIR, ERDEC
ATTN: SCDRB-RTT,
L BICKFORD
S FUNK
G GOLDSMITH
I SWANN

1 CDR, USAOC&S
ATTN: TECH LIB

6 CDR, USATECOM
ATTN: AMSTE-SI-F
AMSTE-CL
AMSTE-EV-O
AMSTE-TA-F
AMSTE-ML
AMSTE-TE-V

NO. OF COPIES	ORGANIZATION
86	DIR, USARL
	ATTN: AMSRL-CI-S, A. MARK
	AMSRL-CP-TI, J. POLK
	AMSRL-SL,
	J. WADE (433)
	J. SMITH (433)
	AMSRL-SL-I, M. STARKS (433)
	AMSRL-SL-B, P. DEITZ (328)
	AMSRL-SL-BA, J. WALBERT (1068)
	AMSRL-SL-BG, A. YOUNG (433)
	AMSRL-SL-BL, M. RITONDO (328)
	AMSRL-SL-BS, D. BELY (328)
	AMSRL-SL-BV,
	J. MORRISSEY (247)
	W. BAKER (247)
	J. COLLINS (247)
	L. MOSS (247) (5 CYS)
	W. WINNER (247)
	AMSRL-CI-C,
	M. TAYLOR
	AMSRL-WT-NC,
	R. LOTTERO
	R. LOUCKS (20 CYS)
	P. MULLER
	R. THANE
	J. SULLIVAN
	R. RALEY
	G. FERGUSON
	S. SCHRAMEL
	C. MERMAGEN
	A. MIHALCIN
	AMSRL-WT-TB, J. CONDON
	AMSRL-WT-TD, P. KINGMAN
	AMSRL-WT-W, C. MURPHY
	AMSRL-WT-WA,
	B. MOORE
	H. ROGERS
	F. BRANDON
	T. GORDON BROWN
	W. D'AMICO
	B. DAVIS (20 CYS)
	D. HEPNER
	M. HOLLIS
	R. MCGEE
	AMSRL-WT-WB, A. BARAN
	AMSRL-WT-WD, G. THOMSON
	AMSRL-WT-WE,
	R. HAUSER
	W. JOHNSON
	J. THOMAS
	J. WITAS
	AMSRL-WT-WG, L. PUCKETT
	AMSRL-W-WC, T. HAUG
	AMSRL-HR-SB, W. HANLON
	AMSRL-HR-SD, J. KALB

NO. OF COPIES ORGANIZATION

2 BUNDESAMT FÜR WEHRTECHNIK
UND BESCHAFFUNG
ATTN: K KÖHLER
TECH LIB
POSTFACH 7360
5400 KOLENZ, GERMANY

2 DEFENSE RESEARCH ESTABLISHMENT
SUFFIELD
ATTN: D. RITZEL
TECH LIB
PO BOX 4000
MEDICINE HAT
ALBERTA, T1A 8K6 CANADA

4 DSTO, MATERIALS RESEARCH
LABORATORY
ATTN: N. BURMAN
D. SAUNDERS
M. BUCKLAND
TECH LIB
PO BOX 50
ASCOT VALE
VICTORIA, AUSTRALIA 3032

2 INDUSTRIEANLAGEN-
BETRIEBSGESGELLSCHAFT MBH
ATTN: TECH LIB
H. DIEKHOFF
ABTEILUNG FINITE
BERECHNUNGSVERFAHREN
EINSTEINSTRAβE 20, D-8012 OTTOBRUNN

8 MINISTRY OF DEFENSE
ATOMIC WEAPONS ESTABLISHMENT
ATTN: M. GERMAN
J. THREAGOLD
W. BABBAGE
B. BOGARTZ
I. SMITH
J. TATE
M. KING
TECH LIB
FOULNESS, ESSEX, SS3 9XE, UK

NO. OF COPIES ORGANIZATION

4 MINISTRE DE LA DEFENSE
CENTRE D'ETUDE DE GRAMAT
ATTN: S. GRATIAS
E. CANTON
D. MERGNAT
TECH LIB
46500 GRAMAT, FRANCE

2 MINISTERE DE L'EQUIPMENT
LABORATOIRE D'ESSAIS D'EQUIPEMENTS
D'ABRIS
ATTN: TECH LIB
D. FAU
BASE DE VIROULOU-ALVIGNAC
46500 GRAMAT, FRANCE

2 NATIONAL DEFENSE RESEARCH INSTITUTE
WEAPONS TECHNOLOGY DEPARTMENT
ATTN: H. AXELSSON
TECH LIB
PO BOX 98
S-147 00 TUMBA, SWEDEN

3 NORWEGIAN DEFENSE CONSTRUCTION SERVICE
TEST AND DEVELOPMENT SECTION
ATTN: TECH LIB
A. JENSSEN
OSLO MIL/AKERSHUS
OSLO, NORWAY

3 STORES AND CLOTHING RESEARCH AND
DEVELOPMENT ESTABLISHMENT
ATTN: S. ELTON
S. CROSS
TECH LIB
FLAGSTAFF RD
ESSEX, CO2 7SS, UK

3 WEHRWISSENSCHAFTLICHE DIENSTELLE FÜR
SPRENGMITTEL UND SONDERTECHNIK
ATTN: M. KLAUS
L. KLUBERT
TECH LIB
OBERJETTENBERG
8230 SCHNIZLREUTH, GERMANY

NO. OF
COPIES ORGANIZATION

2 WEHRWISSENSCHAFTLICHE DIENSTELLE
DER BUNDESWEHR FÜR ABC-SCHUTZ
ATTN: W. REHMANN
TECH LIB
HUMBOLTSTRAβE/POSTFACH 1142
3042 MÜNSTER, GERMANY

1 DEWEY MCMILLAN & ASSOCIATES, INC.
ATTN: J. DEWEY
1741 FELTHAM RD
VICTORIA, BC V8N 2A4, CANADA

USER EVALUATION SHEET/CHANGE OF ADDRESS

This Laboratory undertakes a continuing effort to improve the quality of the reports it publishes. Your comments/answers to the items/questions below will aid us in our efforts.

1. ARL Report Number ARL-TR-859 Date of Report September 1995

2. Date Report Received _____

3. Does this report satisfy a need? (Comment on purpose, related project, or other area of interest for which the report will be used.) _____

_____

_____

4. Specifically, how is the report being used? (Information source, design data, procedure, source of ideas, etc.)

_____

_____

_____

5. Has the information in this report led to any quantitative savings as far as man-hours or dollars saved, operating costs avoided, or efficiencies achieved, etc? If so, please elaborate. _____

_____

_____

6. General Comments. What do you think should be changed to improve future reports? (Indicate changes to organization, technical content, format, etc.) _____

_____

_____

_____

CURRENT ADDRESS

_____
Organization

_____
Name

_____
Street or P.O. Box No.

_____
City, State, Zip Code

7. If indicating a Change of Address or Address Correction, please provide the Current or Correct address above and the Old or Incorrect address below.

OLD ADDRESS

_____
Organization

_____
Name

_____
Street or P.O. Box No.

_____
City, State, Zip Code

(Remove this sheet, fold as indicated, tape closed, and mail.)

(DO NOT STAPLE)